"Hey farmer, farmer, put away your DDT

I don't care about spots on my apples,

Leave me the birds and the bees – please"

-Joni Mitchell

University of Alberta

Enantiomer- and Isomer-Specific Fate of Persistent Organic Pollutants in the Environment

by

Matthew Stephen Ross

A thesis submitted to the Faculty of Graduate Studies and Research
in partial fulfillment of the requirements for the degree of

Doctor of Philosophy

Department of Chemistry

©Matthew Stephen Ross
Spring 2011
Edmonton, Alberta

This thesis is dedicated to my parents, Barbara and Stephen.

Abstract

This thesis discusses the fate of individual enantiomers and isomers of organohalogen compounds (OHCs) in the environment and the development of analytical methods to facilitate such determinations.

A novel proof of principle anion attachment atmospheric pressure photoionization (AA-APPI) method was developed. Minimal matrix effects, increased sensitivity and lower limits of detection were found in sediment extracts spiked with hexabromocyclododecane (HBCD) compared to atmospheric pressure photoionization. AA-APPI offers a simple means of further extending the range of compounds ionizable by photoionization, while maintaining minimal matrix effects.

Enantiomer fractions (EFs) of chiral OHCs were determined in the blood and eggs of glaucous gulls from Svalbard, Norway, to determine the enantioselectivity of OHC maternal transfer. No differences were found between the EFs for any analyte in female gulls compared to those found in egg yolk. This indicates that processes involved in the maternal transfer of OHCs to eggs do not modulate the stereochemical ratio between enantiomers.

EFs of polychlorinated biphenyl (PCB) atropisomers were determined in the sediment and biota from an estuary heavily contaminated with highly chlorinated PCB congeners. Non-racemic EFs were found in sediment, likely the result of microbial dechlorination. EFs in grass shrimp mirrored those of sediment, but non-racemic EFs in fish species and bottlenose dolphins were likely

a result of both uptake of non-racemic proportions of PCBs from the diet and enantioselective biotransformation.

OHC EFs were investigated in captive sledge dogs fed OHC-polluted minke whale blubber, to gain greater understanding of the biotransformation capacity of a model polar bear surrogate species. Sledge dogs biotransformed OHCs enantioselectively, and the comparative enantiomer-specific biotransformation capacity showed similar and contrasting results based on individual compounds/congeners.

The isomer-specific fate of perfluorooctane sulfonamide (PFOSA) was investigated in male Sprague-Dawley rats. PFOSA elimination occurred isomer-specifically, resulting in a depletion of branched PFOSA isomers in blood. Isomer-specific formation of PFOS was also observed. The significant enrichment of 5*m*-PFOS and the depletion of the alpha branched PFOS isomer provide the first *in vivo* evidence that exposure to PFOS precursor compounds alters the isomer pattern of PFOS in biota.

Acknowledgments

The acknowledgments—the place where I get to thank and recognize all those who helped move this thesis to completion. It is unfortunate that there is neither enough time nor enough room to acknowledge everyone, and for those who I have forgotten, I apologize.

I will begin by thanking my advisors, Charles Wong and Jonathan Martin. I appreciate the opportunity I had to work with each of you. I know that the guidance and knowledge that I gained from each of you has helped me to grow considerably as a scientist, and for that I am thankful.

I was fortunate to be a part of two research groups filled with wonderful people, and I'm glad I had the opportunity to work with each of them. Nick W, Jon B, and Derek B were all instrumental in helping complete the work presented in this thesis, and I am indebted to each.

I think John Lennon and Paul McCartney said it best when they wrote "I get by with a little help from my friends". Without their support, I know that the completion of this thesis would not have been possible. I would like to thank Haley for her unwavering love and support, and her unending patience with me. I am also grateful to Sherri, Brian, Echo, Vicki, Craig and Ev for all the coffee, conversations, and adventures. The time we spent together made my time in Canada a wonderful and memorable experience.

Finally, to my family. I can't express enough how much having your love and support has helped me to get here today. Thank you.

Table of Contents

Chapter 2: Comparison of Electrospray Ionization, Atmospheric Pressure Photoionization, and Anion Attachment Atmospheric Pressure Photoionization for the Analysis of Hexabromocyclododecane Enantiomers in Environmental Samples

Chapter 6: Isomer-Specific Biotransformation of Perfluorooctane

List of Tables

List of Figures

List of Symbols, Nomenclature, or Abbreviations

1,4-DBB   1,4-dibromobutane

AA-APPI   anion attachment atmospheric pressure photoionization

ANOVA   analysis of variance

APPI   atmospheric pressure photoionization

B.W.   body weight

BPDM   benzphetamine-N-demethylase

CC   *cis*-chlordane

C_{max} maximum concentration

CRM   certified reference material

CYP   cytochrome p-450

DDT   1,1,1-trichloro-2,2-bis-(p-chlorophenyl) ethane

ECF   electrochemical fluorination

EF   enantiomer fraction

EI   electron impact

ESI   electrospray ionization

eV   electron volts

GC-MS   gas chromatography-mass spectrometry

HBCD   hexabromocyclododecane

HCH   hexachlorocyclohexane

HEPX   heptachlor *exo*-epoxide

HPLC   high performance liquid chromatography

i.p.	intraperitoneal
K_{ow}	octanol-water partition coefficient
LC-MS	liquid chromatography-mass spectrometry
LOD	limit of detection
LOQ	limit of quantification
MAP	mercapturic acid pathway
ME	matrix effects
MeSO2-PCB	methylsulfonyl polychlorinated biphenyl
MFO	mixed function oxidase
mL	milliliter
MRM	multiple reaction monitoring
NEtFOSA	N-ethyl perfluorooctane sulfonamide
NEtFOSE	N-ethyl perfluorooctane sulfonamidoethanol
ng	nanogram
NOEL	no observed effects level
NOW	Northwater Polynya
OC	organochlorine
OH-PCB	hydroxylated polychlorinated biphenyl
OXY	oxychlordane
PBDE	polybrominated diphenyl ether
PCB	polychlorinated biphenyl
PFC	perfluorinated compound
PFOA	perfluorooctanoic acid

PFOS	perfluorooctane sulfonate
PFOSA	perfluorooctane sulfonamide
PFOSF	perfluorooctane sulfonylfluoride
POP	persistent organic pollutant
SIM	selective ion monitoring
TC	*trans*-chlordane

Chapter 1

Persistent Organic Pollutants and the Use of Chiral and Isomer-Specific Analyses

1.1 Introduction

Persistent organic pollutants (POPs) are a class of environmental contaminants, which are generally anthropogenic in origin, recalcitrant to environmental degradation processes, can migrate long distances from the point of release, bioaccumulate, and elicit toxic effects.

After release to the environment, POPs may sorb strongly to soil and sediment and resist environmental degradation processes such as hydrolysis and photolysis. The recalcitrant nature of POPs allows them to persist in the environment for decades. For example, the use of chlordane for agricultural purposes was discontinued in the United States in 1983 (1), yet it can still be frequently detected at high concentrations in the US (2). Furthermore, POPs are generally highly hydrophobic and lipophilic, and partition into the fat of organisms, where they may be stored and remain unmetabolized. This combination of physical properties and resistance to metabolism causes accumulation of POPs in humans and wildlife, and concentrations may also increase through foodwebs. One example is polar bears from East Greenland, which have concentrations of polychlorinated biphenyls in their livers that were 50-fold higher than in the blubber of their main prey item, ringed seals (3).

Most POPs also have sufficiently high vapor pressures to allow them to partition from sediments or water into the atmosphere. This, combined with a resistance towards atmospheric degradation process, allows for POPs to be transported to remote regions of the globe via long-range atmospheric transport.

High concentrations of POPs have been, and continue to be, detected in the Arctic environment (4), hundreds of miles away from the nearest point of release.

Two generalized groups of POPs exist. First, legacy POPs are organochlorines that were first used in the mid 1940's and subsequently banned or heavily restricted in North America in the 1970's and 1980's. Most are first-generation organochlorine pesticides, such as 1,1,1-trichloro-2,2-*bis*-(*p*-chlorophenyl) ethane (DDT), hexachlorocyclohexane (HCH), aldrin, and chlordane. Some of these compounds found widespread use in agriculture and as general-purpose insecticides before concerns arose regarding their potential for adverse affects to human health. Other legacy POPs include chlorinated industrial chemicals, such as hexachlorbenzene and polychlorinated biphenyls (PCBs). In 2001, 91 nations signed a treaty in Stockholm, Sweden, banning or restricting the use of twelve legacy POPs (5), including chlordanes, DDT, and PCBs.

A second group of contaminants are considered to be new or "emerging POPs", that have either been recently added to the list of controlled chemicals under the Stockholm Convention on Persistent Organic Pollutants, or which are currently being reviewed for addition to this list. These compounds include such chemicals as the polybrominated diphenyl ethers (PBDEs) and hexabromocyclododecane (HBCD) brominated flame retardants, as well as perfluorooctane sulfonate (PFOS) and its precursors. These compound are similar to legacy POPS in that they are persistent, bioaccumulative, toxic, and may undergo long-range global transport. However, these compounds continue to be

3

manufactured and used, or their manufacture has only recently been discontinued. The Stockholm Convention was amended in May 2009, when HCH and penta- and octa-PBDE formulations use was restricted. At this time, PFOS and its precursors were added to Annex B of the Stockholm Convention, which still allows the use of PFOS and its precursors for many applications, while the production of two PBDE formulations was banned. HBCD is currently under review for inclusion to the Stockholm Convention.

Despite restrictions on their use, human and wildlife exposure to POPs continues. POPs are still being emitted from older stocks of chemicals, such as products manufactured prior to restrictions (6), while the continued production of some POPs by non-signatory countries will inevitably result in continued release to the environment. In fact, after a sharp decrease in concentrations of PCBs in humans following restrictions on their production, concentrations have begun to level off in the last two decades (6), likely due to continued exposure to PCPs. Furthermore, even after 60 years of use, the human health effects of some POPs remains unclear (7), and it is likely that our understanding of their adverse health effects will continue to grow. Therefore, there is a continued need to monitor these chemicals in humans and the environment, and to gain a deeper understanding of their environmental fate processes so that the future toxicological risks may be predicted.

The broad aim of this thesis is to investigate the processes affecting the fate of POPs in the environment. More specifically, this thesis looks at the fate of

individual POP isomers and enantiomers, two terms that will be discussed in much greater detail in forthcoming sections. It was hypothesized that environmental and biological fate processes will lead to the differential enrichment of POP isomers and enantiomers, and that the study of POP isomer and enantiomer patterns will not only lead to insight into the processes affecting the environmental fate of POPs, but may also be used to determine POP sources.

1.2 Chirality and Isomers

The three-dimensional structure of a compound has a profound effect on its environmental fate and toxicity. Stereoisomerism describes compounds that possess the same chemical formula and bond arrangement, but differ in the spatial arrangement of their bonds (8). One example is the *cis-* and *trans-* arrangement of substituents around a double bond. Due to the crude synthetic processes by which they were manufactured, most POPs are composed of different stereoisomers (hereafter referred to simply as isomers). For instance, the manufacture of PCBs resulted in a mixture of compounds that have the same number of chlorine atoms, but vary in the location of the chlorine substituent on the biphenyl backbone. Isomers can have different physical and chemical properties, and thus will likely behave differently in the environment, possess different toxicities, and undergo biological processing in different ways. For instance, the boiling point of γ-HCH is 323°C, while the boiling point of α-HCH is only 288°C (9). Similarly, of the five isomers present in technical HCH, only the γ isomer is the active pesticide

(9). Due to the possibility of such differences, it is important to understand the environmental fate of individual isomers for all POPs.

A sub-class of stereoisomerism is chirality. A chiral compound exists as two non-superimposable mirror images, referred to as enantiomers (8). Chiral molecules are characterized by a lack of symmetry. The most simple example of chirality is a tetrahedral carbon with 4 different substituents bound to it. Other examples of chirality exist, such as atropisomerism, in which chirality is induced due to hindered rotation about a bond. Chirality is also known as optical isomerism, because the two enantiomers of a chiral substance will rotate plane polarized light in different directions (8). A 1:1 mixture of enantiomers is referred to as a racemic mixture.

In contrast to isomers, enantiomers possess identical physical and chemical properties. For this reason, abiotic environmental processes such as volatilization, photolysis, and deposition will not lead changes in the proportion of enantiomers. However, enantiomers can interact with other chiral molecules, such as proteins, differently. As will be discussed in further detail, differential interactions with biological molecules can lead to differences between enantiomers with respect to the speed of biological transformations by enzymes, toxicokinetics, or affinity for the same toxicological receptor (which are generally proteins). Only recently have the enantiomers of chiral POPs and environmental contaminants been studied carefully. There is therefore a considerable lack of knowledge available regarding the environmental fate, biological fate, and

toxicological properties of individual POP enantiomers.

Understanding the fate of individual enantiomers is important for a number of reasons. Firstly, enantiomers may elicit different toxicological effects, such as the differences in estrogenicity between enantiomers of *o,p´*-DDT. The (*R*)-(-)-*o,p´*-DDT enantiomer is an estrogen mimic, while (*S*)-(+)-*o,p´*-DDT had negligible estrogenicity (10). Therefore, the use of non-enantioselective analytical techniques in exposure assessment, or a lack of understanding of enantiomer-specific fate and effects could lead to uncertainty in environmental risk assessments (11).

Secondly, the use of enantioselective analysis can provide a means of probing biological processes that might affect the environmental fate of POPs. The manufacture and subsequent release of chiral POPs to the environment occurs as a racemic mixture. However, as will be discussed in greater detail in forthcoming sections, biological processes can alter the enantiomer distribution, leading to the detection of non-racemic proportions in some samples. The detection of non-racemic proportions of a compound provides strong evidence for biological processing, and allows insight into processes that may otherwise be missed when using achiral techniques. For instance, Warner et al. (12) determined that the invertebrate, *Mysis relicta*, could biotransform PCBs, a process not previously thought to be occurring in lower trophic level organisms.

Finally, enantiomer distributions can be used to apportion POP sources. For example, sources of chlorinated pesticides to the atmosphere have been

determined to be from historic weathered sources which have volatilized from the soil (13), while sources of PCBs to the Hudson River Estuary were found to be due to deposition of sediment from upstream, rather than from fresh inputs (14). Information on POP sources is important from a regulatory, litigious, toxicological, and risk assessment point of view.

1.3 Overview of Chiral POPs

This thesis discusses a number of different POPs. Below is a brief introduction to the POPs most frequently encountered in the following chapters.

1.3.1 Hexachlorocyclohexane (HCH)

Hexachlorocyclohexane (Figure 1-1) was used widely as a broad based insecticide beginning in 1945 and, although the γ-isomer (also known as lindane) continues to be used in the North America as a medicinal treatment for head lice and scabies (15), the general use of HCH in agriculture was banned in the United States and Canada in the late 1970's (15).
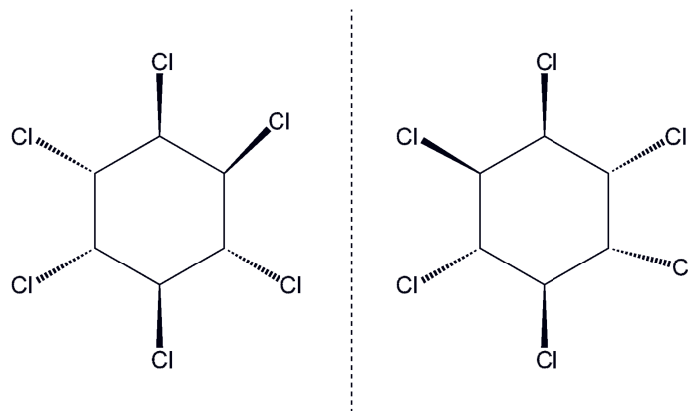
Figure 1-1: *Structure of α-HCH enantiomers.*

Technical HCH is produced through the photochlorination of benzene, a process that could theoretically result in the production of eight isomers that differ based on the axial and equatorial arrangement of the chlorine atoms (15). However, technical HCH is predominantly composed of only five isomers: α (60-70%), β (5-12%), γ (10-12%), δ (6-10%), and ε (3-4%) (16). Of these isomers, only α-HCH is chiral.

HCH is efficiently absorbed *in vivo*, with 95% of a single dose being absorbed within 4 days by rats (17). *In vivo*, HCH is biotransformed to a number of metabolites, mostly consisting of dechlorinated di- through pentachlorinatedcyclohexanes (9). HCH is generally less persistent in organisms than other POPs, and does not appear to biomagnify substantially (18).

α-HCH was the first POP for which individual enantiomers were successfully separated, and thus the first measurements of individual enantiomers

in the environment were for α-HCH (19,20). These initial studies revealed non-racemic distributions of α-HCH in the North Sea (19,20). Since this time, α-HCH has become one of the most studied chiral POPs, and has been detected in non-racemic proportions in the atmosphere (21), soil and sediment (22), ocean water (23), and in a multitude of organisms (18,24,25). A more detailed review of the fates of individual HCH isomers and enantiomers can be found elsewhere (15,26).

1.3.2 Polychlorinated Biphenyls (PCBs)

As a class, PCBs are composed of 209 individual compounds, called congeners, which vary from one another by the number and arrangement of chlorine atoms around a biphenyl backbone. Each ring is substituted with between one and five chlorines (Figure 1-2). PCBs are named based on the degree and pattern of chlorination about the biphenyl ring (27).

$x + y = 1\text{-}10$
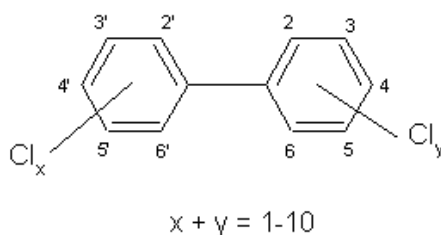
Figure 1-2: *The general structure of PCBs.*

Due to the way in which they are synthesized, PCBs were produced as

mixtures containing dozens of congeners with varying degrees of chlorination. These commercial mixtures were typically named based on the weight percent of chlorine that they contained (e.g., Aroclor 1254 and Aroclor 1268 are composed of 54% and 68% chlorine, respectively). Commercial mixtures were colorless liquids, with low flammability, low vapor pressures, and low water solubility. Such properties made PCBs popular for use as dielectrics in capacitors and transformers, as well as in paints, adhesives, sealants, and lubricating oils (28). However, it is these same physical properties that make PCBs the ubiquitous and persistent environmental contaminants that they are today. More highly chlorinated PCBs degrade very slowly in the environment and are able to bioaccumulate in organisms due to their high (i.e. >4000) octanol-water partition coefficients (K_{ow}) and general resistance to metabolism.

Seventy-eight of the 209 possible PCB congeners are chiral by atropisomersism (29), although only 19 are stable under environmental conditions (30,31). In order for a particular PCB congener to be chiral and stable in the environment, two criteria must be met. First, congeners must possess an asymmetric substitution pattern around the biphenyl backbone. Secondly, the congener must possess three or four *ortho*-substituted chlorines. The bulkiness of the chlorine atoms at the *ortho* positions provides enough steric hindrance that the phenyl rings are not free to rotate about the central carbon-carbon bond (Figure 1-3) (30,31).
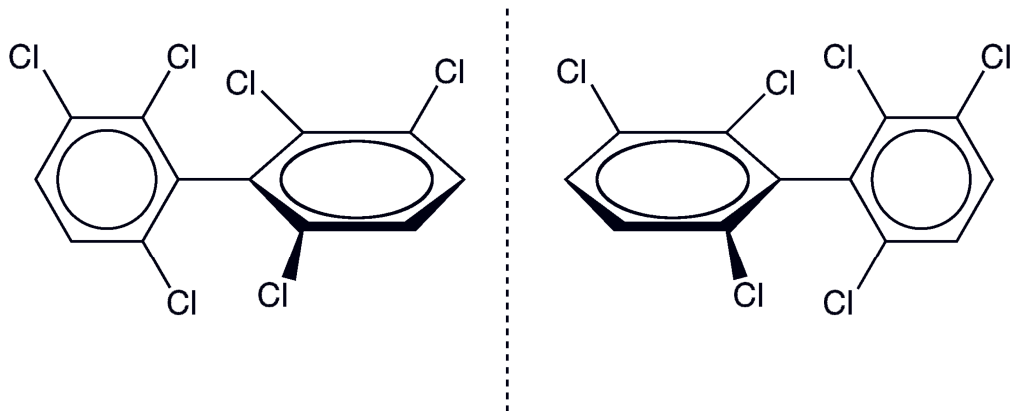
Figure 1-3: *2,2′,3,3′,6,6′-hexachlorobiphenyl (PCB 136) drawn in its non-planar conformation as an example of atropisomerism in PCBs.*

Non-racemic distributions of PCBs have been determined in the environment, including humans and wildlife. However, a thorough review of the occurrence of non-racemic distributions is beyond the scope of this introduction. Several reviews on the subject were recently published (26,32).

The metabolism of PCBs may also result in the formation of several stable chiral metabolites, which have themselves been detected in non-racemic proportions in the environment. The initial step in the metabolism of PCBs can proceed with the cytochrome P-450 (CYP) catalyzed formation of an arene oxide (33). Arene oxides are short-lived intermediates and spontaneously isomerize to form either *para* or *meta* hydroxylated metabolites. Alternatively, oxidation can proceed by the direct insertion of oxygen by CYP isozymes, generally at the *meta* position (34,35). The resulting hydroxylated PCBs (OH-PCBs) bind strongly to the thyroxine-binding protein transthyretin (36,37), resulting in accumulation in

the blood of organisms (38). Recently, an enantioselective gas chromatography method was developed which allowed for the separation of OH-PCB enantiomers (39). While it has yet to be employed to investigate the enantiomer distribution of OH-PCBs in wildlife, non-racemic distributions of several hydroxylated metabolites were found in rats administered PCB 136 (39).

Methylsulfonyl PCB metabolites (Figure 1-4) are formed from the conjugation of the arene oxide, formed during phase I metabolism, with glutathione. This conjugate is then degraded through the mercapturic acid pathway (MAP) to the resulting metabolites (40). The metabolism of chiral PCBs via the MAP can result in the formation of chiral methylsulfonyl PCBs (41). The addition of the $MeSO_2$ moiety to an achiral PCB can also create asymmetry about the biphenyl bond, resulting in chiral tri- and tetra-*ortho*-chlorinated $MeSO_2$-PCBs. Non-racemic distributions of $MeSO_2$-PCBs have been detected in wildlife (42,43) and in rats exposed to racemic PCB 132 (44,45).
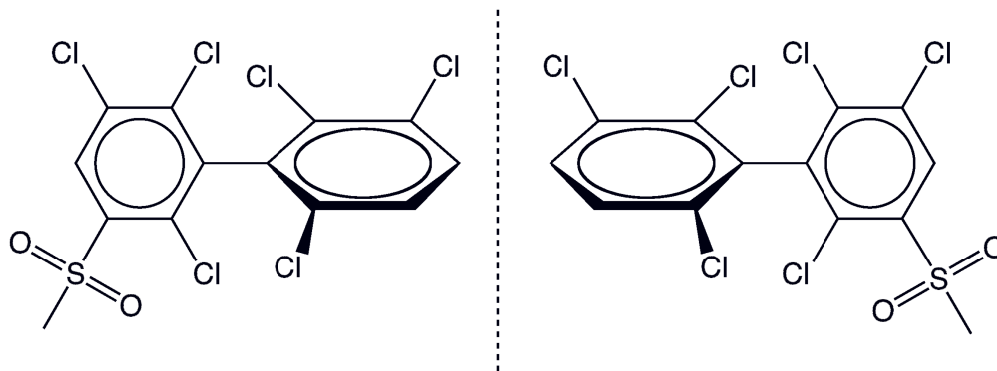
Figure 1-4: *5-MeSO$_2$-2,2´,3,3´,4,4´,6-hexachlorbiphenyl (5-MeSO$_2$-PCB 149) drawn in its non-planar confirmation as an example of atropisomerism in PCB metabolites.*

1.3.3 Chlordane Compounds

Chlordane (Figure 1-5) is a chlorinated cyclodiene pesticide widely used in the United States from 1948 until 1988, primarily for the control of termites. Chlordane is formed via a Diels-Alder reaction between hexachlorocyclopentadiene and cyclopentadiene, followed by further chlorination. Similar to other POPs discussed here, this synthetic process does not result in a single compound; rather, commercial mixtures of chlordane are comprised of approximately 140 components (46). The two most prominent compounds are *cis-* and *trans*-chlordane, which comprise between 60-70% of technical chlordane (47). Other major constituents include heptachlor and *cis-* and *trans*-nonachlor (47).
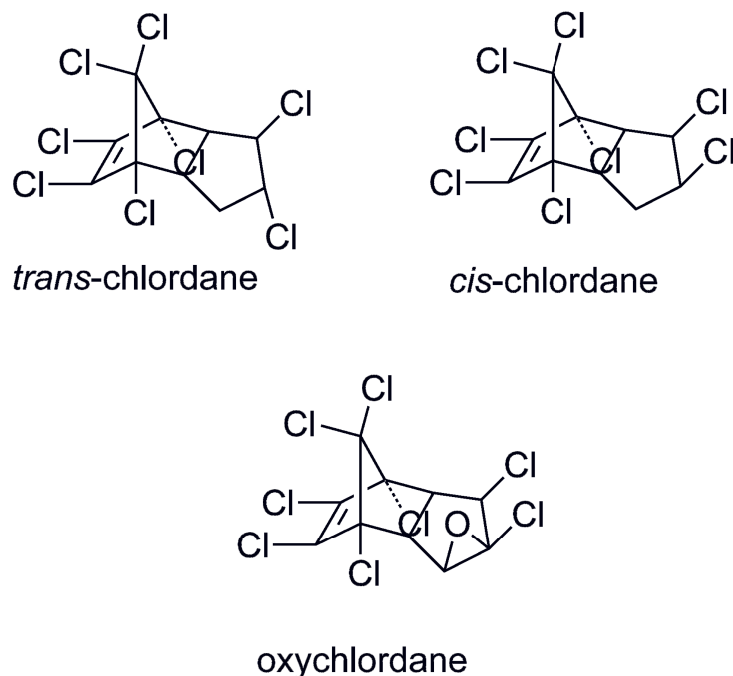
Figure 1-5: *cis- and trans-Chlordane isomers and the epoxide metabolite, oxychlordane.*

Like other hydrophobic compounds, chlordane is efficiently absorbed across the gastrointestinal or respiratory tract, with 50-75% of a single dose being absorbed by rats and mice (48). *Cis-* and *trans*-chlordane possess moderately high log K_{ow} values of 6.10 and 6.22, respectively (49), and accumulate in lipid-rich tissues of the body such as the adipose tissue and liver (48). Both *cis-* and *trans*-chlordane have also been found to biomagnify (18).

While the overall metabolic scheme of *cis-* and *trans*-chlordane is not fully elucidated, the metabolism of *cis*-chlordane appears to proceed slightly faster than *trans*-chlordane (50), although the metabolism of either isomer results

in the formation of oxychlordane (Figure 1-5) as the major metabolite (48). After rats were administered a single oral dose of a 3:1 mixture of *cis*- and *trans*-chlordane, 30-40% of the dose was recovered as oxychlordane in the tissues (50). Oxychlordane is not a terminal metabolite of chlordane, as it may undergo further metabolism (48), but it is quite resistant to any further metabolism. The half-life of oxychlordane in the fat of rats was 24 days, compared to 5.9 and 7.1 days for *cis*- and *trans*-chlordane, respectively (51). Moreover, oxychlordane is itself persistent and bioaccumulative, and continues to be widely detected in the tissues of humans (52,53) and wildlife (54,55), twenty years after the use of chlordane was banned.

The *in vivo* dechlorination of chlordane also results in the formation of heptachlor (Figure 1-6) (48), which was itself used as an agricultural insecticide. The metabolism of heptachlor (and thus of chlordane as well) results in the formation of heptachlor epoxide (56), another persistent metabolite. The half-life of heptachlor epoxide (Figure 1-6) in rats has been measured to be 15 days (51). Furthermore, the microbial degradation of *cis*- and *trans*-chlordane may also result in the formation of oxychlordane and heptachlor epoxide (57).
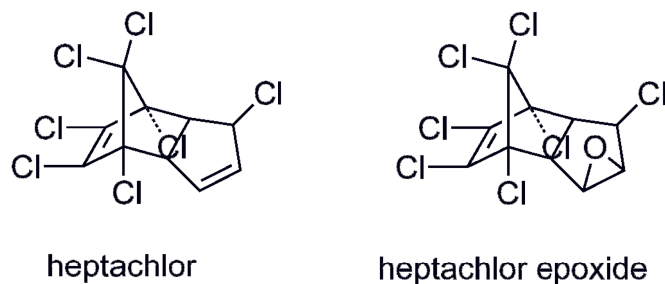
Figure 1-6: *Structures of heptachlor and heptachlor epoxide.*

A number of components of technical chlordane are chiral, but *cis-* and *trans-*chlordane, heptachlor, and their chiral oxidation products, oxychlordane and heptachlor epoxide, will be a focus of this thesis.

1.4 Enantiomer-Specific Toxicity of Chiral POPs

As mentioned previously, individual enantiomers can interact with proteins and other biomolecules with different affinities, and thus have the potential to exhibit considerably different toxic effects. The influence of chirality on the pharmacology of a compound is well established in the pharmaceutical literature (58), and while the literature on the toxicity of individual POP enantiomers is sparse, differences in the toxicity of enantiomers have been demonstrated.

Enantiomers of several chiral PCB congeners have been shown to induce drug metabolizing enzymes to different extents (59,60). Racemic PCB 88, PCB 139, and PCB 197 were shown to induce CYP 450 and benzphetamine-*N*-

demethylase (BPDM, a measure of CYP3A4 activity) activity in chick embryo hepatocytes (60). The (+) and (-) enantiomers of PCB 88 and PCB 197 showed similar potencies, but (+)-PCB 139 was a significantly more potent inducer of CYP 450 than the (-)-enantiomer. The (-)-enantiomers of PCB 88 and PCB 197 were both more potent inducers of BPDM activity than the (+)-enantiomers, but the (+)-enantiomer of PCB 139 was more potent than its antipode. Similar results were seen *in vivo* for PCB 139 and 197 (59).

Ortho-chlorinated PCB congeners have been shown to have neurotoxic effects, and these effects may be mediated through enantioselective mechanisms (61). Individual enantiomers of PCB 84 differed in their potency for increasing the translocation of protein kinase C from the cytosol to the cell membrane in the rat cerebral granular cells, although racemic PCB 84 was more effective than either enantiomer alone (61). Likewise, racemic PCB 84 was a stronger inhibitor of Ca^{2+} uptake in rat cerebral microsomes than either enantiomer, and only subtle differences were observed between (+)- and (-)-PCB 84 (61). The finding that racemic PCB 84 displayed more potency on these two measures of neurotoxicity was surprising, and may suggest that enantiomers of PCB 84 act synergistically (61).

The (-)-enantiomer of PCB 136 increased the sensitivity of ryanodine receptors (62), which are broadly expressed Ca^{2+} release channels necessary in cellular signaling and muscle contractions. They were also shown to induce the

release of accumulated Ca^{2+} in kidney microsomal vesicles by stereospecifically binding and activating ryanodine receptors (62). In addition, the lack of any activation by the (+)-enantiomer, or the fact that the (+)-enantiomer lacked any apparent competitive inhibition of this process, indicates that the 3-dimensional structure of the PCB plays a greater role in the interactions with the ryanodine receptors than the physical properties of the PCB congener (62).

Enantiomer-specific toxicity has been demonstrated for other POPs as well. For instance, (*R*)-(-)-*o,p´*-DDT was found to be a weak estrogen mimic in a yeast reporter gene system, while (*S*)-(+)-*o,p´*-DDT had negligible estrogenic effects (10). The (*R*)-(-)-*o,p´*-DDT enantiomer was similarly found to increase cell proliferation and transcription of the pS2 gene in MCF-7 human breast carcinoma cells, likely through binding to the estrogen receptor (63). In contrast to the synergistic toxicity of racemic PCB 84, the toxicity of racemic *o,p´*-DDT was in-between that of the (*R*) and (*S*) enantiomers.

1.5 Processes Altering Enantiomer Distributions

A number of review articles have recently been published that discuss, in detail, methods for the separation and detection of enantiomers in the environment (64,65), and the occurrence and fate of individual POP enantiomers (26,66). Therefore, a detailed discussion of these topics will not be addressed here. Instead, the following sections address the biological processes that may alter the

enantiomer distribution of chiral POPs in the environment.

It is appropriate to note here that enantiomer distributions in the environment are often quantified using enantiomer fractions (EF) as a metric (67). The EF is equal to the chromatographic peak area of the first eluting enantiomer (E1) divided by the sum peak areas of the first and second (E2) eluting enantiomers. However, if the optical rotation and elution order of the enantiomers are known, then the EF is equal to area of the (+)-enantiomer divided by the sum area of the (+)- and (-)-enantiomers.

1.5.1 Microorganisms

The ability for microorganisms to degrade POPs has been well established. For PCBs, anaerobic degradation proceeds through the removal of chlorine atoms, resulting in the formation of lower chlorinated congeners (68). Similar processes occur for other chlorinated POPs as well (69).

While the observation of non-racemic distributions of chiral POPs in sediment and soil would suggest enantioselective degradation by microorganisms, the ability for anaerobic microbes to preferentially degrade one enantiomer over the other was established by Pakdeesusuk et al. (70). In microcosm studies using sediment from Lake Hartwell, South Carolina, no enantioselective degradation of either PCB 132 or PCB 149 was observed, despite a decrease in concentrations. However, the degradation products of these two congeners, PCBs 91 and 95, respectively, were found in non-racemic proportions. This indicated that

enantioselective dechlorination of PCBs is congener-specific. Furthermore, no dechlorination activity was observed in autoclaved microcosms, providing unequivocal evidence for the microorganism mediated enantioselective dechlorination.

Enantioselective degradation has also been found in aerobic bacteria, supporting the finding of non-racemic distributions of chiral POPs in soil. Singer et al. (71) investigated the enantioselective biotransformation of PCBs 45, 84, 91, and 95 by two gram-negative strains and 3 gram-positive strains of bacteria. Similar to anaerobic degradation, aerobic degradation was dependent on both the congener and the strain. Furthermore, bacteria were cultured in the presence of biphenyl, (*S*)-(+)-carvone, or *p*-cymene. Differences in the co-substrate also lead to differences in the direction of enantioselectivity, even within the same strain. In contrast, however, García-Ruiz (72) found no enantioselective degradation for eight PCB congeners, including PCBs 91 and 95, in microcosms inoculated with the culture strain *Jonibacter sp*. Such differences make clear the species-specific, as well as congener-specific, differences in enantioselective microbial mediated degradation. Marine sediment microbes from the North Sea have also been shown to degrade α-HCH enantioselectively (73).

The differences between microorganism species and communities in their isomer preferences and ability to enantioselectively degrade POPs bears itself out in field studies. Reversals in the enantiomer preference between sediment microorganisms in the Hudson River (74) from those in the Housatonic River in

Connecticut (75) have been found for the degradation of PCB 91. Similarly, nine congeners (PCBs 91, 95, 136, 149, 174, 176, and 183) were found to be racemic in the sediment of the River Elsenz in Germany (76), although most of these congeners have been detected in non-racemic proportions in river sediment from various locations throughout the United States (75).

Differences in enantioselectivity not only vary from site to site, but may also vary substantially within a single location. Sediment cores from Lake Hartwell, SC, had substantial differences in enantiomer distributions depending on depth, often times with complete reversals of enantiomer preferences (77). These differences were attributed to differences in the microbial communities at varying depths.

While the influence of many environmental factors, including pH, organic carbon content, and temperature, as well as the presence of other co-contaminants, have yet to be thoroughly examined (26), it is clear that variations in microbial communities can have profound effects on the enantiomer enrichment of chiral POPs in the environment.

1.5.2 Biota

In vivo processes may result in the alteration of the observed enantiomer profile, including absorption from the gastrointestinal tract, distribution and disposition processes, metabolism, and excretion. Investigations into the enrichment of PCB enantiomers have received the most attention in the literature,

22

although several studies have investigated the enantiomer enrichment of other POPs in laboratory experiments.

1.5.2.1 Pharmacokinetics

In perhaps the most comprehensive study on chiral POP pharmacokinetics to date, Kania-Korwel et al. investigated the enantioselective clearance, accumulation, and blood elimination half-lives of seven chiral PCB congeners in female mice (78). An increased maximum concentration (C_{max}) of the second-eluting enantiomer of PCBs 91, 95, 149 and 176 over that of the first-eluting enantiomer was generally found in all tissues examined, except for the brain. Moreover, terminal phase blood half-lives were significantly longer for E1-PCB 95, (-)-PCB 132, and (-)-PCB 136 than their antipodes. With the exception of PCB 174, terminal phase blood half-lives of all other congeners were different than their antipode, albeit not statistically significantly. Finally, the bioavailability normalized clearance (CL/F), a descriptor of the volume of blood which is cleared of xenobiotic per unit time, was significantly greater for the first eluting enantiomer of all congeners. The differences in kinetic parameters between individual enantiomers lead to a greater accumulation of the second-eluting enantiomer of all congeners except PCB 136 and PCB 174.

The enantioselective handling of chiral POPs has been investigated in other species as well. Rats exposed to oxychlordane, *cis*-chlordane, and *trans*-

chlordane for 28 days showed a significant enrichment in the (-) enantiomer of all three compounds over the 56 days following termination of dosing (79). Likewise, rainbow trout (*Oncorhynchus mykiss*) significantly enriched individual enantiomers of *trans*-chlordane and PCBs 91 and 136 in the 200 days following removal of an exposure source (80, 81). An enrichment of (+)-α-HCH was found in the blood and tissues of mice administered a single dose of racemic α-HCH. These studies shed light on the differences in pharmacokinetic parameters between enantiomers, and makes clear that the biological handling differs between individual enantiomers. However, the mechanism by which such non-racemic distributions of enantiomers arise is currently unclear.

1.5.2.2 Absorption

The absorption of PCBs through the walls of the intestinal lumen occurs rapidly by passive diffusion. Given the passive nature of uptake, it would be expected that no enantioselectivity would be observed. This is indeed the case in carp exposed to technical chlordane via water for 3 days. No enantioselectivity was observed during the uptake phase, although enrichment of individual enantiomers of *cis*- and *trans*-chlordane was observed during depuration (82). In mice, enantioselective uptake was suggested based on differences in C_{max} values between enantiomers for several PCB congeners (78). However, examination of feces of mice given a single gavage dose of PCB 136 revealed racemic EFs immediately post-dose, due to the excretion of unabsorbed racemic PCB 136 (83),

providing evidence that the absorption of chiral PCBs (and by extension other passively absorbed chiral POPs) occurs with no enantiomeric bias.

1.5.2.3 Distribution

Clear differences in the tissue distribution of individual enantiomers of several chiral OCs have been noted in wildlife. For instance, in bowhead whales, the enantiomer fractions of PCBs 91, 135, and 149, as well as *cis-* and *trans-* chlordane, were significantly higher in the blubber than in the liver (84,85). The most extreme examples, however, have been found for α-HCH in brain tissues. Double crested cormorants (86), harbor seals (87,88), and fur seals (89) were all found to have a large excess of (+)-α-HCH in brain tissues. In neonatal fur seals, an EF of 0.97 was detected for α-HCH in the brain (88).

The differences in tissue distribution observed in wildlife have been confirmed in laboratory experiments. Kania-Korwel et al. (90) investigated the tissue distribution of individual enantiomers of PCBs 95 and 149, and found significant differences between storage tissues (liver, skin, adipose tissue) and most non-storage tissues (i.e., blood). Furthermore, EFs of *trans*-chlordane were significantly different in rats between abdominal fat and the liver (79). Differences in tissue distribution varied depending on the route of administration, with the greatest enrichment of (+)-PCB 136 being found in the brain tissues of mice given a single intraperitoneal (i.p.) injection of PCB 136, while the liver was the most enriched in (+)-PCB 136 when mice were administered PCB 136 orally

(91).

Despite these studies, no mechanism of enantiomer enrichment could be deduced. Evidence that the initial distribution of PCBs to the tissues is an enantioselective process was presented by Lehmler et al. (92), who found rats that had received an i.p injection of racemic PCB 84 showed an enrichment of the (+)-enantiomer after three and six days in all tissues, except the spleen. After six days, there was no statistical difference in the enantiomer distribution between the various tissues. Additionally, there was no time dependent enrichment of the (+)-enantiomer observed. Likewise, a similar enrichment in (+)-PCB 136 was found in mice administered a single i.p injection of PCB 136, with no significant change in the EF of individual tissues between 3 and 6 days (91). The lack of enantiomer enrichment with time suggests that the enrichment is a result of the initial distribution process, as it is unlikely that the selective binding of (+)-PCB 84 or (+)-PCB 136 is the same in all tissues, and enantioselective metabolism or enantioselective redistribution would have resulted in a time dependent enrichment of one of the enantiomers (92). However, time dependent changes in the EF were observed in other species for PCB 136 (81), and for other compounds (79). These differences may indicate considerable species- and compound-specific mechanisms for enantiomer enrichment. Conversely, it may be that the initial distribution process does occur enantioselectively, but 6 days may not be enough time to fully observe other enantioselective processes that may occur.

The enantioselective uptake of α-HCH in the brain has been investigated

in detail. In rats administered a subcutaneous injection of racemic α-HCH, EFs in the brain exceeded 0.9 within 24 hours of exposure (93). Likewise, mice and quail administered α-HCH orally both enriched (+)-α-HCH in brain tissues (94). In mice, this enrichment was opposite to what was observed in other tissues, where (-)-α-HCH was preferentially enriched. Investigations into the mechanisms of enrichment showed that α-HCH was not enantioselectively metabolized *in vitro* by brain tissue slices or nerve cell cultures *in vivo*. This led to the conclusion that the enrichment of (+)-α-HCH was due to enantioselective transport across the blood-brain barrier (93,94). As (+)-α-HCH is generally found enriched in the brain in biota, the selectivity of the blood-brain barrier towards (+)-α-HCH appears to be conserved among species.

1.5.3 Metabolic Processes

1.5.3.1 In Vitro

The oxidation of PCBs and other OCs is catalyzed by mixed function oxidases (MFOs), namely CYP enzymes. Buser and Müeller (95) were the first to investigate the hypothesis that enantioselectivity in the metabolism of OCs by MFOs results in the enrichment of enantiomers observed *in vivo*. Using rat liver microsomes, it was found that the degradation of heptachlor results in a depletion of the (+)-enantiomer, resulting in an EF of 0.26. This was coupled with the formation of (+)-heptachlor epoxide in highly non-racemic proportions (EF=0.78), yielding strong evidence for the role of MFOs in the enantiomer

enrichment in wildlife.

The enantioselective metabolism of 8 chiral PCB congeners was investigated *in vitro* using purified rat CYP 2B1 and human CYP 2B6 by Warner et al. (96). PCBs 45, 84, 91, 95, 132, and 136 were significantly enriched after 50-minute incubations, while PCBs 149 and 183 remained racemic throughout. Oxidative metabolism was confirmed by the detection of OH-PCBs 45, 91, 95, and 132.

Furthermore, differences in the binding efficiency of individual enantiomers to CYP enzymes have been noted. A higher binding efficiency, as deduced from an increase in difference between the UV spectral maxima and minima, was found for (+)-PCB 136 (97). Using antibodies to inhibit the binding of PCB 136 to different subfamilies, PCB 136 bound most strongly to CYP 2B isozymes. The stronger binding of (+)-PCB 136 to CYP 2B enzymes, implies preferential metabolism of the (+)-enantiomer, contrasting the observation of an enrichment of (+)-PCB 136 *in vivo* (83,90,91,98,99). The authors therefore suggest that the enrichment of (+)-PCB 136 observed *in vivo* is due to the hepatic sequestration of the (+)-enantiomer and the elimination or metabolism of the (-)-enantiomer (97). These results appear to contrast the results obtained by Warner et al. (96), who found that (+)-PCB 136 was preferentially metabolized when incubated with rat CYP 2B1 enzymes. However, Warner et al. only investigated the metabolism of a single enzyme, while multiple other CYP 2B isozymes are present in microsomes and may interact with PCB 136 differently than CYP

2B1.

While the results of Warner et al. (96) and Buser and Müller (95) provide unequivocal evidence for the role of MFOs and metabolism as a significant driver of enantiomer enrichment in biota, other *in vivo* process may still play a role, and the situation becomes further complicated when whole organisms are investigated.

1.5.3.2 In Vivo

Despite evidence from *in vitro* studies, the role of MFOs in the enrichment of individual enantiomers *in vivo* still remains unclear. PCBs and chlordane induce the enzymes responsible for their own metabolism. However, *in vivo*, the induction of MFOs does not appear to alter the enantiomeric enrichment. For instance, a significant dose-dependent enrichment of PCB 136 was found in female mice (99). However, at higher concentrations of PCBs (which would presumably induce CYP 2B isozymes) significantly less enantiomer enrichment of PCB 136 was observed (99). The decrease in enrichment was attributed to the saturation of the enzymes or protein systems responsible for the enantiomer enrichment. The lack of effect of enzyme induction on enantiomer enrichment was further examined in mice pretreated with β-naphthoflavone, phenobarbital, or dexamethasone in order to induce CYP 1A, CYP 2B, or CYP 3A, respectively (100). Three days after receiving a single oral dose of PCB 136 (50 mg/kg b.w.) the EF of PCB 136 was similar amongst treatment groups, despite significant

differences in PCB 136 concentrations amongst the groups. It should be noted, however, that these results should only be interpreted in regards to PCBs, and caution should be made in extrapolating to other chiral compounds. No studies have specifically tested the influence of enzyme induction on the enantioselective pharmacokinetics of other POPs.

In vivo, the pharmacokinetics of chiral compounds is further influenced by exposure to co-contaminants, or their presence within the organism. In rats exposed to extracts of soil contaminated with Chlorofen, a technical mixture of PCBs used predominantly in Europe, EFs of PCBs 95 and 149 deviated less from racemic than did EFs of these two congeners in rats exposed to Aroclor 1254 (90). The two mixtures employed in this study contained different PCB congeners, suggesting that differences in the congener profiles and relative concentrations of individual congeners may have played a role in altering the enantiomer profiles of PCBs 95 and 149. Such a finding was also suggested in vitro for PCB 132, which was enantioselectively metabolized when incubated alone with purified human CYP 2B6, but not when PCB 132 was incubated together with the other seven congeners (96). This implies that competition for the enzyme active site occurred when CYP 450s were incubated with multiple congeners (96).

1.5.3.3 Metabolite Formation

The metabolism of several chiral compounds results in the formation of

stable metabolites, which are themselves chiral and detected at high concentrations in the environment. Heptachlor epoxide and oxychlordane, metabolites of heptachlor and *cis*- and *trans*-chlordane, respectively, have been found in non-racemic proportions in a variety of species, including fish (84), whales (84), seals (101), polar bears (18), and birds (102). The detection of non-racemic metabolites may imply formation from the enantioselective metabolism of parent compounds; however, non-racemic distributions may also arise from the non-enantioselective metabolism of the parent compound followed by enantioselective elimination of the metabolite. Warner et al. (103) demonstrated the enantioselective formation of oxychlordane in the freshwater invertebrate *Mysis relicta*. Mysids, exposed to a suite of OC contaminants, preferentially eliminated (+)-*trans*-chlordane, with a concomitant increase in (+)-oxychlordane. Similarly, in male and female rats administered *trans*-chlordane orally for 28 days, an enrichment of the (-)-enantiomer was observed (79). This observation was coupled with the finding of an enrichment of (-)-oxychlordane in the tissues of rats. Female rats from this study were initially enriched in (+)-oxychlordane, but 28 days after the last dose of *trans*-chlordane, an enrichment of (-)-oxychlordane was observed. The initial finding of an enrichment of (+)-oxychlordane strongly suggests that enantioselective metabolism of *trans*-chlordane occurred, while the continued further enrichment of (+)-oxychlordane over time suggests that (-)-oxychlordane is preferentially eliminated.

In male and female Sprague-Dawley rats, non-racemic distributions of

several hydroxylated metabolites of PCB 136 were found, demonstrating that the formation of OH-PCBs can occur enantioselectively (39). OH-PCBs are strongly retained in the blood of biota due to protein binding, and are formed *in vitro* from chiral PCBs congeners (96).

Upon administration of PCB 132, a strong enrichment of (R)-4-MeSO$_2$-PCB 132 and (R)-5-MeSO$_2$-PCB 132, with EFs of 1.0 and 0.95, respectively, was observed, while the parent compound, PCB 132, was non-racemic (EF=0.2) (45). In the same study, rats administered enantiopure standards of E1-PCB 132 only formed (R)-4-MeSO$_2$-PCB 132 and (R)-5-MeSO$_2$-PCB 132. Similarly, only the (S)-MeSO$_2$-PCB 132 enantiomers were observed after administration of E2-PCB 132. These results suggest that the metabolism of E1-PCB 132 is responsible for the enrichment of (R)-MeSO$_2$ enantiomers of PCB 132. However, *in vitro* studies have shown the enantioselective degradation of MeSO$_2$-PCB 149 when ($\pm$)-MeSO$_2$-PCB 149 was incubated with rat hepatocytes (104). While this finding does not preclude the enantioselective formation of MeSO$_2$-PCB 149, it does demonstrate that the non-racemic distributions of PCB MeSO$_2$ metabolites do not arise solely from enantioselective formation.

1.5.4 Excretion

Only a few studies to date have investigated the possibility of enantioselective excretion, and it has generally been found that the excretion of chiral POPs occurs non-enantioselectively. In rats administered PCB 136, non-racemic distributions were found in the feces; however, the enantiomer distribution was similar to that observed in the liver (83,99,100). Likewise, the enantiomer distribution of $MeSO_2$-PCB 136 in feces was comparable to various tissues, thus providing no evidence for enantioselective excretion (45).

1.5.5 Maternal Transfer

Females are able to transfer significant proportions of their contaminant body burdens to their offspring, providing another route of elimination. Few studies have investigated the enantioselectivity of this phenomenon. Similar EFs were found between neonatal fur seals, stillborn fur seal pups, and female fur seal milk (89), implicating non-enantioselective transfer. Lack of enantioselective maternal transfer has also been noted in avian species and their eggs. While non-racemic EFs have been found in bird eggs, glaucous gulls transfered their body burden of OC contaminants to their eggs in a non-enantioselective manner (Chapter 4 of this thesis). Given the sensitivity of the fetus to environmental contamination, an understanding of the exposure to individual enantiomers of POPs is warranted.

Due to the lipophilicity of most POPs, unmetabolized compounds can

partition into other high lipid and high volume compartments, such as milk, providing another route of elimination (105). Racemic and non-racemic ratios of the parent PCB compounds have been found in human and wildlife milk samples (106). PCB 149 was racemic in these human milk samples, but both PCB 95 and PCB 132 were slightly non-racemic (107,108). No paired milk-tissue comparisons have been made; therefore, it is difficult to ascertain the enantioselectivity of this process. However, the milk of fur seals was found to be similar to that of fat and liver tissues, implying that the lactational transfer of OCs occurs non-enantioselectively (106).

1.5.6 Other Complicating Factors

Many other factors have been demonstrated, either directly or correlatively, to influence enantiomer distributions. For instance, enantiomer distributions of *cis*-chlordane and MC5 (a chiral octachlordane) were significantly more enriched in grey seals suffering from poor nutritional status (109). This is explained by a decline in nutritive intake, leading to the mobilization of fat reserves for energy and the subsequent release of stored OC pollutants back into the blood stream where they are subject to metabolism in various organs (109).

Significant sex differences have also been found to play a role in the enantioselective disposition and elimination of chiral POPs. After receiving a *trans*-chlordane dose daily by oral gavage for 28 days, female rats were enriched

in (+)-oxychlordane, while males were enriched in the antipode (79). Similar results were found after analogous dosing with *trans*-nonachlor, which is dechlorinated *in vivo* to *trans*-chlordane. During the 56-day depuration phase, both males and females eliminated (+)-oxychlordane, but at different rates. Sex differences have also been noted to occur in wild cod (*Gadus morhua*), with males and females enriching opposing enantiomers of *trans*-chlordane (110). It is unclear why such sex differences exist, although differences in the induction of CYP subfamilies differs between male and female rats (111), and such differences may play a role in the differences in EFs observed between sexes (79). Differences in EFs between sexes have yet to be reported for PCBs, possibly due to the lack of effect that enzyme induction has on altering the enantiomer profile.

Differences among individuals of the same species in biological handling of chiral compounds also exist. Significant differences in the elimination of *o,p'*-DDD were found in Göttingen minipig, with EFs ranging from 0.2 to 0.7 in adipose tissue (112). This demonstrates that even amongst individuals of the same species, antipodes of a single compound can be preferentially enriched (112). Such differences were attributed to differences in genetic polymorphisms amongst individuals.

Perhaps the most complicating factor to interpreting enantiomer distributions in biota is the significant inter-species differences in biotransformation of chiral OCs. Such differences were noted to occur in wildlife, and only recently have laboratory based studies confirmed this. As

discussed earlier, rats given a single oral dose of racemic α-HCH enriched the (+)-enantiomer, while an enrichment of (-)-α-HCH was found in quail. This unequivocally demonstrates that species-specific differences exist, not only in the magnitude of enrichment, but also in the direction of enantiomer enrichment. Furthermore, such differences exist even amongst closely related species. Rainbow trout and Arctic char, both members of the *salmonidae* family, were found to similarly enrich (+)-PCB 149 and eliminate PCBs 95 and PCB 174 non-enantioselectively (80,82,113). However, an inversion of the EF of PCB 136 and *trans*-chlordane was found between these two species.

It is clear that differences in the biological handling between enantiomers results in an enrichment of one enantiomer over the other in organisms. Evidence suggests that this is a result of enantioselective metabolism by MFOs, although other processes, such as enantioselective distribution or selective sequestration of one enantiomer, cannot yet be ruled out. Furthermore, significant complications in the interpretation of EFs arise due to the considerable impacts that other factors such as sex, nutritional status, age, and inter-individual variability may have on the enrichment of individual enantiomers.

1.6 Overview of Perfluorooctane Sulfonate and its Precursors

Perfluorinated compounds (PFCs) are another class of pervasive environmental contaminants investigated in this thesis. The most ubiquitous PFC

is perfluorooctane sulfonate ($C_8F_{17}SO_3^-$; PFOS; Figure 1-7). PFOS is detected at high concentrations in the blood and tissues of wildlife from remote regions of the world (114,115), and in the blood of humans globally (116-118). Furthermore, PFOS persists in the environment and bioaccumulates in biota (119). What follows is a brief review, as it relates to this thesis, of the environmental fate of PFOS isomers and a discussion of the role PFOS precursors play in contributing to environmental levels of PFOS.
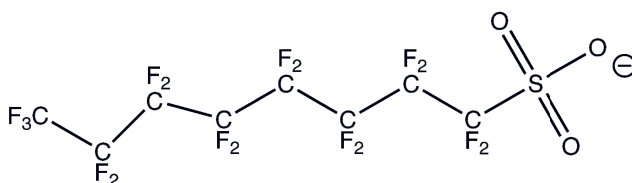
Figure 1-7: *Structure of linear perfluorooctane sulfonate (PFOS).*

Despite the ubiquity and high concentrations of PFOS detected in the environment, PFOS itself had relatively minor commercial use, with its primary use being in aqueous firefighting foams (120). The predominant globally manufactured PFC was perfluorooctane sulfonylfluoride ($C_8F_{17}SO_2F$; PFOSF) (120), which is used as the main synthetic precursor to PFOS and related sulfonamides. In contrast to the other contaminants discussed thus far, all of which were banned from widespread use in North America in the late 1970s, the bulk of PFOSF manufacturing did not begin until 1975. Large volume manufacturing and use continued until 2001, when PFOSF based chemicals were

voluntarily phased out by the primary manufacturer, the 3M Co., due to the widespread detection of PFOS in the environment (115) and humans (121).

The manufacture of PFOSF occurred by electrochemical fluorination (ECF), a crude synthetic process in which an electrical current is applied to a mixture of linear octane sulfonylfluoride and hydrogen fluoride (122). The process caused perfluorination of the hydrocarbons, but also carbon-carbon bond breakages and a rearrangement of the carbon backbone. This resulted in a mixture of branched and linear PFOSF isomers (Figure 1-8), as well as longer and shorter chain impurities (122). PFOSF was further derivatized through its sulfonyl moiety to form a series of alkyl, acrylate, or phosphate perfluorooctane sulfonamides (122). It was these derivatives that found the most extensive commercial use, due to their chemical stabilities and effective surfactant properties. Such uses include stain repellants for carpets, furniture, and clothing, oil repellent coatings for food packaging, ink additives, cleaning products, and even as insecticides (122). Technical mixtures of PFOS are composed of approximately 30% branched isomers and 70% linear isomers. Although little is known about the isomer composition of PFOSF or derivatives, it is expected that the isomer pattern of PFOS precursors is similar to that of technical PFOS.
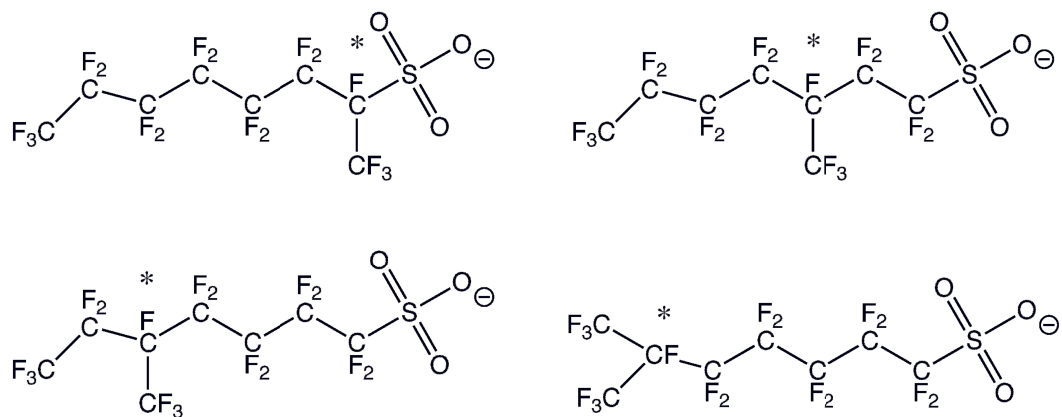
Figure 1-8: *Structures of branched PFOS isomers. Asterisk indicates location of branching.*

Little information is available about the isomer-specific fate of PFOS and PFOS precursors in the environment, although a thorough review was recently published (123). Data on the branched isomer composition of PFOS in abiotic environmental samples are limited, but were in the range of 43-56% linear PFOS in Lake Ontario water, and from 81-89% linear PFOS in Lake Ontario sediment (124). It was suggested that the increased proportion of branched isomers observed in Lake Ontario water might be due to preferential adsorption of the linear isomer to sediment. Similarly, branched isomers were enriched in water from the Atlantic Ocean and Mississippi River (125). Limited information is available on the abiotic fractionation of PFOS isomers in the environment, although there is evidence to suggest that there are differences between isomers in some physical properties, such as water solubility (126) and hydrophobicity (127), which may lead to differences in their environmental fate.

Biological processing of PFOS also influences the isomer composition. Rats administered technical PFOS preferentially eliminated branched isomers more quickly than the linear (128,129), with similar results in rainbow trout (130). These results largely corroborate wildlife studies, with the majority of studies reporting depletion of the branched isomers and an enrichment of the linear isomer (124,131-134); however, there are some exceptions reported (133,134). On the other hand, an enrichment of branched PFOS isomers (i.e., >30% branched) is found in humans (135,136). Pooled serum samples from the United States contained 29 to 41% branched isomers (135), while the percentage of branched isomers in archived serum samples from Norway ranged from 22% to 47%, with the percentage of branched isomers becoming greater in recent years (136). Given the known rat pharmacokinetics of PFOS isomers (i.e., more rapid elimination of branched isomers compared to the linear), the finding of enriched proportions of branched isomers in humans is intriguing. Assuming similar isomer-specific pharmacokinetics in humans, such enrichment is theoretically impossible if exposure is only to PFOS.

One possible explanation for this enrichment in humans is by exposure to PFOS precursor compounds. Derivatives of PFOSF are considered to be PFOS precursors (Figure 1-9), because they may degrade to PFOS through abiotic environmental degradation pathways or biological degradation. The biotic and abiotic transformation of PFOS precursors to PFOS was recently reviewed (137), and will therefore not be covered here in detail .
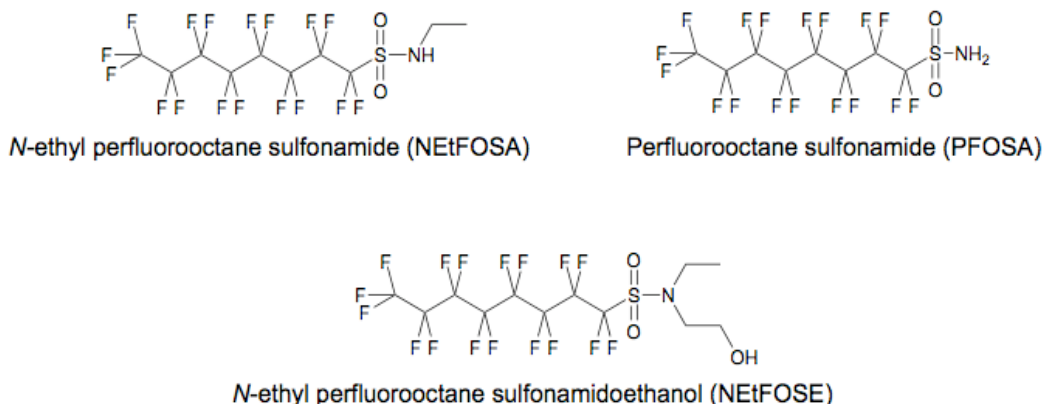
Figure 1-9: *Structures of representative PFOS precursor compounds.*

An important point, however, is that abiotic degradation of PFOS precursors to PFOS is not conclusive in the environment, although the degradation of larger PFOS precursors (i.e., acrylate and phosphate polymers) to smaller precursors has been demonstrated (137). In contrast, the efficient biological transformation of PFOS precursors to PFOS is likely a significant environmental fate process. *In vitro*, Xu et al. (138) elucidated the pathways of *N*-ethyl perfluorooctane sulfonamidoethanol ($C_8F_{17}SO_2NH(C_2H_5)$; NEtFOSE) metabolism in human and rat liver slices, microsomes, and isolated CYP isozymes. The primary metabolite formed in all three systems was perfluorooctane sulfonamide ($C_8F_{17}SO_2NH_2$; PFOSA). However, Xu et al. (138) were able to detect the formation of PFOS from PFOSA in rat liver slices only (i.e., no PFOS was formed in hepatocytes or microsomes), but even in liver slices the biotransformation rate was very slow. Benskin et al. (139) were also unable to

detected PFOS in their microsomal studies of NEtFOSA. Only a single study (140) has reported the formation of PFOS from a PFOS precursors in microsomal preparations, although trout liver microsomes were used in this work. Thus, certain fish species may have an increased capacity to biotransform PFOS-precursors to PFOS, relative to humans and rats.

Despite inconsistent findings *in vitro*, the metabolism of PFOS precursors to PFOS has been confirmed *in vivo*, and the extent of biotransformation is quite high. Several studies have investigated the *in vivo* metabolism of NEtFOSE. After receiving a dose of 5 mg/kg for 21 days by gastric intubation, rats metabolized approximately 9.5% of the total dose to PFOS, with all the other metabolites accounting for only 1.1% (141). In a separate study, Seacat et al. reported that 20% of an oral dose of NEtFOSE was converted to PFOS in rats (142). In rats given an oral dose (5 mg/kg by gavage) of PFOSA, 32% the dose was recovered as PFOS in the serum and liver 4 days after dosing (143). Other body tissues were not analyzed, but the total yield of PFOS must therefore have been considerably higher than 32%.

While it is clear that PFOS precursors may contribute to the overall PFOS body burden in animals or humans, the relative contribution of precursors is unclear. Exposure models have been used to estimate the importance of precursors to PFOS body burdens, using percentage yields of PFOS precursor to PFOS of 20% (144,145). With the exception of a "highly exposed" group, these studies concluded that the relative contribution of precursors was minor (e.g., <10%)

(144,145).

The use of PFOS isomer signatures as a way of qualitatively or quantitatively assessing the relative contribution of precursor compounds has been suggested (137), as has the use of isomer patterns of PFOS as means to track environmental fate processes of PFOS (123). To date, however, no studies have attempted to use PFOS isomer profiles to apportion PFOS sources, likely due to a lack of knowledge on the environmental behavior and fate of PFOS precursors. However, the technique does hold promise, as isomer profiles in human serum differ amongst countries, with serum and plasma samples from the UK and Australia having a significantly greater proportion of branched isomers than serum samples from Sweden (146), for example. Furthermore, site-specific differences in the PFOS isomeric composition amongst herring gull eggs in the Great Lakes region has also been reported (132). Such differences may be suggestive of different exposure sources, although a number of other factors, such as individual differences in pharmacokinetics, may also play a role in affecting PFOS isomer profiles.

Despite the phase-out of PFOSF based manufacturing by the 3M Co., it is expected that exposure to PFOS and PFOSF based chemicals will continue. This is due to the on-going production of PFOSF based chemicals in China and the presence of PFOSF based chemicals in pre-2001 consumer products, which may still be in use today. It is therefore imperative to continue to gain knowledge of the fate of individual PFOS isomers, as well as an understanding of human and

43

wildlife exposure pathways.

1.7 Thesis Outline

This thesis presents five original studies that aim to answer several of the questions presented in this introduction.

Chapter 2 describes the analytical method development of a novel anion attachment atmospheric pressure photoionization (AA-APPI) mass spectrometry method. AA-APPI has been suggested as a means of expanding the range of compounds that may be analyzed by LC-MS, and has been found to enhance the ionization of some macromolecules (e.g., peptides, polymers) that were unable to be ionized by other techniques. In this study, AA-APPI was compared to APPI, using hexabromocyclododecane enantiomers as a model compound, to provide proof of principle of the use of AA-APPI for small molecule analysis.

Chapter 3 investigates the potential for enantioselective biotransformation and bioaccumulation of seven PCB atropisomers in the sediment and biota from a sub-tropical estuary heavily contaminated with Aroclor 1268, a technical mixture of highly chlorinated PCB congeners. Enantiomer fractions of PCBs 91, 95, 136, 149, 174, 176, and 183 in marsh sediment, invertebrate, forage and predatory fish species, and bottlenose dolphins were determined.

In Chapter 4 the enantiomer distribution of chiral chlordanes and atropisomeric PCB congeners were determined in the blood plasma of adult male

and female glaucous gulls from three breeding colonies in the Norwegian Arctic to determine the influence of maternal transfer process on the fate of individual enantiomers in avian species.

Chapter 5 compares the enantiomer-specific biotransformation and bioaccumulation dynamics of legacy organochlorine compounds, including PCB, α-HCH, and chlordane compounds, between free-ranging polar bears (*Ursus maritimus*) and captive West Greenland sledge dogs (*Canis familiaris*), a species serving as an ecotoxicological surrogate for polar bears.

Chapter 6 investigates the isomer-specific fate of perfluorooctane sulfonamide, a known PFOS-precursor, and the subsequent isomer-specific formation of PFOS in male Sprague-Dawley rats to test the hypothesis that exposure to precursor compounds (e.g., PFOSA) will lead to differences in the isomer profile of PFOS relative to the parent material.

Finally, Chapter 7 presents the overall conclusions of this thesis, and puts forth recommendations for future work in the area of isomer and enantiomer-specific environmental fate of POPs.

1.8 References

(1)   Toxicological Profile for Chlordane. Agency for Toxic Substances and Disease Registry, Atlanta, GA, 1994.

(2)   Goel, A., McConnell, L.L., Torrents, A., Kuang, Z.H., Hapeman, C.J.,

Meritt, D.W., Alexander, S.T., Scudlark, J.R., Scarborough, R., Environmental Factors Affecting the Levels of Legacy Pesticides in the Airshed of Delaware and Chesapeake Bays, USA. Environmental Toxicology and Chemistry, 29 (2010) 1893-1906.

(3)   Letcher, R.J., Gebbink, W.A., Sonne, C., Born, E.W., McKinney, M.A., Dietz, R., Bioaccumulation and biotransformation of brominated and chlorinated contaminants and their metabolites in ringed seals (Pusa hispida) and polar bears (Ursus maritimus) from East Greenland. Environment International, 35 (2009) 1118- 1124.

(4)   de Wit, C.A., Fisk, A.T., Hobbs, K.E., Muir, D.C.G., Gabrielsen, G.W., Kallenborn, R., Krahn, M.N., Norstrom, R.J., Skaare, J.U., AMAP Assessment 2002: Persistent organic pollutants in the Arctic, Arctic Monitoring and Assessment Programme, Oslo, Norway, 2004.

(5)   What are POPs? From the Stockholm Convention on Persistent Organic Pollutants,   http://chm.pops.int/Convention/The%20POPs/tabid/673/language/en-US/Default.aspx. Accessed January 24, 2011.

(6)   Diamond, M., Harrad, S.J., in Harrad, S.J. (Editor), Persistent Organic Pollutants, Blackwell Publishing Ltd., 2010, p. 241-270.

(7)   Beard, J., DDT and human health. Science of the Total Environment, 355 (2006) 78-89.

(8)   Zumdahl, S.S., Zumdahl, S.A., Chemistry, 5th Ed., Houghton Miflin

Company, Boston, MA, 2000.

(9)   Toxicological Profile of Hexachlorocyclohexane.   Agency for Toxic Substances and Disease Registry, Atlanta, GA, 2005.

(10)   Hoekstra, P.F., Burnison, B.K., Neheli, T., Muir, D.C.G., Enantiomer-specific activity of *o,p*'-DDT with the human estrogen receptor. Toxicology Letters, 125 (2001) 75-81.

(11)   Stanley, J.K., Brooks, B.W., Perspectives on ecological risk assessment of chiral compounds. Integrated Environmental Assessment and Management, 5 (2009) 364-373.

(12)   Warner, N.A., Norstrom, R.J., Wong, C.S., Fisk, A.T., Enantiomeric fractions of chiral polychlorinated biphenyls provide insights on biotransformation capacity of Arctic biota. Environmental Toxicology and Chemistry, 24 (2005) 2763-2767.

(13)   Bidleman, T.F., Harner, T., Wiberg, K., Wideman, J.L., Brice, K., Su, K., Falconer, R.L., Aigner, E.J., Leone, A.D., Ridal, J.J., Kerman, B., Finizio, A., Alegria, H., Parkhurst, W.J., Szeto, S.Y., Chiral pesticides as tracers of air-surface exchange. Environmental Pollution, 102 (1998) 43-49.

(14)   Asher, B.J., Wong, C.S., Rodenburg, L.A., Chiral source apportionment of polychlorinated biphenyls to the Hudson River Estuary atmosphere and food web. Environmental Science & Technology, 41 (2007) 6163-6169.

(15)   Willett, K.L., Ulrich, E.M., Hites, R.A., Differential toxicity and

environmental fates of hexachlorocyclohexane isomers. Environmental Science & Technology, 32 (1998) 2197-2207.

(16)   Kutz, F.W., Wood, P.H., Bottimore, D.P., Organochlorine pesticides and polychlorinated-biphenyls in human adipose-tissue. Reviews of Environmental Contamination and Toxicology, 120 (1991) 1-82.

(17)   Albro, P.W., Thomas, R., Intestinal-absorption of hexachlorobenzene and hexachlorocyclohexane isomers in rats. Bulletin of Environmental Contamination and Toxicology, 12 (1974) 289-294.

(18)   Wiberg, K., Letcher, R.J., Sandau, C.D., Norstrom, R.J., Tysklind, M., Bidleman, T.F., The enantioselective bioaccumulation of chiral chlordane and alpha-HCH contaminants in the polar bear food chain. Environmental Science & Technology, 34 (2000) 2668-2674.

(19)   Faller, J., Huhnerfuss, H., Konig, W.A., Ludwig, P., Gas-chromatographic separation of the enantiomers of marine organic pollutants - distribution of alpha-HCH enantiomers in the North-Sea. Marine Pollution Bulletin, 22 (1991) 82-86.

(20)   Faller, J., Huhnerfuss, H., Konig, W.A., Krebber, R., Ludwig, P., Do marine bacteria degrade alpha-hexachlorocyclohexane stereoselectively. Environmental Science & Technology, 25 (1991) 676-678.

(21)   Jantunen, L.M., Helm, P.A., Ridal, J.J., Bidleman, T.F., Air-water gas exchange of chiral and achiral organochlorine pesticides in the Great Lakes. Atmospheric Environment, 42 (2008) 8533-8542.

(22)   Wang, W., Li, X.H., Wang, X.F., Wang, X.Z., Lu, H., Jiang, X.N., Xu, X.B., Levels and chiral signatures of organochlorine pesticides in urban soils of Yinchuan, China. Bulletin of Environmental Contamination and Toxicology, 82 (2009) 505-509.

(23)   Jantunen, L.M.M., Bidleman, T.F., Organochlorine pesticides and enantiomers of chiral pesticides in Arctic Ocean water. Archives of Environmental Contamination and Toxicology, 35 (1998) 218-228.

(24)   Moisey, J., Fisk, A.T., Hobson, K.A., Norstrom, R.J., Hexachlorocyclohexane (HCH) isomers and chiral signatures of alpha-HCH in the Arctic marine food web of the Northwater Polynya. Environmental Science & Technology, 35 (2001) 1920-1927.

(25)   Tanabe, S., Kumaran, P., Iwata, H., Tatsukawa, R., Miyazaki, N., Enantiomeric ratios of alpha-hexachlorocyclohexane in blubber of small cetaceans. Marine Pollution Bulletin, 32 (1996) 27-31.

(26)   Wong, C.S., Warner, N.A., in Harrad, S.J. (Editor), Persistent Organic Pollutants, Blackwell Publishing Ltd., 2010, p. 71-136.

(27)   Ballschmiter, K., Zell, M., Analysis of polychlorinated-biphenyls (PCB) by glass-capillary gas-chromatography - composition of technical Aroclor-PCB and Clophen-PCB mixtures. Fresenius Zeitschrift Fur Analytische Chemie, 302 (1980) 20-31.

(28)   Erickson, M., in Robertson, L., Hansen, L.G. (Editors), PCBs: Recent

advances in environmental toxicology and health effects, The University of Kentucky Press, Lexington, KY, 2001, p. xi-xxx.

(29)   Kaiser, K.L.E., Optical-activity of polychlorinated biphenyls. Environmental Pollution, 7 (1974) 93-101.

(30)   Harju, M.T., Haglund, P., Determination of the rotational energy barriers of atropisomeric polychlorinated biphenyls. Fresenius Journal of Analytical Chemistry, 364 (1999) 219-223.

(31)   Schurig, V., Reich, S., Determination of the rotational barriers of atropisomeric polychlorinated biphenyls (PCBs) by a novel stopped-flow multidimensional gas chromatographic technique. Chirality, 10 (1998) 316-320.

(32)   Lehmler, H.J., Harrad, S.J., Huhnerfuss, H., Kania-Korwel, I., Lee, C.M., Lu, Z., Wong, C.S., Chiral polychlorinated biphenyl transport, metabolism, and distribution: A review. Environmental Science & Technology, 44 (2010) 2757-2766.

(33)   Sundstrom, G., Hutzinger, O., Safe, S., Metabolism of chlorobiphenyls - Review. Chemosphere, 5 (1976) 267-298.

(34)   Preston, B.D., Miller, J.A., Miller, E.C., Nonarene oxide aromatic ring hydroxylation of 2,2',5,5'-tetrachlorobiphenyl as the major metabolic pathway catalyzed by phenobarbital-induced rat-liver microsomes. Journal of Biological Chemistry, 258 (1983) 8304-8311.

(35)   Koga, N., Kikuichinishimura, N., Hara, T., Harada, N., Ishii, Y., Yamada,

H., Oguri, K., Yoshimura, H., Purification and characterization of a newly identified isoform of cytochrome-P450 responsible for 3-hydroxylation of 2,5,2',5'-tetrachlorobiphenyl in hamster liver. Archives of Biochemistry and Biophysics, 317 (1995) 464-470.

(36)   Gutleb, A.C., Cenijn, P., van Velzen, M., Lie, E., Ropstad, E., Skaare, J.U., Malmberg, T., Bergman, A., Gabrielsen, G.W., Legler, J., In vitro assay shows that PCB metabolites completely saturate thyroid hormone transport capacity in blood of wild polar bears (Ursus maritimus). Environmental Science & Technology, 44 (2010) 3149-3154.

(37)   Lans, M.C., Spiertz, C., Brouwer, A., Koeman, J.H., Different competition of thyroxine-binding to transthyretin and thyroxine-binding globulin by hydroxy-PCBs, PCDDs and PCDFs. European Journal of Pharmacology-Environmental Toxicology and Pharmacology Section, 270 (1994) 129-136.

(38)   Bergman, A., Klassonwehler, E., Kuroki, H., Selective retention of hydroxylated PCB metabolites in blood. Environmental Health Perspectives, 102 (1994) 464-469.

(39)   Kania-Korwel, I., Vyas, S.M., Song, Y., Lehmler, H.J., Gas chromatographic separation of methoxylated polychlorinated biphenyl atropisomers. Journal of Chromatography A, 1207 (2008) 146-154.

(40)   Bakke, J.E., Bergman, A.L., Larsen, G.L., Metabolism of 2,4',5-trichlorobiphenyl by the mercapturic acid pathway. Science, 217 (1982) 645-647.

(41)   Nezel, T., Muller-Plathe, F., Muller, M.D., Buser, H.R., Theoretical considerations about chiral PCBs and their methylthio and methylsulfonyl metabolites being possibly present as stable enantiomers. Chemosphere, 35 (1997) 1895-1906.

(42)   Chu, S.G., Covaci, A., Haraguchi, K., Voorspoels, S., Van de Vijver, K., Das, K., Bouquegneau, J.M., De Coen, W., Blust, R., Schepens, P., Levels and enantiomeric signatures of methyl sulfonyl PCB and DDE metabolites in livers of harbor porpoises (Phocoena phocoena) from the southern North Sea. Environmental Science & Technology, 37 (2003) 4573-4578.

(43)   Wiberg, K., Letcher, R., Sandau, C., Duffe, J., Norstrom, R., Haglund, P., Bidleman, T., Enantioselective gas chromatography mass spectrometry of methylsulfonyl PCBs with application to Arctic marine mammals. Analytical Chemistry, 70 (1998) 3845-3852.

(44)   Larsson, C., Ellerichmann, T., Huhnerfuss, H., Bergman, A., Chiral PCB methyl sulfones in rat tissues after exposure to technical PCBs. Environmental Science & Technology, 36 (2002) 2833-2838.

(45)   Norstrom, K., Eriksson, J., Haglund, J., Silvari, V., Bergman, A., Enantioselective formation of methyl sulfone metabolites of 2,2',3,3',4,6'-hexachlorobiphenyl in rat. Environmental Science & Technology, 40 (2006) 7649-7655.

(46)   Dearth, M.A., Hites, R.A., Complete analysis of technical chlordane using

negative ionization mass-spectrometry. Environmental Science & Technology, 25 (1991) 245-254.

(47)   Buchert, H., Class, T., Ballschmiter, K., High-resolution gas-chromatography of technical chlordane with electron-capture selective and mass selective detection. Fresenius Zeitschrift Fur Analytische Chemie, 333 (1989) 211-217.

(48)   Nomeir, A.A., Hajjar, N.P., Metabolism of chlordane in mammals. Reviews of Environmental Toxicology and Chemistry, 100 (1987) 1-22.

(49)   Simpson, C.D., Wilcock, R.J., Smith, T.J., Wilkins, A.L., Langdon, A.G., Determination of octanol-water partition coefficients for the major components of technical chlordane. Bulletin of Environmental Contamination and Toxicology, 55 (1995) 149-153.

(50)   Barnett, J.R., Dorough, H.W., Metabolism of chlordane in rats. Journal of Agricultural and Food Chemistry, 22 (1974) 612-619.

(51)   Dearth, M.A., Hites, R.A., Depuration rates of chlordane compounds from rat fat. Environmental Science & Technology, 25 (1991) 1125-1128.

(52)   Polder, A., Skaare, J.U., Skjerve, E., Loken, K.B., Eggesbo, M., Levels of chlorinated pesticides and polychlorinated biphenyls in Norwegian breast milk (2002-2006), and factors that may predict the level of contamination. Science of the Total Environment, 407 (2009) 4584-4590.

(53)   Dearth, M.A., Hites, R.A., Chlordane accumulation in people.

Environmental Science & Technology, 25 (1991) 1279-1285.

(54)   Bentzen, T.W., Muir, D.C.G., Amstrup, S.C., O'Hara, T.M., Organohalogen concentrations in blood and adipose tissue of Southern Beaufort Sea polar bears. Science of the Total Environment, 406 (2008) 352-367.

(55)   Braune, B.M., Mallory, M.L., Gilchrist, H.G., Letcher, R.J., Drouillard, K.G., Levels and trends of organochlorines and brominated flame retardants in Ivory Gull eggs from the Canadian Arctic, 1976 to 2004. Science of the Total Environment, 378 (2007) 403-417.

(56)   Tashiro, S., Matsumura, F., Metabolism of trans-nonachlor and related chlordane components in rat and man. Archives of Environmental Contamination and Toxicology, 7 (1978) 113-127.

(57)   Beeman, R.W., Matsumura, F., Metabolism of cis-chlordane and trans-chlordane by a soil microorganism. Journal of Agricultural and Food Chemistry, 29 (1981) 84-89.

(58)   Smith, S.W., Chiral toxicology: It's the same thing...only different. Toxicological Sciences, 110 (2009) 4-30.

(59)   Puttmann, M., Mannschreck, A., Oesch, F., Robertson, L., Chiral effects in the induction of drug metabolizing enzymes using synthetic atropisomers of polychlorinated biphenyls (PCBs). Biochemical Pharmacology, 38 (1989) 1345-1352.

(60)   Rodman, L.E., Shedlofsky, S.I., Mannschreck, A., Puttmann, M., Swim,

A.T., Robertson, L.W., Differential potency of atropisomers of polychlorinated-biphenyls on cytochrome-P450 induction and uroporphyrin accumulation in the chick-embryo hepatocyte culture. Biochemical Pharmacology, 41 (1991) 915-922.

(61)   Lehmler, H.J., Robertson, L.W., Garrison, A.W., Kodavanti, P.R.S., Effects of PCB 84 enantiomers on [H-3]-phorbol ester binding in rat cerebellar granule cells and Ca-45(2+)-uptake in rat cerebellum. Toxicology Letters, 156 (2005) 391-400.

(62)   Pessah, I.N., Lehmler, H.J., Robertson, L.W., Perez, C.F., Cabrales, E., Bose, D.D., Feng, W., Enantiomeric specificity of (-)-2,2',3,3',6,6'-hexachlorobiphenyl toward ryanodine receptor types 1 and 2. Chemical Research in Toxicology, 22 (2009) 201-207.

(63)   Wang, L.M., Zhou, S.S., Lin, K., Zhao, M.R., Liu, W.P., Gan, J.Y., Enantioselctive estrogenicity of o,p'-dichlorodiphenyltrichloroethane in the MCF-7 human breast carcinoma cell line. Environmental Toxicology and Chemistry, 28 (2009) 1-8.

(64)   Eljarrat, E., Guerra, P., Barcelo, D., Enantiomeric determination of chiral persistent organic pollutants and their metabolites. TRAC-Trends in Analytical Chemistry, 27 (2008) 847-861.

(65)   Huhnerfuss, H., Shah, M.R., Enantioselective chromatography-A powerful tool for the discrimination of biotic and abiotic transformation processes of chiral environmental pollutants. Journal of Chromatography A, 1216 (2009) 481-502.

(66)   Wong, C.S., Environmental fate processes and biochemical transformations of chiral emerging organic pollutants. Analytical and Bioanalytical Chemistry, 386 (2006) 544-558.

(67)   Harner, T., Wiberg, K., Norstrom, R., Enantiomer fractions are preferred to enantiomer ratios for describing chiral signatures in environmental analysis. Environmental Science & Technology, 34 (2000) 218-220.

(68)   Bedard, D., in Robertson, L., Hansen, L.G. (Editors), PCBs: Recent advances in environmental toxicology and health effects, The University of Kentucky Press, Lexington, KY, 2001, p. 27-33.

(69)   Kobayashi, H., Rittmann, B.E., Microbial removal of hazardous organic-compounds. Environmental Science & Technology, 16 (1982) A170-A183.

(70)   Pakdeesusuk, U., Jones, W.J., Lee, C.M., Garrison, A.W., O'Niell, W.L., Freedman, D.L., Coates, J.T., Wong, C.S., Changes in enantiomeric fractions during microbial reductive dechlorination of PCB132, PCB149, and Aroclor 1254 in Lake Hartwell sediment microcosms. Environmental Science & Technology, 37 (2003) 1100-1107.

(71)   Singer, A.C., Wong, C.S., Crowley, D.E., Differential enantioselective transformation of atropisomeric polychlorinated biphenyls by multiple bacterial strains with different inducing compounds. Applied and Environmental Microbiology, 68 (2002) 5756-5759.

(72)   Garcia-Ruiz, C., Andres, R., Valera, J.L., Laborda, F., Marina, M.L.,

Monitoring the stereoselectivity of biodegradation of chiral polychlorinated biphenyls using electrokinetic chromatography. Journal of Separation Science, 25 (2002) 17-22.

(73) Ludwig, P., Huhnerfuss, H., Konig, W.A., Gunkel, W., Gas-chromatographic separation of the enantiomers of marine pollutants. 3. Enantioselective degradation of alpha-hexachlorocyclohexane and gamma-hexachlorocyclohexane by marine microorganisms. Marine Chemistry, 38 (1992) 13-23.

(74) Wong, C.S., Hoestra, P.F., Karlsson, H., Backus, S.M., Mabury, S.A., Muir, D.C.G., Enantiomer fractions of chiral organochlorine pesticides and polychlorinated biphenyls in standard and certified reference materials. Chemosphere, 49 (2002) 1339-1347.

(75) Wong, C.S., Garrison, A.W., Foreman, W.T., Enantiomeric composition of chiral polychlorinated biphenyl atropisomers in aquatic bed sediment. Environmental Science & Technology, 35 (2001) 33-39.

(76) Glausch, A., Blanch, G.P., Schurig, V., Enantioselective analysis of chiral polychlorinated biphenyls in sediment samples by multidimensional gas chromatography electron-capture detection after steam distillation-solvent extraction and sulfur removal. Journal of Chromatography A, 723 (1996) 399-404.

(77) Wong, C.S., Pakdeesusuk, U., Morrissey, J.A., Lee, C.M., Coates, J.T.,

Garrison, A.W., Mabury, S.A., Marvin, C.H., Muir, D.C.G., Enantiomeric composition of chiral polychlorinated biphenyl atropisomers in dated sediment cores. Environmental Toxicology and Chemistry, 26 (2007) 254-263.

(78)   Kania-Korwel, I., El-Komy, M., Veng-Pedersen, P., Lehmler, H.J., Clearance of polychlorinated biphenyl atropisomers is enantioselective in female C57Bl/6 mice. Environmental Science & Technology, 44 (2010) 2828-2835.

(79)   Bondy, G.S., Coady, L., Doucet, J., Armstrong, C., Kriz, R., Liston, V., Robertson, P., Norstrom, R., Moisey, J., Enantioselective and gender-dependent depletion of chlordane compounds from rat tissues. Journal of Toxicology and Environmental Health-Part a-Current Issues, 68 (2005) 1917-1938.

(80)   Buckman, A.H., Wong, C.S., Chow, E.A., Brown, S.B., Solomon, K.R., Fisk, A.T., Biotransformation of polychlorinated biphenyls (PCBs) and bioformation of hydroxylated PCBs in fish. Aquatic Toxicology, 78 (2006) 176-185.

(81)   Wong, C.S., Lau, F., Clark, M., Mabury, S.A., Muir, D.C.G., Rainbow trout (Oncorhynchus mykiss) can eliminate chiral organochlorine compounds enantioselectively. Environmental Science & Technology, 36 (2002) 1257-1262.

(82)   Seemamahannop, R., Berthod, A., Maples, M., Kapila, S., Armstrong, D.W., Uptake and enantioselective elimination of chlordane compounds by common carp (Cyprinus carpio, L.). Chemosphere, 59 (2005) 493-500.

(83)   Kania-Korwel, I., Hornbuckle, K.C., Robertson, L.W., Lehmler, H.J.,

Influence of dietary fat on the enantioselective disposition of 2,2',3,3',6,6'-hexachlorobiphenyl (PCB 136) in female mice. Food and Chemical Toxicology, 46 (2008) 637-644.

(84)   Hoekstra, P.F., O'Hara, T.M., Karlsson, H., Solomon, K.R., Muir, D.C.G., Enantiomer-specific biomagnification of alpha-hexachlorocyclohexane and selected chiral chlordane-related compounds within an Arctic marine food web. Environmental Toxicology and Chemistry, 22 (2003) 2482-2491.

(85)   Hoekstra, P.F., Wong, C.S., O'Hara, T.M., Solomon, K.R., Mabury, S.A., Muir, D.C.G., Enantiomer-specific accumulation of PCB atropisomers in the bowhead whale (Balaena mysticetus). Environmental Science & Technology, 36 (2002) 1419-1425.

(86)   Iwata, H., Tanabe, S., Iida, T., Baba, N., Ludwig, J.P., Tatsukawa, R., Enantioselective accumulation of alpha-hexachlorocyclohexane in northern fur seals and double crested cormorants: Effects of biological and ecological factors in the higher trophic levels. Environmental Science & Technology, 32 (1998) 2244-2249.

(87)   Huhnerfuss, H., Faller, J., Kallenborn, R., Konig, W.A., Ludwig, P., Pfaffenberger, B., Oehme, M., Rimkus, G., Enantioselective and nonenantioselective degradation of organic pollutants in the marine ecosystem. Chirality, 5 (1993) 393-399.

(88)   Vetter, W., Schurig, V., Enantioselective determination of chiral

organochlorine compounds in biota by gas chromatography on modified cyclodextrins. Journal of Chromatography A, 774 (1997) 143-175.

(89)   Mossner, S., Spraker, T.R., Becker, P.R., Ballschmiter, K., Ratios of Enantiomers of alpha-HCH and determination of alpha-HCH, beta-HCH, and gamma-HCH isomers in brain and other tissues of neonatal northern fur seals (Callorhinus ursinus). Chemosphere, 24 (1992) 1171-1180.

(90)   Kania-Korwel, I., Garrison, A.W., Avants, J.K., Hornbuckle, K.C., Robertson, L.W., Sulkowski, W.W., Lehmler, H.J., Distribution of chiral PCBs in selected tissues in the laboratory rat. Environmental Science & Technology, 40 (2006) 3704-3710.

(91)   Kania-Korwel, I., Shaikh, N.S., Hornbuckle, K.C., Robertson, L.W., Lehmler, H.J., Enantioselective disposition of PCB 136 (2,2',3,3',6,6'-hexachlorobiphenyl) in C57BL/6 mice after oral and intraperitoneal administration. Chirality, 19 (2007) 56-66.

(92)   Lehmler, H.J., Price, D.J., Garrison, A.W., Birge, W.J., Robertson, L.W., Distribution of PCB 84 enantiomers in C57BL/6 mice. Fresenius Environmental Bulletin, 12 (2003) 254-260.

(93)   Ulrich, E.M., Willett, K.L., Caperell-Grant, A., Bigsby, R.M., Hites, R.A., Understanding enantioselective processes: A laboratory rat model for alpha-hexachlorocyclohexane accumulation. Environmental Science & Technology, 35 (2001) 1604-1609.

(94)   Yang, D.B., Li, X.Q., Tao, S., Wang, Y.Q., Cheng, Y., Zhang, D.Y., Yu, L.C., Enantioselective behavior of alpha-HCH in mouse and quail tissues. Environmental Science & Technology, 44 (2010) 1854-1859.

(95)   Buser, H.R., Muller, M.D., Enantioselective determination of chlordane components, metabolites, and photoconversion products in environmental-samples using chiral high-resolution gas-chromatography and mass-spectrometry. Environmental Science & Technology, 27 (1993) 1211-1220.

(96)   Warner, N.A., Martin, J.W., Wong, C.S., Chiral polychlorinated biphenyls are biotransformed enantioselectively by mammalian cytochrome P-450 isozymes to form hydroxylated metabolites. Environmental Science & Technology, 43 (2009) 114-121.

(97)   Kania-Korwel, I., Hrycay, E.G., Bandiera, S.M., Lehmler, H.J., 2,2',3,3',6,6'-hexachlorobiphenyl (PCB 136) atropisomers interact enantioselectively with hepatic microsomal cytochrome P450 enzymes. Chemical Research in Toxicology, 21 (2008) 1295-1303.

(98)   Kania-Korwel, I., Hornbuckle, K.C., Peck, A., Ludewig, G., Robertson, L.W., Sulkowski, W.W., Espandiari, P., Gairola, C.G., Lehmler, H.J., Congener-specific tissue distribution of Aroclor 1254 and a highly chlorinated environmental PCB mixture in rats. Environmental Science & Technology, 39 (2005) 3513-3520.

(99)   Kania-Korwel, I., Hornbuckle, K.C., Robertson, L.W., Lehmler, H.J.,

Dose-dependent enantiomeric enrichment of 2,2 ',3,3 ',6,6 '-hexachlorobiphenyl in female mice. Environmental Toxicology and Chemistry, 27 (2008) 299-305.

(100)   Kania-Korwel, I., Xie, W., Hornbuckle, K.C., Robertson, L.W., Lehmler, H.J., Enantiomeric enrichment of 2,2 ',3,3 ',6,6 '-hexachlorobiphenyl (PCB 136) in mice after induction of CYP enzymes. Archives of Environmental Contamination and Toxicology, 55 (2008) 510-517.

(101)   Fisk, A.T., Holst, M., Hobson, K.A., Duffe, J., Moisey, J., Norstrom, R.J., Persistent organochlorine contaminants and enantiomeric signatures of chiral pollutants in ringed seals (Phoca hispida) collected on the east and west side of the Northwater Polynya, Canadian Arctic. Archives of Environmental Contamination and Toxicology, 42 (2002) 118-126.

(102)   Fisk, A.T., Moisey, J., Hobson, K.A., Karnovsky, N.J., Norstrom, R.J., Chlordane components and metabolites in seven species of Arctic seabirds from the Northwater Polynya: relationships with stable isotopes of nitrogen and enantiomeric fractions of chiral components. Environmental Pollution, 113 (2001) 225-238.

(103)   Warner, N.A., Wong, C.S., The freshwater invertebrate Mysis relicta can eliminate chiral organochlorine compounds enantioselectively. Environmental Science & Technology, 40 (2006) 4158-4164.

(104)   Huhnerfuss, H., Bergman, A., Larsson, C., Peters, N., Westendorf, J., Enantioselective transformation of atropisomeric PCBs or of their methylsulfonyl

metabolites by rat hepatocytes? Organohalogen Compounds, 62 (2003) 265-268.

(105) Matthews, H.B., Dedrick, R.L., Pharmacokinetics of PCBs. Annual Review of Pharmacology and Toxicology, 24 (1984) 85-103.

(106) Mossner, S., Barudio, I., Spraker, T.S., Antonelis, G., Early, G., Geraci, J.R., Becker, P.R., Ballschmiter, K., Determination of HCHs, PCBs, and DDTs in brain-tissues of marine mammals of different age. Fresenius Journal of Analytical Chemistry, 349 (1994) 708-716.

(107) Blanch, G.P., Glausch, A., Schurig, V., Determination of the enantiomeric ratios of chiral PCB 95 and 149 in human milk samples by multidimensional gas chromatography with ECD and MS(SIM) detection. European Food Research and Technology, 209 (1999) 294-296.

(108) Glausch, A., Hahn, J., Schurig, V., Enantioselective determination of chiral 2,2',3,3',4,6'-hexachlorobiphenyl (PCB-132) in human-milk samples by multidimensional gas-chromatography electron-capture detection and by mass-spectrometry. Chemosphere, 30 (1995) 2079-2085.

(109) Wiberg, K., Bergman, A., Olsson, M., Roos, A., Blomkvist, G., Haglund, P., Concentrations and enantiomer fractions of organochlorine compounds in Baltic species hit by reproductive impairment. Environmental Toxicology and Chemistry, 21 (2002) 2542-2551.

(110) Karlsson, H., Oehme, M., Skopp, S., Burkow, I.C., Enantiomer ratios of chlordane congeners are gender specific in cod (Gadus morhua) from the Barents

Sea. Environmental Science & Technology, 34 (2000) 2126-2130.

(111) Bondy, G., Curran, I., Doucet, J., Armstrong, C., Coady, L., Hierlihy, L., Fernie, S., Robertson, P., Barker, M., Toxicity of trans-nonachlor to Sprague-Dawley rats in a 90-day feeding study. Food and Chemical Toxicology, 42 (2004) 1015-1027.

(112) Cantillana, T., Lindstrom, V., Eriksson, L., Brandt, I., Bergman, A., Interindividual differences in o,p'-DDD enantiomer kinetics examined in Gottingen minipigs. Chemosphere, 76 (2009) 167-172.

(113) Wiberg, K., Andersson, P.L., Berg, H., Olsson, P.E., Haglund, P., The fate of chiral organochlorine compounds and selected metabolites in intraperitoneally exposed Arctic char (Salvelinus alpinus). Environmental Toxicology and Chemistry, 25 (2006) 1465-1473.

(114) Butt, C.M., Berger, U., Bossi, R., Tomy, G.T., Levels and trends of poly- and perfluorinated compounds in the Arctic environment. Science of the Total Environment, 408 (2010) 2936-2965.

(115) Giesy, J.P., Kannan, K., Global distribution of perfluorooctane sulfonate in wildlife. Environmental Science & Technology, 35 (2001) 1339-1342.

(116) Roosens, L., D'Hollander, W., Bervoets, L., Reynders, H., Van Campenhout, K., Cornelis, C., Van Den Heuvel, R., Koppen, G., Covaci, A., Brominated flame retardants and perfluorinated chemicals, two groups of persistent contaminants in Belgian human blood and milk. Environmental

Pollution, 158 (2010) 2546-2552.

(117) Toms, L.M.L., Calafat, A.M., Kato, K., Thompson, J., Harden, F., Hobson, P., Sjodin, A., Mueller, J.F., Polyfluoroalkyl chemicals in pooled blood serum from infants, children, and adults in Australia. Environmental Science & Technology, 43 (2009) 4194-4199.

(118) Calafat, A.M., Wong, L.Y., Kuklenyik, Z., Reidy, J.A., Needham, L.L., Polyfluoroalkyl chemicals in the US population: Data from the National Health and Nutrition Examination Survey (NHANES) 2003-2004 and comparisons with NHANES 1999-2000. Environmental Health Perspectives, 115 (2007) 1596-1602.

(119) Martin, J.W., Whittle, D.M., Muir, D.C.G., Mabury, S.A., Perfluoroalkyl contaminants in a food web from Lake Ontario. Environmental Science & Technology, 38 (2004) 5379-5385.

(120) Paul, A.G., Jones, K.C., Sweetman, A.J., A first global production, emission, and environmental inventory for perfluorooctane sulfonate. Environmental Science & Technology, 43 (2009) 386-392.

(121) Hansen, K.J., Clemen, L.A., Ellefson, M.E., Johnson, H.O., Compound-specific, quantitative characterization of organic: Fluorochemicals in biological matrices. Environmental Science & Technology, 35 (2001) 766-770.

(122) 3M Co. Perfluorochemical use, distribution, and release overview. Available in the U.S. EPA Accession Record AR-226-0550. (1999).

(123) Benskin, J.P., De ytSilva, A.O., Martin, J.W., Isomer profiling of

perfluorinated substances as a tool for source tracking: A review of early findings and future applications. Reviews of Environmental Contaminant Toxicology, 208 (2010) 111-160.

(124)   Houde, M., Czub, G., Small, J.M., Backus, S., Wang, X.W., Alaee, M., Muir, D.C.G., Fractionation and bioaccumulation of perfluorooctane sulfonate (PFOS) isomers in a Lake Ontario food web. Environmental Science & Technology, 42 (2008) 9397-9403.

(125)   Benskin, J.P., Yeung, L.W.Y., Yamashita, N., Taniyasu, S., Lam, P.K.S., Martin, J.W., Perfluorinated acid isomer profiling in water and quantitative assessment of manufacturing source. Environmental Science & Technology, 44 (2010) 9049-9054.

(126)   Arsenault, G., Chittim, B., McAlees, A., McCrindle, R., Riddell, N., Yeo, B., Some issues relating to the use of perfluorooctane sulfonate (PFOS) samples as reference standards. Chemosphere, 70 (2008) 616-625.

(127)   Benskin, J.P., Bataineh, M., Martin, J.W., Simultaneous characterization of perfluoroalkyl carboxylate, sulfonate, and sulfonamide isomers by liquid chromatography-tandem mass spectrometry. Analytical Chemistry, 79 (2007) 6455-6464.

(128)   Benskin, J.P., De Silva, A.O., Martin, L.J., Arsenault, G., McCrindle, R., Riddell, N., Mabury, S.A., Martin, J.W., Disposition of perfluorinated acid isomers in Sprague-Dawley rats; Part 1: Single dose. Environmental Toxicology

and Chemistry, 28 (2009) 542-554.

(129) De Silva, A.O., Benskin, J.P., Martin, L.J., Arsenault, G., McCrindle, R., Riddell, N., Martin, J.W., Mabury, S.A., Disposition of perfluorinated acid isomers in Sprague-Dawley rats; Part 2: Subchronic dose. Environmental Toxicology and Chemistry, 28 (2009) 555-567.

(130) Sharpe, R.L., Benskin, J.P., Laarman, A.H., MacLeod, S.L., Martin, J.W., Wong, C.S., Goss, G.G., Perfluorooctane sulfonate toxicity, isomer-specific accumulation, and maternal transfer in Zebrafish (Danio rerio) and rainbow trout (Oncorhynchus mykiss). Environmental Toxicology and Chemistry, 29 (2010) 1957-1966.

(131) Chu, S.G., Letcher, R.J., Linear and branched perfluorooctane sulfonate isomers in technical product and environmental samples by in-port derivatization-gas chromatography-mass spectrometry. Analytical Chemistry, 81 (2009) 4256-4262.

(132) Gebbink, W.A., Letcher, R.J., Linear and branched perfluorooctane sulfonate isomer patterns in herring gull eggs from colonial sites across the Laurentian Great Lakes. Environmental Science & Technology, 44 (2010) 3739-3745.

(133) Lloyd, A.S., Bailey, V.A., Hird, S.J., Routledge, A., Clarke, D.B., Mass spectral studies towards more reliable measurement of perfluorooctanesulfonic acid and other perfluorinated chemicals (PFCs) in food matrices using liquid

chromatography/tandem mass spectrometry. Rapid Communications in Mass Spectrometry, 23 (2009) 2923-2938.

(134)   Powley, C.R., George, S.W., Russell, M.H., Hoke, R.A., Buck, R.C., Polyfluorinated chemicals in a spatially and temporally integrated food web in the Western Arctic. Chemosphere, 70 (2008) 664-672.

(135)   Riddell, N., Arsenault, G., Benskin, J.P., Chittim, B., Martin, J.W., McAlees, A., McCrindle, R., Branched perfluorooctane sulfonate isomer quantification and characterization in blood serum samples by HPLC/ESI-MS(/MS). Environmental Science & Technology, 43 (2009) 7902-7908.

(136)   Haug, L.S., Thomsen, C., Bechert, G., Time trends and the influence of age and gender on serum concentrations of perfluorinated compounds in archived human samples. Environmental Science & Technology, 43 (2009) 2131-2136.

(137)   Martin, J.W., Asher, B.J., Beesoon, S., Benskin, J.P., Ross, M.S., PFOS or PreFOS? Are perfluorooctane sulfonate precursors (PreFOS) important determinatns of human and environmental perfluorooctane sulfonate (PFOS) exposure? Journal of Environmental Monitoring, 12 (2010) 1979-2004.

(138)   Xu, L., Krenitsky, D.M., Seacat, A.M., Butenhoff, J.L., Anders, M.W., Biotransformation of N-ethyl-N-(2-hydroxyethyl)perfluorooetanesulfonamide by rat liver microsomes, cytosol, and slices and by expressed rat and human cytochromes P450. Chemical Research in Toxicology, 17 (2004) 767-775.

(139)   Benskin, J.P., Holt, A., Martin, J.W., Isomer-specific biotransformation

rates of a perfluorooctane sulfonate (PFOS)-precursor by cytochrome P450 isozymes and human liver microsomes. Environmental Science & Technology, 43 (2009) 8566-8572.

(140)   Tomy, G.T., Tittlemier, S.A., Palace, V.P., Budakowski, W.R., Braekevelt, E., Brinkworth, L., Friesen, K., Biotransformation of N-ethyl perfluorooctanesulfonamide by rainbow trout (Onchorhynchus mykiss) liver microsomes. Environmental Science & Technology, 38 (2004) 758-762.

(141)   Xie, W., Wu, Q., Kania-Korwel, I., Tharappel, J.C., Telu, S., Coleman, M.C., Glauert, H.P., Kannan, K., Mariappan, S.V.S., Spitz, D.R., Weydert, J., Lehmler, H.J., Subacute exposure to N-ethyl perfluorooctanesulfonamidoethanol results in the formation of perfluorooctanesulfonate and alters superoxide dismutase activity in female rats. Archives of Toxicology, 83 (2009) 909-924.

(142)   Seacat, A.M., Thomford, P.J., Hansen, K.J., Clemen, L.A., Eldridge, S.R., Elcombe, C.R., Butenhoff, J.L., Sub-chronic dietary toxicity of potassium perfluorooctanesulfonate in rats. Toxicology, 183 (2003) 117-131.

(143)   Seacat, A., Toxicokinetic study of perfluorooctane sulfonamide (PFOSA; T-7132.2) in rats. Available in the U.S. EPA Accession Record AR-226-0328. (2000).

(144)   Vestergren, R., Cousins, I.T., Trudel, D., Wormuth, M., Scheringer, M., Estimating the contribution of precursor compounds in consumer exposure to PFOS and PFOA. Chemosphere, 73 (2008) 1617-1624.

(145) Fromme, H., Tittlemier, S.A., Volkel, W., Wilhelm, M., Twardella, D., Perfluorinated compounds - Exposure assessment for the general population in western countries. International Journal of Hygiene and Environmental Health, 212 (2009) 239-270.

(146) Karrman, A., Langlois, I., van Bavel, B., Lindstrom, G., Oehme, M., Identification and pattern of perfluorooctane sulfonate (PFOS) isomers in human serum and plasma. Environment International, 33 (2007) 782-788.

Chapter 2

Comparison of Electrospray Ionization, Atmospheric Pressure Photoionization, and Anion Attachment Atmospheric Pressure Photoionization for the Analysis of Hexabromocyclododecane Enantiomers in Environmental Samples

71

2.1 Introduction

In recent years, liquid chromatography-mass spectrometry (LC-MS) has become increasingly popular for use in environmental analysis, and while a number of ionization techniques exist, electrospray ionization (ESI) remains the most widely used. However, while ESI is extremely sensitive for polar compounds, many environmental compounds are non-polar, and are therefore difficult to analyze using this technique. In 2000, atmospheric pressure photoionization (APPI) was developed as a complementary technique to ESI, and provides a means of ionizing low-polarity compounds (1). For some analytes, APPI offers greater sensitivity (2,3) and larger dynamic ranges (4,5) than ESI. Furthermore, APPI may offer other advantages over ESI for environmental analyses. APPI ionization has been found to be less susceptible to matrix effects than ESI for a variety of analytes (4,6,7). Matrix effects occur when the ionization efficiency of an analyte is either enhanced or suppressed, and is often attributed to matrix materials that co-elute with the analyte. This change in the analyte response can hamper quantification by leading to inaccurate and imprecise measurements of analyte concentration.

More recently, the use of anion attachment APPI (AA-APPI) has been suggested as a means of further expanding the range of compounds ionizable by APPI (8). In general, the ionization of analytes by APPI relies on the presence of a photoionizable dopant, a low molecular weight compound with an ionization potential below that of the energies of the emitted photons. The dopant is

introduced into the source, where it is photoionized to release a thermal electron. This, in turn, may initiate a series of gas phase reactions, subsequently yielding either a positively or negatively charged analyte ion (9). In AA-APPI, analytes are ionized by the formation of a negatively charged adduct species within the source. The use of stable adducts to enhance the ionization of non-polar compounds in APPI, particularly large molecules such as peptides and polymers, has been demonstrated through the use of chlorinated solvents or chlorinated eluents (8,10,11). However, to date this technique has not been shown to be applicable to small molecules, nor, to the best of my knowledge, do studies exist comparing the use of AA-APPI to other techniques, such as ESI or APPI.

Hexabromocyclododecane (HBCD) is a brominated flame retardant commonly added to consumer products, such as polystyrene foams and textiles, to reduce their flammability (12). Within the last decade, increasing concentrations of HBCD have been found in air, sediment, biota, and human blood and milk (13). HBCD is present in the environment as a mixture of three major diastereomers: α, β, and γ (Figure 2-1). Each diastereomer is chiral, and therefore each exists as a pair of enantiomers (14). The chirality of a compound may have profound impacts on a compound's fate and behavior in the environment. For instance, individual enantiomers may vary in bioaccumulation, metabolism, and toxicology (15-19). Therefore, the need exists to analyze chiral compounds on an enantiomer-specific basis in order to understand better the environmental fate of individual enantiomers. However, the accurate quantification of enantiomers is

73

often hampered by matrix effects, as matrix effects may have a more detrimental effect on the quantification of enantiomers than on the sum mixture of enantiomers, as commonly measured by non-enantioselective chromatography as a single peak (20). This study provides the first comparison of the analytical characteristics and matrix effects of APPI and AA-APPI, using HBCD as an environmentally relevant model compound. In doing so, proof of principle evidence on the use of AA-APPI for the purposes of quantifying small molecules is provided.
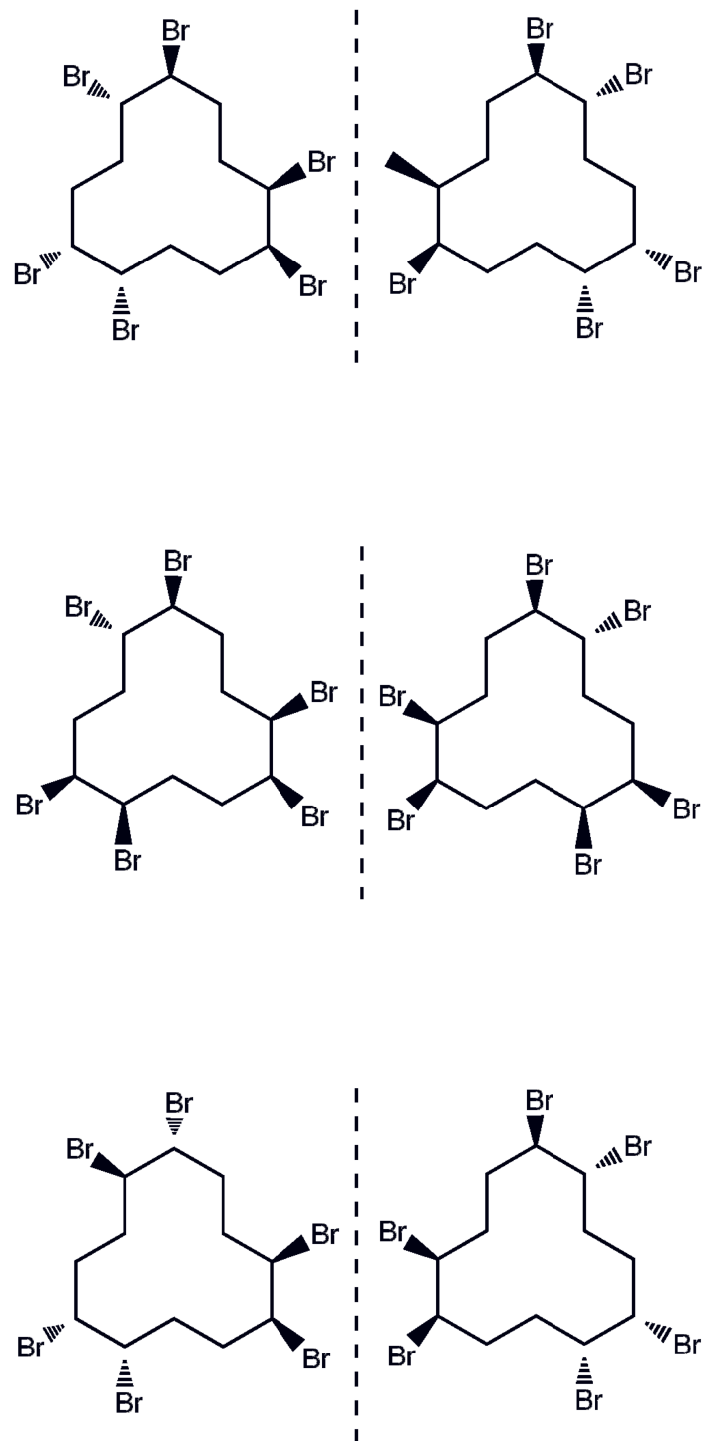
Figure 2-1: *Structures of major HBCD diastereomers and enantiomers.*

75

2.2 Materials and Methods

2.2.1 Chemicals and Reagents

Individual HBCD standards (α, β, and γ) were purchased from Accustandard (New Haven, CT, USA) and all were greater than 99% pure. Individual deuterated (d_{18}) HBCD isomers, of at least 98% chemical and isotopic purity, were purchased from Wellington Laboratories (Guelph, ON, Canada). HPLC grade methanol, acetonitrile, and toluene, as well as pesticide grade hexane and acetone were purchased from Fisher Scientific (Ottawa, ON, Canada), as was anhydrous sodium sulfate. Milli-Q water was obtained via a Millipore (Billerica, MA, USA) water filtration system. 1,4-Dibromobutane (99% purity) was purchased from VWR (Mississauga, ON, Canada). Silica gel (70-230 mesh) was purchased from Sigma Aldrich (Oakville, ON, Canada). Certified Reference Material EC-5 (Lake Ontario sediment, certified for polyaromatic hydrocarbons, chlorobenzenes, and polychlorinated biphenyls) was obtained from Environment Canada.

2.2.2 Liquid Chromatography/Mass Spectrometry

For all experiments, an Agilent 1100 HPLC system coupled to an Applied Biosystems QTrap 2000 (Foster City, CA, USA) triple quadrupole mass spectrometer was used. Enantiomer separation was achieved on a Nucleodex β-PM enantioselective column (4.6 × 200 mm, 5 μm d_p, Macherey-Nagel, Bethlehem, PA, USA) using an eluent of 49% acetonitrile:30% methanol:21%

H$_2$O initially held for two minutes, then changed linearly to 59.5% acetonitrile:30% methanol:10.5% H$_2$O over 20 minutes at 500 μL min^{-1} (21). This gradient was accomplished on a binary pump using 70:30 water/methanol as the A solvent and 70:30 acetonitrile/methanol as the B solvent and changing the eluent composition from 30:70 A:B to 15:85 A:B over the course of the run (22). Unless otherwise noted, an injection volume of 20 μL was used for all experiments. Chromatographic conditions were kept constant among source experiments.

Mass spectrometric experiments were carried out with a Photospray source (Applied Biosystems). Source parameters were optimized individually for all three sources in a similar manner. Optimization was done using a 1:1:1 mixture of all three native diastereomers (300 ng mL^{-1} each). An equal mixture of all three isomers was chosen in order not to place undue emphasis on one isomer over the others, as the mass spectral response may vary among isomers. This solution was introduced into the eluent flow via a tee connection at 20 μL min^{-1} using a syringe pump (Hamilton, Reno, NV, USA). The eluent was flowed at 500 μL min^{-1}, and the composition was 77.5% A:22.5% B, which represents the midpoint in the gradient used for analysis. Optimization was carried out by systematically changing the user-adjustable source parameters to maximize the ion intensity of either the [M – H]$^-$ (APPI) or [M + Br]$^-$ (AA-APPI) ion (Table 2-1).

Table 2-1: *Optimized MS/MS variables. a.u. = arbitrary units as per instrumentation used.*

Parameter	Units	AA-APPI $m/z= 722\rightarrow 79$	APPI $m/z= 640\rightarrow 79$
Dwell time	ms	100	100
Collision cell entrance potential	V	-32	-34
Curtain gas	a.u.	20	20
Collision gas	a.u.	10	5
Source temperature	ºC	300	400
Sheath gas	a.u.	600	60
Turbo gas	a.u.	0	90
Ion spray voltage	V	-1100	-1200
Declustering potential	V	-14	-18
Entrance potential	V	-5	-5
Collision energy	eV	-52	-52
Collision cell exit potential	V	-2	-2

Unless otherwise noted, for all experiments and analyses, the carrier solvent or photoionization dopant was flowed into the source in conjunction with the auxiliary gas at 50 μL min^{-1} using either a syringe pump or a pneumatic delivery system (23). For APPI experiments, toluene was used as the photoionization dopant.

2.2.3 Carrier Solvent Optimization

Prior to AA-APPI experiments and analyses, several experiments were carried out to determine the best source of bromide and the optimum carrier solvent (i.e., co-solvent being tested as a possible dopant) that would maximize the formation of the [M + Br]⁻ ion. All experiments were carried out by injecting the analyte directly into the eluent flow, which was coupled to the mass

spectrometer without any chromatographic column attached. For the first experiment, 15 brominated aliphatic and alicyclic compounds of varying structures and degrees of bromination, were selected for screening due to their ready availability in our lab and their solubility in non-polar solvents. These compounds were characterized by their ability to fragment within the source to form bromide ions (m/z 79 and 81). This was done by injecting 10 μL of a 1% solution (v/v) of each compound in toluene. The LC eluent composition was held constant at 77.5% A: 22.5% B at a rate of 500 μL min^{-1}. Full scan mass spectra were collected for each compound over the mass range of m/z 60-400 to determine the dominant ions formed through photoionization and to monitor the formation of m/z 79 and 81 ions. To determine the necessity of a photoionizable carrier solvent on the formation of the bromide ions, this experiment was carried out with and without the addition of toluene introduced with the auxiliary gas at 50 μL min^{-1}.

Individual brominated compounds were further screened based on the formation of the [M + Br]$^-$ adduct, in order to determine whether or not the formation of the [M + Br]$^-$ adduct ion was based solely on the amount of Br$^-$ formed from a particular compound, or whether other factors were involved. A 1:1:1 mixture of HBCD diastereomers (100 ng mL^{-1} final concentration) was spiked into solutions containing 1% (v/v) of individual brominated compounds in toluene. These solutions were injected (10 μL) into the eluent flow as described above, and the [M + Br]$^-$ → Br$^-$ transition was monitored by multiple reaction

monitoring (MRM).   No additional source of dopant was used during this experiment. Based on these two experiments, 1,4-dibromobutane (1,4-DBB) was chosen for use as the bromide source for the rest of the study.

From the first experiment, it was found that the use of a photoionizable carrier solvent was necessary for the formation of bromide ions. Therefore, the carrier solvent was optimized based on its ability to function as a dopant (i.e., photoionize within the source), as the dopant has been found to affect the ionization of analytes in APPI (1,2,24). The carrier solvent was optimized by injecting 5 μL of 1% (v/v) 1,4-DBB in either toluene, anisole, acetone, acetonitrile, hexane, heptane or methanol, and collecting full scan mass spectra from m/z 60-400. No additional dopant was used in these experiments. From the collected spectra, the abundance of bromide ions was compared between the different solvents. Next, the effects of the carrier solvent selection on the formation of HBCD adducts was investigated. A 1:1:1 mixture of HBCD diastereomers (1 μg mL^{-1} each) was added to the eluent flow via a tee connection, and 10 μL injections of 1% (v/v) 1,4-DBB in either toluene, anisole, acetone, acetonitrile, hexane, heptane or methanol was injected into the LC with no additional source of dopant. The transitions from both the [M + Br]$^-$ → Br$^-$ and [M − H]$^-$ → Br$^-$ were monitored by MRM. The resultant peak areas were integrated using Analyst software (Applied Biosystems), and compared amongst the solvents.

Finally, the influence of the brominated compound concentration on the

formation of $[M + Br]^-$ was investigated. The formation of $[M + Br]^-$ was measured at 5 different concentrations of 1,4-DBB dissolved in toluene, ranging from 0.05% (v/v) to 2% (v/v). Each solution was introduced into the source in conjunction with the auxiliary gas at 50 μL min^{-1}. A 1:1:1 mixture of HBCD diastereomers (1 μg mL^{-1} each) was injected (10 μL) into the eluent flow and the formation of the $[M + Br]^-$ ion was monitored.

For calibration curve and matrix experiments, MRM was used for analyte detection. For APPI experiments, the transitions from $[M - H]^- \rightarrow Br^-$ (m/z 640.6 $\rightarrow$ 78.9 and 80.9) was used, while for AA-APPI experiments, the transitions from $[M + Br]^- \rightarrow Br^-$ (m/z 722.6 $\rightarrow$ 78.9 and 80.9) was monitored. The d_{18}-labeled isomers were detected using analogous transitions. All results are reported as the parent ion to m/z 78.9 transition.

2.2.4 Determination of Analytical Variables

For the determination of analytical parameters, a single set of standard solutions was made up in methanol by solvent exchanging and serially diluting the initial stock standards. Each solution contained HBCD diastereomers in a 1:1:1 ratio, ranging in concentration from 1-1000 ng mL^{-1} for each diastereomer, and also contained 100 ng mL^{-1} of each d_{18}-labeled diastereomer. Analysis of each solution was done in triplicate on each source, producing a calibration curve for each individual enantiomer. From this, analytical variables such as linearity, limits of detection (LOD, mean signal of the blank + 3 × standard deviation of the

81

blank) and limits of quantification (LOQ, mean signal of the blank + 10 ×
standard deviation of the blank) were determined on an enantiomer-specific basis.

2.2.5 Matrix Effects Experiments

The effect of co-extracted matrix materials from sediment samples on the
analysis of HBCDs was compared among ionization methods. For this, a post-
extraction addition method was done utilizing reference sediment as the matrix
material. Using a 1:1 mixture of acetone:hexane, 3 g of CRM EC-5 was extracted
overnight by Soxhlet extraction. Extracts were cleaned up by acidified silica gel
chromatography, using 8 g of deactivated silica gel which had been 50% acidified
by H_2SO_4 (25,26). While a number of other extraction and cleanup procedures
exist for HBCDs, this method was chosen as it likely retains much of the matrix
material in the final extract. After cleanup, samples were divided into two aliquots
and reduced in volume to 200 μL. The first aliquot was fortified with 40 ng of
1:1:1 mixture of HBCD diastereomers as well as a 40 ng of a 1:1:1 mixture of d_{18}-
labeled HBCDs. The second aliquot remained unspiked. Extracts were then
analyzed by LC-MS/MS on all three sources.

2.2.6 Data Analysis

For flow injection analysis experiments, ion intensities and analyte peaks
were integrated with Analyst software. Model-fitting software (PeakFit v.4.0,
Systat, San Jose, CA, USA) was used to determine the peak areas in

chromatographic runs. This software was used due to the fact that some enantiomer peaks partially coeluted and other methods of peak integration may lead to erroneous measurements of the EFs (27). For all analyses, peaks were fit to an exponentially modified Gaussian function, and all peak widths were assumed to remain constant. These parameters were chosen as they best modeled the peak shape in these experiments.

2.3 Results and Discussion

2.3.1 Selection of AA-APPI Bromine Source

The use of stable adducts to enhance the ionization of non-polar compounds in APPI has previously been demonstrated, and was found to be particularly useful for large molecules such as peptides and polymers (8,10,11). The formation of the adduct ion in these studies was achieved through the use of chlorinated eluents or solvents, both of which are incompatible with the reversed phase eluents needed to separate the HBCD enantiomers (22). Therefore, to form the $[M + Br]^-$ ion, a source of bromide ions was introduced into the source in conjunction with a photoionizable carrier solvent, rather than adding brominated compounds or bromine salts into the eluent, as is typically done when generating adducts for ESI analyses.

To demonstrate the feasibility of using this technique, 15 brominated compounds were screened (Figure 2-2), in order to determine their ability to fragment and form Br^- ions within the source. With the addition of toluene, all of

the brominated compounds investigated could be fragmented to some degree. The dominant ion for all of the screened compounds was Br⁻.
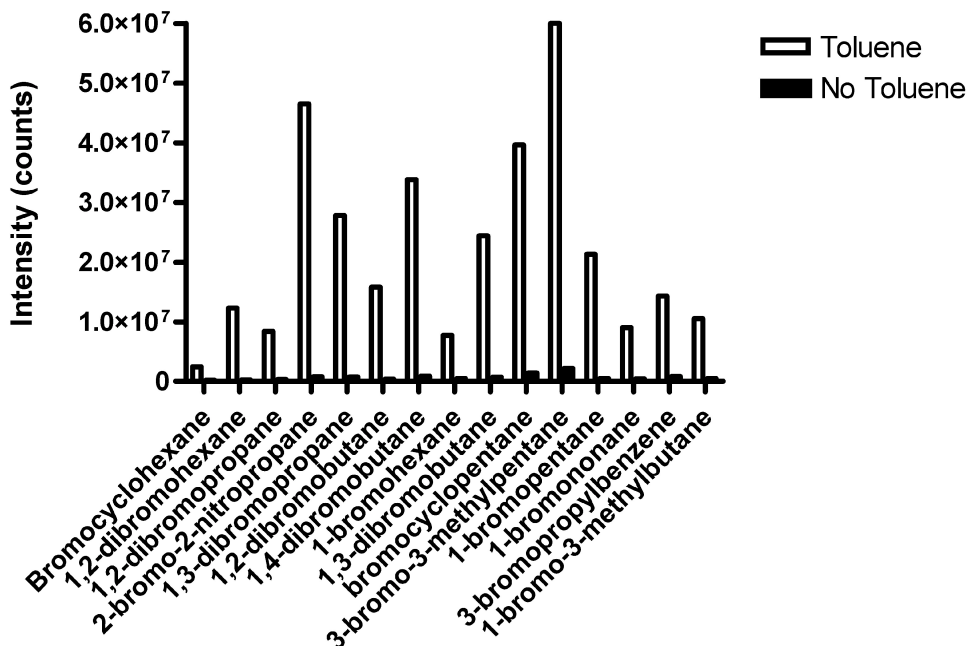
Figure 2-2: *Intensity of Br⁻ ion (m/z 79) formed with and without toluene as the dopant for the 15 screened brominated compounds.*

For all of the compounds tested, there was at least an order of magnitude difference between the amount of ions formed with and without toluene (Figure 2-2), indicating the necessity of a photoionizable solvent to facilitate the ionization of the brominated compounds. Additionally, all investigated compounds produced similar amounts of [M + Br]⁻ adduct ions, and were within a three-fold difference of each other (Figure 2-3).
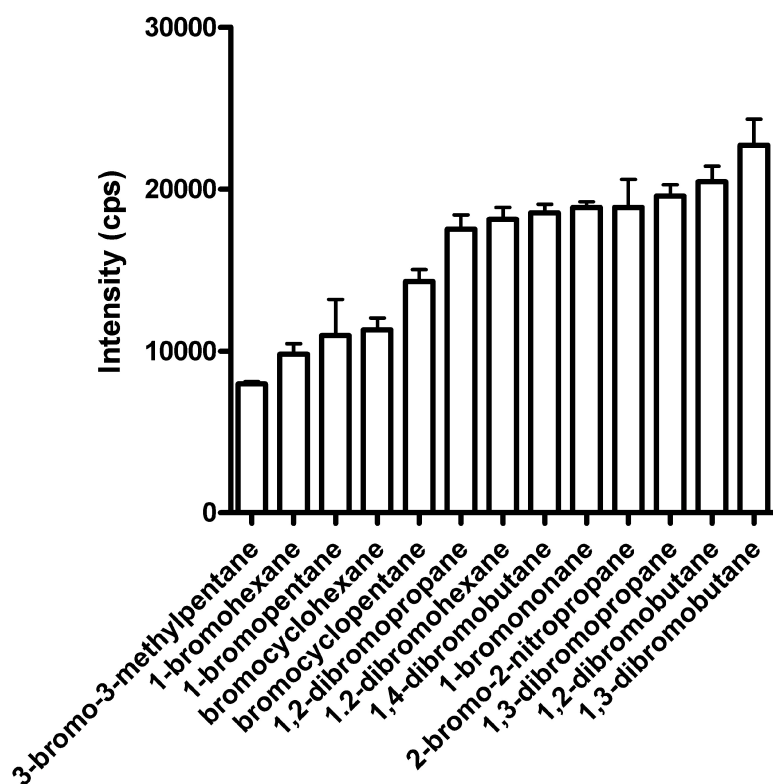
Figure 2-3: The intensity of the $[M+Br]^- \rightarrow Br^-$ multiple reaction monitoring transition for the 15 screened brominated compounds in toluene (1% vol./vol.) with 100 ng mL^{-1} of a 1:1:1 mixture of α-, β-, γ-HBCD. Data represents the mean±standard error.

While selecting compounds to be screened, an attempt was made to choose compounds of varying structures and degrees of bromination. However, it was difficult to determine if there were any trends among the compounds in terms of the amount of bromide ions formed, based on the limited number of compounds investigated this experiment. Furthermore, a comprehensive study of possible bromide sources was beyond the scope of this study. Due to the similarities among compounds, experiments were continued with 1,4-dibromobutane (1,4-DBB), as it was readily available in our lab. Based on other experiments using

1,4-DBB as a bromide source, there was a large excess of Br⁻ ions in the source during HBCD analyses, even at low concentrations of 1,4-DBB (data not shown). Given the similarities in bromide and [M+Br]⁻ formation found among compounds, it is likely that most of the other brominated compounds investigated would have produced such an excess. This may indicate that the structure or choice of brominated compound may be of minor importance in determining the formation of the resulting [M + Br]⁻ ion.

2.3.2 Selection of AA-APPI Carrier Solvent

Previous studies have found that the selection of the photoionization dopant has significant impacts on the analyte intensities in APPI (2,24,28,29). Therefore the influence of the photoionization of the carrier solvent on the formation of Br⁻ ions was investigated. This was done by monitoring the amount of Br⁻ ions formed from the photoionization of 1,4-DBB in various carrier solvents, encompassing a range of ionization potentials (IP, Table 2-2). In addition, anisole, toluene, and acetone have also been shown to impact the ionization of analytes in APPI (2,24,28,29).

Table 2-2: *Ionization potentials of carrier solvents.*

Compound	IP (eV)[a]
1,4-Dibromobutane	10.15
Toluene	8.83
Anisole	8.2
Acetone	9.7
Heptane	9.93
Hexane	10.13
Methanol	10.83

[a] From reference (30)

From these experiments, it was found that the fragmentation of 1,4-DBB and the formation of bromide ions in the source were not dependent simply on the presence of a photoionizable solvent, but was also dependent on the IP of the carrier solvent in which the 1,4-DBB was dissolved. Toluene and anisole, which have the lowest IPs of the selected solvents, produced a significantly higher abundance of bromide ions than the other tested carrier solvents ($p < 0.05$). Following this observation, an inverse relationship was found between the amount of bromide ions produced and the ionization potential of the carrier solvent (Figure 2-4A).
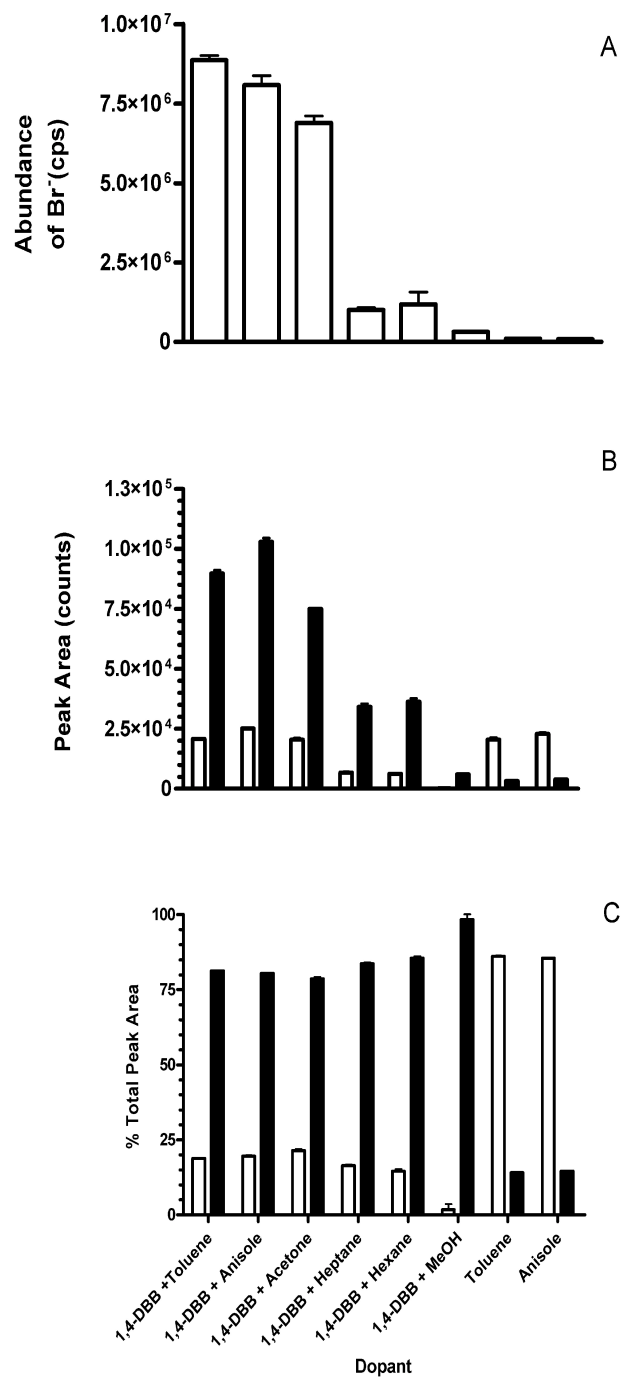
Figure 2-4: *Mean intensity (±standard error) of (A) bromide (m/z 79) and (B) peak areas of [M – H]⁻ and [M + Br]⁻ ions in various possible carrier solvents, and the (C) percentage of total peak area of each ion in the various carrier solvents. Total peak area equals the sum peak area of the [M – H]⁻ and [M + Br]⁻ produced by flow injection analysis. In (B) and (C), [M – H]⁻ is represented by white bars and [M + Br]⁻ is represented as black bars.*

Of the carrier solvents investigated, only toluene, anisole, and acetone have ionization potentials less than the predominant photon energy produced by the krypton lamp used in this study (<10 eV). Therefore, these compounds are able to be ionized and release an electron into the source. However, bromide ions were formed even in the presence of heptane, hexane, and methanol, all solvents with an IP very near or greater than 10 eV. As mentioned earlier, a small proportion of the photons produced may also have energies of 10.6 eV, which is greater than the IP of heptane or hexane. Therefore, some ionization of these compounds may be expected, and may explain the observed formation of bromide in the presence of these solvents. Methanol, however, has an IP of 10.8 eV. The bromide ions detected when using methanol as a carrier solvent may be attributed to the photoionization of 1,4-DBB itself, although this is unlikely given the lack of observation of a positive bromocyclobutane ion (31). Alternatively, the formation of bromide ions in the presence of solvents with IPs greater than 10 eV may be due to the presence of electrons formed from the irradiation of the steel surfaces within the source (32). Furthermore, an electron capture-dissociation mechanism is supported by the lack of finding of either an M^- or $[M - H]^-$ ion in the 1,4-DBB mass spectrum (data not shown), which would have indicated that other ionization processes, such as electron capture or proton transfer, were responsible for the ionization of 1,4-DBB.

Next, the effect of the carrier solvent on the formation of HBCD adducts was investigated. Through FIA experiments, it was discovered that the $[M + Br]^-$

ion was predominantly formed, although a small percentage of [M – H]⁻ ions were formed as well (Figure 2-5). In order to maximize the formation of the [M + Br]⁻ ion while minimizing [M – H]⁻ formation, an investigation of how the ionization potential of the carrier solvent may influence the formation of both [M + Br]⁻ and [M – H]⁻ ions was carried out, using FIA and monitoring the [M – H]⁻ → Br⁻ and [M + Br]⁻ → Br⁻ transitions. As with the previous experiment, there was a significant impact on the formation of [M + Br]⁻ with the use of a photoionizable carrier solvent.
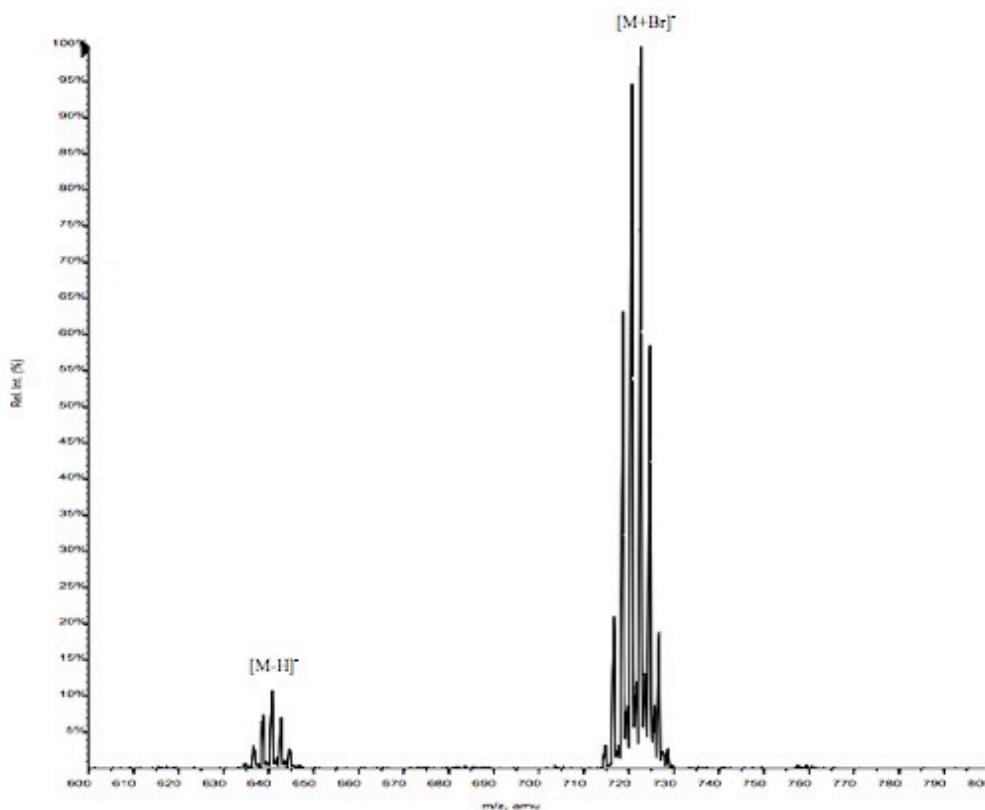
Figure 2-5: *APPI mass spectrum of HBCD diastereomers with 1% (v/v) 1,4-DBB in toluene as the carrier solvent, showing the formation of the [M – H]⁻ (m/z 640.6) and [M + Br]⁻ (m/z 722.6) ions.*

The intensity of the [M + Br]⁻ → Br⁻ transition signal followed the same trend as

seen for the formation of bromide, with toluene and anisole producing the highest signal for the $[M + Br]^-$ → Br^- transition (Figure 2-4B). This observation was not surprising, given that the amount of Br^- initially formed was itself dependent on the solvent used. However, there was little impact on the formation of $[M – H]^-$ ions by the various carrier solvents. There was no significant difference in the percentage of $[M – H]^-$ formed with the use of toluene, anisole or acetone, although all three of these solvents formed a significantly higher percentage of $[M – H]^-$ than did hexane. Moreover, with the exception of methanol, there was a general similarity in the percentage of $[M – H]^-$ formed (Figure 2-4C). No differences were found in the intensity of $[M – H]^-$ ions formed with and without the addition of 1,4-DBB, in either toluene or anisole. Competition between the formation of the adduct ion and the deprotonated analyte ion has been observed previously (8,11). The formation of either $[M – H]^-$ or $[M + Br]^-$ ions is a result of several competing reactions occurring within the source, although this data would indicate that the formation of $[M – H]^-$ occurs independently of the presence of bromide. Given the near-constant intensities of the $[M – H]^-$ ions, it may be that the formation of $[M – H]^-$ occurs quickly until a steady state is reached, at which point unreacted HBCD molecules may form brominated adducts. However, based on the results of this study, the mechanism and kinetics of these competing reactions is unknown, and warrants further investigation. Furthermore, if the formation of the $[M – H]^-$ ion could be suppressed, then an increase in the formation of the $[M + Br]^-$ ion would likely be seen. However, total suppression

of the [M − H]⁻ ion would only add an additional 20% maximum to the [M + Br]⁻
ions formed (Figure 2-4C).

Additionally, the formation of [M − H]⁻ from the in-source fragmentation
of [M + Br]⁻ and subsequent loss of HBr is unlikely. The collision induced
dissociation of the adduct ion at various collisions energies ranging from 10 to 60
eV was investigated, and found that the only ion formed in these experiments was
Br⁻ (data not shown). Therefore, any insource fragmentation would likely result
in the formation of Br⁻ and neutral HBCD. Previous studies have found that the
collision induced dissociation of chloride adducts of HBCD (formed during ESI)
dissociated to form [M − H]⁻. This was not observed in this study, likely due to
the lower gas phase acidity of HBr compared to that of HCl (33,34).

Finally, the concentration of 1,4-DBB in toluene was optimized. The
formation of [M + Br]⁻ was measured at 5 different concentrations of 1,4-DBB,
ranging from 0.05% (v/v) to 2% (v/v). At concentrations greater than 0.1%, there
was no effect of concentration on [M + Br]⁻ formation (Figure 2-6).
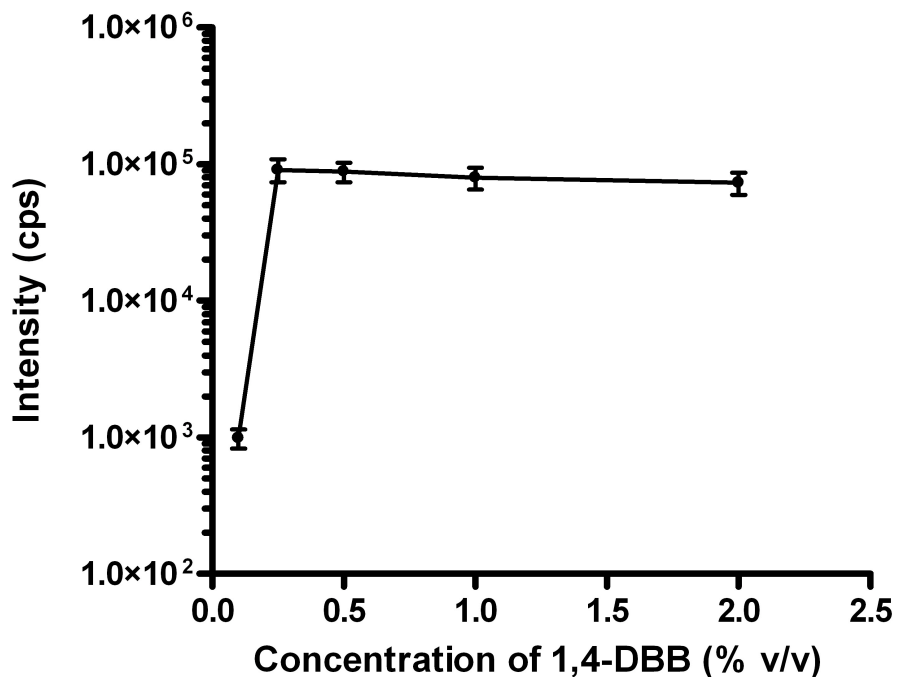
Figure 2-6: *The effect of the concentration of 1,4-dibromobutane in toluene on the intensity of the [M + Br]⁻ → Br⁻ multiple reaction monitoring transition. Data points represent mean ± 1 standard deviation.*

2.3.3 Comparison of Analytical Performance Between APPI-Based Methods

To compare the analytical performance of APPI and AA-APPI, five-point calibration curves, encompassing a concentration range of 3 orders of magnitude (1 ng mL⁻¹ to 1000 ng mL⁻¹ of each racemic diastereomer), were prepared and analyzed in triplicate with each method. Individual enantiomers were separated using an enantioselective LC-MS/MS method (21,22). Individual enantiomers were identified based on the elution order reported by Heeb et al. (14). The peak area of each enantiomer was then fit to a linear regression line. From this, analytical parameters were determined on an enantiomer-specific basis.

93

For all comparisons, the $[M - H]^- \rightarrow 79$ and $[M + Br]^- \rightarrow 79$ transitions were used, as this is the transition most commonly used in the literature. Previous studies that have investigated the use of chloride adducts for the analysis of HBCDs by ESI have used the $[M + Cl]^- \rightarrow [M - H]^-$ transition for detection in MRM mode (35,36). However, through the use of flow injection and infusion experiments, it was found that the only daughter ion formed by the collision induced dissociation of the $[M + Br]^-$ ion was *m/z* 79 and 81.

For all enantiomers, the calibration curves produced by both methods were linear over the concentration ranges examined, with an average r^2 of 0.997 and 0.933 for the AA-APPI and APPI methods, respectively (Table 2-3). However, the average response factors (slope of the regression line) varied, depending on the diastereomer. Using AA-APPI, the γ- and β-HBCD isomers had equivalent response factors, which were more than 5-fold higher than that of the α isomer. Conversely, in APPI, the β isomer had a 3-fold higher response factor than did either the γ or α isomers, which were nearly equivalent. These differences in response factors between isomers and between methods translated into corresponding trends for LODs (Table 2-4), with the γ isomer having the lowest LOD using AA-APPI, which was 4.6 fold lower than the LOD using APPI. The LODs of the α and β isomer, however, were equivalent between the two methods. For both response factors and LODs, there were no differences between enantiomers of an individual isomer, regardless of method.

Table 2-3: *Linear regression results for calibration curves of individual enantiomers produced by APPI and AA-APPI.*

Enantiomer	AA-APPI		APPI
	Equation[1]	r^2	Equation[1]
(-)-α-HBCD	y=17.0x+2.9	0.998	y=6.8x+4.7
(+)-α-HBCD	y=17.4x+3.1	0.997	y=6.3x+5.7
(-)-β-HBCD	y=88.9x+22.5	0.998	y=22.9x+13.7
(+)-β-HBCD	y=88.1x+23.0	0.996	y=21.3x+14.8
(+)-γ-HBCD	y=91.7x+23.7	0.996	y=6.7x+4.8
(-)-γ-HBCD	y=91.4x+18.4	0.997	y=6.4x+4.8

[1]Units of X are ng

It should be noted that, while the LODs of the β and α isomers were similar between APPI and AA-APPI, the peak height response of the α, β, and γ isomers in AA-APPI were 3, 4, and 10 fold higher, respectively, than that of APPI. However, these enhancements in signal did not translate into equivalent decrease in LODs, due to the nearly 5-fold increase in background noise in AA-APPI. This increased noise was likely due to the addition of the 1,4-DBB.

Table 2-4: Analytical performance characteristics of AA-APPI and APPI.

Enantiomer	Limit of detection (LOD)				Limit of quantification (LOQ)			
	AA-APPI		APPI		AA-APPI		APPI	
	Mass (pg)	Standard Dev.	Mass (pg)	Standard Dev.	Mass (pg)	Standard Dev.	Mass (pg)	Standard Dev.
(-)-α-HBCD	459	6	370	101	1380	19	1180	323
(+)-α-HBCD	449	6	390	96	1350	19	1250	308
(-)-β-HBCD	88	2	110	28	264	5	350	88
(+)-β-HBCD	89	2	120	27	266	5	370	86
(+)-γ-HBCD	85	2	370	81	256	5	1180	259
(-)-γ-HBCD	104	2	480	127	311	5	1540	407

The selective enhancement in the LODs of the γ isomer was interesting, as was the observation that the LODs of β and α isomers were only slightly or negligibly increased from APPI to AA-APPI. The enhancement of the γ isomer by AA-APPI may be linked to differences in the physical-chemical properties between diastereomers. For instance, Suzuki et al. (37) found differences between the three diastereomers in terms of cavity diameter, dipole/dipole interactions, and charge density distributions. The differences in charge density distribution were attributed to the higher response of β-HBCD in the formation of the $[M + Cl]^-$ adduct, and may play a role in the differences observed in this study. Furthermore, differences in the octanol-water partition coefficient (K_{ow}) among diastereomers have been reported. Hayward et al. found γ-HBCD to have the largest K_{ow} (and thus the most non-polar) (38), while Mariussen et al. (39) and Goss et al. (40) have found γ-HBCD to be the second most polar diastereomer, after β-HBCD. Due to the uncertainty in the physical properties of HBCD, it is difficult to speculate as to the cause of the increase in response of the γ isomer. Regardless, it is clear that the influence of chemical and physical properties on the ionization of an analyte by AA-APPI requires further investigation.

2.3.4 Matrix Effects

The effects of co-extracted matrix material were evaluated in two ways. First, the extent of ion suppression or enhancement of individual enantiomers was quantified using a post-extraction addition technique. Sediment samples were

extracted and spiked with a 1:1:1 mix of HBCDs prior to analysis. The same mixture of HBCDs was also spiked into methanol, and the resulting peak areas from the spiked sediment samples were compared to those from the methanolic solution. The percentage of ion suppression or enhancement was then quantified:

$$ME=\left(\frac{B}{A}-1\right)x\,100$$

(Equation 2-1)

where A is the peak area of the enantiomer in methanol, and B is the peak area of the enantiomer in the extracted sediment samples. If no suppression or enhancement of the response was occurring, the calculated percentage of matrix effects using the above formula would be zero, whereas percentages less than zero indicate ion suppression is occurring and values greater than zero indicate that the analyte signal is being enhanced.

The analyte signal was generally enhanced for all diastereomers (Figure 2-5). Matrix effects in AA-APPI ranged from -1.5% for (-)-α-HBCD to 5.9% for (+)-α-HBCD, while the average matrix effects across all enantiomers was 2.2%. Similarly, the average matrix effects found in APPI ranged from 1.2% to 19.5%, although with the exception of (+)-γ-HBCD, all were less than a 10% enhancement. Both methods were very precise, with average RSDs of 3.5% and 4.3% for AA-APPI and APPI, respectively.
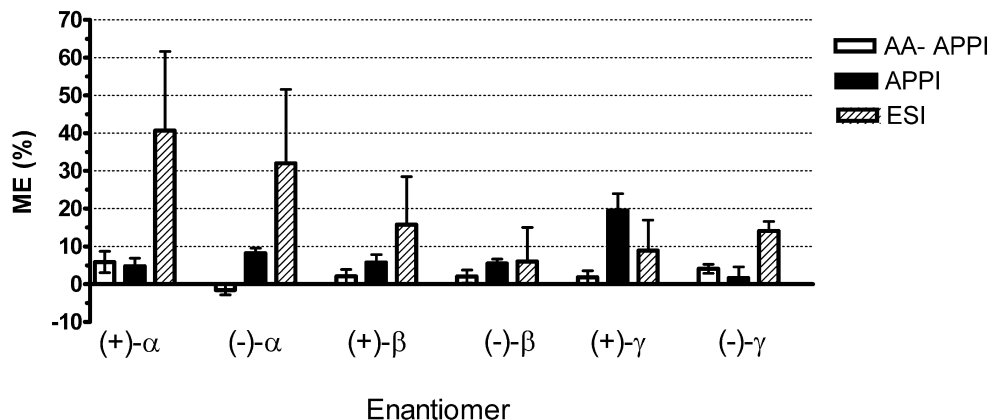
Figure 2-7: *Matrix effects on individual enantiomers in ESI, AA-APPI and APPI. Data represents mean ± standard error.*

For all diastereomers, no differences in the matrix effects between the two enantiomers were observed. In addition, the effect of any HBCDs already present in the sediment extracts prior to spiking may be ruled out, as sediment extracts that remained unspiked were analyzed and found to contain no detectable levels of HBCDs. Therefore, any signal enhancement must be attributed to matrix effects.

To compare these methods to the more commonly used techniques, all of the spiked sediment extracts and methanolic solutions were analyzed by ESI. Matrix effects in ESI ranged from 6.0% to 40.7% (Figure 2-5), values which were similar to matrix effects found in food samples when using chloride adducts to quantify HBCDs by ESI (36). It was clear that both APPI and AA-APPI showed considerable improvement over ESI in regards to matrix effects. The results from this study support many other studies which found a reduction in the matrix

99

effects through the use of APPI compared to ESI (4,6,7).

Secondly, the effect of matrix effects on the quantification of enantiomers was investigated. This was done by determining the enantiomer fractions (EF) (41) of HBCD enantiomers from the same extracts as described previously, and comparing them across the methods. The EF is equal to the peak area of the (+) enantiomer divided by the total peak area of the (+) and (-) enantiomers. It was assumed that the solution spiked into the sediment samples was racemic and that the mass spectral response factor between individual enantiomers is identical. Therefore, any deviations from a racemic EF of 0.5 were attributed to matrix effects.

Previous studies have reported that the EFs found using ESI deviated from 0.5, even in standard solutions containing racemic proportions of HBCD diastereomers (20,21). The non-racemic EFs have been attributed to differential effects of matrix between the two enantiomers or due to the differences in the ionization environment between the two enantiomers during the gradient elution (20,21). The accurate measurement of EFs is essential, as it has been found that even small changes in the measured EF may lead to significant effects on the interpretation of enantiomer-specific data (27).

Using similar chromatography as previous studies, it was found that AA-APPI and APPI produced nearly racemic EFs for all diastereomers (Table 2-5). Enantiomer fractions produced using AA-APPI were racemic for all diastereomers, ranging from 0.492 to 0.507. Using APPI, EFs deviated slightly

from non-racemic and had larger variation than the EFs found using AA-APPI. This can likely be attributed to the low signal-to-noise ratio for these samples and the difficulty accurately fitting peaks under such conditions (24). These results agree with the above post-addition spike data, with the lack of observed matrix effects subsequently leading to more accurate quantification of enantiomers in the samples.

Atmospheric pressure photoionization has previously been demonstrated to produce fewer matrix effects than ESI for the trace analysis of environmental contaminants in biological matrices (42). While only sediment samples were used in the current study, a similar lack of matrix effects for AA-APPI in biological matrices is expected. How biological matrices may affect the measurement of the enantiomer distribution, however, must be investigated further.

Table 2-5: *Enantiomer fractions of HBCD diastereomers in post-extraction spiked certified reference material EC-5 sediment samples.*

	AA-APPI		APPI		ESI	
	EF	Standard Dev.	EF	Standard Dev.	EF	Standard Dev.
α-HBCD	0.507	0.013	0.510	0.017	0.506	0.009
β-HBCD	0.503	0.005	0.516	0.013	0.509	0.025
γ-HBCD	0.492	0.003	0.521	0.016	0.489	0.036

It should be noted that for HBCDs, ESI produced a 5-25 fold lower LOD than either APPI or AA-APPI (data not shown). The ESI LODs were consistent with previous results (20-22). The differences in ionization efficiency of an analyte among the different ionization methods will be based on the physical-chemical properties of the analyte. Despite the decrease in sensitivity compared to ESI that is seen here for HBCDs, analysis by AA-APPI and APPI has been shown be advantageous for some analytes (2-5). Furthermore, the ability to reduce matrix effects and yield more accurate results may offset the reduction in sensitivity for other analytes. While the use of a mass-labeled internal standard may compensate for matrix effects and lead to more accurate quantification of the EF (20), for many compounds, chiral or otherwise, mass-labeled versions are unavailable. For these analytes, the use of APPI or AA-APPI may lead to more accurate quantification of such analytes.

2.4 Conclusions

Through the inclusion of brominated compounds into the dopant flow, a novel method for the formation of adduct species by APPI and the viability of AA-APPI for the analysis of small molecules is demonstrated, using HBCD as a model compound. Lower limits of detection were produced through the use of AA-APPI compared to APPI, particularly for the γ-HBCD isomer. Moreover, AA-APPI was relatively unaffected by matrix effects from extracted sediment, similar to APPI, and considerably less so than ESI. While matrix effects may be

compensated for using isotopically labeled standards, as is the case for HBCDs, there is a lack of such standards available for many environmentally relevant compounds. Therefore, the use of AA-APPI and APPI is an attractive technique to quantify enantiomers in environmental samples for those compounds for which an isotopically labeled standard is unavailable.

2.5 References

(1)   Robb, D.B., Covey, T.R., Bruins, A.P., Atmospheric pressure photoionisation: An ionization method for liquid chromatography-mass spectrometry. Analytical Chemistry, 72 (2000) 3653-3659.

(2)   Itoh, N., Aoyagi, Y., Yarita, T., Optimization of the dopant for the trace determination of polycyclic aromatic hydrocarbons by liquid chromatography/dopant-assisted atmospheric-pressure photoionization/mass spectrometry. Journal of Chromatography A, 1131 (2006) 285-288.

(3)   Riu, A., Zalko, D., Debrauwer, L., Study of polybrominated diphenyl ethers using both positive and negative atmospheric pressure photoionization and tandem mass spectrometry. Rapid Communications in Mass Spectrometry, 20 (2006) 2133-2142.

(4)   Theron, H.B., van der Merwe, M.J., Swart, K.J., van der Westhuizen, J.H., Employing atmospheric pressure photoionization in liquid chromatography/tandem mass spectrometry to minimize ion suppression and

matrix effects for the quantification of venlafaxine and O-desmethylvenlafaxine. Rapid Communications in Mass Spectrometry, 21 (2007) 1680-1686.

(5)   Hakala, K.S., Laitinen, L., Kaukonen, A.M., Hirvonen, J., Kostiainen, R., Kotiaho, T., Development of LC/MS/MS methods for cocktail dosed Caco-2 samples using atmospheric pressure photoionization and electrospray ionization. Analytical Chemistry, 75 (2003) 5969-5977.

(6)   Takino, M., Tanaka, T., Yamaguchi, K., Nakahara, T., Atmospheric pressure photo-ionization liquid chromatography/mass spectrometric determination of aflatoxins in food. Food Additives and Contaminants Part A-Chemistry Analysis Control Exposure & Risk Assessment, 21 (2004) 76-84.

(7)   Marchi, I., Rudaz, S., Selman, M., Veuthey, J.L., Evaluation of the influence of protein precipitation prior to on-line SPE-LC-API/MS procedures using multivariate data analysis. Journal of Chromatography B-Analytical Technologies in the Biomedical and Life Sciences, 845 (2007) 244-252.

(8)   Song, L.G., Wellman, A.D., Yao, H.F., Bartmess, J.E., Negative ion-atmospheric pressure photoionization: Electron capture, dissociative electron capture, proton transfer, and anion attachment. Journal of the American Society for Mass Spectrometry, 18 (2007) 1789-1798.

(9)   Kauppila, T.J., Kotiaho, T., Kostiainen, R., Bruins, A.P., Negative ion-atmospheric pressure photoionization-mass spectrometry. Journal of the American Society for Mass Spectrometry, 15 (2004) 203-211.

(10)   Delobel, A., Roy, S., Touboul, D., Gaudin, K., Germain, D.P., Baillet, A., Brion, F., Prognon, P., Chaminade, P., Laprevote, O., Atmospheric pressure photoionization coupled to porous graphitic carbon liquid chromatography for the analysis of globotriaosylceramides. Application to Fabry disease. Journal of Mass Spectrometry, 41 (2006) 50-58.

(11)   Keki, S., Torok, J., Nagy, L., Zsuga, M., Atmospheric pressure photoionization mass spectrometry of polyisobutylene derivatives. Journal of the American Society for Mass Spectrometry, 19 (2008) 656-665.

(12)   Alaee, M., Arias, P., Sjodin, A., Bergman, A., An overview of commercially used brominated flame retardants, their applications, their use patterns in different countries/regions and possible modes of release. Environment International, 29 (2003) 683-689.

(13)   Covaci, A., Gerecke, A.C., Law, R.J., Voorspoels, S., Kohler, M., Heeb, N.V., Leslie, H., Allchin, C.R., de Boer, J., Hexabromocyclododecanes (HBCDs) in the environment and humans: A review. Environmental Science & Technology, 40 (2006) 3679-3688.

(14)   Heeb, N.V., Schweizer, W.B., Kohler, M., Gerecke, A.C., Structure elucidation of hexabromocyclododecanes - a class of compounds with a complex stereochemistry. Chemosphere, 61 (2005) 65-73.

(15)   Smith, S.W., Chiral toxicology: It's the same thing...only different. Toxicological Sciences, 110 (2009) 4-30.

(16)   Warner, N.A., Martin, J.W., Wong, C.S., Chiral polychlorinated biphenyls are biotransformed enantioselectively by mammalian cytochrome P-450 isozymes to form hydroxylated metabolites. Environmental Science & Technology, 43 (2009) 114-121.

(17)   Buckman, A.H., Wong, C.S., Chow, E.A., Brown, S.B., Solomon, K.R., Fisk, A.T., Biotransformation of polychlorinated biphenyls (PCBs) and bioformation of hydroxylated PCBs in fish. Aquatic Toxicology, 78 (2006) 176-185.

(18)   Wong, C.S., Mabury, S.A., Whittle, D.M., Backus, S.M., Teixeira, C., DeVault, D.S., Bronte, C.R., Muir, D.C.G., Organochlorine compounds in Lake Superior: Chiral polychlorinated biphenyls and biotransformation in the aquatic food web. Environmental Science & Technology, 38 (2004) 84-92.

(19)   Wiberg, K., Letcher, R.J., Sandau, C.D., Norstrom, R.J., Tysklind, M., Bidleman, T.F., The enantioselective bioaccumulation of chiral chlordane and alpha-HCH contaminants in the polar bear food chain. Environmental Science & Technology, 34 (2000) 2668-2674.

(20)   Marvin, C.H., MacInnis, G., Alaee, M., Arsenault, G., Tomy, G.T., Factors influencing enantiomeric fractions of hexabromocyclododecane measured using liquid chromatography/tandem mass spectrometry. Rapid Communications in Mass Spectrometry, 21 (2007) 1925-1930.

(21)   Janak, K., Covaci, A., Voorspoels, S., Becher, G.,

Hexabromocyclododecane in marine species from the Western Scheldt Estuary: Diastereoisomer- and enantiomer-specific accumulation. Environmental Science & Technology, 39 (2005) 1987-1994.

(22)   Dodder, N.G., Peck, A.M., Kucklick, J.R., Sander, L.C., Analysis of hexabromocyclododecane diastereomers and enantiomers by liquid chromatography/tandem mass spectrometry: Chromatographic selectivity and ionization matrix effects. Journal of Chromatography A, 1135 (2006) 36-42.

(23)   McCulloch, R.D., Robb, D.B., Blades, M.W., A dopant introduction device for atmospheric pressure photoionization with liquid chromatography/mass spectrometry. Rapid Communications in Mass Spectrometry, 22 (2008) 3549-3554.

(24)   Kauppila, T.J., Kostiainen, R., Bruins, A.P., Anisole, a new dopant for atmospheric pressure photoionization mass spectrometry of low proton affinity, low ionization energy compounds. Rapid Communications in Mass Spectrometry, 18 (2004) 808-815.

(25)   Marvin, C.H., Tomy, G.T., Alaee, M., MacInnis, G., Distribution of hexabromocyclododecane in Detroit River suspended sediments. Chemosphere, 64 (2006) 268-275.

(26)   de Boer, J., Allchin, C., Law, R., Zegers, B., Boon, J.P., Method for the analysis of polybrominated diphenylethers in sediments and biota. TRAC-Trends in Analytical Chemistry, 20 (2001) 591-599.

(27)   Asher, B.J., D'Agostino, L.A., Way, J.D., Wong, C.S., Harynuk, J.J., Comparison of peak integration methods for the determination of enantiomeric fraction in environmental samples. Chemosphere, 75 (2009) 1042-1048.

(28)   Smith, D.R., Robb, D.B., Blades, M.W., Comparison of dopants for charge exchange ionization of nonpolar polycyclic aromatic hydrocarbons with reversed-phase LC-APPI-MS. Journal of the American Society for Mass Spectrometry, 20 (2009) 73-79.

(29)   Robb, D.B., Smith, D.R., Blades, M.W., Investigation of substituted-benzene dopants for charge exchange ionization of nonpolar compounds by atmospheric pressure photoionization. Journal of the American Society for Mass Spectrometry, 19 (2008) 955-963.

(30)   Sunagawa, T., Shimamori, H., Temperature dependence of low-energy electron attachment to $CHCl_3$. International Journal of Mass Spectrometry, 205 (2001) 285-291.

(31)   Staley, R.H., Wieting, R.D., Beauchamp, J.L., Carbenium ion stabilities in gas-phase and solution - ion-cyclotron resonance study of bromide transfer-reactions involving alkali ions, alkyl carbenium ions, acyl cations, and cyclic halonium ions. Journal of the American Chemical Society, 99 (1977) 5964-5972.

(32)   Basso, E., Marotta, E., Sergalia, R., Tubaro, M., Traldi, P., On the formation of negative ions in atmospheric pressure photoionization conditions.

Journal of Mass Spectrometry, 38 (2003) 1113-1115.

(33)   Zhu, J.H., Cole, R.B., Formation and decompositions of chloride adduct ions, [M+Cl]$^{(-)}$, in negative ion electrospray ionization mass spectrometry. Journal of the American Society for Mass Spectrometry, 11 (2000) 932-941.

(34)   Cole, R.B., Zhu, J.H., Chloride anion attachment in negative ion electrospray ionization mass spectrometry. Rapid Communications in Mass Spectrometry, 13 (1999) 607-611.

(35)   Galindo-Iranzo, P., Quintanilla-Lopez, J.E., Lebron-Aguilar, R., Gomara, B., Improving the sensitivity of liquid chromatography-tandem mass spectrometry analysis of hexabromocyclododecanes by chlorine adduct generation. Journal of Chromatography A, 1216 (2009) 3919-3926.

(36)   Gomara, B., Lebron-Aguilar, R., Quintanilla-Lopez, J.E., Gonzalez, M.J., Development of a new method for the enantiomer specific determination of HBCD using an ion trap mass spectrometer. Analytica Chimica Acta, 605 (2007) 53-60.

(37)   Suzuki, S., Hasegawa, A., Determination of hexabromocyclododecane diastereoisomers and tetrabromobisphenol A in water and sediment by liquid chromatography/mass spectrometry. Analytical Sciences, 22 (2006) 469-474.

(38)   Hayward, S.J., Lei, Y.D., Wania, F., Comparative evaluation of three high-performance liquid chromatography-based K-ow estimation methods for highly hydrophobic organic compounds: Polybrominated diphenyl ethers and

hexabromocyclododecane. Environmental Toxicology and Chemistry, 25 (2006) 2018-2027.

(39)   Mariussen, E., Haukås, M., Arp, H.P.H., Goss, K.U., Borgen, A., Sandanger, T.M., Relevance of 1,2,5,6,9,10-hexabromocyclododecane diastereomer structure on partitioning properties, column-retention and clean-up procedures. Journal of Chromatography A, 1217 (2010) 1441-1446.

(40)   Goss, K.U., Arp, H.P.H., Bronner, G., Niederer, C., Partition behavior of hexachlorocyclohexane isomers. Journal of Chemical and Engineering Data, 53 (2008) 750-754.

(41)   Harner, T., Wiberg, K., Norstrom, R., Enantiomer fractions are preferred to enantiomer ratios for describing chiral signatures in environmental analysis. Environmental Science & Technology, 34 (2000) 218-220.

(42)   Chu, S., Letcher, R.J., Analysis of fluorotelomer alcohols and perfluorinated sulfonamides in biotic samples by liquid chromatography-atmospheric pressure photoionization mass spectrometry. Journal of Chromatography A, 1215 (2008) 92-99.

Chapter 3

Enantioselectivity of Polychlorinated Biphenyl Atropisomers in Sediment and Biota from the Turtle/Brunswick River Estuary, Georgia, USA

3.1 Introduction

Due to their persistence within the environment, polychlorinated biphenyls (PCBs, Figure 1-2) continue to pose risks to humans and biota more than 30 years after their use was discontinued. High concentrations of PCBs are still found in some environmental compartments. In aquatic environments, their hydrophobicity causes PCBs to partition into sediments, where they may be taken up by lower trophic level organisms and enter the food web.

Microbially-mediated reductive dehalogenation is one possible transformation process for highly chlorinated PCBs in anaerobic sediments. Sediment microbes remove chlorine atoms from highly chlorinated congeners, resulting in an enrichment of lower chlorinated congeners in the environment (1). The presence of *in situ* dechlorination activity can be inferred by analyzing congener and homolog patterns in sediments and comparing those to congener and homolog patterns found in the original Aroclor mixtures (2-4). While such techniques provide strong evidence for microbial activity, they do no necessarily prove that it exists, as changes in congener patterns may also result from vaporization or selective sorption. Furthermore, dechlorination rates may also be sufficiently slow to make it difficult to detect changes in the congener patterns over short durations of time.

The use of enantioselective analytical techniques and the detection of non-racemic proportions of chiral molecules can provide unequivocal evidence for biological activity. Nineteen of the 209 PCB congeners are chiral and exist in the

environment as stable atropisomers (5). These congeners were released into the environment as racemic mixtures, and although individual enantiomers possess identical physical and chemical properties, non-racemic distributions of PCB enantiomers have been found in sediment and biota samples (6,7). Biological processing may change the enantiomer distribution of a compound within the environment due to differential interaction between enantiomers with other chiral molecules, such as proteins. Previous studies have found that dechlorination of PCBs by sediment microbes and *in vivo* biotransformation by biota can occur in an enantioselective manner (8-12). Therefore, the use of enantioselective analysis and the detection of non-racemic enantiomer distributions provides a sensitive means of detecting and tracing biologically-mediated processes, for instance the presence of microbial dehalogenation activity, that may otherwise be difficult to detect using achiral methods (13,14).

The LCP Chemicals Superfund site, a marshfront industrial site located on the margins of the Turtle/Brunswick estuary in southeastern Georgia, USA (Figure 3-1), was home to an oil refinery, a power plant, and a paint manufacturing plant over the past 70 years. Most recently, a chlor-alkali plant operated on the site from 1955 to 1994. During this time, industrial wastes were discharged directly into the surrounding marsh areas known as Purvis Creek. This resulted in the sediment from the marsh and creek areas surrounding the LCP site being highly contaminated with mercury and Aroclor 1268, an uncommon PCB formulation comprised primarily of octa- to decachlorinated biphenyls (Table 3-1) (15).
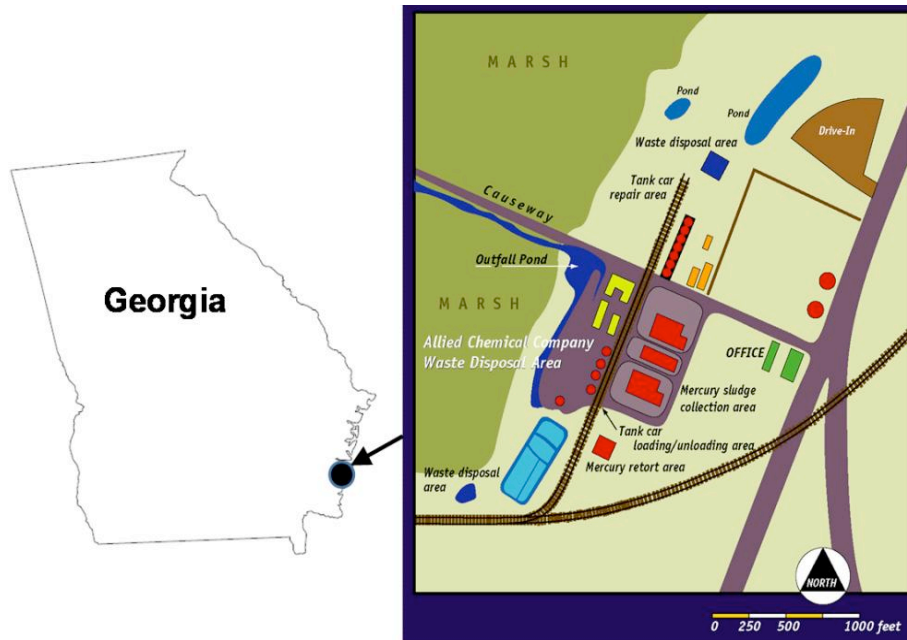
Figure 3-1: Map of the study area.

Previous studies on the site have found that the highly chlorinated PCBs are bioavailable to organisms, which has also resulted in widespread contamination of local biota (16,17). However, due to the recalcitrance of these congeners, these studies were not designed to investigate whether biotransformation was occurring, either in sediments or biota.

Table 3-1: *Polychlorinated biphenyl relative homolog distributions (%) in Aroclor 1268 and marsh sediments from the LCP Superfund site, Brunswick, GA.*

Homolog	Aroclor 1268[a]	Marsh Sediment[ab]
di-	0	0
tri-	0.006	0.16
tetra-	0.12	0.30
penta-	0.19	1.57
hexa-	4.38	7.2
hepta-	10.1	14.6
octa-	45	33.1
nona-	35	37.9
deca-	4.8	5.2

[a] Data from (15)

[b] Average of left and right south marsh transect.

In this study, the enantiomer distribution of seven chiral PCB congeners was analyzed in sediment cores from the contaminated estuary around the LCP Superfund site to determine whether or not microbial dechlorination was occurring at this site. Additionally, the high proportion of heptachlorinated biphenyls found in biota at this site provide a unique opportunity to investigate the enantioselective behavior of highly chlorinated PCB homologs. Therefore, enantiomer distributions were determined in invertebrates, fish species, and resident dolphins to determine the extent of enantioselective biotransformation

occurring within these species. This study provides insight into the biological processing occurring at the LCP Superfund site, and allows for a further understanding of the environmental behavior of highly chlorinated PCBs.

3.2 Materials and Methods

3.2.1 Sample Collection

Three sediment core samples were collected using a polyvinylchloride push core (7.6 cm diameter × 61 cm length) from two areas of the intertidal marsh (Figure 3-1). Intact cores were sealed with end caps lined with solvent-rinsed aluminum foil and were sectioned using solvent-rinsed stainless implements upon return to the lab. All sediment samples were stored frozen at -20°C in pre-cleaned glass (I-Chem) jars prior to analysis. The south marsh area (cores NSM and LCP) is located adjacent to waste pits on the LCP Superfund site, and is characterized by high concentrations of PCBs and mercury (15,18). A causeway bisects the marsh area, and sediments collected from the north side of the causeway (core 311A) contain significantly lower concentrations of PCBs.

Biota was collected from various locations around the LCP site in an effort to represent the basic trophic levels of the local estuarine food web. Grass shrimp (*Palaemonetes pugio*), an abundant crustacean macroinvertebrate in estuaries of this region, were collected from Purvis Creek by dip netting (16). Silver perch (*Bairdiella chrysoura*), spot (*Leiostomus xanthurus*), spotted seatrout (*Cynoscion*

nebulosus), and striped mullet (*Mugil cephalus*) were collected from Purvis Creek by trawl, gill and cast netting (19). These fish species were collected to represent likely prey items of the bottlenose dolphins (*Tursiops truncatus)*, the predominant marine mammal species that frequent the region's estuaries (20). Blubber samples from free ranging bottlenose dolphins were collected from the Turtle/Brunswick estuary by means of a dart biopsy (20,21).

3.2.2 Sample Analysis

The procedures for the extraction and achiral analysis of sediment and biota samples have been described in detail elsewhere (16,19,20,22). Briefly, sediment samples were extracted by Soxhlet extraction in CH_2Cl_2 and cleaned up by activated silica column chromatography, followed by sulfur removal by activated copper. Whole-body composite grass shrimp samples were extracted similarly, but cleaned up by Florisil® column chromatography. Composite fish samples (~5g) and dolphin blubber samples (0.5-1.0 g) were extracted in triplicate with CH_2Cl_2 using a Dionex 200 ASE system (Salt Lake City, UT). Lipids were removed by gel permeation chromatography, and the fraction containing the PCBs was subsequently cleaned up on a glass column packed with 1% water-deactivated Florisil® (Fisher Scientific, Fair Lawn, NJ, USA).

Total PCB analysis was carried out by GC coupled to an electron capture detector. A DB-1 (30 m × 0.25 mm × 0.25 μm d_f, J&W Scientific, Folsom, CA,

USA) or DB-XLB (30 m × 0.25 mm × 0.25 μm d_f, J&W Scientific) fused silica column was used for separation of individual PCB congeners (16,19,20,22).

Enantioselective analysis was performed on an Agilent 5890 GC-MS using electron impact ionization (EI) and selected ion monitoring (SIM). Separation of enantiomers was achieved using multiple chiral columns and previously published conditions (23,24). A Chirasil-Dex column (25 m × 0.25 mm i.d. × 0.25 μm d_f, Varian, Walnut Creek, CA, USA) was used for the separation of PCBs 91, 95, 136, 149, 174 and 176, and results were confirmed on a Cyclosil-B column (30 m × 0.25 mm × 0.25 μm d_f, J&W Scientific). A BGB-172 column (30 m × 0.25 mm × 0.18 μm d_f, Analytik, Adiswil, Switzerland) was used for the separation of PCBs 132 and 183.

In order to assure that no coelutions with other PCB homologs was occurring, all columns were calibrated with standard solutions containing all 209 PCB congeners (24). In addition, results of the enantiomer separations of PCBs 91, 95, 136, 149 and 176 were compared between the Chirasil-Dex and Cyclosil-B columns. Data points with enantiomer fractions (see below) that were not in agreement between the two columns within ±0.032, based on the 95% confidence interval of repeated measurements of racemic standards on these columns (14), were assumed to have interferences and were removed from the data set. Replicate injections of standards yielded racemic compositions for all congeners, with EFs ranging from 0.495 to 0.505.

3.2.3 Data Analysis

For enantiomer analyses, all peaks were integrated using model-fitting software (PeakFit v.4.0, Systat, San Jose, CA, US) to allow for more accurate quantification of partially coeluting peaks (25).

Results are expressed as enantiomer fractions (EFs), which are used to quantify the stereoisomer distribution of a sample (26). The EF is defined as the peak area of the first eluted enantiomer (E1) divided by the sum area of both enantiomers for those congeners where the elution order of the enantiomers on a particular column is unknown (PCBs 95 and 183). However, if the elution order is known (all other congeners), then the EF was determined using the peak area of the (+) enantiomer divided by the sum peak area of the (+) and (-) enantiomers.

Comparisons amongst all groups (standards, sediment, and biota) were carried out by one-way analysis of variance (ANOVA) with $\alpha=0.05$.

3.3 Results and Discussion

3.3.1 Sediment Cores

All PCB congeners investigated were found in non-racemic proportions in at least one of the sediment core samples (Figure 3-2). PCBs 183, 174, and 136 were non-racemic in all cores and at all depths. PCB 149 was generally racemic, but was found to be non-racemic in two cores (311A, 12 cm; NSM, 15 cm). Likewise, PCB 91 was only non-racemic at a single depth (North Marsh, 7 cm). Lower chlorinated congeners (<6 chlorines) were found sporadically within the

cores, and were detectable at some depths, but not others. Heptachlorinated congeners, with the exception of PCB 176 in the North Marsh core, were detectable in all cores. The measurement of non-racemic EFs in sediment samples indicates that biotransformation has occurred within the marsh sediments. Biotransformation was likely the result of microbially-mediated reductive dechlorination, given the anaerobic conditions of the sediment at these depths. Previous studies have concluded that microbial dechlorination activity towards Aroclor 1268 (27) and higher PCB homologs in general (28) is limited.
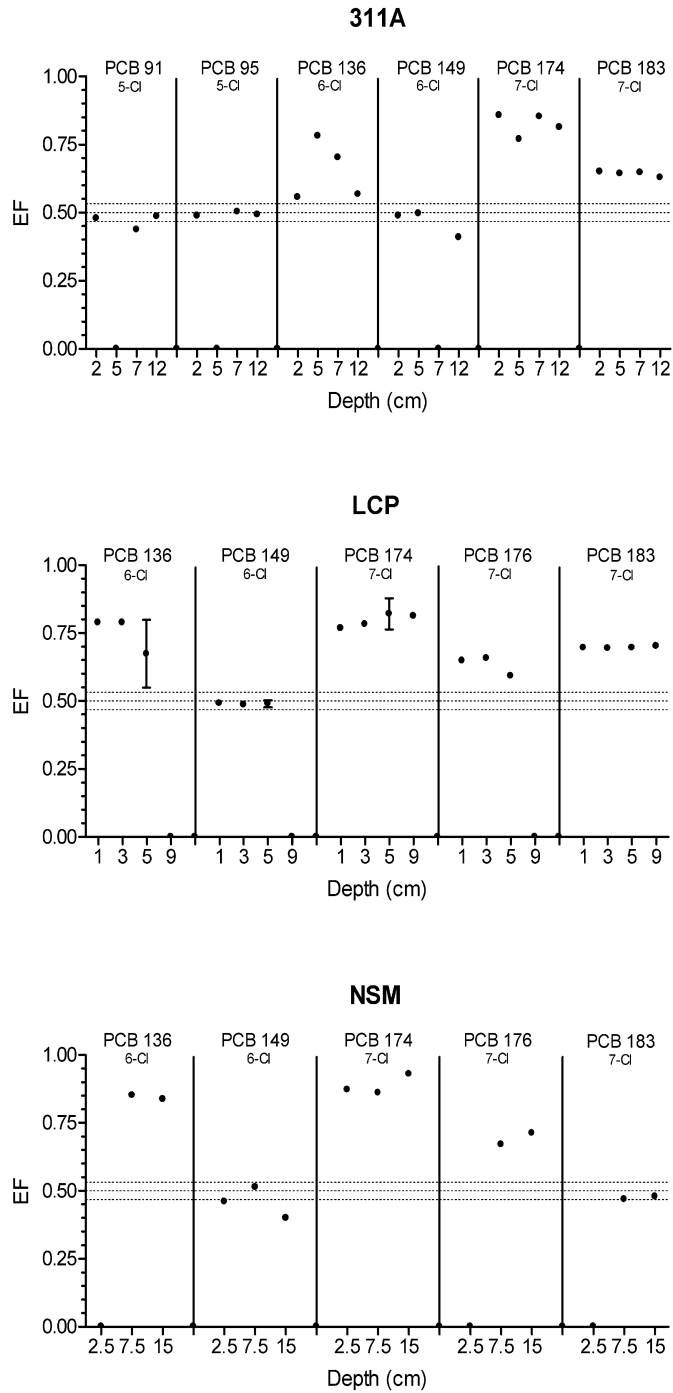
Figure 3-2: *Enantiomer fractions (EFs) at various depths in sediment cores collected from north marsh area (311A) and south marsh areas (LCP and NSM) from the LCP Superfund site in Georgia. Horizontal dashed lines represent the racemic EF value of 0.5 and the 95% confidence interval of racemic standards (±0.032). Numbers below congener names represent degree of chlorination.*

Microcosm studies investigated the dechlorination activity of microbes in sediments from the marsh area and found significant dechlorination of the primer (2,3,4,5,6-pentachlorobiphenyl), indicating that microbial dechlorination at this site is possible (27). However, during a 1-yr incubation period, no measurable decrease in the concentration of hexa- to decachlorinated biphenyls was found (27). This was attributed to the high concentrations of heavy metals found at this location or the reduced bioavailability of the more highly chlorinated congeners, rather than a limitation in the dechlorination capability of the sediment microbes (15,27). The formation of non-racemic EFs in the sediment confirms that even congeners with more than six chlorines were bioavailable to microbes, and that microbial dechlorination had occurred at this site.

For all cores, there was little change in EF with depth, and no correlation between total PCB concentrations and EF. Furthermore, despite differences in total PCB concentrations, EFs among the locations were similar, regardless of depth. PCB 136 is an exception, with a spike in enantiomer enrichment in the north marsh core, and a decrease in enrichment in the south marsh core. Wong et al. (13) found EFs to vary with depth in sediment cores from Lake Hartwell, SC, and in some instances, found reversals in the EF for some congeners. No reversals in EF were found in this study, possibly indicating a consistency in the microbial communities at different depths. Alternatively, the lack of any variation in EF with depth in this study may be due to a cessation of microbial dechlorination activity in the sediments. The decline or cessation of reductive

dechlorination activity over time has been found in other sediment cores from other locations (2,13,29,30), and the lack of reductive dechlorination found in previous studies from this site may be attributable to this decline in activity.

The non-racemic quantities of PCBs 91, 136, 174, 176 and 183 in the sediments is indicative that these congeners were either being degraded or formed enantioselectively. The preference for microbes to degrade one enantiomer over the other under anaerobic conditions has been previously shown in controlled microcosm studies (11). The direction and magnitude of enantioselective microbial degradation of PCB congeners occurs in a site-specific manner *in situ*. EFs of PCB 91 in the sediment cores were found to be of similar magnitude and direction of enrichment to that which had previously been seen in the Housatonic River and Lake Hartwell, but opposite of that seen in the Hudson River (7). In addition, PCB 95, which was found to be racemic in this study, was extremely enriched in the second eluted enantiomer in microcosm studies and sediment cores from Lake Hartwell (11,13).

Literature data for the enantioselective dechlorination of more highly chlorinated congeners is sparse. Non-racemic EFs of PCB 174 and 176 have been measured in several sites across the US, and in sediment cores from Lake Hartwell, SC (7,13). For PCB 174, all of these locations were found to be slightly enriched in the (+)-enantiomer. Surficial sediment samples from Lake Hartwell, however, contained highly non-racemic EFs of PCB 174 (EF=0.788, converted from enantiomer ratio) in a single site (7), which is more closely in line with the

EFs observed in this study. Enantiomer fractions of PCB 176 are generally enriched in the (-)-enantiomer, the exception being Lake Hartwell sediment, which was slightly enriched in the (+)-enantiomer (7). Observations of PCB 183 in non-racemic proportions are limited, with only two observations occurring in the White River Basin of Indiana, and in Hudson River Sediment Standard Reference Material (SRM 1939a) (7,31). All of the EFs observed to date for PCB 183 show only a slight enrichment, which is in stark contrast to the results seen in this study, which found sediment samples to be highly enriched in the first eluting enantiomer. Such differences in the magnitude and direction of EF shifts among sites has been attributed differences in species and/or activities of the microbial communities found at those sites (7,13).

A key difference between this and previous studies is the environment in which the sediments were collected. Most other studies investigated sites in freshwater environments, which may differ significantly in the microbial populations from those in saltwater or estuarine environments. In particular, sulfate reducing bacteria are much more abundant in estuarine and marine sediments compared to freshwater environments. Non-racemic EFs of PCBs 95 and 149 have been found in the Hudson River estuary, although their presence was attributed to the transport of contaminated sediment containing non-racemic EFs from the upper Hudson River (32). A lack of enantioselective biodegradation has been found in marine sediments for chlordanes and toxaphene congeners (33,34), which may imply that marine microorganisms lack the ability to degrade

chlorinated organic pollutants enantioselectively. These results contrast this, with the finding of non-racemic EFs, particularly of more highly chlorinated congeners, in the estuarine sediment from this location.

In general, reductive dechlorination pathways favor the removal of flanked *meta* and *para* chlorines first, resulting in decreased abundance of highly chlorinated congeners, and an increase in the less chlorinated congeners (1). A number of dechlorination pathways or processes have been determined to occurring the environment. These processes are characterized and identified based on the homolog and position on the biphenyl ring targeted for dechlorination (1). Individually characterized processes have been given letter names for identification. Based on Palekar et al. (27), several reductive dechlorination pathways may be occurring at this site. The dechlorination of 2,3,4,5,6-pentachlorobiphenyl in sediments from this site followed two dechlorination pathways, depending on whether 2,3,4,5,6-pentachlorobiphenyl was initially *meta*- or *para*-dechlorinated. The *meta*-initiated route appears to proceed through process N, which preferentially removes flanked *meta*-chlorines from penta- to nonachlorinated biphenyls. Processes P and H may also be occurring at this site, as both processes remove flanked *para* chlorines from tetra- to heptachlorinated biphenyls.

The use of enantioselective analysis alone makes it difficult to conclude which dechlorination processes were occurring. The enantioselective dechlorination of several congeners in this study may yield the formation of other

chiral congeners in non-racemic amounts; for example, the formation of PCBs 91 or 95 from PCB 149 (7). These chiral daughter congeners may in turn be enantioselectively degraded, making it difficult to determine whether the non-racemic EFs observed for a particular congener arose from enantioselective formation or degradation. Therefore, observation of a non-racemic parent congener and non-racemic daughter compound does not necessarily mean that conversion of a chiral parent to a chiral daughter congener has occurred. However, the use of chiral analysis and the comparison of possible parent-daughter congeners does make it possible determine which processes are **not** occurring at a particular site.

This can be exemplified at this site, where enantioselective analysis suggests that it is unlikely that the reductive dechlorination of the more highly chlorinated congeners proceeds through the preferential removal of flanked *para* chlorines. The removal of a flanked *para* chlorine from PCB 183 would have formed PCB 149, which was found to be racemic, and which in turn can form PCBs 91 or 95. The observation of non-racemic proportions of PCB 183 and racemic proportions of PCB 149 indicate that this dechlorination pathway is not occurring, as the *para* dechlorination of PCB 183 would have yielded non-racemic proportions of PCB 149, even if this process itself were not enantioselective.

Furthermore, it would appear that process H, which removes doubly flanked *meta* chlorines (1) was not active at this site. The reductive

127

dechlorination of PCB 174 by this process would also have yielded PCB 149. PCB 174 was found in non-racemic proportions, and therefore, dechlorination by process H would have yielded non-racemic proportions of PCB 149. The observation of racemic proportions of PCB 149 can eliminate process H as a likely dechlorination pathway occurring at this location. Based on this, it seems unlikely that the formation of PCB 183 from the removal of a doubly flanked *meta* chlorine from chiral PCB 196 was occurring. The *para*-dechlorination of PCB 196 could also lead to the formation of PCB 174 (7). PCB 196 is a major component of Aroclor 1268, and is found in high concentration at this site (15). Therefore the dechlorination of this congener may be a significant pathway leading to the formation of lower chlorinated congeners. Kuipers et al. (28) have reported that the only heptachlorinated biphenyl metabolite formed from the dechlorination of PCB 196 was PCB 183. PCB 196 is also the most highly chlorinated chiral congener present in the environment. However, despite published methods on the separation of PCB 196 (24,35), insufficient separation was achieved of individual enantiomers from other coeluting octachlorinated biphenyls to accurately quantify the enantiomer distribution. It is therefore unknown whether or not PCB 196 has been enantioselectively degraded, and whether the non-racemic proportions of PCB 183 were due to enantioselective formation or degradation.

The non-racemic proportions of PCB 91 observed in this study are most likely due to enantioselective degradation. PCB 91 may be formed from the

removal of a doubly flanked *meta* chlorine from PCB 132, the removal of a *meta* chlorine from PCB 149, or the removal of a *para* chlorine from achiral PCB 139. However, as discussed earlier, PCB 149 was found to be racemic, and thus would not form non-racemic quantities of PCB 91. Furthermore, the removal of doubly flanked *meta* chlorines has already been shown to likely not be occurring at this site. This is further suggested by the two measurements of PCB 132, which were both found to be racemic (EF=0.496, data not shown). Therefore, the likely degradation pathway for PCB 91 is through meta dechlorination to form PCB 51. A similar pathway was observed in Lake Hartwell microcosms, where PCB 132 was found to remain racemic throughout the incubation period, despite a decrease in concentration and the concurrent formation of non-racemic PCB 91 and PCB 51 (11).

In summary, it would appear that neither *para* dechlorination nor dechlorination of doubly flanked *meta* chlorines from penta- to heptachlorinated congeners was occurring in sediments at this site. This is not to say that these two processes were not occurring with lower chlorinated congeners. Without detailed congener-specific characterization, however, it is difficult to conclusively say which reductive dechlorination processes are occurring at the LCP site, as it is possible for mixed populations of bacteria to cohabitate the same area, and thus lead to multiple dechlorination pathways occurring (3). Results from this study do strongly indicate, however, that microbial reductive dechlorination was occurring at the LCP site.

3.3.2 Biota

Non-racemic quantities of three PCB congeners (PCBs 136, 174, and 183) were observed in grass shrimp (Figure 3-3), whereas, in contrast, PCB 149 was found to be racemic. For all congeners, the EFs measured in shrimp did not vary significantly from the EFs found in the sediment, indicating that the observed non-racemic EFs likely resulted from uptake of non-racemic proportions of PCBs from the sediment, rather than *in vivo* biotransformation. Results from this study are in line with previous studies that found a lack of enantioselective biotransformation capability in marine crustaceans, both for PCBs and other chlorinated organic contaminants. However, freshwater crustaceans (*Mysis relicta*) were shown to be capable of eliminating PCBs enantioselectively, both in the field and in laboratory studies (9,14). Results from this study would suggest that grass shrimp are unable to bioprocess PCBs in an enantioselective manner, or that such as process is overwhelmed by uptake of racemic proportions of PCBs via the diet. Furthermore, our results do not preclude the possibility that achiral biotransformation and/or elimination is occurring.
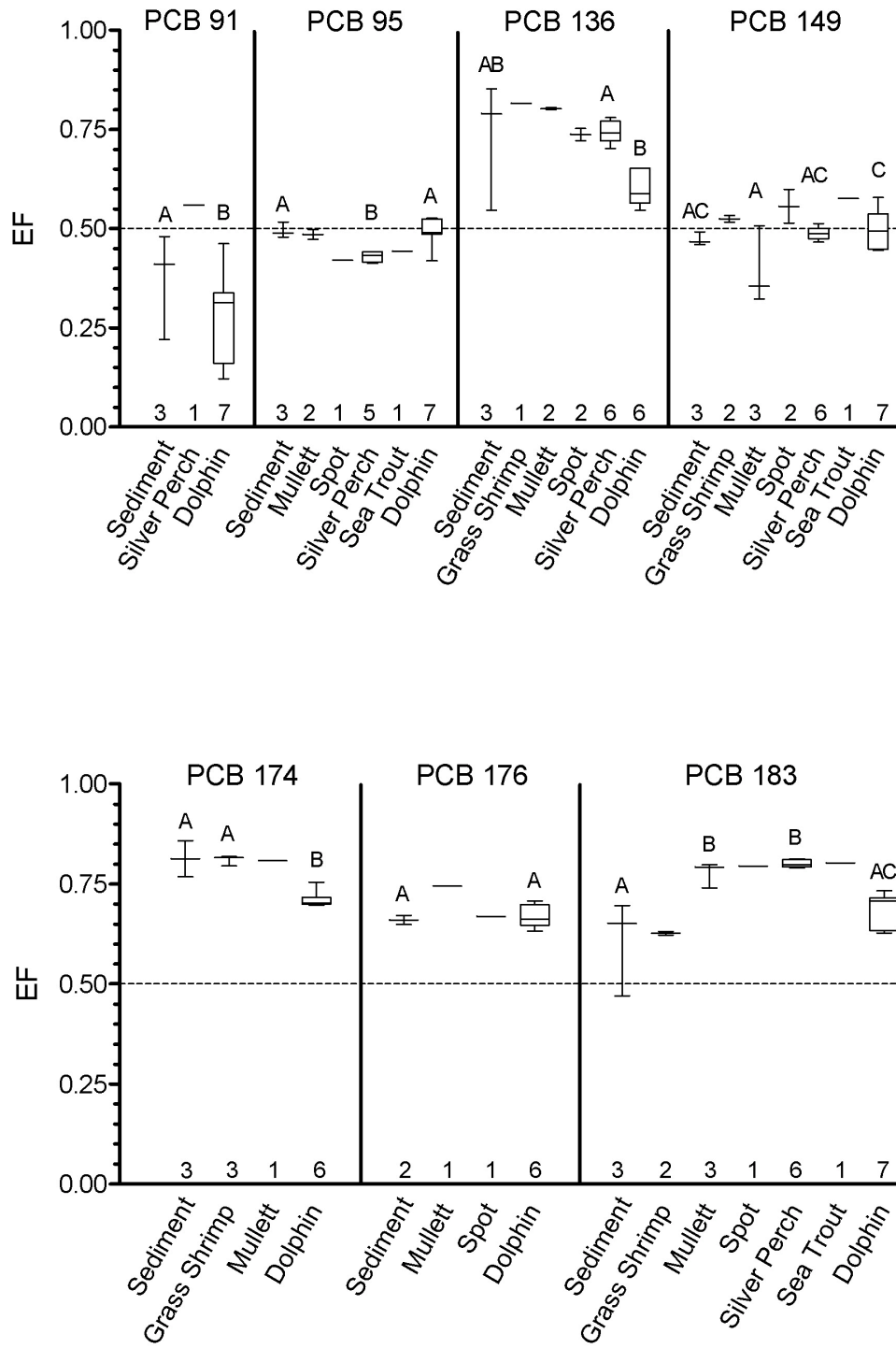
Figure 3-3: *Box and whisker plots of enantiomer fractions (EFs) in sediment and biota from the Turtle/Brunswick estuary. Numbers above X-axis represent number of samples. For a particular congener, samples with the same letters above them are not statistically different from one another.*

Fish species from the Purvis Creek, near the LCP Superfund site, are all heavily contaminated with PCBs and other organochlorine contaminants. The congener profiles are dominated by octa- to decachlorinated biphenyls, and are indicative of contamination by Aroclor 1268 (19,22). All fish species were found to contain non-racemic proportions of PCBs, and for most congeners, EFs amongst species were similar (Figure 3-3). The exceptions to this, however, were PCBs 95 and 149. PCB 95 was found to be racemic in striped mullet, but significantly enriched in the second eluted enantiomer in silver perch. All species, with the exception of mullet, contained racemic proportions of PCB 149. Composite mullet samples were significantly enriched in (-)-PCB 149. For all other congeners, there were no differences in the EFs amongst species. These similarities would indicate similarities in uptake and/or biotransformation of PCBs amongst these four species, which is supported by of a lack of discernible difference amongst species in PCB conger profiles (19).

The measurement of non-racemic proportions of PCBs within an organism does not, in and of itself, indicate that biotransformation within the organism is occurring. Exposure and subsequent uptake of non-racemic quantities of PCBs, followed by non-enantioselective or no biotransformation may also lead to non-racemic EFs in an organism (33). In order to ascertain whether or not biotransformation was occurring, enantiomer distributions within an organism must be compared to that of its exposure source. Due to the low number of detectable congeners in grass shrimp, fish EFs were compared to those found in

132

the top layer of the sediment cores, as this likely represents the distribution of enantiomers to which the base of the food web is exposed to. The exception to this was the NSM core, which lacked detectable levels of several congeners in the uppermost layer. Due to the constancy of the EFs measured in the cores, the top most layer with detectable levels of PCBs 91, 95, 136, 176, and 183 (generally 8-10 cm) were used for statistical testing.

Significant differences between sediment and fish EFs were found only for PCBs 95 and 183, indicating that these species may be biotransforming these congeners enantioselectively. Racemic proportions of PCB 95 were found in mullet, while EFs in perch were enriched in the second eluted enantiomer of PCB 95 and significantly different from those found in sediment. A slight enrichment in the second eluted enantiomer of PCB 95 was also detected in spot and seatrout, although EFs were only measurable in single samples of each species, and consequently enrichment of this congener should be interpreted with caution. An opposite trend was found for PCB 149, with mullet being significantly more enriched in (-)-PCB 149, with all other fish species mirroring EFs found in the sediment. Thus, mullet appeared unable to biotransform PCB 95 enantioselectively, but are able to biotransform PCB 149 in a enantioselective manner.

Fish species are generally considered to have low biotransformation capacity towards PCBs, although they have been found to biotransform some congeners enantioselectively (8,12,36). Field studies have found non-racemic

EFs of congeners in fish species that differed from those found in their prey or sediment, and enantioselective elimination has been confirmed in laboratory experiments. Results from this study are consistent with results from Lake Superior and rivers from the United States (6,14), where forage fish were found to be capable of biotransforming PCB 95. In contrast to our findings, these studies, as well as laboratory based studies, found some of the fish species investigated can biotransform PCB 136 in an enantioselective manner. Enantiomer fractions of PCBs have yet to be reported in any of the fish species investigated in this study, and it is difficult to draw conclusions based on comparisons to other species, as it is clear that species differ in their capability for enantioselective biotransformation (14).

PCB 183 was found to be non-racemic, with EFs shifted relative to sediment by all fish species in this study (Figure 3-3). Generally, PCB 183 is found to be non-biotransformed in fish. The exception to this is trout from Lake Superior, which have been found to be enriched in the second eluting enantiomer. PCB 183 has also been found in non-racemic proportions in mammalian and avian species. PCB 183 is often considered difficult to metabolize, with low rates of elimination from organisms. This congener lacks vicinal *meta-para* hydrogens, the presence of which makes a congener more susceptible to biotransformation by CYP 2B-like enzymes. However, the lack of vicinal *meta-para* hydrogens does not necessarily preclude metabolism by CYP 2B-like enzymes, as only a single unsubstituted *meta* or *para* position is necessary for the formation of hydroxylated

metabolites. The finding of enantioselective biotransformation of PCB 183 in these and other species may indicate other process or other enzymes may also be responsible for the observed non-racemic distributions. Alternatively, the non-racemic proportions of PCB 183 in fish may be the result of uptake from prey that also exhibited a non-racemic EF and that were not analyzed in this study.

With the exception of PCBs 136 and 149, dolphins were found to have non-racemic distributions of all PCB congeners investigated (Figure 3-3). Non-racemic EFs have previously been found in cetaceans. Striped dolphins from the Mediterranean were found to contain non-racemic quantities of PCBs 95, 149, 174, and 176 (37) and PCBs 95, 149 and 176 were found to be non-racemic in bottlenose dolphins found stranded along the Italian coast (38). Non-racemic EFs of PCBs 95, 132, and 149 have also been found in adult harbour porpoises (*Phocoena phocoena*) from the North Sea (39). These studies, however, did not characterize the enantiomer distribution in any prey species, and therefore, it is unknown whether or not these non-racemic EFs are due to biotransformation, or uptake of non-racemic proportions from prey.

The EFs measured in this study were enriched in the same direction for PCBs 95 and 176 as those found in other dolphins, although in the opposite direction than EFs of PCB 95 found in harbour porpoises (39). In addition, this study found that EFs are considerably more enriched in a single enantiomer than those previously found in cetaceans. Because of the enantiomer enrichment observed in prey species, this is likely due to a combination of exposure to highly

135

non-racemic EFs in the food web from this estuary, as well as *in vivo* biotransformation. Although these animals are likely year round residents of this region (20), the duration and seasonality of exposure to Aroclor 1268 contaminated prey for these animals may also play a role in interpreting these EF signatures.

A comparison of EFs in dolphins to those in prey species indicates that dolphins may be biotransforming several PCB congeners enantioselectively. Significant differences between EFs in dolphins and those in fish species were found for PCBs 95, 136, 149, and 183. In general, EFs in dolphins were less enriched (closer to racemic) than EFs observed in fish. This may indicate that the biotransformation processes occurring in dolphins are enantioselective towards the antipode of the enantiomers favored in fish. The ability of cetaceans to biotransform PCBs enantioselectively has been found in bowhead whale (*Balaena mysticetus*), which had significantly different EFs for PCBs 91, 135, 149, 174, 176, and 183 than those found in zooplankton (*Calanus* spp.), their primary prey item (40).

The observation that dolphins may be enantioselectively biotransforming highly chlorinated PCBs, based on comparisons of EFs between dolphins and likely prey, is a novel and significant finding. Dolphins are generally regarded as having a low capability to biotransform PCBs with six or more chlorines, or those congeners with 3 or more *ortho* chlorines (41). However, all of the congeners investigated in this study contain more than three *ortho* chlorines, and 5 of the 7

congeners contain six or more chlorines. Furthermore, congeners with no vicinal *meta-para* hydrogens and more than three *ortho* chlorines were found to have no susceptibility towards biotransformation. PCB 183 fits this criteria, yet dolphins appear to be biotransforming this congener enantioselectively. Our results are corroborated by the finding of methylsulfonyl PCBs, the primary end product of PCB metabolism, in highly non-racemic proportions in harbour porpoises (42).

An alternate explanation may be the influence of other prey species that were not measured in this study and that contain racemic or near racemic proportions of these congeners. The EF contribution from prey species to the body burden of a predator species is a weighted average of EFs found in prey species and the frequency at which that prey item is consumed (14). Given the limited biotransformation capability of dolphins observed in other studies, exposure to more racemic sources of PCBs may "dilute" the observed EF, shifting it closer to racemic. While evidence suggest that these dolphins are feeding almost exclusively on prey from the Turtle/Brunswick estuary, they may inhabit more open water regions of the estuary for unknown periods of time, as opposed to the inshore tidal creeks from which fish samples were collected. This difference may be enough to expose dolphins to prey items that contain more racemic distributions of PCBs.

A significant correlation between total PCB concentration and EFs of PCBs 91 (r^2=0.79, p=0.007) and 149 (r^2=0.58, p=0.05) was also found (Figure 3-4). EFs of PCB 91 became more enriched in the first eluting enantiomer as

concentrations increase, while EFs of PCB 149 became less enriched. Correlations between EF and PCB concentration have been found in lake trout and for male bowhead whales (14,40). It is currently unclear why such a correlation exists, although a similar correlation between EF and concentration has been linked to variation in feeding habits in other species (43).
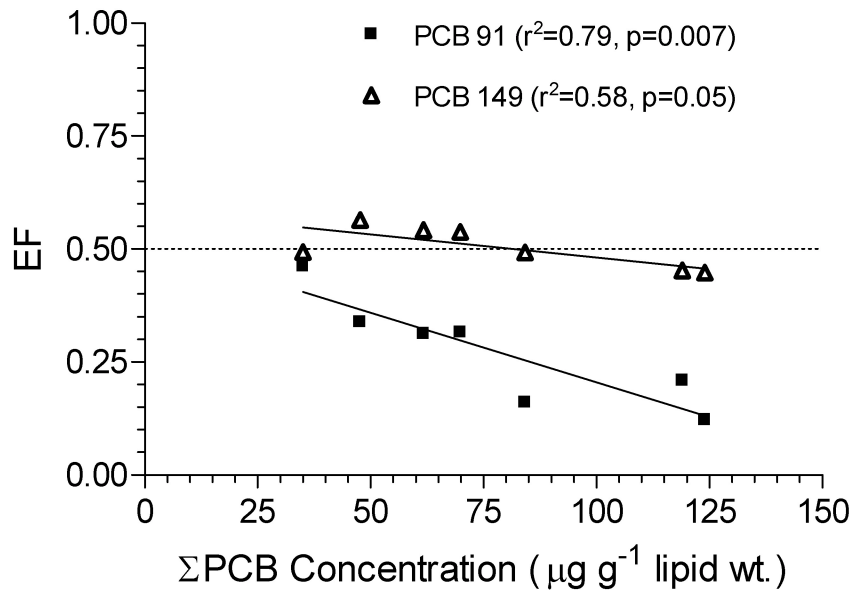
Figure 3-4: Linear regression of total PCB concentrations versus enantiomer fraction (EF) of PCB 91 and PCB 149 in bottlenose dolphin blubber from the Turtle/Brunswick estuary.

3.4 Conclusions

Non-racemic EFs measured in marsh sediments confirms the presence of reductive dechlorination activity at this site. Furthermore, biota contained highly non-racemic EFs, likely the result of a combination of uptake of non-racemic

138

proportions of these congeners from the diet, and *in vivo* biotransformation. While further studies should be conducted to determine how PCB concentration, trophic level, and feeding ecologies affect EFs, this study exemplifies how the use of chiral analysis may be used to detect biotransformation processes that were otherwise thought not to be occurring.

3.5 References

(1)   Bedard, D., in Robertson, L., Hansen, L.G. (Editors), PCBs: Recent advances in environmental toxicology and health effects, The University of Kentucky Press, Lexington, KY, 2001, p. 27-33.

(2)   Magar, V.S., Johnson, G.W., Brenner, R.C., Quensen, J.F., Foote, E.A., Durell, G., Ickes, J.A., Peven-McCarthy, C., Long-term recovery of PCB-contaminated sediments at the Lake Hartwell Superfund site: PCB dechlorination. 1. End-member characterization. Environmental Science & Technology, 39 (2005) 3538-3547.

(3)   Bedard, D.L., May, R.J., Characterization of the polychlorinated biphenyls in the sediments of Woods Pond: Evidence for microbial dechlorination of Aroclor 1260 in situ. Environmental Science & Technology, 30 (1996) 237-245.

(4)   Brown, J.F., Bedard, D.L., Brennan, M.J., Carnahan, J.C., Feng, H., Wagner, R.E., Polychlorinated biphenyl dechlorination in aquatic sediments. Science, 236 (1987) 709-712.

(5)   Kaiser, K.L.E., Optical-activity of polychlorinated biphenyls. Environmental Pollution, 7 (1974) 93-101.

(6)   Wong, C.S., Garrison, A.W., Smith, P.D., Foreman, W.T., Enantiomeric composition of chiral polychlorinated biphenyl atropisomers in aquatic and riparian biota. Environmental Science & Technology, 35 (2001) 2448-2454.

(7)   Wong, C.S., Garrison, A.W., Foreman, W.T., Enantiomeric composition of chiral polychlorinated biphenyl atropisomers in aquatic bed sediment. Environmental Science & Technology, 35 (2001) 33-39.

(8)   Wong, C.S., Lau, F., Clark, M., Mabury, S.A., Muir, D.C.G., Rainbow trout (Oncorhynchus mykiss) can eliminate chiral organochlorine compounds enantioselectively. Environmental Science & Technology, 36 (2002) 1257-1262.

(9)   Warner, N.A., Wong, C.S., The freshwater invertebrate Mysis relicta can eliminate chiral organochlorine compounds enantioselectively. Environmental Science & Technology, 40 (2006) 4158-4164.

(10)   Singer, A.C., Wong, C.S., Crowley, D.E., Differential enantioselective transformation of atropisomeric polychlorinated biphenyls by multiple bacterial strains with different inducing compounds. Applied and Environmental Microbiology, 68 (2002) 5756-5759.

(11)   Pakdeesusuk, U., Jones, W.J., Lee, C.M., Garrison, A.W., O'Niell, W.L., Freedman, D.L., Coates, J.T., Wong, C.S., Changes in enantiomeric fractions during microbial reductive dechlorination of PCB132, PCB149, and

Aroclor 1254 in Lake Hartwell sediment microcosms. Environmental Science & Technology, 37 (2003) 1100-1107.

(12)   Buckman, A.H., Wong, C.S., Chow, E.A., Brown, S.B., Solomon, K.R., Fisk, A.T., Biotransformation of polychlorinated biphenyls (PCBs) and bioformation of hydroxylated PCBs in fish. Aquatic Toxicology, 78 (2006) 176-185.

(13)   Wong, C.S., Pakdeesusuk, U., Morrissey, J.A., Lee, C.M., Coates, J.T., Garrison, A.W., Mabury, S.A., Marvin, C.H., Muir, D.C.G., Enantiomeric composition of chiral polychlorinated biphenyl atropisomers in dated sediment cores. Environmental Toxicology and Chemistry, 26 (2007) 254-263.

(14)   Wong, C.S., Mabury, S.A., Whittle, D.M., Backus, S.M., Teixeira, C., DeVault, D.S., Bronte, C.R., Muir, D.C.G., Organochlorine compounds in Lake Superior: Chiral polychlorinated biphenyls and biotransformation in the aquatic food web. Environmental Science & Technology, 38 (2004) 84-92.

(15)   Kannan, K., Maruya, K.A., Tanabe, S., Distribution and characterization of polychlorinated biphenyl congeners in soil and sediments from a Superfund site contaminated with Aroclor 1268. Environmental Science & Technology, 31 (1997) 1483-1488.

(16)   Maruya, K.A., Lee, R.E., Biota-sediment accumulation and trophic transfer factors for extremely hydrophobic polychlorinated biphenyls. Environmental Toxicology and Chemistry, 17 (1998) 2463-2469.

(17)   Kannan, K., Nakata, H., Stafford, R., Masson, G.R., Tanabe, S., Giesy, J.P., Bioaccumulation and toxic potential of extremely hydrophobic polychlorinated biphenyl congeners in biota collected at a superfund site contaminated with Aroclor 1268. Environmental Science & Technology, 32 (1998) 1214-1221.

(18)   Winger, P.V., Lasier, P.J., Geitner, H., Toxicity of sediments and pore-water from Brunswick Estuary, Georgia. Archives of Environmental Contamination and Toxicology, 25 (1993) 371-376.

(19)   Pulster, E.L., Smalling, K.L., Maruya, K.A., Polychlorinated biphenyls and toxaphene in preferred prey fish of coastal southeastern US bottlenose dolphins (Tursiops truncatus). Environmental Toxicology and Chemistry, 24 (2005) 3128-3136.

(20)   Pulster, E.L., Smalling, K.L., Zolman, E., Schwacke, L., Maruya, K.A., Persistent organochlorine pollutants and toxaphene congener profiles in bottlenose dolphins (Tursiops truncatus) frequenting the Turtle/Brunswick River Estuary, Georgia, USA. Environmental Toxicology and Chemistry, 28 (2009) 1390-1399.

(21)   Pulster, E.L., Maruya, K.A., Geographic specificity of Aroclor 1268 in bottlenose dolphins (Tursiops truncatus) frequenting the Turtle/Brunswick River Estuary, Georgia (USA). Science of the Total Environment, 393 (2008) 367-375.

(22)   Maruya, K.A., Lee, R.F., Aroclor 1268 and toxaphene in fish from a

southeastern US Estuary. Environmental Science & Technology, 32 (1998) 1069-1075.

(23)   Wong, C.S., Hoestra, P.F., Karlsson, H., Backus, S.M., Mabury, S.A., Muir, D.C.G., Enantiomer fractions of chiral organochlorine pesticides and polychlorinated biphenyls in standard and certified reference materials. Chemosphere, 49 (2002) 1339-1347.

(24)   Wong, C.S., Garrison, A.W., Enantiomer separation of polychlorinated biphenyl atropisomers and polychlorinated biphenyl retention behavior on modified cyclodextrin capillary gas chromatography columns. Journal of Chromatography A, 866 (2000) 213-220.

(25)   Asher, B.J., D'Agostino, L.A., Way, J.D., Wong, C.S., Harynuk, J.J., Comparison of peak integration methods for the determination of enantiomeric fraction in environmental samples. Chemosphere, 75 (2009) 1042-1048.

(26)   Harner, T., Wiberg, K., Norstrom, R., Enantiomer fractions are preferred to enantiomer ratios for describing chiral signatures in environmental analysis. Environmental Science & Technology, 34 (2000) 218-220.

(27)   Palekar, L.D., Maruya, K.A., Kostka, J.E., Wiegel, J., Dehalogenation of 2,6-dibromobiphenyl and 2,3,4,5,6-pentachlorobiphenyl in contaminated estuarine sediment. Chemosphere, 53 (2003) 593-600.

(28)   Kuipers, B., Cullen, W.R., Mohn, W.W., Reductive dechlorination of nonachlorobiphenyls and selected octachlorobiphenyls by microbial enrichment

cultures. Environmental Science & Technology, 33 (1999) 3579-3585.

(29)   Pakdeesusuk, U., Lee, C.M., Coates, J.T., Freedman, D.L., Assessment of natural attenuation via in situ reductive dechlorination of polychlorinated bipheny is in sediments of the Twelve Mile Creek arm of Lake Hartwell, SC. Environmental Science & Technology, 39 (2005) 945-952.

(30)   Bzdusek, P.A., Christensen, E.R., Lee, C.M., Pakdeesusuk, U., Freedman, D.L., PCB congeners and dechlorination in sediments of Lake Hartwell, South Carolina, determined from cores collected in 1987 and 1998. Environmental Science & Technology, 40 (2006) 109-119.

(31)   Morrissey, J.A., Bleackley, D.S., Warner, N.A., Wong, C.S., Enantiomer fractions of polychlorinated biphenyls in three selected Standard Reference Materials. Chemosphere, 66 (2007) 326-331.

(32)   Asher, B.J., Wong, C.S., Rodenburg, L.A., Chiral source apportionment of polychlorinated biphenyls to the Hudson River estuary atmosphere and food web. Environmental Science & Technology, 41 (2007) 6163-6169.

(33)   Vetter, W., Maruya, K.A., Congener and enantioselective analysis of toxaphene in sediment and food web of a contaminated estuarine wetland. Environmental Science & Technology, 34 (2000) 1627-1635.

(34)   Li, X.Q., Yang, L.J., Jans, U., Melcer, M.E., Zhang, P.F., Lack of enantioselective microbial degradation of chlordane in Long Island Sound

sediment. Environmental Science & Technology, 41 (2007) 1635-1640.

(35)   Haglund, P., Isolation and characterization of polychlorinated biphenyl (PCB) atropisomers. Chemosphere, 32 (1996) 2133-2140.

(36)   Wiberg, K., Andersson, P.L., Berg, H., Olsson, P.E., Haglund, P., The fate of chiral organochlorine compounds and selected metabolites in intraperitoneally exposed Arctic char (Salvelinus alpinus). Environmental Toxicology and Chemistry, 25 (2006) 1465-1473.

(37)   Reich, S., Jimenez, B., Marsili, L., Hernandez, L.M., Schurig, V., Gonzalez, M.J., Congener specific determination and enantiomeric ratios of chiral polychlorinated biphenyls in striped dolphins (Stenella coeruleoalba) from the Mediterranean sea. Environmental Science & Technology, 33 (1999) 1787-1793.

(38)   Jimenez, O., Jimenez, B., Gonzalez, M.J., Isomer-specific polychlorinated biphenyl determination in cetaceans from the Mediterranean Sea: Enantioselective occurrence of chiral polychlorinated biphenyl congeners. Environmental Toxicology and Chemistry, 19 (2000) 2653-2660.

(39)   Chu, S.G., Covaci, A., Van de Vijver, K., De Coen, W., Blust, R., Schepens, P., Enantiomeric signatures of chiral polychlorinated biphenyl atropisomers in livers of harbour porpoises (Phocoena phocoena) from the southern North Sea. Journal of Environmental Monitoring, 5 (2003) 521-526.

(40)   Hoekstra, P.F., Wong, C.S., O'Hara, T.M., Solomon, K.R., Mabury, S.A., Muir, D.C.G., Enantiomer-specific accumulation of PCB atropisomers in the

bowhead whale (Balaena mysticetus). Environmental Science & Technology, 36 (2002) 1419-1425.

(41)   Tanabe, S., Watanabe, S., Kan, H., Tatsukawa, R., Capacity and mode of PCB metabolism in small cetaceans. Marine Mammal Science, 4 (1988) 103-124.

(42)   Chu, S.G., Covaci, A., Haraguchi, K., Voorspoels, S., Van de Vijver, K., Das, K., Bouquegneau, J.M., De Coen, W., Blust, R., Schepens, P., Levels and enantiomeric signatures of methyl sulfonyl PCB and DDE metabolites in livers of harbor porpoises (Phocoena phocoena) from the southern North Sea. Environmental Science & Technology, 37 (2003) 4573-4578.

(43)   Ross, M.S., Verreault, J., Letcher, R.J., Gabrielsen, G.W., Wong, C.S., Chiral organochlorine contaminants in blood and eggs of glaucous gulls (Larus hyperboreus) from the Norwegian Arctic. Environmental Science & Technology, 42 (2008) 7181-7186.

Chapter 4

Chiral Organochlorine Contaminants in Blood and Eggs of

Glaucous Gulls (Larus hyperboreus) from the Norwegian Arctic

4.1 Introduction

Despite the discontinued use of many organochlorine (OC) compounds, their environmental persistence continues to result in high concentrations in biota. Of particular concern are birds and mammals feeding at the top of the food webs. Glaucous gulls (*Larus hyperboreus*) breeding in Svalbard, in the Norwegian Arctic, occupy an apical position in the Arctic marine food web, and accumulate some of the highest body burdens of polychlorinated biphenyls (PCBs) and other legacy OC contaminants relative to other Arctic avian species and populations (1). In addition, glaucous gulls accumulate a variety of pollutants of emerging environmental concern, such as brominated flame retardants (2,3) and fluorinated compounds (4). High concentrations of organic contaminants have been linked to a variety of potentially chemical-induced biological effects in this species ((5) and references therein). Over the last decade, monitoring studies in the Norwegian Arctic have utilized glaucous gull whole blood, blood plasma, and eggs to monitor environmental contamination in the Norwegian Arctic (5-8).

Some OC contaminants are chiral, and are present in the environment as pairs of enantiomers (e.g., OC pesticides) or atropisomers (e.g., PCBs, hereafter referred to as enantiomers). Despite being released into the environment as racemic mixtures, non-racemic distributions of some chiral organochlorine compounds have been detected in tissues of a variety of organisms. Non-racemic distributions are evidence of biological processes that alter these stereochemical ratios. Thus, enantioselective analysis provides a sensitive means of detecting

such processes within individuals and/or food webs. Enantiomers may also possess different toxicological properties (9-11). For example, (+)-PCB 139 is a more potent inducer of ethoxyresorufin-*O*-deethylase activity than (-)-PCB 139 in chick embryo hepatocyte cultures (10). Due to potential enantiomer-specific differences in toxicity, it is important to understand the exposure of organisms to individual enantiomers, particularly when exposure occurs during sensitive life-stages, such as during avian ovogenesis and chick development.

A number of environmental monitoring programs have routinely used the eggs of avian species to assess exposure levels of adult birds to environmental contaminants (1,12), and to investigate maternal transfer of OC contaminants to eggs. Eggs are an advantageous medium to sample, as they are generally easy to collect, and egg contaminant concentrations can directly reflect concentrations in the mother at the time of laying (13). Non-racemic distributions of some chiral OC pollutants have been found in the eggs of raptors and seabirds (14-17), although why those distributions arose is not fully understood. The enrichment or depletion of one enantiomer over the other in eggs may be due to the direct transfer of non-racemic proportions of OCs from the mother to the egg. Alternatively, the enrichment may be due to enantioselective maternal transfer of contaminants to eggs, or to microbial degradation in unfertilized eggs (15). To evaluate the reliability of eggs as an option for monitoring of chiral pollutants, the mechanism by which chiral contaminants are transferred to eggs must be understand, and the degree to which the distribution of enantiomers in eggs

reflects that of the overall breeding adult population.

The objectives of the present study were two-fold. The first was to determine the enantiomer distribution of chiral OC contaminants in the blood plasma of adult male and female glaucous gulls from Svalbard, and to compare these to known chiral distributions in other Arctic populations. Secondly, enantiomer signatures were determined in the yolk of freshly laid, unincubated eggs collected concurrently from within the same nesting colonies. These signatures were compared to those found in female glaucous gull plasma to determine whether the maternal transfer of OC contaminants occurs in an enantioselective manner, and to assess the feasibility of using eggs as a means of monitoring chiral signatures within a top predator seabird population.

4.2 Materials and Methods

4.2.1 Sample Collection

Blood samples were collected from live-trapped adult male (n=19) and female (n=30) glaucous gulls from three breeding colonies less than 20 km apart on Bear Island (74°22'N, 19°05'E) in the Svalbard archipelago (Norwegian Arctic) during the nesting period between May and June 2006. Glupen, the southernmost colony, is part of the major seabird breeding colony, consisting mainly of black legged kittiwakes (*Rissa tridactyla*), northern fulmars (*Fulmarus glacialis*) and common and Brünnich's guillemots (*Uria aalge* and *Uria lomvia*). Teltvika is the northernmost breeding colony, and is located furthest from the

major seabird breeding colony. Kapp Harry is an intermediate site, located between Glupen and Teltvika. From each site, the third-laid egg from random three-egg clutches was collected concurrently (n=31) from the same colonies shortly after laying (<3 days) and prior to any embryo development. Further details on the sampling location, animal capture, and sampling methods can be found elsewhere (2,18).

4.2.2 Extraction and Cleanup

Sample extraction and cleanup was performed as described previously (5), with no modification. Briefly, plasma samples were denatured by addition of 1 mL HCl and 3 mL of 2-propanol, and analytes were extracted by liquid-liquid extraction with methyl-*tert*-butyl-ether/*n*-hexane (50:50 volume to volume ratio). Whole eggs were separated into yolk and albumen components, and yolks were homogenized and ground with anhydrous Na_2SO_4. Egg homogenates were added to an extraction column and extracted with dichloromethane/*n*-hexane (45:55 volume to volume ratio). Lipids were removed from yolk samples by gel permeation chromatography. For yolk and plasma samples, four fractions, containing PCBs (fraction 1, F1), OC pesticides and byproducts (F2), heptachlor epoxide and dieldrin (F3), and aryl sulfones (F4), were collected by Florisil cleanup chromatography. All four fractions were quantified by achiral gas chromatography-mass spectrometry (GC-MS, see below). For enantioselective analysis, the first three fractions were recombined and analyzed by chiral GC-MS.

4.2.3 Chemical Analysis

Achiral analyte separation and quantification was performed on an Agilent 6890 (Agilent Technologies, Palo Alto, CA, USA) gas chromatograph-mass spectrometer (GC-MS) with electron impact (EI) ionization. Analytes were separated on a DB-5 column (30 m × 0.25 mm internal diameter, i.d. × 0.25 μm film thickness, d_f, J&W Scientific, Folsom, CA, USA) as previously described (19).

Enantiomer analysis of PCB congeners was carried out on an Agilent 5890 GC-MS with EI ionization and selected ion-monitoring (20). A Chirasil-Dex column (25 m × 0.25 mm × 0.25 μm d_f, Varian, Walnut Creek, CA, USA) was used for the separation of PCBs 95 and 149. A BGB-172 column (30 m × 0.25 mm i.d. × 0.18 μm d_f, Analytik, Adiswil, Switzerland) was used for the separation of PCB 183 (21). All OC pesticides were analyzed on an Agilent 6890 GC-MS in electron capture negative ionization mode (22), using methane as the reagent gas at a rate of 40 ml/min. Separation of oxychlordane and heptachlor epoxide was achieved on a BGB-172. *trans*-Chlordane and *cis*-chlordane were separated on a Betadex-120 column (30 m × 0.25 mm × 0.25 μm d_f, Supelco, Oakville, ON, Canada).

4.2.4 Data Analysis

Due to partial coelution of some enantiomers, model-fitting software (PeakFit v.4.0, Systat, San Jose, CA, USA) was used for peak integrations and the

152

deconvolution of partially co-eluting peaks as previously described (23-25). Enantiomer fractions (EFs) were used to quantify enantiomer distributions (26). For compounds with unknown enantiomer elution order (PCB 95 on Chirasil-Dex and PCB 183 on BGB-172) (23), the EF is defined as E1/(E1+E2), where E1 and E2 are the peak areas of the first-eluted enantiomer and second-eluted enantiomer, respectively. For all other analytes (PCB 149, oxychlordane, heptachlor epoxide, *cis*- and *trans*-chlordane) the EF was determined as the peak area of the (+)-enantiomer divided by the sum of the peak areas of the (+) and (-) enantiomers (22,27). Enantiomer fractions are presented as mean ± 1 standard error unless otherwise noted. Racemic mixtures have a theoretical EF of 0.5, and mean measured EFs of all racemic standards ranged from 0.492 to 0.502, depending on the analyte (Table 4-1). Non-racemic distributions of analytes were determined by comparing median EFs of samples to that of standards (Mann-Whitney test). Non-parametric tests were used for this comparison only, due to the significant differences in the variances between the samples and standards. A one-way analysis of variance (ANOVA) with Tukey honestly-significant-difference post-hoc test was used to determine differences in EFs among categories (e.g., male plasma, female plasma, and yolk). For all statistical analyses, the level of significance was set at 0.05.

4.3 Results and Discussion

4.3.1 Achiral Analysis

A comprehensive discussion of the concentrations and congener/compound profiles of the present plasma samples is found in Verreault *et al*. (19). Concentrations of Σ_{58}PCB (58 congeners; Individual congeners: CB31/28, 33/20, 52, 49, 47/48, 44, 42, 64/41, 74, 70/76, 95, 66, 56/60, 92, 101/90, 99, 97, 87, 85, 110, 151, 149, 118, 114, 146, 153, 105, 179, 141, 130, 176, 137, 138, 158, 178, 187, 183, 128, 167, 174, 177, 202, 171, 156, 200, 157, 172, 180, 170/190, 189, 199, 196/203, 208, 195, 207, 194, 206) and $\Sigma_6$chlordane (oxychlordane, heptachlor epoxide, *trans*-chlordane, *cis*-chlordane, *trans*-nonachlor, and *cis*-nonachlor) in plasma and yolk (Figure 4-1) were comparable to those previously reported in glaucous gull plasma and eggs from Svalbard (3,18,28,29). Furthermore, consistent with previous studies, in which samples also were collected shortly after egg laying (i.e., within three days following clutch completion), Σ_{58}PCB and $\Sigma_6$chlordane concentrations in female plasma were lower than those found in males. This concentration difference between sexes is evidence that females have transferred a portion of their OC contaminant body burden to their eggs (5,28). All females in the present study had laid three eggs; therefore, the maternal transfer effect was consistent for all female birds. Lipid-normalized concentrations of Σ_{58}PCB and $\Sigma_6$chlordane were lower in yolk than in female plasma, which was consistent with previous studies (28).
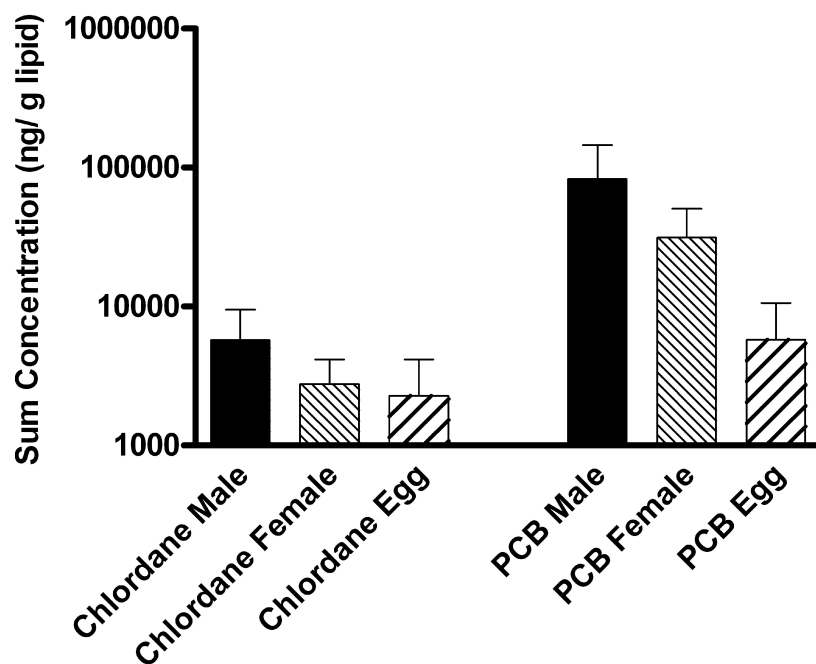
Figure 4-1: *Mean ± standard error of $\Sigma_{58}PCB$ (58 congeners) and Σ_{6}chlordane (6 compounds) concentrations (ng/g lipid weight) in male plasma, female plasma, and egg yolk samples of glaucous gulls from Svalbard, Norwegian Arctic.*

4.3.2 Enantiomers in Adult Plasma

With the exception of *trans*-chlordane, all analytes quantified in plasma (*cis*-chlordane, *trans*-chlordane, oxychlordane, heptachlor epoxide, and PCB 183, Table 4-1) had non-racemic EFs (Figure 4-2). Plasma EFs of all analytes were not correlated either to lipid percentage, breeding colony, or achiral $\Sigma_{58}PCB$ or Σ_{6}chlordane concentrations.
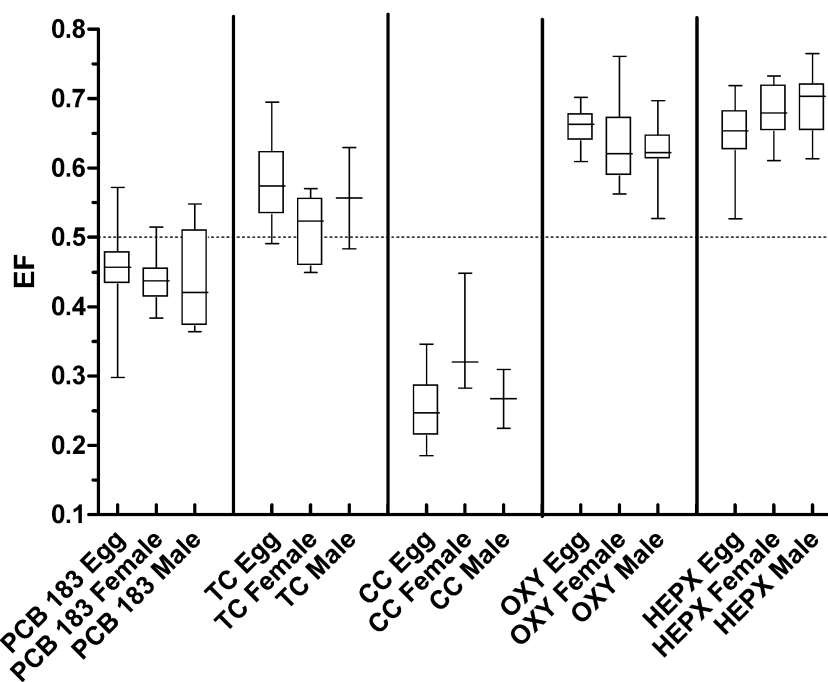
Figure 4-2: *Enantiomer fractions (EF) for organochlorine compounds in eggs and plasma of glaucous gulls from Svalbard, Norwegian Arctic. Box plots defined as follows: Center line, median; boxplot edges, 25th and 75th percentile; whiskers, range of data values. Dotted line represents racemic EF of 0.5. OXY, oxychlordane; TC, trans-chlordane; CC, cis-chlordane; HEPX, heptachlor epoxide.*

Enantiomer distributions of PCBs and chlordanes have previously been determined in liver and muscle tissue samples of glaucous gulls from the Northwater (NOW) polynya (14,30) in northern Baffin Bay (Canadian Arctic). With the exception of *trans*-chlordane, the enantiomer distributions of all analytes from the present study were similar to those from the NOW, both in the magnitude and direction of the enantiomer enrichment (Table 4-1).

Table 4-1: *Mean enantiomer fractions of analytes (±1 standard error) in racemic standards, and egg yolk and plasma samples from Svalbard glaucous gulls.[a]*

	Standard	Egg yolk	Female Plasma	Male Plasma	NOW
PCB 95	0.492±0.001 (n=3)	0.523±0.059 (n=3)	nd	nd	0.609±0.177[b]
PCB 149	0.500±0.001 (n=4)	0.226±0.009 (n=31)	nd	nd	0.227±0.052[b]
PCB 183	0.498±0.002 (n=5)	0.451±0.010 (n=30)	0.439±0.014 (n=8)	0.434±0.028 (n=6)	0.443[a]
trans-Chlordane	0.491±0.001 (n=6)	0.581±0.013 (n=20)	0.513±0.019 (n=6)	0.557±0.073 (n=2)	0.23±0.04[cd]
cis-Chlordane	0.493±0.001 (n=6)	0.255±0.009 (n=28)	0.350±0.050 (n=3)	0.267±0.042 (n=2)	0.30±0.04[cd] 0.26±0.04[ce]
Oxychlordane	0.504±0.001 (n=6)	0.630±0.009 (n=29)	0.634±0.012 (n=19)	0.626±0.011 (n=13)	0.63±0.01[cd] 0.65±0.03[ce]
Heptachlor epoxide	0.502±0.002 (n=5)	0.650±0.009 (n=28)	0.680±0.012 (n=10)	0.693±0.014 (n=10)	0.62±0.01[cd] 0.61±0.07[ce]

[a] Sample sizes are given in parenthesis. Mean (±σ) of EFs found in glaucous gull liver and muscle samples from the Canadian Arctic Northwater Polynya (NOW) are given for comparison.

[b] Data obtained from Warner et al. (30)

[c] Data obtained from Fisk et al. (14)

[d] Enantiomer fractions found in liver samples.

[e] Enantiomer fractions found in muscle samples.

157

The strong similarity in EFs between these two locations suggests overall similarities in the biochemical processes influencing the EFs of bioaccumulated OC contaminants within the food webs at those two locations, despite possible differences in age class, feeding ecologies, and reproductive status between the NOW birds and those of this study. Non-racemic EFs in glaucous gulls may arise due to *in vivo* enantioselective biotransformation of the compounds (30,31), or due to the uptake of food containing non-racemic distributions of these compounds (32). The biochemical pathways mediating the biotransformation of chiral OC compounds are assumed to be generally similar between individuals within a given species, and therefore the extent of biotransformation of chiral compounds between two populations of glaucous gulls is likely to be similar. The EFs observed in adult glaucous gull plasma were most likely steady-state EFs, as OC concentrations in blood of this species have been reported to reach steady-state levels after the first year of breeding (33). Previous studies have determined that wild mummichogs (*Fundulus* sp.) maintained near-constant EFs by continually taking up contaminants with enantiomer distributions which were closer to racemic (34). Therefore, in order for similar steady-state EFs to occur between these two populations, the birds must be consuming prey containing analogous enantiomer distributions of chiral compounds. It has been shown that glaucous gulls from Svalbard and the NOW polynya in the Canadian Arctic feed at similar trophic levels (35), although their diets may include a wide variety of food items that may differ between these two populations. In general, the few

studies investigating EFs in lower trophic level organisms from both Svalbard and the NOW polynya found that they contained EFs of most OC compounds which were closer to racemic than EFs measured in glaucous gulls from these locations (30,36-38). However, *trans*-chlordane was racemic or slightly enriched in the (+)-enantiomer in plasma and egg yolk, in contrast to enrichment of the (-)-enantiomer observed in the NOW polynya birds (14). While the reasons for this observation are unclear, it is possible this is a result of uptake of dietary items already enriched in the (+)-enantiomer. In the Svalbard region, chiral signatures of *trans*-chlordane were near racemic in whole Arctic cod (*Gadus morhua*) (38) and marine invertebrates (39), while (-)-*trans*-chlordane was slightly enriched in muscle and blubber of ringed seals (*Pusa hispida*) from the NOW polynya (36), similar to what was also observed in glaucous gulls there. It is difficult to draw firm conclusions based on the data in this study, but clearly, further work needs be done to understand the relative contributions of diet and of food web structure on the resulting EFs observed in upper trophic level predators.

4.3.3 Enantiomers in Eggs

For OC pesticides and metabolites, an enrichment of (-)-*cis*-chlordane was observed in yolk, while for *trans*-chlordane, heptachlor epoxide, and oxychlordane the (+)-enantiomer was enriched (Figure 4-2). Enantiomer fractions of only three PCB congeners (PCB 95, 149 and 183) were quantifiable in yolk; PCB 95 was racemic, while the PCBs 149 and 183 were non-racemic (Table 4-1).

There were statistically significant differences in PCB 183 and heptachlor

epoxide EFs between the Glupen and Teltvika breeding sites. Heptachlor epoxide

EFs were more racemic, while EFs of PCB 183 deviated more from racemic at

Teltvika compared to Glupen (Figure 4-3).
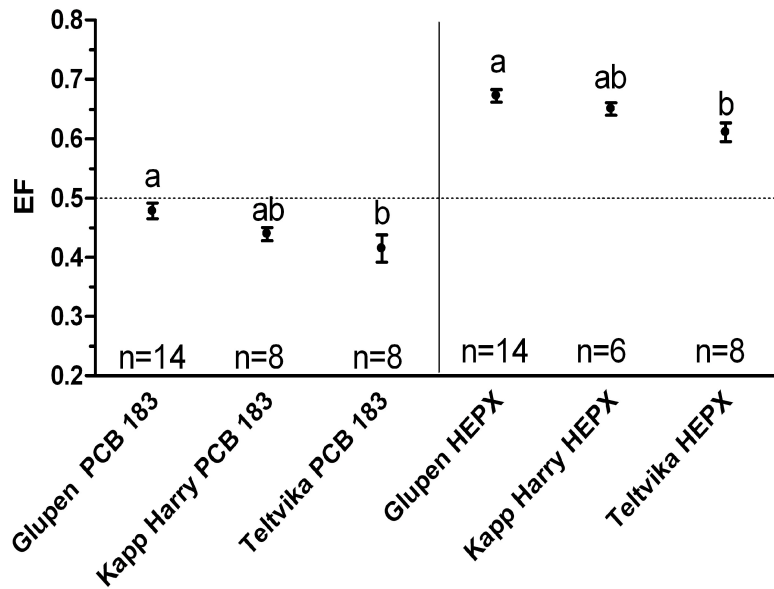
Figure 4-3: *Enantiomer fractions (EFs) for organochlorine compounds in the eggs at the three breeding sites investigated in this study. Points indicate mean value, while error bars indicate standard error. EF distributions sharing a letter designation (a, b) are not statistically different. HEPX, heptachlor epoxide. Dotted line represents theoretical racemic EF (EF = 0.5).*

The EFs of both analytes in the egg yolks from Kapp Harry fell in between and

were not significantly different from EFs from the other sites. To our knowledge,

this is the first time that local differences in biota EFs have been shown.   In

addition, this finding contrasts previous studies in ringed seals, which found no

differences in chlordane EFs between nearby sample locations in the NOW

polynya (36). PCB 183 and heptachlor epoxide EFs were also correlated with egg

160

laying date and with total PCB and chlordane concentrations. With respect to egg laying date, EF signatures of heptachlor epoxide in eggs laid later in the breeding season had deviated less from racemic (p <0.004, r^2=0.27) than those laid earlier in the breeding season, while EFs of PCB 183 became more non-racemic as the breeding season progressed (p <0.002, r^2=0.32) (Figure 4-4a). This observation may partially explain the differences in EFs between sites, as laying dates also varied between sites, with birds from Glupen laying eggs earlier than Teltvika, and birds from Kapp Harry having an intermediate laying date (40). Furthermore, EFs of PCB 183, oxychlordane, and heptachlor epoxide in eggs were correlated with egg $\Sigma_6$chlordane concentrations (Figure 4-4c, p<0.004, r^2=0.29, 0.28, and 0.29, respectively), while PCB 183 (p=0.02 and r^2=0.19) and oxychlordane (p=0.0004 and r^2=0.38) EFs in eggs were also correlated with egg Σ_{58}PCB concentrations (Figure 4-4b). At higher $\Sigma_6$chlordane or Σ_{58}PCB concentrations, PCB 183 deviated more from racemic, while oxychlordane and heptachlor epoxide became more racemic. This trend was similar to what was found for location and laying date. However, there were no significant differences in concentrations of PCBs or chlordanes between nesting sites (40), although eggs laid later in the breeding season had higher concentrations of these two compound classes. Therefore, it is unclear whether location or laying date had a greater effect on EFs, suggesting that other factors may be responsible.

The variation in EFs among locations and throughout the breeding period may be due to differences in the feeding ecologies between birds at the three

nesting sites. In addition to contaminants in eggs only being derived from a long term accumulation in the mothers (endogenous resources) and subsequent transfer to eggs, Verreault et al. (28) suggested that a portion of the contaminant burden in glaucous gull eggs might originate from the transfer of recently ingested contaminants during the ovogenesis. If this is the case, then subtle changes in the diet of birds in different colonies or throughout the breeding season may impact the EF distribution in eggs, if those dietary items contained enantiomer compositions varying from those of the female gull. Variation in feeding ecology in relation to OC concentrations has been documented between neighboring nesting colonies of glaucous gulls from Bear Island (41). Glaucous gulls breeding near large seabird colonies, such as those from Glupen, supplement their diet with seabird eggs and chicks. Thus, gulls from these colonies feed at a higher trophic level and are more contaminated than those breeding at sites farther from large aggregates of seabirds, which tend to feed more on fish and crustaceans (40). Additionally, glaucous gulls may change their dietary preferences as the breeding season progress, possibly to correspond with the egg laying of other seabirds (40). The concentrations and relative proportions of several organic pollutants in egg yolks from this study varied with location and laying date, indicating that location and/or feeding ecology may have significant impacts on the contaminants to which the gulls were exposed (40). These variations in feeding ecology and foraging strategies may lead to the uptake of dietary items containing contaminants of varying EF signatures, leading to differences in the EFs between

sites and throughout the breeding season.

While it is clear that local differences in the egg EFs exist, due to the large number of potentially confounding variables in this study, it is unclear exactly how egg yolk EFs were impacted by ecological factors, such as laying date and foraging behavior. In addition, the effect of dietary composition on egg EFs cannot be fully ascertained, as there have been no studies to date investigating the EFs in lower trophic level prey species from Bear Island. This is the first time that EFs in eggs have been related to any ecological variables, and makes clear the need for further study on how feeding strategies and food web structures impact egg EFs.
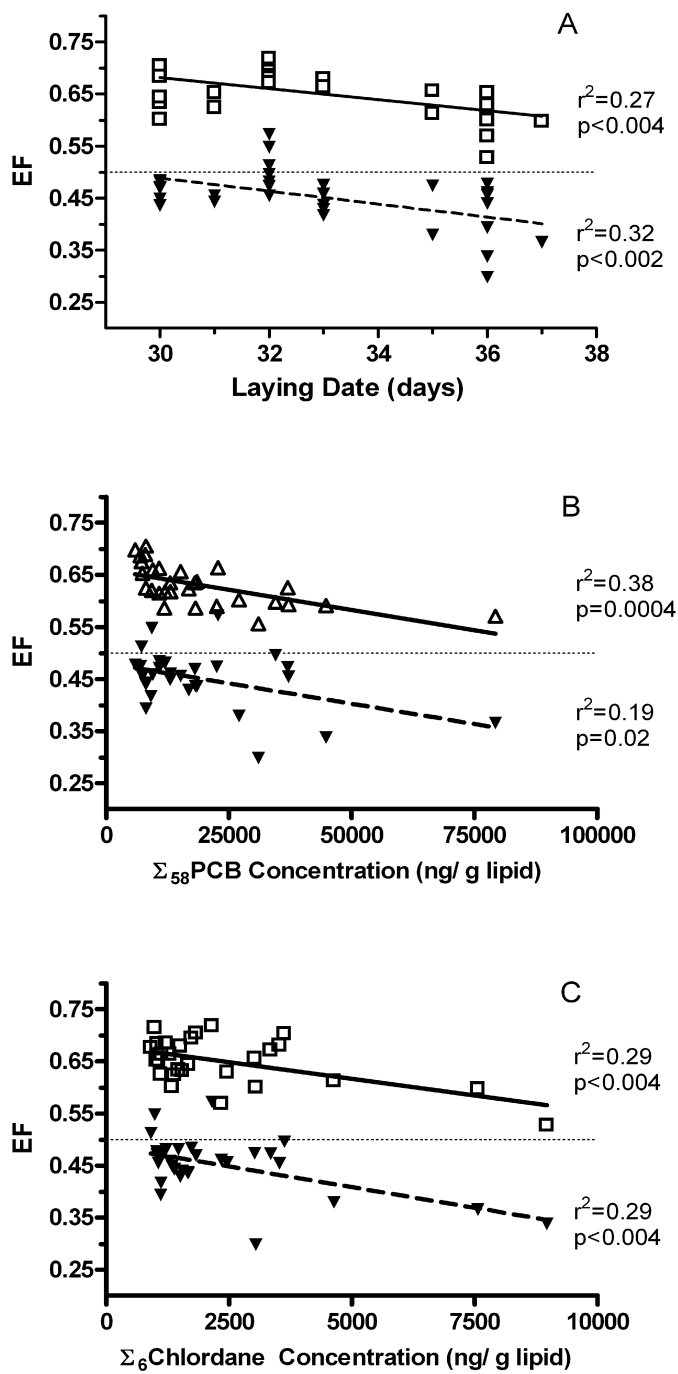
Figure 4-4: *Linear regression of enantiomer fractions (EF) versus (A) laying date, expressed as days after May 1, 2006, (B) $\Sigma_{58}PCB$ and (C) $\Sigma_6$chlordane concentrations in glaucous gull eggs. ▼ PCB 183; □ Heptachlor Epoxide (HEPX); △ Oxychlordane (not shown in subfigure C for simplicity). Dotted line represents theoretical racemic EF (EF = 0.5).*

4.3.4 Maternal Transfer

It has been hypothesized that non-racemic EFs of chiral contaminants in eggs may be the result of either enantioselective microbial degradation in unfertilized or abandoned eggs (16), enantioselective chemical transfer from the female to the eggs (15), or direct transfer of non-racemic distributions of chiral compounds from the female to the eggs (an achiral process). To distinguish among these hypotheses, EFs of several chiral contaminants in female glaucous gull plasma were compared to the EFs in freshly laid eggs collected from the same breeding colony. Because eggs were collected within three days of clutch completion, no microbial degradation had likely taken place. For all analytes, no differences were observed between EFs in female plasma and in eggs (Figure 4-2, Table 4-1), indicating that the transfer of the studied chemicals to eggs occurred non-enantioselectively.

Maternal OC residues are generally associated with lipidoidal material, and the contaminant residues which are transferred to the egg are predominantly derived from these endogenous stores, with an unknown portion from dietary intake (13). At the onset of ovogenesis, endogenous lipid stores are mobilized and transported by the bloodstream to the growing oocyte via lipoproteins (42). Previous studies have found that OC contaminants are associated with several different lipoproteins in blood, including low-density lipoproteins and very low-density lipoproteins, both of which constitute a large proportion of lipoproteins in the blood of laying hens and in the resulting yolk (42-44). This association with

lipoproteins does not appear to be an enantioselective process, as the enantiomer distribution of several OC compounds in plasma was similar to that in other tissues, including the liver (25,45). The lipoproteins, containing both lipids and associated contaminants, are then taken by active transport across the cell membranes of the ovarian follicle. This active transport of proteins across the cell membranes is unlikely to be a process that is enantioselective for OC contaminants, as they are associated with achiral lipids, and are transported across the membrane in conjunction with these lipids. Therefore, the overall process should result in an enantiomer distribution in the eggs mirroring that found in the female. The results of our study are in agreement with this postulated mechanism.

4.3.5 Implications for Biomonitoring

The finding that chiral OC contaminants are transferred to eggs (based on the yolk fraction) non-enantioselectively, and that EFs in eggs are representative of those in female glaucous gull plasma, suggests that egg yolk may be used for biomonitoring of the enantiomeric distribution of chiral OCs in birds. Furthermore, there were no significant differences in EFs in both male and female plasma to EFs in egg yolk (ANOVA, $p > 0.05$). This observation suggests that egg EFs may be representative of the entire glaucous gull breeding population on Bear Island, rather than of females alone. It should be noted, however, that our results are for egg yolk homogenates, and the analysis of whole egg homogenates, including the protein-rich albumen, may yield different results. Furthermore, all

eggs from this study were collected shortly after laying, and that the use of unfertilized or degraded eggs may yield different results due to microbial degradation of the analytes.

An understanding of the enantiomer distribution in avian top predators will allow for insight into the biochemical processing occurring within the food web, and the identification of atypical EFs may help identify disturbances or differences within the given food web (34). Furthermore, with an increased knowledge of enantiomer-specific toxicity, the determination of the enantiomer distribution in eggs will allow for more accurate risk assessments in birds, by taking into account enantiomer-specific exposure. Given the information that can be gleaned from enantioselective analysis, its inclusion into biomonitoring programs is suggested.

4.4 References

(1)   de Wit, C.A., Fisk, A.T., Hobbs, K.E., Muir, D.C.G., Gabrielsen, G.W., Kallenborn, R., Krahn, M.N., Norstrom, R.J., Skaare, J.U., AMAP Assessment 2002: Persistent organic pollutants in the Arctic, Arctic Monitoring and Assessment Programme, Oslo, Norway, 2004.

(2)   Verreault, J., Gebbink, W.A., Gauthier, L.T., Gabrielsen, G.W., Letcher, R.J., Brominated flame retardants in glaucous gulls from the Norwegian Arctic: More than just an issue of polybrominated diphenyl ethers. Environmental Science & Technology, 41 (2007) 4925-4931.

(3)   Verreault, J., Gabrielsen, G.W., Chu, S., Muir, D.C.G., Andersen, M., Hamaed, A., Letcher, R.J., Flame retardants and methoxylated and hydroxylated polybrominated diphenyl ethers in two Norwegian Arctic top predators: Glaucous gulls and polar bears. Environmental Science & Technology, 39 (2005) 6021-6028.

(4)   Verreault, J., Houde, M., Gabrielsen, G.W., Berger, U., Haukas, M., Letcher, R.J., Muir, D.C.G., Perfluorinated alkyl substances in plasma, liver, brain, and eggs of glaucous gulls (Larus hyperboreus) from the Norwegian Arctic. Environmental Science & Technology, 39 (2005) 7439-7445.

(5)   Verreault, J., Letcher, R.J., Muir, D.C.G., Chu, S.G., Gebbink, W.A., Gabrielsen, G.W., New organochlorine contaminants and metabolites in plasma and eggs of glaucous gulls (Larus hyperboreus) from the Norwegian Arctic. Environmental Toxicology and Chemistry, 24 (2005) 2486-2499.

(6)   Barrett, R.T., Skaare, J.U., Gabrielsen, G.W., Recent changes in levels of persistent organochlorines and mercury in eggs of seabirds from the Barents Sea. Environmental Pollution, 92 (1996) 13-18.

(7)   Henriksen, E.O., Gabrielsen, G.W., Skaare, J.U., Validation of the use of blood samples to assess tissue concentrations of organochlorines in glaucous gulls, Larus hyperboreus. Chemosphere, 37 (1998) 2627-2643.

(8)   Bustnes, J.O., Skaare, J.U., Erikstad, K.E., Bakken, V., Mehlum, F., Whole blood concentrations of organochlorines as a dose metric for studies of the

glaucous gull (Larus hyperboreus). Environmental Toxicology and Chemistry, 20 (2001) 1046-1052.

(9)   Ali, I., Aboul-Enein, H.Y., Ghanem, A., Enantioselective toxicity and carcinogenesis. Current Pharmaceutical Analysis, 1 (2005) 109-125.

(10)   Rodman, L.E., Shedlofsky, S.I., Mannschreck, A., Puttmann, M., Swim, A.T., Robertson, L.W., Differential potency of atropisomers of polychlorinated-biphenyls on cytochrome-P450: Induction and uroporphyrin accumulation in the chick-embryo hepatocyte culture. Biochemical Pharmacology, 41 (1991) 915-922.

(11)   Puttmann, M., Mannschreck, A., Oesch, F., Robertson, L., Chiral effects in the induction of drug metabolizing enzymes using synthetic atropisomers of polychlorinated biphenyls (PCBs). Biochemical Pharmacology, 38 (1989) 1345-1352.

(12)   Hebert, C.E., Norstrom, R.J., Zhu, J.P., Macdonald, C.R., Historical changes in PCB patterns in Lake Ontario and Green Bay, Lake Michigan, 1971 to 1982, from herring gull egg monitoring data. Journal of Great Lakes Research, 25 (1999) 220-233.

(13)   Drouillard, K.G., Norstrom, R.J., Quantifying maternal and dietary sources of 2,2',4,4',5,5'-hexachlorobiphenyl deposited in eggs of the ring dove (Streptopelia risoria). Environmental Toxicology and Chemistry, 20 (2001) 561-567.

(14)   Fisk, A.T., Moisey, J., Hobson, K.A., Karnovsky, N.J., Norstrom, R.J., Chlordane components and metabolites in seven species of Arctic seabirds from the Northwater Polynya: relationships with stable isotopes of nitrogen and enantiomeric fractions of chiral components. Environmental Pollution, 113 (2001) 225-238.

(15)   Gomara, B., Gonzalez, M.J., Enantiomeric fractions and congener specific determination of polychlorinated biphenyls in eggs of predatory birds from Donana National Park (Spain). Chemosphere, 63 (2006) 662-669.

(16)   Herzke, D., Kallenborn, R., Nygard, T., Organochlorines in egg samples from Norwegian birds of prey: Congener-, isomer- and enantiomer specific considerations. Science of the Total Environment, 291 (2002) 59-71.

(17)   Kallenborn, R., Planting, S., Haugen, J.E., Nybo, S., Congener-, isomer- and enantiomer-specific distribution of organochlorines in dippers (Cinclus cinclus l.) from Southern Norway. Chemosphere, 37 (1998) 2489-2499.

(18)   Verreault, J., Bech, C., Letcher, R.J., Ropstad, E., Dahl, E., Gabrielsen, G.W., Organohalogen contamination in breeding glaucous gulls from the Norwegian Arctic: Associations with basal metabolism and circulating thyroid hormones. Environmental Pollution, 145 (2007) 138-145.

(19)   Verreault, J., Changes in prolactin in a highly organohalogen-contaminated Arctic top predator seabird, the glaucous gull. General and Comparative Endocrinology, 156 (2008) 569-576.

(20)   Wong, C.S., Hoekstra, P.F., Karlsson, H., Backus, S.M., Mabury, S.A., Muir, D.C.G., Enantiomer fractions of chiral organochlorine pesticides and polychlorinated biphenyls in Standard and Certified Reference Materials. Chemosphere, 49 (2002) 1339-1347.

(21)   Wong, C.S., Garrison, A.W., Enantiomer separation of polychlorinated biphenyl atropisomers and polychlorinated biphenyl retention behavior on modified cyclodextrin capillary gas chromatography columns. Journal of Chromatography A, 866 (2000) 213-220.

(22)   Falconer, R.L., Bidleman, T.F., Szeto, S.Y., Chiral pesticides in soils of the Fraser Valley, British Columbia. Journal of Agricultural and Food Chemistry, 45 (1997) 1946-1951.

(23)   Wong, C.S., Garrison, A.W., Foreman, W.T., Enantiomeric composition of chiral polychlorinated biphenyl atropisomers in aquatic bed sediment. Environmental Science & Technology, 35 (2001) 33-39.

(24)   Asher, B.J., Wong, C.S., Rodenburg, L.A., Chiral source apportionment of polychlorinated biphenyls to the Hudson River Estuary atmosphere and food web. Environmental Science & Technology, 41 (2007) 6163-6169.

(25)   Ulrich, E.M., Willett, K.L., Caperell-Grant, A., Bigsby, R.M., Hites, R.A., Understanding enantioselective processes: A laboratory rat model for alpha-hexachlorocyclohexane accumulation. Environmental Science & Technology, 35

(2001) 1604-1609.

(26)   Harner, T., Wiberg, K., Norstrom, R., Enantiomer fractions are preferred to enantiomer ratios for describing chiral signatures in environmental analysis. Environmental Science & Technology, 34 (2000) 218-220.

(27)   Haglund, P., Wiberg, K., Determination of the gas chromatographic elution sequences of the (+)- and (-)-enantiomers of stable atropisomeric PCBs on Chirasil-Dex. HRC-Journal of High Resolution Chromatography, 19 (1996) 373-376.

(28)   Verreault, J., Villa, R.A., Gabrielsen, G.W., Skaare, J.U., Letcher, R.J., Maternal transfer of organohalogen contaminants and metabolites to eggs of Arctic-breeding glaucous gulls. Environmental Pollution, 144 (2006) 1053-1060.

(29)   Verreault, J., Letcher, R.J., Ropstad, E., Dahl, E., Gabrielsen, G.W., Organohalogen contaminants and reproductive hormones in incubating glaucous gulls (Larus hyperboreus) from the Norwegian Arctic. Environmental Toxicology and Chemistry, 25 (2006) 2990-2996.

(30)   Warner, N.A., Norstrom, R.J., Wong, C.S., Fisk, A.T., Enantiomeric fractions of chiral polychlorinated biphenyls provide insights on biotransformation capacity of Arctic biota. Environmental Toxicology and Chemistry, 24 (2005) 2763-2767.

(31)   Hoekstra, P.F., O'Hara, T.M., Karlsson, H., Solomon, K.R., Muir, D.C.G., Enantiomer-specific biomagnification of alpha-hexachlorocyclohexane

and selected chiral chlordane-related compounds within an Arctic marine food web. Environmental Toxicology and Chemistry, 22 (2003) 2482-2491.

(32)   Wong, C.S., Garrison, A.W., Smith, P.D., Foreman, W.T., Enantiomeric composition of chiral polychlorinated biphenyl atropisomers in aquatic and riparian biota. Environmental Science & Technology, 35 (2001) 2448-2454.

(33)   Bustnes, J.O., Bakken, V., Skaare, J.U., Erikstad, K.E., Age and accumulation of persistent organochlorines: A study of Arctic-breeding glaucous gulls (Larus hyperboreus). Environmental Toxicology and Chemistry, 22 (2003) 2173-2179.

(34)   Vetter, W., Smalling, K.L., Maruya, K.A., Interpreting nonracemic ratios of chiral organochlorines using naturally contaminated fish. Environmental Science & Technology, 35 (2001) 4444-4448.

(35)   Borga, K., Gabrielsen, G.W., Skaare, J.U., Kleivane, L., Norstrom, R.J., Fisk, A.T., Why do organochlorine differences between Arctic regions vary among trophic levels? Environmental Science & Technology, 39 (2005) 4343-4352.

(36)   Fisk, A.T., Holst, M., Hobson, K.A., Duffe, J., Moisey, J., Norstrom, R.J., Persistent organochlorine contaminants and enantiomeric signatures of chiral pollutants in ringed seals (Phoca hispida) collected on the east and west side of the Northwater Polynya, Canadian Arctic. Archives of Environmental

Contamination and Toxicology, 42 (2002) 118-126.

(37)   Wiberg, K., Letcher, R.J., Sandau, C.D., Norstrom, R.J., Tysklind, M., Bidleman, T.F., The enantioselective bioaccumulation of chiral chlordane and alpha-HCH contaminants in the polar bear food chain. Environmental Science & Technology, 34 (2000) 2668-2674.

(38)   Karlsson, H., Oehme, M., Skopp, S., Burkow, I.C., Enantiomer ratios of chlordane congeners are gender specific in cod (Gadus morhua) from the Barents Sea. Environmental Science & Technology, 34 (2000) 2126-2130.

(39)   Borga, K., Bidleman, T.F., Enantiomer fractions of organic chlorinated pesticides in Arctic marine ice fauna, zooplankton, and benthos. Environmental Science & Technology, 39 (2005) 3464-3473.

(40)   Verboven, N., Verreault, J., Letcher, R.J., Gabrielsen, G.W., Evans, E., Maternally derived testosterone and 17β-estradiol in the eggs of Arctic-breeding glaucous gulls in relation to persistent organic pollutants. Comparative Biochemistry and Physiology C-Toxicology & Pharmacology, 2 (2008) 143-151.

(41)   Bustnes, J.O., Erikstad, K.E., Bakken, V., Mehlum, F., Skaare, J.U., Feeding ecology and the concentration of organochlorines in glaucous gulls. Ecotoxicology, 9 (2000) 179-186.

(42)   Burley, R.W., Vadehra, D.V., The Avian Egg: Chemistry and Biology, John Wiley & Sons, New York, NY, USA, 1989.

(43)   Noren, K., Weistrand, C., Karpe, F., Distribution of PCB congeners,

DDE, hexachlorobenzene, and methylsulfonyl metabolites of PCB and DDE among various fractions of human blood plasma. Archives of Environmental Contamination and Toxicology, 37 (1999) 408-414.

(44)   Borlakoglu, J.T., Welch, V.A., Wilkins, J.P.G., Dils, R.R., Transport and cellular uptake of polychlorinated biphenyls (PCBs) 2. Association of individual PCB isomers and congeners with plasma lipoproteins and proteins in the pigeon. Biochemical Pharmacology, 40 (1990) 265-272.

(45)   Kania-Korwel, I., Shaikh, N.S., Hornbuckle, K.C., Robertson, L.W., Lehmler, H.J., Enantioselective disposition of PCB 136 (2,2',3,3',6,6'-hexachlorobiphenyl) in C57BL/6 mice after oral and intraperitoneal administration. Chirality, 19 (2007) 56-66.

Chapter 5

Comparison of the Enantiomer Distribution of Chiral Organochlorine Contaminants in Captive West Greenland Sledge Dogs and Eastern Canadian (Baffin Island) Polar Bears

5.1 Introduction

Polar bears (*Ursus maritimus*) are apex predators within Arctic ecosystems. They biomagnify high concentrations of organohalogen compounds (OHCs), such as certain polychlorinated biphenyls (PCBs), organochlorine pesticides, brominated flame retardants, and persistent metabolites of these compounds in their adipose tissue, internal organs, and blood relative to lower trophic level Arctic species (1). Concentrations of OHCs in polar bears have been correlated with levels of a variety of biomarkers (e.g., endocrine and immunological) (1). For instance, a negative correlation was shown to exist between OHC concentrations and plasma testosterone concentrations in free-ranging male polar bears (2). While such correlations suggest possible deleterious effects from exposure, uncertainty in factors such as age, health, genetic variation, reproductive status, and other life history variables of wild polar bears leaves the direct cause and effect relationship between contaminant body-burdens and observed toxicological impairments for polar bears unclear (3). It is impractical and ethically problematic to conduct experiments on captive polar bears, and thus studies on a model surrogate species are needed to elucidate such relationships.

Recently, the sled dog (*Canis familiaris*) has been investigated for use as a surrogate species to study the bioaccumulation, fate and effects of OHCs and other environmental contaminants in wild polar bears, as well as other members of the *canoidea* superfamily, including Arctic fox (*Alopex lagopus*), Arctic wolf (*Canis lupus arctos*), and wolverine (*Gulo gulo*). The captive West Greenland sled

177

dogs that are the subject of the present study were fed wild minke whale (*Balaenoptera acutorostrata*) blubber, which was naturally contaminated with OHCs, for nearly two years to simulate natural exposure conditions. Results have shown that dogs from the exposed cohort exhibited similar biomarker endpoint changes as those reported for wild polar bears for a number of health related parameters, such as vitamin status (4), sex hormone homeostasis (5), and cellular immune response (6). A comprehensive review of the comparative health and toxicological findings in wild polar bear and surrogate model species can be found elsewhere (3).

Species-specific metabolic differences, due to dissimilarity in cytochrome P-450 (CYP) isozyme substrate specificity, catalytic activity, or expression levels between species, may lead to a differential accumulation or fate of contaminants, or result in varying degrees of formation of toxic metabolites. Such species-specific differences in biotransformation capacity and bioaccumulation of OHCs may thusly affect the toxicological response, and make cross-species extrapolations of toxicity difficult. Investigations into the comparative fate of OHCs between sled dogs and polar bears found both similarities and differences between species (7). Although similarities existed in OHC concentrations between the two species, differences in the inferred biotransformation capability and bioaccumulation of contaminant classes and individual compounds led to variation in contaminant and metabolite patterns between polar bears and sled dogs (7).

Enantioselective analysis has been shown to provide a means of quantifying and observing biological processes, which are often difficult to quantify using other techniques (8-10), and provides an additional method of comparing the bioaccumulation dynamics and biotransformation capabilities and pathways among species. Chiral compounds exist as pairs of non-superimposable mirror images (enantiomers). Environmentally relevant chiral OHCs include 19 atropisomeric PCB congeners (11), many components of technical chlordane and their metabolites, and α-hexachlorocyclohexane (α-HCH). These compounds were released into the environment as racemic mixtures (1:1 mixtures of enantiomers), and because enantiomers possess identical physical and chemical properties, only biological processes (e.g., metabolism, protein binding, active uptake/elimination) will alter the relative proportion of enantiomers in the environment. Within biota, differences in the toxicokinetic behavior between enantiomers will lead to a greater accumulation of one enantiomer over the other (12). In addition, biological effects may differ between enantiomers. For instance, (*R*)-(-)-*o,p´*-DDT enantiomer is a weak estrogen mimic, while (*S*)-(+)-*o,p´*-DDT has negligible estrogenic effects (13). Likewise, individual PCB enantiomers displayed differing potencies towards hepatic enzyme induction (14,15), and in the enhancement of cellular Ca^{2+} release (16). Thus, enantioselective analysis not only provides an additional means of investigating the bioaccumulation dynamics of organisms, but is essential for proper assessment of the risk posed by chiral compounds.

The comparison of OHC enantiomer distributions among species is complicated. One of the most notable factors influencing inter-species differences is the enantiomeric substrate selectivity of the enzymes that catalyze metabolism. For instance, complete inversions of enantiomer enrichment have been found between closely related species in some laboratory experiments (9,17,18). Similarities were found in the enantiomer-specific biotransformation of PCB 95 and 149 between Arctic char and rainbow trout, although opposite enantiomer selectivity was reported for PCB 136 between these two members of the *Salmonidae* family (9,17,18). Likewise, bearded seals (*Erignathus barbatus*) from the coast of Alaska were enriched in (-)-oxychlordane, while ringed seals (*Phoca hispida*) from the same location were enriched in the (+)-enantiomer (19). The interpretation of enantiomer distributions in a given predator species is also influenced by consumption of non-racemic quantities of chiral OHCs from prey items. Enantiomer distributions of OHCs were shown to vary in eggs and plasma of glaucous gull from three nearby breeding colonies in the Norwegian Arctic, and was likely a result of differences in enantiomer distributions of the selected OHCs in the preferential food sources of each colony (20). However, the degree to which the uptake of food-derived enantiomer distributions affects the measured distribution versus biotransformation within the predator has not been investigated.

The objectives of this study were two-fold. The first was to examine the enantiomer distribution of a suite of chiral OHCs in captive West Greenland

180

(Baffin Bay) sled dog adipose, liver, thyroid, adrenal, and brain tissues after 20-month exposure to naturally OHC-contaminated minke whale blubber (exposed cohort) or pork fat (control cohort), in order to understand bioaccumulation dynamics and fate of individual enantiomers within top-predator species in a controlled experiment. Secondly, the enantiomer distributions of chiral OHCs were determined in adipose tissues of free-ranging polar bears from Canadian subpopulations (also in Baffin Bay), and compared to those in West Greenland sled dog adipose tissues. The goal was to better understand species-specific biotransformation capabilities for chiral OHC contaminants, and to examine the feasibility of using surrogate models for cross-species comparisons of enantiomer distributions.

5.2 Materials and Methods

5.2.1 Experimental Design

This research was part of a larger study investigating the overall health effects of persistent environmental contaminants on West Greenland sled dogs. Further details on the experimental design are found elsewhere (6,7,21-24). This animal experiment was conducted under a license granted by the Self-Government of Greenland.

Sixteen 2-month old female sled dogs from the community of Aasiaat, Disco Bay, West Greenland, were divided into control (CON; $n = 8$) and exposed (EXP; $n = 8$) groups. Groups were composed of paired sisters, one in each group,

to minimize age and genetic variation between groups. EXP dogs were exposed (20 month exposure period) to a daily diet of blubber from an individual minke whale collected off the west coast (Baffin Bay) of Greenland as part of a controlled Greenlandic native subsistence hunt. This blubber was naturally contaminated with a suite of OHCs and other environmental contaminants, including mercury and polybrominated diphenyl ethers (PBDEs) (6,7), simulating real-world exposure to multiple contaminants experienced by wild *canoidea* species. The CON group received relatively non-contaminated pork fat classified for human consumption, and for the same feeding duration. Both cohorts were also fed an equivalent amount of standardized Royal Canin Energy 4300/4800 pellets (https://www.royalcanin.com) to fortify the diet with essential vitamins and nutrients not found in either food source. Daily intake of whale blubber or pork fat was 50-200 g/day, leading to an exposure of 10.4-11.7 μg/kg body weight of total OHCs in EXP dogs (25).

CON and EXP dogs were subjected to a variety of health-related toxicological tests throughout the experiment, including blood sampling and immune system challenges (6,25). However, such procedures are not expected to alter the biotransformation capacity of the dogs. Upon termination of the experiment, dogs (mean age 1.5 ± 0.1 years, range 1.5-2 years) were euthanized. Liver, thyroid, brain, adrenal, and subcutaneous adipose tissues were collected and stored at -20 °C until analysis.

Subcutaneous adipose tissue samples were collected from adult and

juvenile polar bears (mean age 6.1 ± 3.0 years) from two subpopulations inhabiting Eastern Baffin Island, Canada: Davis Strait (southern Baffin Island; n=11) and Baffin Bay (northern Baffin Island; n=14). All samples were collected between October 2007 and May 2008 as part of Inuit subsistence hunts. Further details on dates and locations of sample collection, as well as sample handling procedures can be found in (26).

5.2.2 Extraction

Procedures for the extraction and cleanup of sled dog and polar bear tissue samples for PCBs, HCHs, and chlordane-related compounds have been described in detail previously (27,28). Briefly, samples were homogenized with Na_2SO_4 and extracted with either 1:1 acetone/*n*-hexanes (brain tissue) or 1:1 DCM:*n*-hexanes (all other tissues). Lipids were removed with the addition of H_2SO_4 and analytes were fractioned into several chemical classes on a Florisil column. Polar bear adipose tissue was homogenized with sodium sulfate and extracted by pressurized liquid extraction, followed by gel permeation and silica gel chromatography prior to analysis (26).

5.2.3 Chemical Analysis

Non-enantioselective separation and quantification was performed on an Agilent 6890 (Agilent Technologies, Palo Alto, CA, USA) gas chromatograph-mass spectrometer (GC-MS) with electron impact (EI) ionization, as previously

described (7,29,30). Total chlordane (ΣCHL) concentrations are reported as the sum of six chlordane compounds: Heptachlor epoxide (HEPX), oxychlordane, *trans*-chlordane, *cis*-chlordane, *trans*-nonachlor, *cis*-nonachlor. Total PCB (ΣPCB) concentrations in sled dogs and minke whale blubber are reported as the sum of 40 congeners (7), while ΣPCB concentrations in Baffin Island polar bears represent the sum of 74 congeners (26). A complete list of monitored congeners in both species has been published previously (7,26).

Enantiomer analysis of OCs was carried out on a Thermo Trace GC Ultra gas chromatograph coupled to a Thermo DSQII mass spectrometer (ThermoFisher Scientific, Waltham, MA, USA). PCBs were detected with EI ionization and selected ion-monitoring (31). The separation of PCBs 95 and 149 was achieved on a Chirasil-Dex column (25 m $\times$ 0.25 mm i.d. $\times$ 0.25 μm d_f, Varian, Walnut Creek, CA, USA) (32). A BGB-172 column (30 m $\times$ 0.25 mm i.d. $\times$ 0.18 μm d_f, Analytik, Adiswil, Switzerland) was used for the separation of PCB 183 (33). All columns were calibrated with standard solutions containing all 209 PCB congeners to avoid coelutions with other PCB homologs (32). Organochlorine pesticides were detected in electron capture negative ionization mode using previously described methods (34). Methane was used as the reagent gas at a flow rate of 2.5 mL/min. A BGB-172 was used for the separation of oxychlordane and heptachlor epoxide. α-HCH, *trans*-chlordane, and *cis*-chlordane were separated on a Betadex-120 column (30 m $\times$ 0.25 mm i.d. $\times$ 0.25 μm d_f, Supelco, Oakville, ON, Canada).

5.2.4 Data Analysis

Model-fitting software (PeakFit v.4.0, Systat, San Jose, CA, USA) was used for deconvolution and integration of partially co-eluting chromatographic peaks (35-37). Enantiomer fractions (EFs) were used to quantify enantiomer distributions (38). For compounds with unknown enantiomer elution order (PCB 95 on Chirasil-Dex and PCB 183 on BGB-172) (31), the EF is defined as E1/ (E1+E2), where E1 and E2 are the peak areas of the first-eluted enantiomer and second-eluted enantiomer, respectively. For all other analytes the EF was determined as the peak area of the (+)-enantiomer divided by the sum of the peak areas of the (+) and (-) enantiomers (34,39).

Enantiomer fractions and concentration data are presented as mean ±1 standard deviation unless otherwise noted. Mean measured EFs of all racemic standards ranged from 0.493 to 0.499, depending on the analyte. Non-racemic EFs were determined by comparison to racemic standards. Comparisons between and amongst groups were done by Student's *t* test or one-way analysis of variance (ANOVA) with Tukey Honestly Significant Difference post-hoc test, respectively, with $\alpha=0.05$.

5.3 Results and Discussion

5.3.1 Organochlorine Contaminant Concentrations

Elevated concentrations of chlorinated OHCs were detected in naturally contaminated minke whale blubber used for the exposed cohort diet, which had

ΣPCB concentrations and ₓCHL concentrations of 1150±60 and 196±5 ng/g wet weight, respectively (24). None of the analytes were detected in the control cohort diet or dietary supplements (limit of quantification range: 0.01-1.5 ng/g wet wt., depending on the analyte). Exposure to contaminated minke whale blubber lead to increased concentrations of all investigated OHCs in EXP cohort dog tissues. A detailed description of the tissue concentrations and accumulation patterns of OHCs and metabolites in sled dogs arising from exposure to contaminated minke whale blubber was recently published (7), and will not be reiterated here. It is important to point out, however, that after two years of exposure, adipose tissue concentrations of ΣPCB and ΣCHL in EXP sled dogs were 2710 ± 500 ng/g wet wt. and 1480 ± 140 ng/g wet wt., respectively (7). These concentrations were 56-fold higher in ΣPCB and 43-fold higher in ΣCHL than CON dogs (7). Adipose tissue concentrations (mean ± standard deviation) of ΣPCB and ΣCHL in CON dogs were 48 ± 12 ng/g wet wt. and 34 ± 8 ng/g wet wt., respectively.

No differences in ΣPCB and ΣCHL concentrations were found between the Davis Strait and Baffin Bay polar bear subpopulations of Baffin Island (mean concentrations of 3080 ± 2770 ng/g wet wt. and 1150 ± 690 ng/g wet wt., respectively (26). In polar bears and sled dogs, ΣPCB contributed the most to the overall chlorinated OHC body burden. Additionally, oxychlordane was the predominant chlordane compound found in both species. A more detailed description of the non-enantioselective congener and compound distributions in sled dogs and Baffin Island polar bears can be found elsewhere (7,26).

5.3.2 Distributions of OC Enantiomers in Minke Whale Blubber

Enantiomer distributions of α-HCH, *cis*-chlordane, HEPX, and PCB 91 were non-racemic in minke whale blubber (Figures 5-1 and 5-2). α-HCH was enriched in the (+)-enantiomer, while both HPEX and *cis*-chlordane were enriched in the (-)-enantiomer (Figure 5-1). A slight, although not significant (EF=0.565±0.022; p>0.05), enrichment of (+)-oxychlordane was also observed (Figure 5-1). Amongst PCB congeners, only the second-eluting enantiomer of PCB 91 was enriched, while PCB s 95, 149, 174, and 183 were racemic (Figure 5-2). This appears to be the first report of enantiomer distributions of chiral OHCs in minke whale blubber. Similar EFs for chlordanes, α-HCH and PCB 149, both in the magnitude and the direction of enrichment were reported in bowhead whale from Barrow, AK (19). HEPX, on the other hand, was enriched in the (+)-enantiomer in bowhead whales (EF=0.64) (19), in contrast to the enrichment of the antipode in this study.
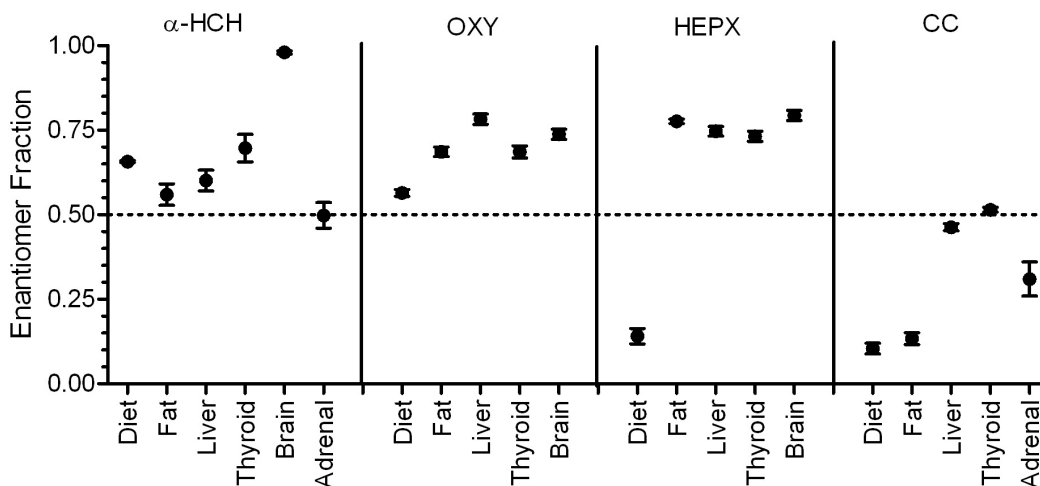
Figure 5-1: *Enantiomer fractions (EFs) for organochlorine compounds in exposed cohort sledge dog tissues and diet. Points indicate mean value, while error bars indicate standard error. OXY, oxychlordane; HEPX, heptachlor epoxide; CC, cis-chlordane. Dotted line represents theoretical racemic EF (EF = 0.5).*

5.3.3 Accumulation and Disposition of Enantiomers in Sledge Dogs

Non-racemic distributions of all analytes except PCB 174 were found in the tissues of EXP sled dogs (Figures 5-1 and 5-2). To increase the understanding of the sled dog enantiomer-specific biotransformation and bioaccumulation capacity, biomagnification factors (BMF; wet weight concentrations of each enantiomer in predator divided by the wet weight concentrations in the prey) from minke whale blubber to EXP sled dog adipose tissue were calculated on an enantiomer-specific basis. An inverse relationship exists between the BMF and the elimination rate constant of a compound, based on the equation $BMF = \alpha F / k_{el}$, where α is the assimilation efficiency (%), F is the feeding rate ($g_{food}\ g_{body\ weight}^{-1}$ day^{-1}), and k_{el} is the elimination rate constant (day^{-1}) (40). Feeding rates will be identical for enantiomers, and assimilation efficiencies should also be identical

188

due to the identical physical properties of enantiomers and the passive absorption

and uptake of hydrophobic compounds (41). The latter assumption is supported

by the observation that enantiomer-specific assimilation efficiencies were similar

for α-HCH, *trans*-chlordane, PCB 95 and PCB 136 enantiomers in rainbow trout

(9). Therefore, the ratio of the enantiomer-specific BMFs provides an

approximation of the biotransformation rate constant of the more highly

accumulated enantiomer relative to its antipode.
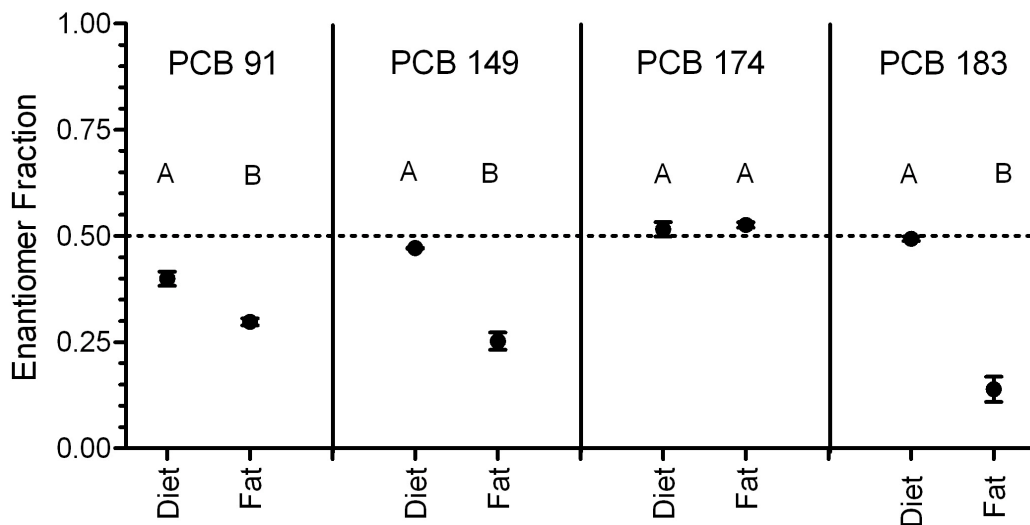
Figure 5-2: *Enantiomer fractions (EFs) for polychlorinated biphenyls in diet (minke whale blubber) and sledge dog fat. Points indicate mean value, while error bars indicate standard error. EF distributions sharing a letter designation are not statistically different. Dotted line represents theoretical racemic EF (EF = 0.5).*

With the exception of (+)-α-HCH, both PCB 149 enantiomers, and the first-

eluting enantiomer of PCB 183, all enantiomers had BMFs greater than 1 in EXP

sled dogs, indicating a propensity for dogs to accumulate these enantiomers from

the diet (Table 5-1). Conversely, those enantiomers for which the BMF was less

than 1 were not being accumulated, and thus were being biotransformed and/or

eliminated more rapidly than they were being absorbed by the sled dogs. Moreover, clear differences in enantiomer-specific bioaccumulation and/or biotransformation were evident. The BMF of (+)-oxychlordane was 1.8-fold higher than that of (-)-oxychlordane, while BMFs of (-)-α-HCH and (-)-PCB 149 were 3.4-fold and 2.5-fold greater than their antipodes, respectively. Clear accumulation of (+)-HEPX was also apparent, as the BMFs of (+)- and (-)-HEPX were 19.5 ± 5.9 and 1.9 ± 0.3, respectively. Although minke whale blubber was enriched in (-)-HEPX, the greater accumulation of (+)-HEPX by sled dogs resulted in an inversion in the enantiomer enrichment of HEPX between minke whale blubber and sled dog tissues (Figure 5-1). Similarly, PCB 183 was racemic in minke whale blubber, but was highly enriched in the second-eluting enantiomer in sled dog adipose tissue (EF=0.139 ± 0.067, Figure 5-2). The differences in biotransformation between individual OHC enantiomers led to a significant enrichment of the (+)-enantiomer of oxychlordane and HEPX, the (-)-enantiomer of α-HCH and PCB 149, and the second eluting enantiomer of PCB 91 and PCB 183 relative to the food. No change in the enantiomer distribution of *cis*-chlordane or PCB 174 was found between the food and adipose tissue, resulting in similarity in BMFs between enantiomers of these two compounds. These changes in OHC EFs between minke whale blubber and sled dog adipose tissues provides strong evidence that sled dogs enantioselectively biotransformed chiral OHCs (Figures 5-1 and 5-2).

Table 5-1: *Biomagnification factors of individual OC enantiomers in West Greenland sledge dog EXP cohort and polar bears from Resolute Bay, Canada.*

| | Biomagnification Factors[a] | | | |
| | EXP Sledge Dogs | | Resolute Bay Polar Bears[b] | |
	BMF	BMF Ratio[c]	BMF	BMF Ratio[d]
(+)-α-HCH	0.60 ± 0.2	3.4	1.4	2.0
(-)-α-HCH	2.0 ± 0.7		0.71	
(+)-HEPX	19.5 ± 5.9	17.9	7.4	3.2
(-)-HEPX	1.1 ± 0.3		2.3	
(+)-OXY	6.6 ± 4.1	1.9	7.1	1.2
(-)-OXY	3.6 ± 1.7		5.8	
(+)-*cis*-Chlordane	30.2 ± 13.5	1.2	0.0043	1.1
(-)-*cis*-Chlordane	24.3 ± 9.2		0.0047	
E1-PCB 91	nd		na	
E2-PCB 91	nd		na	
(+)-PCB 149	0.010 ± 0.005	2.6	na	
(-)-PCB 149	0.025 ± 0.008		na	
E1-PCB 174	nd		na	
E2-PCB 174	nd		na	
E1-PCB 183	0.28 ± 0.15	6.7	na	
E2-PCB 183	1.9 ± 0.10		na	

[a] biomagnification factors (BMF)=concentration of each enantiomer in predator divided by the concentration in the prey

[b] Data from (18)

[c] BMF ratio= BMF of more highly accumulated enantiomer (i.e., higher BMF) divided by the BMF of other enantiomer.

na=data not available

nd=not detected

The mechanism responsible for enantiomer enrichment in biota is unknown at the present time, although it has been suggested that CYP-mediated metabolism may be responsible based on the enantioselective metabolism of PCB congeners by isolated CYP isozymes *in vitro* (42,43).

The second-eluting enantiomer of PCB 183 was eliminated nearly 7 times slower than the first-eluting enantiomer, leading to a significant enrichment of the second eluting enantiomer of PCB 183 in EXP sled dog adipose tissue. PCB 183 is a metabolic precursor to 4-hydroxylated PCB 187 (4-OH-PCB 187), a major OH-PCB congener in the blood of wildlife species, including polar bears (27,44-46). Concentrations of 4-OH-PCB 187 in the present EXP sled dog plasma were reported to be nearly three-fold higher than the second most abundant OH-PCB congener, and represented approximately 25% of the total burden of OH-PCBs in sled dogs (7). Similarly, high concentrations of 4-OH-PCB 187 have also been found in polar bears and other wildlife species (27,44-46). The large ratio of PCB 183 enantiomer-specific BMFs in EXP sled dog adipose tissue and the enrichment of the second eluting PCB 183 enantiomer compared to minke whale blubber suggest substantial biotransformation occurred, which may partially explain the high concentrations of 4-OH-PCB 187 in EXP sled dog blood plasma.

Tissue-specific differences in the accumulation of individual enantiomers were also evident. The direction of enantiomer enrichment of chlordane compounds and α-HCH was similar amongst all tissues of the EXP cohort dogs, although some differences existed in the magnitude of enrichment (Figure 5-1).

Extremely non-racemic EFs (EF= 0.960 ± 0.011) of α-HCH were found in the brain tissue, consistent with the highly enriched EFs of α-HCH found in brains tissues of other species, including seals (47), rats (36), mice and quail (48). Enantiomer-specific differences in α-HCH bioaccumulation have been attributed to selective uptake of the (+)-enantiomer across the blood-brain barrier (36). An enrichment of (+)-α-HCH was found in all tissues relative to the adrenal gland, which was racemic. Similarly, (+)-oxychlordane in the liver was enriched relative to the fat and thyroid, while the (+)-enantiomer of *cis*-chlordane in fat was enriched relative to the other tissues.

Differences in the accumulation of individual OHC enantiomers between tissues has been reported previously, both in wildlife and laboratory animals. Enantiomer fractions of *trans*-chlordane were different in rats between abdominal fat and the liver (49), while differences in the tissue distribution of oxychlordane enantiomers occurred in rats (49) and bowhead whales (19). In bowhead whales, the liver contained racemic proportions of *cis*-chlordane, while adipose tissue was significantly enriched in the (+)-enantiomer (19). Variation in the enantiomer distribution of chiral OHCs between liver and adipose tissue was attributed to metabolism or selective protein binding within the liver (19), although the exact mechanism has yet to be elucidated. However, this is the first time that enantiomer distributions of chiral OHCs have been determined in adrenal or thyroid tissue, and therefore the toxicological significance of such findings is unknown. Although no histological changes in either adrenal or thyroid tissue

were found in exposed sled dogs (3), rats dosed orally with technical chlordane or *trans*-nonachlor (which is metabolized to *trans*-chlordane) developed hypothyroidism and pathological alterations of the thyroid gland (50,51). Therefore, evaluation of the enantiomer-specific toxicological effects of chiral OHCs and further investigation of the distribution of OHC enantiomers in sensitive tissues are warranted.

Enantiomer distributions of chiral OHCs were similar between CON and EXP cohort dogs for most analytes. This may be expected, due to the age and genetic similarity between CON and EXP groups. However, adipose tissue EFs of oxychlordane in CON dogs were significantly more enriched in the (+)-enantiomer than EXP dogs (Table 5-2). This difference likely resulted from the uptake of more racemic enantiomer distributions of oxychlordane from minke whale blubber by EXP cohort dogs. Oxychlordane was not detectable in pork fat, and the EF of oxychlordane in minke whale blubber (Figure 5-1) deviated less from racemic than the distributions measured in the tissues of either EXP or CON dogs (Figure 5-1 and Table 5-2). Enantiomer distributions in sled dogs and wildlife are likely at a steady-state balance between uptake of non-racemic proportions from the food and enantioselective biotransformation (52). Changes in the distribution of OHC enantiomers in prey items or in the magnitude of exposure to non-racemic quantities will thus alter the enantiomer distribution within the consuming organism.

Table 5-2: *Mean enantiomer fractions (± 1 standard deviation) of OCs in tissues of canoidea species.*

	Minke Whale	CON Sledge Dogs[a]	EXP Sledge Dogs[a]	Baffin Bay Polar Bear[a]	Resolute Bay Polar Bear[a]	Wolverine[b]	Arctic Fox[b]
α-HCH	0.657 ± 0.006	0.700 ± 0.196	0.559 ± 0.100	0.639 ± 0.079	0.59	0.423 ± 0.020	0.414 ± 0.036
HEPX	0.141 ± 0.040	nd	0.776 ± 0.022	0.725 ± 0.089	0.69	0.554 ± 0.019	0.732 ± 0.014
OXY	0.565 ± 0.022	0.778 ± 0.040	0.686 ± 0.047	0.560 ± 0.067	0.62	0.712 ± 0.020	0.676 ± 0.019
cis-Chlordane	0.105 ± 0.035	0.131 (n=1)	0.134 ± 0.046	0.299 ± 0.159	0.78	na	0.607 ± 0.035
PCB 91	0.399 ± 0.040	0.321 (n=1)	0.300 ± 0.022	0.666 ± 0.150	na	0.497 ± 0.022	0.546 ± 0.060
PCB 149	0.472 ± 0.003	0.315 (n=1)	0.258 ± 0.060	0.403 ± 0.104	na	0.461 ± 0.030	0.535 ± 0.007
PCB 174	0.516 ± 0.044	0.540 (n=1)	0.526 ± 0.010	nd	na	na	na
PCB 183	0.493 ± 0.015	0.072 (n=1)	0.139 ± 0.067	0.122 ± 0.028	na	na	na

nd=not detected

na=data not available

[a]Adipose tissue

[b]Adipose tissue data from (18).

[c]Liver data (mean ± SD) from (19).

195

5.3.4 Comparative Enantioselective Bioaccumulation

Except for oxychlordane, no differences were found in enantiomer distributions between Baffin Island sub-populations (data not shown). The difference in oxychlordane EFs may be attributable to differences in prey consumption. Davis Strait and Baffin Bay polar bear subpopulations were shown to feed at different trophic levels and employ different foraging strategies, based on stable isotope and dietary fatty acid analysis (53). For the purposes of comparing to sled dogs and other *canoidea* species, both Baffin Island subpopulations were combined into a single data set.

Enantiomer distributions of chiral OHCs have previously been determined in polar bears from Resolute Bay, Canada (54), as well in Arctic fox and wolverines from the Canadian Arctic. The overall enantiomer profiles of chiral OHCs in the current study were comparable among Baffin Island polar bears, captive EXP sled dogs, and other Arctic *canoidea* species (Table 5-2). Similarities in chiral OHC enantiomer distributions amongst *canoidea* species have been noted previously by Hoekstra et al. (55) for Arctic fox, wolverine, and Resolute Bay polar bears. The results from our study agree well with these previous observations based on visual inspection of the enantiomer distributions. Amongst the OHCs determined in all 4 species, the (+)-enantiomer of both oxychlordane and HEPX was enriched (Table 5-2) in EXP sled dogs, Arctic fox (55), wolverines (55), and polar bears (54). Despite similarities in the direction of enrichment, the magnitude of enrichment tended to vary amongst species. For

example, the magnitude of enantiomer enrichment of oxychlordane ranged from an EF of 0.560 in Baffin Island polar bears to 0.712 in wolverines, while EFs of HEPX ranged from 0.554 in wolverines to 0.776 in EXP sled dogs (Table 5-2).

The above comparisons, however, are based solely on measured EFs, with no knowledge of the enantiomer distributions within the underlying food web. To account for the dietary uptake of non-racemic distributions of OHCs, the comparative bioaccumulation dynamics and relative rate constants of individual enantiomers were investigated between sled dogs and polar bears from Resolute Bay (54) (to our knowledge the only data set in which prey species EFs were determined) using enantiomer-specific BMFs (Table 5-2). The average BMF of (+)-oxychlordane between ringed seals and polar bears was 1.22-fold greater than the BMF of (-)-oxychlordane, similar to the 1.8-fold greater BMF of (+)-oxychlordane than (-)-oxychlordane between minke whale blubber and EXP sled dogs (Table 5-1). BMF ratios of greater than unity in both species indicate a preferential elimination of (-)-oxychlordane, although at a rate that is only marginally slower than (+)-oxychlordane. In a similar vein, the BMF of (+)-HEPX in EXP sled dogs was 18 times greater than (-)-HEPX, while in polar bears this ratio was only 3 (Table 5-1). In both species, the greater accumulation of (+)-HEPX led to a reversal in the EF between predator and prey, and ultimately to EFs of similar magnitude. Both HEPX and oxychlordane are persistent metabolites, and non-racemic distributions can arise due to the enantioselective metabolism of the parent compounds, or due to the enantioselective

197

biotransformation/elimination of HEPX or oxychlordane itself. The predominant pathway leading to the non-racemic EFs is unclear, but given the comparability in BMF ratios of oxychlordane enantiomers between both species, it is apparent that similarities exist in the enantioselective bioaccumulation dynamics of oxychlordane between polar bears and sled dogs. Likewise, the similarity in enrichment of (+)-HEPX suggests similar mechanisms of enrichment (e.g., enzyme mediated degradation or elimination of HEPX), but differences in rate determining factors, such as catalytic enzyme activity.

Enantiomer distributions of several analytes varied among species. The enrichment of (-)-*cis*-chlordane found in sled dogs and Baffin Island polar bears contrasts the enrichment of the (+)-*cis*-chlordane observed previously in Arctic fox (55) and Resolute Bay polar bears (54) (Table 5-2). However, no alteration in *cis*-chlordane EF was observed between minke whale blubber and EXP sled dog adipose tissues, suggesting that sled dogs were not biotransforming *cis*-chlordane in an enantioselective manner. A similar lack of enantiomer enrichment of *cis*-chlordane was found between ringed seals and polar bears from Resolute Bay, Canada (54). If other *canoidea* species similarly lack the ability to biotransform *cis*-chlordane enantioselectively, it is possible that the variation amongst species is a result of differences in the enantiomer distribution of *cis*-chlordane within prey items, and the subsequent uptake of an excess of (+)-*cis*-chlordane. Thus the observed EF may be a reflection of the enantiomer distribution within prey items rather than *in vivo* metabolism.

Enantiomer fractions of α-HCH in EXP sled dogs were similar in magnitude and direction to those in Baffin Island polar bears and to α-HCH EFs previously reported for polar bears from Resolute Bay, Canada (54), although the enrichment of (+)-α-HCH in polar bears and EXP sled dogs contrasts the enrichment of (-)-α-HCH in wolverines and Arctic fox (55) (Table 5-2). The enrichment of (+)-α-HCH in EXP sled dogs and polar bears from both Resolute Bay and Baffin Island suggests similarities in the enantioselective biotransformation capabilities between species. However, as already discussed, (+)-α-HCH was enriched in the tissues of EXP sled dogs due to the consumption of minke whale blubber enriched in the (+)-enantiomer, as a greater BMF of (-)-α-HCH indicates EXP sled dogs were preferentially eliminating the (+)-α-HCH. In contrast, a greater BMF of (+)-α-HCH in Resolute Bay polar bears clearly indicates differences in enantiomer preference of the biotransformation systems between these two species, and further highlights the influences of dietary uptake on the interpretation of EFs in biota.

Enantiomer distributions of PCBs 91 and 149 have been measured in Arctic fox, wolverine, polar bears, and sled dogs, while EFs of PCB 183 have only been determined in EXP sled dogs and Baffin Island polar bears. PCB 149 was enriched in the (-)-enantiomer in sled dogs, polar bear, and wolverine, but was enriched in the (+)-enantiomer in Arctic fox. Similarly, biotransformation of PCB 91 in EXP sled dogs resulted in an enrichment of the second eluting enantiomer of PCB 91, whereas the antipode was enriched in polar bears and

Arctic fox (Table 5-2). Enantiomer distributions of PCBs have not been determined in both wild *canoidea* species and their prey, precluding the comparison of enantiomer-specific BMFs between EXP sled dogs and other *canoidea* species. However, racemic distributions of PCB 149 and a considerable enrichment of the second eluting enantiomer of PCB 91 (EF=0.063) were found in ringed seals from the Northwater Polynya (NOW) (56), a nearby area located on the northern tip of Baffin Bay. Assuming similar enantiomer distributions in the ringed seals from Baffin Island, the enrichment of antipodes of PCB 91 between the polar bears and sled dogs suggests differences in the enzyme systems involved in the biotransformation of PCB 91. However, without knowledge of the true enantiomer distributions in ringed seals from Baffin Island, this conclusion remains speculative.

No differences were found in the enantiomer distribution of PCB 183 between EXP sled dogs and Baffin Island polar bears (Table 5-2). As discussed earlier, metabolism of PCB 183 may lead to formation of 4-OH-PCB 187, although 4-OH-PCB 187 may also be formed metabolically from PCB 187. A greater ratio of PCB 187 + PCB 183 to 4-OH-PCB 187, a metric of inferred biotransformation capacity, was found in East Greenland polar bears compared to EXP sled dogs (7). It was postulated that different species-specific biotransformation capacities may be involved in the metabolism of PCB 183 between the two species (7). While the similarities in both direction and magnitude of the PCB 183 enantiomer enrichment between the two species

suggests similarities in enantioselective biotransformation of PCB 183, other factors (e.g., 4-OH-PCB 187 retention or greater metabolic specificity or activity towards PCB 187) not investigated here may also play a role in the differences between species in 4-OH-PCB 187 accumulation.

5.3.5 Conclusions, Perspectives and Recommendations

Previous investigations into comparative non-enantioselective bioaccumulation dynamics between EXP sled dogs and polar bears from East Greenland found similarities in the bioaccumulation dynamics of compound classes (i.e. PCBs, CHLs, etc.) between species, although the accumulation of individual compounds/congeners tended to vary (7). Differences were also found between species in OH-PCB metabolite retention and/or formation, with OH-PCB congener patterns in sled dogs being composed primarily by penta- and hexa-chlorinated congeners. Polar bears accumulated greater concentrations of OH-PCBs and the congener profile was dominated by hepta- and octa-chlorinated congeners (7). The species-specific congener/compound patterns and differences in metabolite formation were attributed to species-specific differences in biotransformation capacity (CYP enzyme content, activity and specificity), selective retention/excretion of congeners and compounds, or differences in dietary influence between species. Similarly, in this study, both similarities and differences in the enantioselective biotransformation and enantiomer accumulation were found between species. While the biochemical processes

mediating the enantioselective biotransformation of OHCs are not well understood, similarities in the direction of enrichment between Resolute Bay polar bears and EXP sled dogs suggest conservation of the substrate specificity responsible for the biotransformation of OHC contaminants between polar bears and sled dogs. However, differences in the relative rates of the biotransformation of individual enantiomers suggest dissimilarity in the rate determining processes (e.g., catalytic enzyme content and/or activity) between species. Due to the lack of data on the enantiomer distributions of chiral OHCs in Baffin Island polar bears, Arctic fox, and wolverine prey items, it is unclear whether such a conclusion may be extrapolated to these species as well, although the similarities in direction of enrichment suggest that it may. However, differences in the enantiomer preferences in biotransformation of OHCs were also found, most notably in the reversal of enantiomer preference of α-HCH between sled dogs and polar bears.

At present, the toxicological implications of enriched enantiomer distributions are unclear. *In vitro*, exposure of rat hepatocytes to (+)-α-HCH resulted in both higher cell death and greater induction of mitosis than (-)-α-HCH (57). The almost exclusive presence of (+)-α-HCH in sledge dog brain tissues, and the enrichment of (+)-α-HCH in both polar bear and sledge dog tissues, suggests the possibility of increased deleterious effects. Enantiomers of several chiral PCB congeners have been shown to induce drug metabolizing enzymes to different extents (14,15). *In vitro,* individual PCB 84 enantiomers differed in

potency for increasing translocation of protein kinase C from the cytosol to the cell membrane in rat cerebral granular cells (58), and the (-)-enantiomer of PCB 136 increased the sensitivity of ryanodine receptors (16), which are broadly expressed Ca^{2+} release channels necessary in cellular signaling and muscle contractions. However, none of these PCB congeners were investigated in the current study, and aside from α-HCH, enantiomer-specific toxicological investigations of other analytes is lacking.

In conclusion, this study further highlights several challenges in understanding and interpreting enantiomer distributions in biota. Changes in EF between CON and EXP dogs illustrate the role that dietary uptake of non-racemic proportions of chiral contaminants has on resulting EFs in biota. Moreover, the reversal in the relative enantiomer-specific biotransformation rate constants between polar bears and sled dogs, despite the similar observed EFs, demonstrates the danger in interpreting EFs in biota or making cross-species comparisons without knowledge of the enantiomer distribution in the underlying foodweb.

5.4 References

(1)   Letcher, R.J., Bustnes, J.O., Dietz, R., Jenssen, B.M., Jorgensen, E.H., Sonne, C., Verreault, J., Vijayan, M.M., Gabrielsen, G.W., Exposure and effects assessment of persistent organohalogen contaminants in Arctic wildlife and fish. Science of the Total Environment, 408 (2010) 2995-3043.

(2)   Oskam, I.C., Ropstad, E., Lie, E., Derocher, A.E., Wiig, O., Dahl, E.,

Larsen, S., Skaare, J.U., Organochlorines affect the steroid hormone cortisol in free-ranging polar bears (Ursus maritimus) at Svalbard, Norway. Journal of Toxicology and Environmental Health-Part A-Current Issues, 67 (2004) 959-977.

(3)   Sonne, C., Health effects from long-range transported contaminants in Arctic top predators: An integrated review based on studies of polar bears and relevant model species. Environment International, 36 (2010) 461-491.

(4)   Kirkegaard, M., Sonne, C., Jakobsen, J., Jenssen, B.M., Letcher, R.J., Dietz, R., Organohalogens in a whale-blubber-supplemented diet affects hepatic retinol and renal tocopherol concentrations in Greenland sled dogs (Canis familiaris). Journal of Toxicology and Environmental Health-Part A-Current Issues, 73 (2010) 773-786.

(5)   Kirkegaard, M., Sonne, C., Dietz, R., Jenssen, B.M., Leifsson, P.S., Jensen, J.E.B., Testosterone concentrations and male genital organ morphology in Greenland sled dogs (Canis familiaris) dietary exposed to organohalogen contaminants. Toxicological & Environmental Chemistry, 92 (2010) 955-967.

(6)   Sonne, C., Dietz, R., Larsen, H.J.S., Loft, K.E., Kirkegaard, M., Letcher, R.J., Shahmiri, S., Moller, P., Impairment of cellular immunity in West Greenland sledge dogs (Canis familiaris) dietary exposed to polluted Minke whale (Balaenoptera acutorostrata) blubber. Environmental Science & Technology, 40 (2006) 2056-2062.

(7)   Verreault, J., Dietz, R., Sonne, C., Gebbink, W.A., Shahmiri, S., Letcher, R.J., Comparative fate of organohalogen contaminants in two top carnivores in

greenland: Captive sledge dogs and wild polar bears. Comparative Biochemistry and Physiology C-Toxicology & Pharmacology, 147 (2008) 306-315.

(8)   Warner, N.A., Wong, C.S., The freshwater invertebrate Mysis relicta can eliminate chiral organochlorine compounds enantioselectively. Environmental Science & Technology, 40 (2006) 4158-4164.

(9)   Wong, C.S., Lau, F., Clark, M., Mabury, S.A., Muir, D.C.G., Rainbow trout (Oncorhynchus mykiss) can eliminate chiral organochlorine compounds enantioselectively. Environmental Science & Technology, 36 (2002) 1257-1262.

(10)   Ross, M.S., Pulster, E.L., Ejsmont, M.B., Chow, E.A., Hessel, C.M., Maruya, K.A., Wong, C.S., Enantioselectivity of polychlorinated biphenyl atropisomers in sediment and biota from the Turtle/River Estuary, Georgia, USA. Marine Pollution Bulletin, (in press).

(11)   Kaiser, K.L.E., Optical-Activity of polychlorinated biphenyls. Environmental Pollution, 7 (1974) 93-101.

(12)   Kania-Korwel, I., El-Komy, M., Veng-Pedersen, P., Lehmler, H.J., Clearance of polychlorinated biphenyl atropisomers is enantioselective in female C57Bl/6 Mice. Environmental Science & Technology, 44 (2010) 2828-2835.

(13)   Hoekstra, P.F., Burnison, B.K., Neheli, T., Muir, D.C.G., Enantiomer-specific activity of o,p'-DDT with the human estrogen receptor. Toxicology Letters, 125 (2001) 75-81.

(14)   Puttmann, M., Mannschreck, A., Oesch, F., Robertson, L., Chiral effects in the induction of drug metabolizing enzymes using synthetic atropisomers of

polychlorinated biphenyls (PCBs). Biochemical Pharmacology, 38 (1989) 1345-1352.

(15)   Rodman, L.E., Shedlofsky, S.I., Mannschreck, A., Puttmann, M., Swim, A.T., Robertson, L.W., Differential potency of atropisomers of polychlorinated-biphenyls on cytochrome-P450 induction and uroporphyrin accumulation in the chick-embryo hepatocyte culture. Biochemical Pharmacology, 41 (1991) 915-922.

(16)   Pessah, I.N., Lehmler, H.J., Robertson, L.W., Perez, C.F., Cabrales, E., Bose, D.D., Feng, W., Enantiomeric specificity of (-)-2,2',3,3',6,6'-hexachlorobiphenyl toward ryanodine receptor types 1 and 2. Chemical Research in Toxicology, 22 (2009) 201-207.

(17)   Buckman, A.H., Wong, C.S., Chow, E.A., Brown, S.B., Solomon, K.R., Fisk, A.T., Biotransformation of polychlorinated biphenyls (PCBs) and bioformation of hydroxylated PCBs in fish. Aquatic Toxicology, 78 (2006) 176-185.

(18)   Wiberg, K., Andersson, P.L., Berg, H., Olsson, P.E., Haglund, P., The fate of chiral organochlorine compounds and selected metabolites in intraperitoneally exposed Arctic char (Salvelinus alpinus). Environmental Toxicology and Chemistry, 25 (2006) 1465-1473.

(19)   Hoekstra, P.F., O'Hara, T.M., Karlsson, H., Solomon, K.R., Muir, D.C.G., Enantiomer-specific biomagnification of alpha-hexachlorocyclohexane and selected chiral chlordane-related compounds within an Arctic marine food web. Environmental Toxicology and Chemistry, 22 (2003) 2482-2491.

(20)   Ross, M.S., Verreault, J., Letcher, R.J., Gabrielsen, G.W., Wong, C.S., Chiral organochlorine contaminants in blood and eggs of glaucous gulls (Larus hyperboreus) from the Norwegian Arctic. Environmental Science & Technology, 42 (2008) 7181-7186.

(21)   Sonne, C., Dietz, R., Kirkegaard, M., Letcher, R.J., Shahmiri, S., Andersen, S., Moller, P., Olsen, A.K., Jensen, A.L., Effects of organohalogen pollutants on haematological and urine clinical-chemical parameters in Greenland sledge dogs (Canis familiaris). Ecotoxicology and Environmental Safety, 69 (2008) 381-390.

(22)   Sonne, C., Fonfara, S., Dietz, R., Kirkegaard, M., Letcher, R.J., Shahmiri, S., Andersen, S., Moller, P., Multiple cytokine and acute-phase protein gene transcription in west Greenland sledge dogs (Canis familiaris) dietary exposed to organic environmental pollutants. Archives of Environmental Contamination and Toxicology, 53 (2007) 110-118.

(23)   Sonne, C., Riget, F.F., Jensen, J.E.B., Hyldstrup, L., Teilmann, J., Dietz, R., Kirkegaard, M., Andersen, S., Letcher, R.J., Jakobsen, J., Does the nutrition profile of vitamins, fatty acids and microelements counteract the negative impact from organohalogen pollutants on bone mineral density in Greenland sledge dogs (Canis familiaris). Environment International, 34 (2008) 811-820.

(24)   Verreault, J., Letcher, R.J., Sonne, C., Dietz, R., Dietary, age and trans-generational effects on the fate of organohalogen contaminants in captive sledge dogs in Greenland. Environment International, 35 (2009) 56-62.

(25)   Kirkegaard, M., Sonne, C., Dietz, R., Letcher, R.J., Jensen, A.L., Hansen, S.S., Jenssen, B.M., Grandjean, P., Alterations in thyroid hormone status in Greenland sledge dogs exposed to whale blubber contaminated with organohalogen compounds. Ecotoxicology and Environmental Safety, 74 (2011) 157-163.

(26)   McKinney, M., Letcher, R., Aars, J., Born, E.W., Branigan, M., Dietz, R., Evans, T.J., Gabrielsen, G.W., Peacock, E., Sonne, C., Flame retardants and legacy contaminants in polar bears from Alaska, Canada, East Greenland and Svalbard, 2005–2008. Environment International, (in press).

(27)   Gebbink, W.A., Sonne, C., Dietz, R., Kirkegaard, M., Riget, F.F., Born, E.W., Muir, D.C.G., Letcher, R.J., Tissue-specific congener composition of organohalogen and metabolite contaminants in East Greenland polar bears (Ursus maritimus). Environmental Pollution, 152 (2008) 621-629.

(28)   Gebbink, W.A., Sonne, C., Dietz, R., Kirkegaard, M., Born, E.W., Muir, D.C.G., Letcher, R.J., Target tissue selectivity and burdens of diverse classes of brominated and chlorinated contaminants in polar bears (Ursus maritimus) from East Greenland. Environmental Science & Technology, 42 (2008) 752-759.

(29)   McKinney, M.A., Stirling, I., Lunn, N.J., Peacock, E., Letcher, R.J., The role of diet on long-term concentration and pattern trends of brominated and chlorinated contaminants in western Hudson Bay polar bears, 1991-2007. Science of the Total Environment, 408 (2010) 6210-6222.

(30)   McKinney, M.A., Peacock, E., Letcher, R.J., Sea ice-associated diet

change increases the levels of chlorinated and brominated contaminants in polar bears. Environmental Science & Technology, 43 (2009) 4334-4339.

(31)   Wong, C.S., Garrison, A.W., Foreman, W.T., Enantiomeric composition of chiral polychlorinated biphenyl atropisomers in aquatic bed sediment. Environmental Science & Technology, 35 (2001) 33-39.

(32)   Wong, C.S., Garrison, A.W., Enantiomer separation of polychlorinated biphenyl atropisomers and polychlorinated biphenyl retention behavior on modified cyclodextrin capillary gas chromatography columns. Journal of Chromatography A, 866 (2000) 213-220.

(33)   Wong, C.S., Hoestra, P.F., Karlsson, H., Backus, S.M., Mabury, S.A., Muir, D.C.G., Enantiomer fractions of chiral organochlorine pesticides and polychlorinated biphenyls in standard and certified reference materials. Chemosphere, 49 (2002) 1339-1347.

(34)   Falconer, R.L., Bidleman, T.F., Szeto, S.Y., Chiral pesticides in soils of the Fraser Valley, British Columbia. J. Agric. Food Chem., 45 (1997) 1946-1951.

(35)   Asher, B.J., D'Agostino, L.A., Way, J.D., Wong, C.S., Harynuk, J.J., Comparison of peak integration methods for the determination of enantiomeric fraction in environmental samples. Chemosphere, 75 (2009) 1042-1048.

(36)   Ulrich, E.M., Willett, K.L., Caperell-Grant, A., Bigsby, R.M., Hites, R.A., Understanding enantioselective processes: A laboratory rat model for alpha-hexachlorocyclohexane accumulation. Environmental Science & Technology, 35 (2001) 1604-1609.

(37)   Wong, C.S., Garrison, A.W., Smith, P.D., Foreman, W.T., Enantiomeric composition of chiral polychlorinated biphenyl atropisomers in aquatic and riparian biota. Environmental Science & Technology, 35 (2001) 2448-2454.

(38)   Harner, T., Wiberg, K., Norstrom, R., Enantiomer fractions are preferred to enantiomer ratios for describing chiral signatures in environmental analysis. Environmental Science & Technology, 34 (2000) 218-220.

(39)   Haglund, P., Wiberg, K., Determination of the gas chromatographic elution sequences of the (+)- and (-)-enantiomers of stable atropisomeric PCBs on Chirasil-Dex. HRC-Journal of High Resolution Chromatography, 19 (1996) 373-376.

(40)   Bruggeman, W.A., Martron, L., Kooiman, D., Hutzinger, O., Accumulation and elimination kinetics of dichlorobiphenyls, trichlorobiphenyls and tetrachlorobiphenyls by goldfish after dietary and aqueous exposure. Chemosphere, 10 (1981) 811-832.

(41)   Gobas, F., McCorquodale, J.R., Haffner, G.D., Intestinal-absorption and biomagnification of organochlorines. Environmental Toxicology and Chemistry, 12 (1993) 567-576.

(42)   Warner, N.A., Martin, J.W., Wong, C.S., Chiral polychlorinated biphenyls are biotransformed enantioselectively by mammalian cytochrome P-450 isozymes to form hydroxylated metabolites. Environmental Science & Technology, 43 (2009) 114-121.

(43)   Buser, H.R., Muller, M.D., Enantioselective determination of chlordane

components, metabolites, and photoconversion products in environmental-samples using chiral high-resolution gas-chromatography and mass-spectrometry. Environmental Science & Technology, 27 (1993) 1211-1220.

(44)   Letcher, R., Klassonwehler, E., Bergman, A., in Paasivita, J. (Editor), The Handbook of Environmental Chemistry -- New Types of Persistent Halogenated Compounds, Springer-Verlag, Heidelberg, 2000, p. 315-359.

(45)   Kunisue, T., Tanabe, S., Hydroxylated polychlorinated biphenyls (OH-PCBs) in the blood of mammals and birds from Japan: Lower chlorinated OH-PCBs and profiles. Chemosphere, 74 (2009) 950-961.

(46)   Jaspers, V.L.B., Dirtu, A.C., Eens, M., Neels, H., Covaci, A., Predatory bird species show different patterns of hydroxylated polychlorinated biphenyls (HO-PCBs) and polychlorinated biphenyls (PCBs). Environmental Science & Technology, 42 (2008) 3465-3471.

(47)   Mossner, S., Spraker, T.R., Becker, P.R., Ballschmiter, K., Ratios of enantiomers of alpha-HCH and determination of alpha-HCH, beta-HCH, and gamma- HCH isomers in brain and other tissues of neonatal northern fur seals (Callorhinus ursinus). Chemosphere, 24 (1992) 1171-1180.

(48)   Yang, D.B., Li, X.Q., Tao, S., Wang, Y.Q., Cheng, Y., Zhang, D.Y., Yu, L.C., Enantioselective behavior of alpha-HCH in mouse and quail tissues. Environmental Science & Technology, 44 (2010) 1854-1859.

(49)   Bondy, G.S., Coady, L., Doucet, J., Armstrong, C., Kriz, R., Liston, V., Robertson, P., Norstrom, R., Moisey, J., Enantioselective and gender-dependent

depletion of chlordane compounds from rat tissues. Journal of Toxicology and Environmental Health-Part A-Current Issues, 68 (2005) 1917-1938.

(50)   Bondy, G., Curran, I., Doucet, J., Armstrong, C., Coady, L., Hierlihy, L., Fernie, S., Robertson, P., Barker, M., Toxicity of trans-nonachlor to Sprague-Dawley rats in a 90-day feeding study. Food and Chemical Toxicology, 42 (2004) 1015-1027.

(51)   Lu, B., Zhan, P., Time-dependent effects of chlordane on thyroid histological structure and function in rats. Toxicological & Environmental Chemistry, 92 (2010) 813 - 821.

(52)   Vetter, W., Smalling, K.L., Maruya, K.A., Interpreting nonracemic ratios of chiral organochlorines using naturally contaminated fish. Environmental Science & Technology, 35 (2001) 4444-4448.

(53)   McKinney, M.A., Letcher, R.J., Aars, J., Born, E.W., Branigan, M., Dietz, R., Evans, T.J., Gabrielsen, G.W., Muir, D.C.G., Peacock, E., Sonne, C., Regional contamination versus regional dietary differences: Understanding geographic variation in brominated and chlorinated contaminant levels in polar bears. Environmental Science & Technology, 45 (2011) 896-902.

(54)   Wiberg, K., Letcher, R.J., Sandau, C.D., Norstrom, R.J., Tysklind, M., Bidleman, T.F., The enantioselective bioaccumulation of chiral chlordane and alpha-HCH contaminants in the polar bear food chain. Environmental Science & Technology, 34 (2000) 2668-2674.

(55)   Hoekstra, P.F., Braune, B.M., Wong, C.S., Williamson, M., Elkin, B.,

Muir, D.C.G., Profile of persistent chlorinated contaminants, including selected chiral compounds, in wolverine (Gulo gulo) livers from the Canadian Arctic. Chemosphere, 53 (2003) 551-560.

(56)   Warner, N.A., Norstrom, R.J., Wong, C.S., Fisk, A.T., Enantiomeric fractions of chiral polychlorinated biphenyls provide insights on biotransformation capacity of Arctic biota. Environmental Toxicology and Chemistry, 24 (2005) 2763-2767.

(57)   Möller, K., Hünerfuss, H., Wölfe, D., Differential effects of the enantiomeres of α-hexachlorcyclohexane (α-hch) on cytotoxicity and growth stimulation in primary rat hepatocytes. Organohalogen Compounds, 29 (1996).

(58)   Lehmler, H.J., Robertson, L.W., Garrison, A.W., Kodavanti, P.R.S., Effects of PCB 84 enantiomers on [h-3]-phorbol ester binding in rat cerebellar granule cells and ca-45(2+)-uptake in rat cerebellum. Toxicology Letters, 156 (2005) 391-400.

Chapter 6

Isomer-Specific Biotransformation of Perfluorooctane

Sulfonamide in Sprague-Dawley Rats

6.1 Introduction

Synthetic derivatives of perfluorooctane sulfonyl fluoride (PFOSF; $C_8F_{17}SO_2F$) were widely used in a variety of consumer products since the early 1950s, including in firefighting foams and stain repellant coatings for carpet, paper, and textiles. Perfluorooctane sulfonate (PFOS; $C_8F_{17}SO_3^-$; Figure 1-7) is one commercial derivative of PFOSF, but it is also a known biodegradation product of most other PFOSF derivatives. PFOS has garnered much regulatory and scientific scrutiny owing to its persistence and pervasiveness in the environment, and its bioaccumulative (1-3) and toxicological characteristics (4). PFOS has been detected in most environmental compartments globally, including in remote regions of the Arctic (5-7), and in the blood of humans in most countries (8,9). PFOS has been linked to developmental effects (10-12) and other toxicological impairments, including induction of peroxisome proliferation (13), increased liver weight and hepatocellular adenomas (14), and altered thyroid homeostasis (12,15).

Despite the ubiquity of PFOS, the routes by which humans and wildlife are exposed to PFOS remain unclear, although two general routes are involved. The first is direct exposure to PFOS through the diet or the ingestion of dust (8). The second route involves indirect exposure through absorption of PFOS-precursor compounds, such as various perfluorooctane sulfonamides ($C_8F_{17}SO_2NRR'$; Figure 1-9), and the subsequent biotransformation of these to

PFOS. PFOS itself is not metabolized, and the formation of PFOS as a terminal metabolite from perfluorooctane sulfonamides has been demonstrated *in vitro* (16,17) and *in vivo* (18,19). The relative magnitude by which either of these routes contributes to the overall body burden of PFOS, however, remains unclear. Models suggest that precursor exposure may account for between 10% and 40% of the daily intake of PFOS (8,20). However, considerable uncertainty exists in these estimates, largely due to the lack of data on the pharmacokinetics of PFOS-precursor compounds in animals, and the difficulty in extrapolating across species.

It has been suggested that the use of PFOS isomer patterns may be a biomarker of PFOS exposure sources (21). The manufacture of PFOS and its precursors occurred exclusively by electrochemical fluorination (ECF) (22), a synthetic method that produces a mixture of linear and branched isomers (Figure 1-8). This process resulted in a consistent isomeric composition of 70 ± 1.1% (mean ± standard deviation) linear isomer and 30 ± 0.8% branched isomers (23) over decades of manufacturing by the 3M Co., whom manufactured the bulk (~80%) of PFOS worldwide (24). Furthermore, from the limited data available, the isomeric composition of manufactured PFOS-precursors was similar to that of PFOS (21). Therefore, PFOS isomer profiles in environmental or biological samples that differ significantly from 70% linear indicate that isomer-specific fate processes are active in the environment or organisms. By studying and understanding such processes, the variety of PFOS isomer signatures observed in

216

biomonitoring studies may, one day, be interpreted to assist in tracking the sources of PFOS exposure.

Branching of long perfluorinated chains can have considerable effects on the biological processing of perfluorinated compounds. For instance, in rats and fish, branched isomers of perfluorooctanoate (PFOA) are eliminated more quickly than the linear isomer, resulting in blood isomer profiles that are enriched in the linear isomer relative to the dose (25-27). Similarly, fish preferentially bioconcentrate the linear PFOS isomer (28), and rats eliminate branched isomers preferentially in the urine, resulting in shorter half-lives in the blood for most branched isomers compared to linear (25,26). Based on these studies, it is anticipated that direct exposure to PFOS should result in isomer patterns in humans and wildlife that contain fewer branched isomers than the manufactured material (i.e. ≤30%). While this is generally true in wildlife biomonitoring (29-33), some instances have been reported where the branched isomer content in human blood is greater than 40% (34,35). The reasons for such enrichment remain unknown, but *in vitro* evidence suggests that isomer-specific metabolism of PFOS precursors may be one explanation. Branched isomers of *N*-ethyl perfluorooctane sulfonamide (NEtFOSA; $C_8F_{17}SO_2NH(C_2H_5)$) were *N*-deethylated more quickly than the linear isomer *in vitro*, leading to an initial enrichment in the branched isomers of perfluorooctane sulfonamide (PFOSA; $C_8F_{17}SO_2NH_2$) (36). However, to date, no studies have investigated the isomer-specific metabolism of a PFOS-precursor *in vivo* and the influence this might

217

have on the resulting PFOS isomer profile in blood and tissues.

Here, the *in vivo* isomer-specific fate of PFOSA at environmentally relevant concentrations is investigated to test the hypothesis that the isomer profile of its metabolite, PFOS, would be different from the parent material. PFOSA was chosen for study because it is a known PFOS-precursor and is a primary intermediate metabolite in the metabolism of higher molecular weight PFOS precursors (18). PFOSA is also relevant because it is detectable in the environment (37-39), and in the blood and tissues of humans (9) and wildlife (40,41).

6.2 Materials and Methods

6.2.1 Isomer Nomenclature

The nomenclature used here for all PFOS isomers is based on a previously published convention (42). Mono-perfluoromethyl isomers were named according to the carbon number on which the branching was situated. For example, 4*m*-PFOS refers to perfluoro-4-methyl-heptanesulfonate. The linear and isopropyl isomers are named as *n*- and *iso*-PFOS, respectively. Di-perfluoromethyl PFOS isomers were integrated together and are referred to collectively as Σdimethyls.

The linear isomer of PFOSA (*n*-PFOSA) in ECF PFOSA was identified based on an authentic linear standard. Due to the lack of authentic standards for branched PFOSA isomers, ECF PFOSA isomers measured in this study were

identified simply as Br1, Br2, and Br3 on the basis of elution order (earliest to latest). Based on visual appearance of the chromatograms, Br1 was not a pure isomer but was comprised of at least three coeluting isomers, integrated here as a single peak. Assuming an analogous elution pattern to PFOS isomers, Br1 likely represents the dimethyl branched PFOSA isomers, Br2 may be a coelution of 3 or 4 monomethyl isomers, and Br3 is likely *iso*-PFOSA (42); however these assignments could not be confirmed.

6.2.2 Standards and Reagents

High performance liquid chromatography (HPLC) grade methanol, pesticide grade acetone, and formic acid (99%, Acros Organics) were purchased from Fisher Scientific (Ottawa, ON, Canada). Water was obtained via a Millipore (Billerica, MA, USA) water filtration system. Standards of mixed PFOS isomers (brPFOSK), perfluoro-*n*-[$^{13}C_8$]octanesulfonamide ($^{13}C_8$-PFOSA), and perfluoro-*n*-[1,2,3,4-$^{13}C_4$]octanesulfonate ($^{13}C_4$-PFOS) were purchased from Wellington Laboratories (Guelph, ON, Canada). ECF PFOSA (>98% purity) and ECF PFOS were provided by the 3M Co. (St. Paul, MN, USA). Based on NMR analysis, the ECF PFOSA, used for spiking the rat chow, was composed of 70.9% (weight percent) *n*-PFOSA (Table 6-1).

Table 6-1: *Isomer composition (%) of 3M manufactured ECF PFOSA and PFOS.*

Isomer	Isomer composition (%)	
	ECF PFOSA[1]	ECF PFOS[2]
Linear	70.9	70
Internal Monomethyl	15.2	17
Isopropyl	9.1	10.3
Alpha	3.2	1.6
Σdimethyl	0.33	0.4

[1]NMR data of ECF PFOSA provide by the 3M Co.

[2]Data from (57)

6.2.3 Dose Preparation

Spiking of rat chow was carried out by adding 750 g of LabDiet 5001 Laboratory Rodent Diet (PMI Nutrition International, St. Paul, MN, USA) to a 2 L round bottom flask, filling the flask with enough acetone to cover the rat chow, and spiking with ECF PFOSA dissolved in acetone. The flask was manually shaken for one minute, allowed to sit overnight, and the acetone was subsequently removed by rotary evaporation. Rat chow was then placed onto a sheet of cleaned aluminum foil and allowed to air-dry overnight. The diet for the control group was prepared similarly, but without the addition of PFOSA.

6.2.4 Animal Husbandry

Twelve 8-week old male Sprague-Dawley rats were obtained from the University of Alberta Biosciences Animal Service (University of Alberta, Edmonton, AB, Canada). Rats were housed two rats per cage in a temperature and light controlled facility until the end of the uptake phase, after which rats were housed one per cage. Prior to the beginning of the experiment, rats were acclimated to their surroundings and routine handling for 41 days. All experimental procedures were approved by the University of Alberta Animal Policy and Welfare Committee.

6.2.5 Experimental Design

Prior to exposure, rats were randomly divided into control (*n*=4) and experimental (*n*=8) groups. For the duration of the uptake phase (77 days), experimental rats were given *ad libitum* access to ECF PFOSA spiked food. Control rats were given *ad libitum* access to unspiked food. On day 77, 3 experimental rats and 2 control rats were euthanized by CO_2. The remaining rats were switched to a diet of unspiked food for an additional 27 days (depuration phase), at which point all remaining rats were euthanized by CO_2. Every one to two weeks throughout the uptake and depuration phases, two rats from the experimental group were placed into metabolic cages for 24 hours to collect urine and feces; the same two rats were used throughout the experiment.

6.2.6 Sample Collection

Blood samples were collected throughout the experiment at predetermined times, and the weight of individual animals was regularly recorded. Small volume blood samples (~ 500 µL) were collected by puncturing the lateral tail vein with a 22-gauge needle and allowing the blood to drip directly into preweighed Vacutainer® tubes (BD Biosciences, Mississauga, ON, Canada) coated with lithium heparin. Large volume blood samples were collected from CO_2 euthanized rats at the end of the uptake and depuration phases by cardiac puncture using 18-gauge needles and 10 mL plastic syringes. Blood was immediately ejected into preweighed heparanized Vacutainer® tubes. All tissue samples were excised immediately after euthanasia and transferred to 15 or 50 mL polypropylene centrifuge tubes (Corning, New York, NY, USA).

Urine samples were collected from metabolic cage rats in 250 mL polycarbonate beakers and were transferred to 50 mL polypropylene centrifuge tubes. Feces were collected with methanol rinsed tweezers and transferred to 15 or 50 mL polypropylene centrifuge tubes. All samples were stored at -20 °C until analysis.

6.2.7 Extraction

All blood samples were extracted with methanol using a modification of the method developed by Tomy et al. (43), which was previously shown to

conserve PFOS isomer profiles (31). All small volume blood samples were extracted directly in the Vacutainer® collection tubes. For large volume blood samples, a 500 μL aliquot of whole blood was removed and transferred to 15 mL centrifuge tubes for extraction. Prior to extraction, all blood samples were spiked with an internal standard mix containing 25 ng each of $^{13}C_4$-PFOS and $^{13}C_8$-PFOSA. Samples were then vortexed briefly, and allowed to sit for 10 minutes. Following this, 3 mL of methanol were added to the samples and tubes were shaken manually for 5 minutes. Samples were centrifuged for 15 minutes and the supernatant was transferred to a clean 15 mL centrifuge tube. The extraction process was repeated twice more and supernatants were combined. Samples were concentrated by nitrogen evaporation to approximately 100 μL, transferred to autosampler vials, and diluted to 500 μL with 50:50 methanol:water.

For tissue and feces extractions, whole brain, lung, heart, kidney, testes, spleen, 2 g sub-samples of fat, muscle and feces, or a 0.5 g sub-sample of liver were transferred to individual polypropylene centrifuge tubes and spiked with the internal standard mix. Tissues were homogenized in 1 to 2 mL of methanol with a Polytron hand blender and extracted using the method described above. Methanolic extracts were evaporated to approximately 100 μL, diluted with 10 mL of water, and cleaned up by solid phase extraction on 6 cc Oasis HLB SPE cartridges (Waters Co., Milford, MA, USA). Cartridges were conditioned with 5 mL of methanol and 5 mL of water prior to the loading of the sample onto the cartridges. Samples were then washed with 5 mL of 50:50 methanol:water and

analytes were eluted with 10 mL of methanol. These were reduced in volume to approximately 100 μL, transferred to autosampler vials and diluted to 500 μL with 50:50 methanol:water.

Aliquots (2 mL) of urine were transferred to individual polypropylene centrifuge tubes, spiked with the internal standard mix, diluted with 10 mL of water, and extracted by the same solid phase extraction method as above.

6.2.8 Instrumental Analysis

Isomer-specific analysis of PFOS and PFOSA was carried out using a slight modification of the method developed by Benskin et al (25,42). Analyses were carried out using an Agilent 1100 HPLC system coupled to either an API 5000 or QTrap 2000 mass spectrometer (Applied Biosystems, Foster City, CA, USA). Isomers were separated with a FluoroSep RP Octyl column (3 μm, 100 Å, 150 × 2.1 mm i.d., ES Industries, West Berlin, NJ, USA). Gradient elution was used with an initial eluent composition of 50% A (H_2O and 5 mM formic acid, adjusted to pH 4) and 50% B (methanol), and a flow rate of 200 μL min^{-1}. Initial conditions were held for 0.3 min, before being ramped to 64% B by 1.9 min, 78% B by 40 min, and 100% B by 69 min. Final conditions were held for 13 min, before returning to initial conditions. The mass spectrometer was operated in negative electrospray ionization mode, and mass spectral data was collected by multiple reaction monitoring for PFOS and PFOSA isomers.

The presence of *N*-glucuronide conjugates in whole blood, liver, feces, and urine was investigated by operating the mass spectrometer with negative electrospray ionization in product ion scanning mode, scanning for the products of the glucuronide conjugate (*m/z* 674) and its sodium adduct (*m/z* 696) (17,44). In addition, precursors of *m/z* 176 (anhydroglucuronic acid), *m/z* 480 ($C_8F_{17}SO_2^-$), and *m/z* 498 (PFOSA) were also investigated.

6.2.9 Data Analysis

Linear and branched isomers of PFOS were quantified individually with isomer-specific calibration curves based on the known isomer composition of brPFOSK (35,42), and using $^{13}C_4$-PFOS as the internal standard. Sum of dimethyl (Σdimethyl) PFOS isomers were quantified by summing the response of the first three eluting dimethyl isomers in the *m/z* 499 → 130 transition. PFOSA isomers were quantified using the known isomer composition of the NMR-characterized standard (Table 6-1). The total branched isomer content was also known (Table 6-1), thus Σbranched isomers were quantified by a calibration curve of the summed peak areas of Br1, Br2, and Br3 in the *m/z* 498 → 78 transition. Due to the lack of isomer-specific PFOSA standards, only the linear and Σbranched isomers could be quantified.

Body masses (g) for individual rats were fit to an exponential growth

function, $ln(mass)=(a \times t) + ln\ b$, where a is the growth rate (g d^{-1}), t is time (d), and b is the initial mass (g). Concentrations of PFOS and PFOSA in blood samples were corrected for growth dilution by multiplying concentrations of individual isomers by $1 + (a \times t\ /\ b)$, where a and b are derived from the exponential growth model of the rat masses over the course of the experiment (26).

Elimination kinetics of n-PFOSA were determined by fitting the growth corrected concentrations to the first order rate equation $C=C_0e^{-kt}$, where C_0 is the concentration (ng g^{-1}) in the blood at the end of the uptake phase, t is the total time of the depuration phase (days), and k is the elimination rate constant. Half-lives were calculated as $t_{1/2}=ln\ (2)/k$. For Br2 and Br3, the relative response of each isomer (relative to ^{13}C-PFOSA) was calculated and fit to the first order elimination model.

Unfortunately, there were background concentrations of n-PFOS in control rats that obfuscated the PFOS profiles of exposed rats. For example, concentrations of n-PFOS in control rats sometimes reached 25% of the concentration in experimental rats. Thus, the mean concentration of n-PFOS (and any minor branched isomers) in control animals was used to correct the PFOS profile of exposed animals. The detection of n-PFOS in controls was not from laboratory contamination, but rather was likely due to accumulation from background levels in unspiked food (see below).

226

6.2.10 QA/QC

Isotopically labeled internal standards of branched PFOS or PFOSA isomers were unavailable. Thus matrix effects were evaluated using a post extraction standard addition technique in blood and tissues of control rats. ECF PFOS and PFOSA (25 ng of each) was spiked and the relative response of each isomer (relative to ^{13}C-PFOSA) was compared to that a standard spiked in methanol. There were no differences in the percentage of total branched PFOS isomers between spiked whole blood and the standard. For PFOSA, no matrix effects were observed in the blood. A small, albeit significant, suppression of the total branched PFOSA isomers was observed for both food and urine; however, the suppression was less than 10%. A greater suppression was found in the feces and tissues, averaging 17% in the feces, and 37% in both the fat and liver.

6.3 Results and Discussion

6.3.1 Spiked Food Concentrations

Due to the large quantities of spiked food required, several individual batches were created during the exposure. Due to batch-to-batch variability, the exposure also varied during the experiment. The mean spiked food concentration was 2.1 ± 0.5 ng g^{-1} total PFOSA, with concentrations ranging from 1.3 to 2.6 ng g^{-1} (Table 6-2). Nonetheless, the percentage of branched PFOSA isomers was similar among all batches ($22 \pm 1\%$). In all control food, PFOSA was below

limits of quantification (<0.02 ng g^{-1}). Unfortunately, PFOS was detectable in control and spiked food at similar concentrations (0.38 to 3.1 ng g^{-1}), and the isomer profile was composed of greater than 87% *n*-PFOS.

Table 6-2: *Individual batches of spiked and control food, the experimental day administered, total PFOSA concentration, percentage of total branched isomers of PFOSA, and daily dose of total PFOSA.*

Batch	Day	[Total PFOSA] (ng g⁻¹)[1]	Percentage of Total Branched Isomers (%)	Daily Intake (ng kg-1 day-1)[1]
Control Food				
1	0-50	<LOD	n/a[2]	0.64 ± 0.32
2	51-77	<LOD	n/a[2]	0.45 ± 0.39
Spiked Food				
1	0-11	2.59 ± 0.13[a]	23 ± 1	103 ± 5
2	12-24	1.84 ± 0.49[bc]	23 ± 1	73 ± 19
3	25-50	2.14 ± 0.22[ab]	20 ± 1	85 ± 9
4	51-73	1.36 ± 0.12[c]	22 ± 1	54 ± 5
5	74-77	2.56 ± 0.12[a]	22 ± 1	101 ± 5
Control Average		<LOD	n/a[2]	na
Spiked Average		2.10 ± 0.53	22 ± 1	83 ± 21

[1]Values with differing superscripts within a column indicates statistically significant differences ($p<0.$

[2]No branched PFOSA isomers were detected in control food

229

6.3.2 Food Consumption

Food consumption per cage was measured every week by weighing food before and after administration. Over the course of the experiment, food consumption remained relatively constant, with daily food consumption averaging 39.6 ± 15.0 g day^{-1} kg^{-1} rat^{-1}. There were no differences in average food consumption between experimental and control groups.

The average daily intake of total PFOSA for exposed rats was 83 ± 21 ng kg^{-1} day^{-1}. The high variability was a consequence of the batch-to-batch variability of spiked food concentration, and the range of daily PFOSA intakes are presented in Table 6-2. Over the course of the uptake period, the total PFOSA dose to individual rats was approximately 4.1.

6.3.3 Body Weight and General Observations

No mortality or overt adverse effects were observed. The low concentrations used were assumed to be well below the no observed effects level (NOEL), based on a NOEL for PFOS of 370 mg kg^{-1} d^{-1} in a 14-day dietary exposure (14). There were also no significant differences in growth rates between control and experimental treatment groups, or in the mean mass of the two groups at the end of the experiment (*t*-test, $p>0.05$; data not shown).

6.3.4 Disposition of Total PFOSA

Exposure to ECF PFOSA in spiked food led to the detection of Br2-, Br3-, and *n*-PFOSA in blood and tissues. Mean blood concentrations reached steady state by day 22 (26.9 ± 19.4 ng g^{-1}; Figure 6-1), with no statistically significant change in the concentration through to day 62. This time to steady state was consistent with the blood half-life determined during the depuration phase for total PFOSA (6.1 ± 4.1 d^{-1}). By theory, 94% of the steady state concentration is reached within 4 half-lives. On the last day of sampling during the uptake phase (day 77), however, concentrations of total PFOSA had decreased to 18.8 ± 12.0 ng g^{-1}. This decrease was likely attributable to the significantly lower concentrations of PFOSA in the batch of food administered prior to this sampling point (Figure A-4-1). In an attempt to normalize the uptake phase data for variations in food concentration, diet-blood accumulation factors (AF) for total PFOSA in the blood were calculated at each sampling point by dividing the concentration of PFOSA in the blood by the mean total PFOSA concentration in food over each ten day period prior to the sampling point. Average AFs on individual samples days ranged from 10.2 ± 4.5 to 14.6 ± 5.2, with an overall average across all sampling points of 13.0 ± 1.6. Consistent with steady state conditions, no change in the AF was observed from day 22 to day 77 (Figure 6-2). It should be noted, however, that AFs were calculated only for the purposes of normalizing for variation in food concentrations, and therefore should be considered as approximates only.
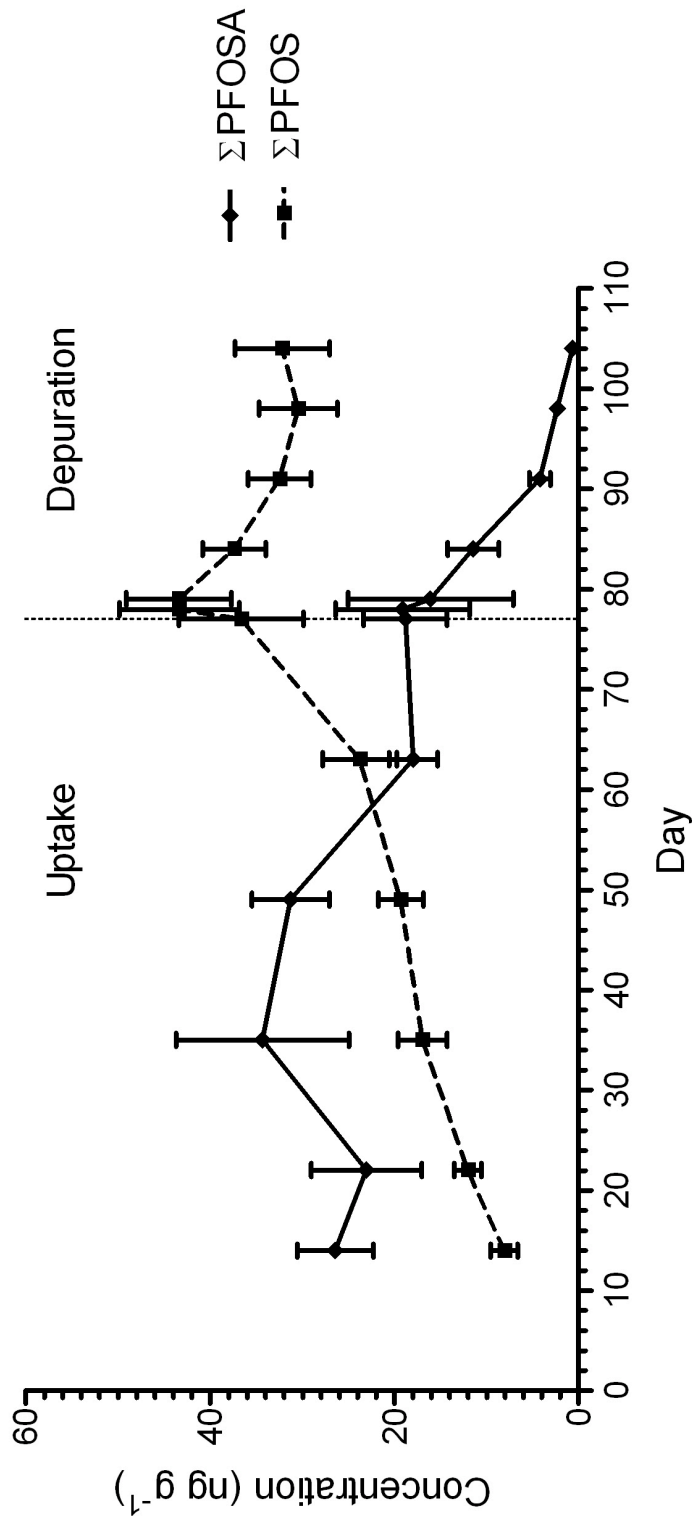
Figure 6-1: *Growth corrected whole blood concentrations of ΣPFOSA and ΣPFOS during uptake (days 0 to 77) and depuration (days 78-104) phases. Each point represents the mean ± 1 standard error for n=8 up to day 77 and n=5 between days 78 and 104. Vertical dashed line delineates the end of the uptake phase.*

232

Sparse pharmacokinetic data for PFOSA are available in the literature for comparison. In rats given a single gavage dose of PFOSA, the apparent half-life in the liver was 5.2 days, while in the blood plasma it was estimated to be less than 4 days (18). To date, most pharmacokinetic data available for PFOSA are based on exposure to NEtFOSA, a higher molecular weight PFOS-precursor that is rapidly *N*-deethylated to yield PFOSA. PFOSA serum half-lives in rats dosed by a single gavage dose of NEtFOSA, or via the food for 35 days, ranged from 4.2 days to 10.8 days, respectively (45,46). The blood half-life of total PFOSA reported here is also similar to half-lives reported for total PFOSA in sheep administered an intravenous or intraruminal bolus dose of NEtFOSA (2.1-3.1 days) (47).
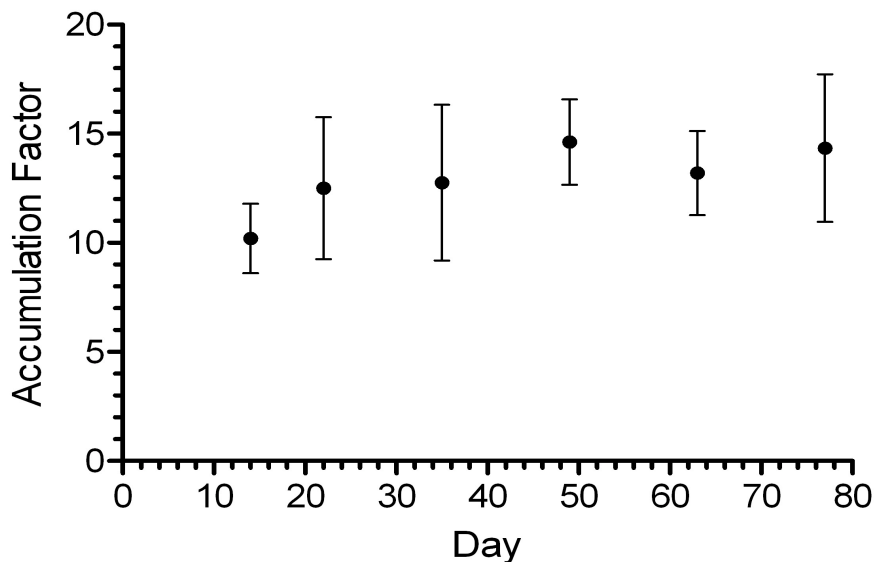
Figure 6-2: *Whole blood dietary accumulation factors of total PFOSA during uptake phase (days 0 to 77). Each point represents the mean ± 1 standard error for n=8.*

Furthermore, the time to reach steady state is consistent with previous studies, where apparent steady state concentrations of PFOSA were reached within seven days in rats exposed via their diet to NEtFOSA (45).

Tissue PFOSA concentrations were all lower than in blood. At the end of the uptake phase, concentrations of total PFOSA were highest in well-perfused organs, with the highest concentrations in spleen (5.79 ± 0.58 ng g^{-1}), followed by the lung, liver and kidney tissues (Figure A-4-2A). It is interesting to note the higher concentrations in the spleen, which is responsible for filtering and removing old red blood cells, may be a result of the high binding efficiency of PFOSA to red blood cells. PFOSA concentrations in whole blood have been reported to be up to 26-fold higher than in serum (47-49). However, no significant differences were found in PFOSA concentrations amongst tissues, with the exception of fat and testes, which were significantly lower than blood. The tissue distribution observed in this study is generally consistent with previous studies on the disposition of PFOSA (47,50), although other studies have reported higher concentrations of PFOSA in liver than in blood serum (18). This discrepancy may again be a result of the high binding efficiency of PFOSA to red blood cells, as whole blood was analyzed in this study.
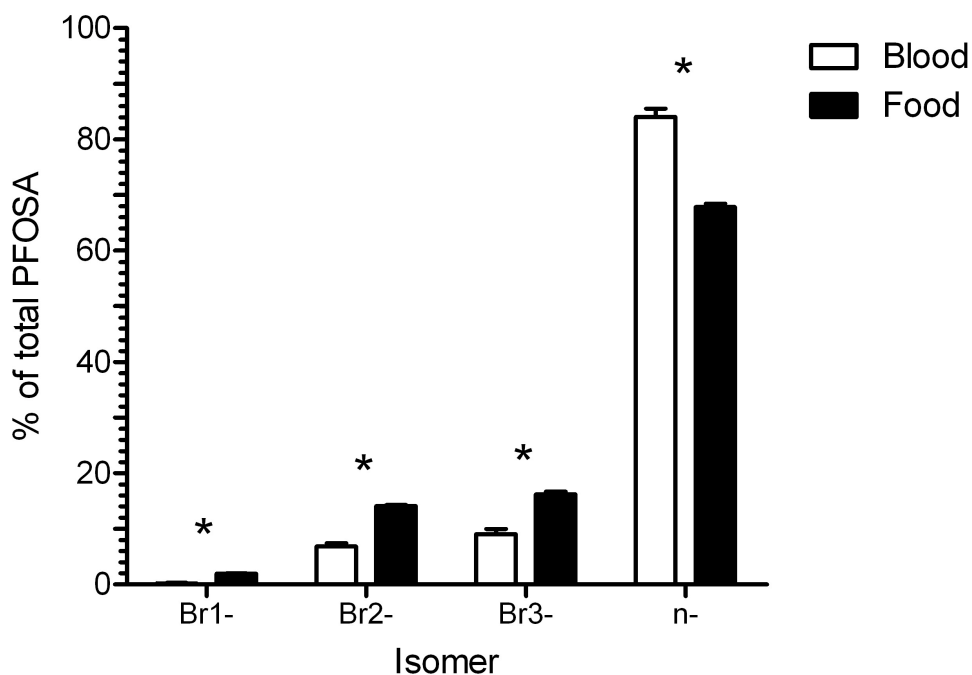
Figure 6-3: Percentage of individual PFOSA isomers in spiked food and whole blood of rats after 77 days of exposure to electrochemically fluorinated PFOSA. The asterisk indicates significant differences between food and blood.

6.3.5 Disposition of PFOSA Isomers

Isomer profiles of PFOSA throughout the uptake phase revealed clear evidence for isomer-specific accumulation. The average percentage of branched isomers in blood at the end of uptake was $15 \pm 7\%$, with a significant depletion of Br1-, Br2-, and Br3-PFOSA compared to spiked food (Figure 6-3). While the percentage of branched PFOSA isomers in blood varied throughout the uptake phase, it was always less than that in the food (22 ± 1 % branched isomers) (Figure 6-4). Likewise, all tissues contained a lower percentage of branched

isomers than the food (Figure A-4-2B). Mean PFOSA isomer compositions in tissues ranged from 6.5 ± 1.5% in heart to 14 ± 10% in fat, although there were no statistically significant differences among tissues. Although it was detected in the spiked food, Br1-PFOSA (presumably diperfluoromethyl branched isomers) was only intermittently detected at low concentrations in the blood, and was never detected in tissues. This may be due to a combination of factors, including the low concentrations of these isomers in the spiked food, rapid excretion (Br1-PFOSA was detectable in feces), or possible rapid biotransformation.

The relative enrichment of *n*-PFOSA in blood and tissues is a result of the preferential elimination or metabolism of branched PFOSA isomers. Br2-, Br3-, and *n*-PFOSA were rapidly eliminated from the blood during the depuration phase with half-lives of 2.5 ± 1.0, 3.7 ± 1.2, and 5.9 ± 4.6 days, respectively. Similar to the blood, branched PFOSA isomers were more rapidly eliminated from the tissues than the linear isomer. For example, by the end of the depuration phase, only *n*-PFOSA was detectable in all tissues (with the exception of blood).

The preferential excretion of branched PFOSA isomers via urine or feces were considered as possible explanations for the relative deficiency of branched PFOSA isomers in blood and tissues. No PFOSA was detected in urine, but total PFOSA concentrations increased in feces during the study, reaching a maximum of 47.1 ng g^{-1} on day 72, the last day of sampling in the uptake phase. However, *n*-PFOSA was always enriched in the feces relative to food (Figure A-4-3A), with

236
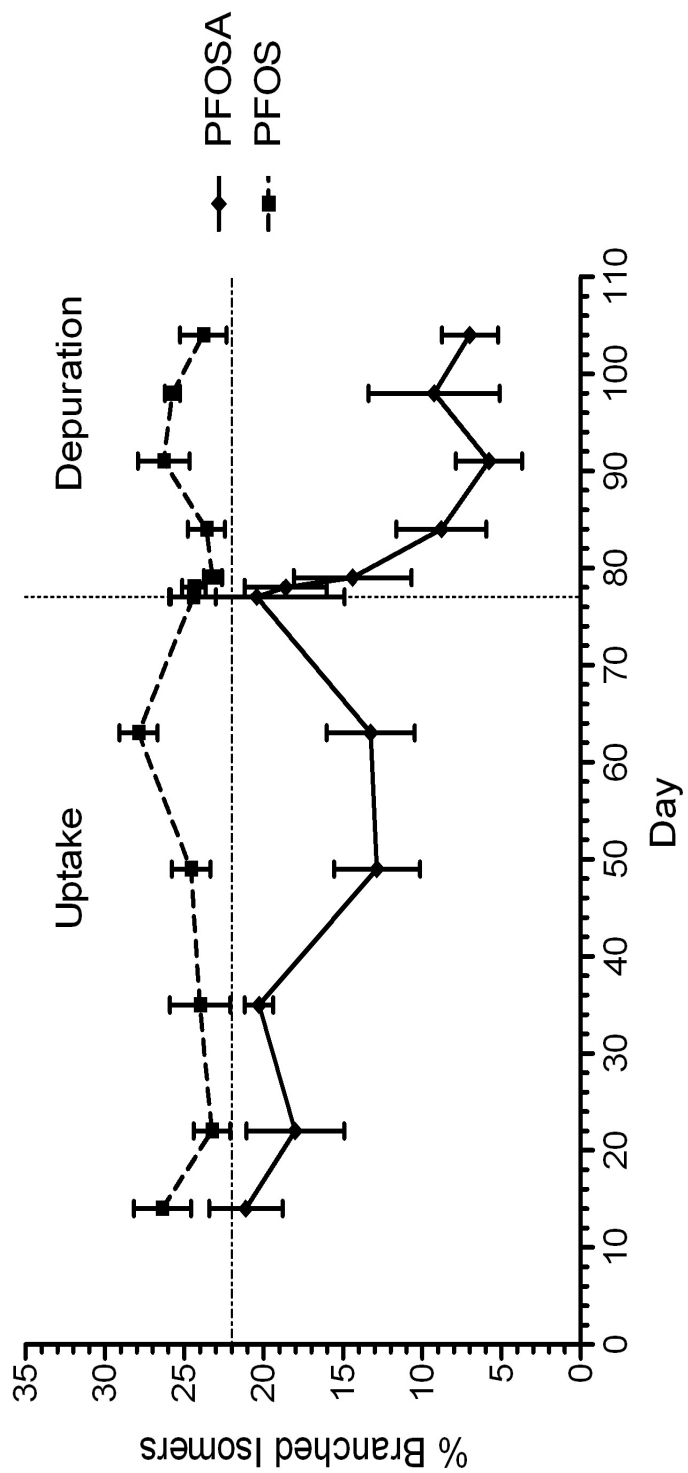
Figure 6-4: *Percentage of total branched isomers of PFOS and PFOSA in whole blood during uptake (days 0 to 77) and depuration (days 78 to 104) phases. Each point represents the mean ± 1 standard error for n=8 up to day 77 and n=5 between days 78 and 104. Vertical dashed line delineates the end of the uptake phase. Horizontal dashed line represents the mean percentage of branched PFOSA isomers in the food.*

237

an average branched isomer percentage in the feces across the entire uptake phase of 13 ± 5%, indicating that excretion of PFOSA was not the mechanism leading to the relative depletion of branched PFOSA in rat blood and tissues. The responsible mechanism must therefore have been metabolism, either to PFOS or some phase II conjugate. No phase II (*N*-glucuronide) conjugates of PFOSA were detected in this study, although glucuronidation appears to be a minor metabolic pathway of PFOSA in rats; 3% of a total NEtFOSA dose was excreted as an *N*-glucuronide conjugate (48).

Although PFOSA and other PFOS-precursors have been detected in human blood and in the tissues of wildlife (1), few studies have investigated the isomer profile of PFOS-precursors in environmental samples. An enrichment of both PFOS and PFOSA branched isomers (~60% branched isomer content) was found in seawater from the German Bight (51), although it was unclear whether this isomer composition is reflective of manufactured PFOSA, the breakdown of other precursor compounds, or an enrichment of branched PFOSA isomers due to environmental fractionation. Similarly, an enrichment in branched PFOSA isomers was found in wastewater treatment plant effluent (52). In contrast, the isomer profile in human blood was found to be dominated by the linear isomer, with only two branched isomers (corresponding to Br2 and Br3 in this study) being detected (42), similar to what has been found in this study. These studies indicate that branched isomers of PFOS-precursors are present and detectable in the environment, although considerably more work must be done in order to

ascertain how environmental fate processes affect individual isomers.

6.3.6 Isomer-Specific Formation of PFOS

Eight branched PFOS isomers, in addition to *n*-PFOS, were detected in the blood and tissues of rats exposed to ECF PFOSA. In contrast to the rapid steady-state reached for PFOSA, a slow increase in concentrations of individual PFOS isomers was observed throughout the uptake phase (Figure 6-1). Total PFOS concentrations peaked at 43.4 ± 12.8 ng g^{-1} on day 78, with other isomers reaching maximum concentrations on day 77 or 78, depending on the isomer. The isomer profile of PFOS in blood remained relatively constant throughout the experiment. No significant changes in the percentage of total branched isomers were observed after day 22 (Figure 6-4), with the exception of on day 64 when the percentage of branched isomer increased slightly (28 ± 3 % branched isomers). While the percentage of branched PFOS isomers was always greater than that of PFOSA in food, the difference was only statistically significant on day 64. At the end of the uptake phase, the liver had a significantly enriched branched PFOS isomer profile (32 ± 3% branched isomers), relative to PFOSA in food (Figure A-4-4). However, this enrichment may have been a simple result of PFOS pharmacokinetics, rather than isomer-specific PFOS formation from PFOSA. For example, the preferential elimination of *n*-PFOS into bile and feces, and the selective retention of the branched isomers in the liver, was observed by Benskin et al. (25). This possibility is supported by the fact that, in all other tissues, the

isomer composition was generally enriched in *n*-PFOS, relative to the blood and food; also similar to previous findings when ECF PFOS was administered directly (25,26). The finding of significant differences in branched isomer content between tissues highlights that the choice of tissue being examined may influence the observed isomer compositions. Thus, individual tissues may not necessarily accurately reflect the isomer composition of the blood or the exposure source.

The isomer-specific excretion pathways of PFOS were similar to those reported previously (25). A slight enrichment of branched PFOS isomers was observed in the urine (mean= 26% branched), with a greater percentage of branched isomers than in the food (22 ± 1 % branched isomers) from day 22 until termination of the experiment (Figure A-4-3B). Conversely, feces were slightly enriched in the linear isomer, with branched isomer percentages ranging from 16% to 20% (mean= 16%) (Figure A-4-3B). At no point was the percentage of branched PFOS isomers in feces greater than in the food. The preferential elimination of the linear isomer via the feces is consistent with the observed enrichment of the branched isomers in the liver, and consistent with previous observations (25).

In humans, the percentage of branched PFOS isomers in serum is quite variable. Archived serum samples from Norway ranged from 22% branched content to 47%, with the percentage of branched isomers becoming greater in recent years (53). Likewise, pooled serum samples from the United States contained 29 to 41% branched isomers (35). However, a significant difference in

the percentage of branched isomers has been reported among studies in different countries. Serum and plasma samples from the UK and Australia were composed of a significantly greater proportion of branched isomers than serum samples from Sweden (34), which may indicate differences in exposure sources between these locations.

Despite the lack of clear total branched PFOS enrichment in the blood of rats in the current study, isomer-specific analysis yielded interesting results. The rank order of individual isomer concentrations in blood was similar to ECF PFOS, with *n*-PFOS being present at the highest concentrations, followed by *iso-* > 5*m-* > 4*m-* ≈ Σdimethyls > 3*m-* ≈ 1*m*-PFOS. However, when the proportions of individual isomers were examined, clear differences between the patterns of individual isomers in blood and ECF PFOS emerged (Figure 6-5). The most notable difference was a relative deficiency of 1*m*-PFOS, and relative enrichment of 5*m*-PFOS in blood (Figure 6-5).

1*m*-PFOS was the most slowly eliminated PFOS isomer, and had the highest propensity to accumulate relative to the other isomers (25,26). Thus, excretion processes cannot explain the observed relative depletion of 1*m*-PFOS. Given its known slow elimination in Sprague-Dawley rats, it was expected that relatively high levels of 1*m*-PFOS should be observed, because the α-branched PFOSA isomer constituted approximately 3.2% of the ECF PFOSA used in this study (Table 6-2). The observed relative depletion of 1*m*-PFOS may be due to the reduced absorption or metabolism of the α-branched PFOSA isomer.
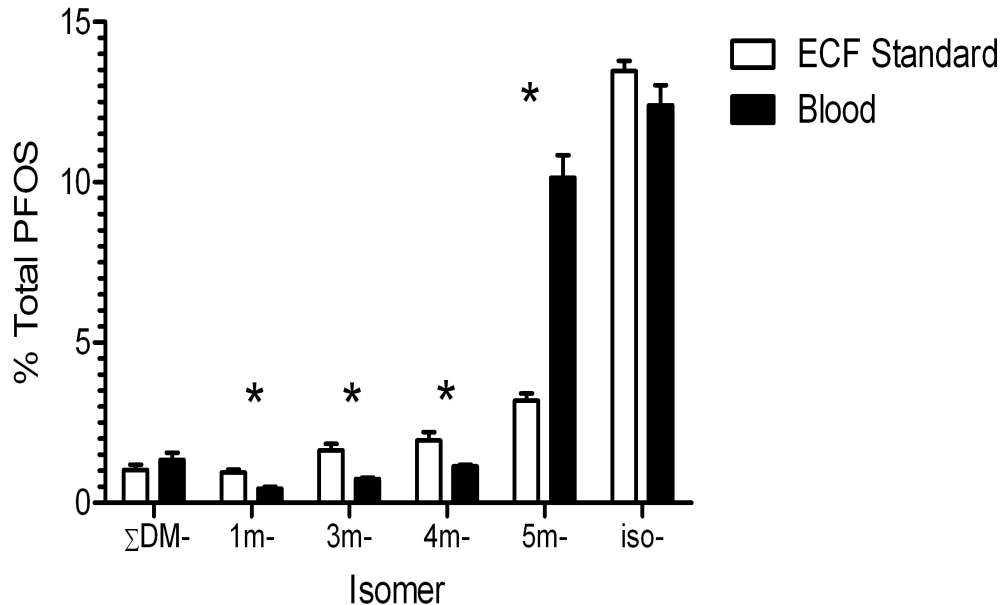
Figure 6-5: Percentage of individual PFOS isomers in the whole blood of rats at the end of the uptake phase (day 77) and in a 3M manufactured electrochemically fluorinated PFOS standard. ΣDM; sum dimethyl-PFOS. The asterisk indicates significant differences between blood and standard. n-PFOSA has been omitted for clarity.

In contrast, a significant enrichment in the proportion of 5*m*-PFOS was observed in the blood. The enrichment was significantly greater than the enrichment of 3*m*-PFOS, which is present in ECF PFOS in similar percentages to 5*m*-PFOS and is excreted at a similar rate (25,26). This enrichment is therefore either a reflection of the preferential metabolism of the 5*m*-PFOSA isomer, or the preferential absorption 5*m*-PFOSA and its subsequent metabolism; 5*m*-PFOS was preferentially absorbed relative to the linear isomer in rats given a single gavage dose of ECF PFOS (25).

242

Few studies to date have investigated the profile of individual PFOS isomers in the blood of humans or wildlife, despite that the utility of monitoring individual isomers has been demonstrated. Gebbink et al. (30) recently showed that the proportion of individual PFOS isomers in glaucous gull eggs varied among breeding colonies from the Great Lakes region. These differences, as the author pointed out, may be due in part to differences in PFOS-precursor exposure. While differences in the percentage of total branched isomers differentiated a single location from the remainder, a number of sites could be differentiated from one another based on percentages of individual isomers. Such differences cannot yet be linked to definite sources, but the ability to separate different populations of the same species based on PFOS isomer patterns is an important first step in use of isomer-specific analysis as a source tracking technique.

While the cause(s) of the enrichment of branched PFOS isomers observed in human serum remains unclear, the lack of any observable enrichment in total branched isomer content in the current study does not preclude the possibility that metabolism of precursor compounds are playing a role. Large interspecies differences exist in the biological handling of perfluorinated compounds (54,55), and it may be that rodent models do not accurately reflect the processes and pharmacokinetics that are occurring in humans. For instance, the reported half-life of PFOS in humans is 5.6-5.9 years (56), considerably greater than the half-life in rats, which varies from 30 to 100 days, depending on the isomer and route of

exposure (25,26). Given such differences between humans and rats, and the lack of data available on the isomer-specific pharmacokinetics in humans, caution should be exercised in the over interpretation of our results and their extrapolation to human biomonitoring studies. Furthermore, it is important to note that the observed PFOS isomer pattern in humans and wildlife is dependent not only on the metabolism of PFOSA to PFOS, but also on the metabolism of higher molecular weight precursors to PFOSA, as the isomer-specific metabolism of other precursors will also influence the isomer composition of PFOS in blood.

6.4 References

(1)   Houde, M., Martin, J.W., Letcher, R.J., Solomon, K.R., Muir, D.C.G., Biological monitoring of polyfluoroalkyl substances: A review. Environmental Science & Technology, 40 (2006) 3463-3473.

(2)   Martin, J.W., Whittle, D.M., Muir, D.C.G., Mabury, S.A., Perfluoroalkyl contaminants in a food web from Lake Ontario. Environmental Science & Technology, 38 (2004) 5379-5385.

(3)   Tomy, G.T., Pleskach, K., Ferguson, S.H., Hare, J., Stern, G., Macinnis, G., Marvin, C.H., Loseto, L., Trophodynamics of some PFCs and BFRs in a western Canadian Arctic marine food web. Environmental Science & Technology, 43 (2009) 4076-4081.

(4)   Lau, C., Anitole, K., Hodes, C., Lai, D., Pfahles-Hutchens, A., Seed, J.,

Perfluoroalkyl acids: A review of monitoring and toxicological findings. Toxicological Sciences, 99 (2007) 366-394.

(5)   Butt, C.M., Berger, U., Bossi, R., Tomy, G.T., Levels and trends of poly- and perfluorinated compounds in the Arctic environment. Science of the Total Environment, 408 (2010) 2936-2965.

(6)   Giesy, J.P., Kannan, K., Global distribution of perfluorooctane sulfonate in wildlife. Environmental Science & Technology, 35 (2001) 1339-1342.

(7)   Martin, J.W., Smithwick, M.M., Braune, B.M., Hoekstra, P.F., Muir, D.C.G., Mabury, S.A., Identification of long-chain perfluorinated acids in biota from the Canadian Arctic. Environmental Science & Technology, 38 (2004) 373-380.

(8)   Fromme, H., Tittlemier, S.A., Volkel, W., Wilhelm, M., Twardella, D., Perfluorinated compounds - exposure assessment for the general population in western countries. International Journal of Hygiene and Environmental Health, 212 (2009) 239-270.

(9)   Kannan, K., Corsolini, S., Falandysz, J., Fillmann, G., Kumar, K.S., Loganathan, B.G., Mohd, M.A., Olivero, J., Van Wouwe, N., Yang, J.H., Aldous, K.M., Perfluorooctanesulfonate and related fluorochemicals in human blood from several countries. Environmental Science & Technology, 38 (2004) 4489-4495.

(10)   Olsen, G.W., Butenhoff, J.L., Zobel, L.R., Perfluoroalkyl chemicals and human fetal development: An epidemiologic review with clinical and

toxicological perspectives. Reproductive Toxicology, 27 (2009) 212-230.

(11)   Case, M.T., York, R.G., Christian, M.S., Rat and rabbit oral developmental toxicology studies with two perfluorinated compounds. International Journal of Toxicology, 20 (2001) 101-109.

(12)   Luebker, D.J., York, R.G., Hansen, K.J., Moore, J.A., Butenhoff, J.L., Neonatal mortality from in utero exposure to perfluorooctanesulfonate (PFOS) in Sprague-Dawley rats: Dose-response, and biochemical and pharamacokinetic parameters. Toxicology, 215 (2005) 149-169.

(13)   Berthiaume, J., Wallace, K.B., Perfluorooctanoate, perflourooctanesulfonate, and N-ethyl perfluorooctanesulfonamido ethanol; peroxisome proliferation and mitochondrial biogenesis. Toxicology Letters, 129 (2002) 23-32.

(14)   Seacat, A.M., Thomford, P.J., Hansen, K.J., Clemen, L.A., Eldridge, S.R., Elcombe, C.R., Butenhoff, J.L., Sub-chronic dietary toxicity of potassium perfluorooctanesulfonate in rats. Toxicology, 183 (2003) 117-131.

(15)   Lau, C., Thibodeaux, J.R., Hanson, R.G., Rogers, J.M., Grey, B.E., Stanton, M.E., Butenhoff, J.L., Stevenson, L.A., Exposure to perfluorooctane sulfonate during pregnancy in rat and mouse. II: Postnatal evaluation. Toxicological Sciences, 74 (2003) 382-392.

(16)   Tomy, G.T., Tittlemier, S.A., Palace, V.P., Budakowski, W.R., Braekevelt, E., Brinkworth, L., Friesen, K., Biotransformation of N-ethyl

perfluorooctanesulfonamide by rainbow trout (Onchorhynchus mykiss) liver microsomes. Environmental Science & Technology, 38 (2004) 758-762.

(17) Xu, L., Krenitsky, D.M., Seacat, A.M., Butenhoff, J.L., Anders, M.W., Biotransformation of N-ethyl-N-(2-hydroxyethyl)perfluorooetanesulfonamide by rat liver microsomes, cytosol, and slices and by expressed rat and human cytochromes P450. Chemical Research in Toxicology, 17 (2004) 767-775.

(18) Seacat, A., Toxicokinetic study of perfluorooctane sulfonamide (PFOSA; t-7132.2) in rats. Available in the U.S. EPA accession record AR-226-0328. (2000).

(19) Xie, W., Wu, Q., Kania-Korwel, I., Tharappel, J.C., Telu, S., Coleman, M.C., Glauert, H.P., Kannan, K., Mariappan, S.V.S., Spitz, D.R., Weydert, J., Lehmler, H.J., Subacute exposure to N-ethyl perfluorooctanesulfonamidoethanol results in the formation of perfluorooctanesulfonate and alters superoxide dismutase activity in female rats. Archives of Toxicology, 83 (2009) 909-924.

(20) Vestergren, R., Cousins, I.T., Trudel, D., Wormuth, M., Scheringer, M., Estimating the contribution of precursor compounds in consumer exposure to PFOS and PFOA. Chemosphere, 73 (2008) 1617-1624.

(21) Benskin, J.P., De Silva, A.O., Martin, J.W., Isomer profiling of perfluorinated substances as a tool for source tracking: A review of early findings and future applications. Reviews of Environmental Contaminant Toxicology, in press (2010).

(22)   Paul, A.G., Jones, K.C., Sweetman, A.J., A first global production, emission, and environmental inventory for perfluorooctane sulfonate. Environmental Science & Technology, 43 (2009) 386-392.

(23)   Reagen, W., Lindstrom, K., Jacoby, C., Purcell, R., Kestner, T., Payfer, R., Miller, J., in Society of Environmental Toxicology and Chemistry 28th North American Meeting Platform Presentation, Milwaukee, WI, 2007.

(24)   Armitage, J.M., Schenker, U., Scheringer, M., Martin, J.W., MacLeod, M., Cousins, I.T., Modeling the global fate and transport of perfluorooctane sulfonate (PFOS) and precursor compounds in relation to temporal trends in wildlife exposure. Environmental Science & Technology, 43 (2009) 9274-9280.

(25)   Benskin, J.P., De Silva, A.O., Martin, L.J., Arsenault, G., McCrindle, R., Riddell, N., Mabury, S.A., Martin, J.W., Disposition of perfluorinated acid isomers in Sprague-Dawley rats; part 1: Single dose. Environmental Toxicology and Chemistry, 28 (2009) 542-554.

(26)   De Silva, A.O., Benskin, J.P., Martin, L.J., Arsenault, G., McCrindle, R., Riddell, N., Martin, J.W., Mabury, S.A., Disposition of perfluorinated acid isomers in Sprague-Dawley rats; part 2: Subchronic dose. Environmental Toxicology and Chemistry, 28 (2009) 555-567.

(27)   De Silva, A.O., Tseng, P.J., Mabury, S.A., Toxicokinetics of perfluorocarboxylate isomers in rainbow trout. Environmental Toxicology and Chemistry, 28 (2009) 330-337.

(28)   Sharpe, R.L., Benskin, J.P., Laarman, A.H., MacLeod, S.L., Martin, J.W., Wong, C.S., Goss, G.G., Perfluorooctane sulfonate toxicity, isomer-specific accumulation, and maternal transfer in zebrafish (Danio rerio) and rainbow trout (Oncorhynchus mykiss). Environmental Toxicology and Chemistry, 29 (2010) 1957-1966.

(29)   Chu, S.G., Letcher, R.J., Linear and branched perfluorooctane sulfonate isomers in technical product and environmental samples by in-port derivatization-gas chromatography-mass spectrometry. Analytical Chemistry, 81 (2009) 4256-4262.

(30)   Gebbink, W.A., Letcher, R.J., Linear and branched perfluorooctane sulfonate isomer patterns in herring gull eggs from colonial sites across the Laurentian Great Lakes. Environmental Science & Technology, 44 (2010) 3739-3745.

(31)   Houde, M., Czub, G., Small, J.M., Backus, S., Wang, X.W., Alaee, M., Muir, D.C.G., Fractionation and bioaccumulation of perfluorooctane sulfonate (PFOS) isomers in a Lake Ontario food web. Environmental Science & Technology, 42 (2008) 9397-9403.

(32)   Lloyd, A.S., Bailey, V.A., Hird, S.J., Routledge, A., Clarke, D.B., Mass spectral studies towards more reliable measurement of perfluorooctanesulfonic acid and other perfluorinated chemicals (PFCs) in food matrices using liquid chromatography/tandem mass spectrometry. Rapid Communications in Mass Spectrometry, 23 (2009) 2923-2938.

(33)   Powley, C.R., George, S.W., Russell, M.H., Hoke, R.A., Buck, R.C., Polyfluorinated chemicals in a spatially and temporally integrated food web in the western Arctic. Chemosphere, 70 (2008) 664-672.

(34)   Karrman, A., Langlois, I., van Bavel, B., Lindstrom, G., Oehme, M., Identification and pattern of perfluorooctane sulfonate (PFOS) isomers in human serum and plasma. Environment International, 33 (2007) 782-788.

(35)   Riddell, N., Arsenault, G., Benskin, J.P., Chittim, B., Martin, J.W., McAlees, A., McCrindle, R., Branched perfluorooctane sulfonate isomer qantification and characterization in blood serum samples by HPLC/ESI-MS(/MS). Environmental Science & Technology, 43 (2009) 7902-7908.

(36)   Benskin, J.P., Holt, A., Martin, J.W., Isomer-specific biotransformation rates of a perfluorooctane sulfonate (PFOS)-precursor by cytochrome P450 isozymes and human liver microsomes. Environmental Science & Technology, 43 (2009) 8566-8572.

(37)   Senthilkumar, K., Ohi, E., Sajwan, K., Takasuga, T., Kannan, K., Perfluorinated compounds in river water, river sediment, market fish, and wildlife samples from Japan. Bulletin of Environmental Contamination and Toxicology, 79 (2007) 427-431.

(38)   Kim, S.K., Kannan, K., Perfluorinated acids in air, rain, snow, surface runoff, and lakes: Relative importance of pathways to contamination of urban lakes. Environmental Science & Technology, 41 (2007) 8328-8334.

(39)   So, M.K., Miyake, Y., Yeung, W.Y., Ho, Y.M., Taniyasu, S., Rostkowski, P., Yamashita, N., Zhou, B.S., Shi, X.J., Wang, J.X., Giesy, J.P., Yu, H., Lam, P.K.S., Perfluorinated compounds in the Pearl River and Yangtze River of China. Chemosphere, 68 (2007) 2085-2095.

(40)   Bossi, R., Riget, F.F., Dietz, R., Temporal and spatial trends of perfluorinated compounds in ringed seal (Phoca hispida) from Greenland. Environmental Science & Technology, 39 (2005) 7416-7422.

(41)   Smithwick, M., Norstrom, R.J., Mabury, S.A., Solomon, K., Evans, T.J., Stirling, I., Taylor, M.K., Muir, D.C.G., Temporal trends of perfluoroalkyl contaminants in polar bears (Ursus maritimus) from two locations in the North American Arctic, 1972-2002. Environmental Science & Technology, 40 (2006) 1139-1143.

(42)   Benskin, J.P., Bataineh, M., Martin, J.W., Simultaneous characterization of perfluoroalkyl carboxylate, sulfonate, and sulfonamide isomers by liquid chromatography-tandem mass spectrometry. Analytical Chemistry, 79 (2007) 6455-6464.

(43)   Tomy, G.T., Halldorson, T.H.J., Tittlemier, S.A., Methanolic extraction of poly- and perfluorinated alkyl acids from biota. Organohalogen Compounds, 67 (2005) 787-789.

(44)   Xu, L., Krenitsky, D.M., Seacat, A.M., Butenhoff, J.L., Tephly, T.R., Anders, M.W., N-glucuronidation of perfluorooctanesulfonamide by human, rat,

dog, and monkey liver microsomes and by expressed rat and human UDP-glucuronosyltransferases. Drug Metabolism and Disposition, 34 (2006) 1406-1410.

(45) Grossman, M.R., Mispagel, M.E., Bowen, J.M., Distribution and tissue elimination in rats during and after prolonged dietary exposure to a highly fluorinated sulfonamide pesticide. Journal of Agricultural and Food Chemistry, 40 (1992) 2505-2509.

(46) Manning, R.O., Bruckner, J.V., Mispagel, M.E., Bowen, J.M., Metabolism and disposition of Sulfluramid, a unique polyfluorinated insecticide, in the rat. Drug Metabolism and Disposition, 19 (1991) 205-211.

(47) Vitayavirasuk, B., Bowen, J.M., Pharmacokinetics of Sulfluramid and its metabolite desethylsulfluramid after intravenous and intraruminal administration of sulfluramid to sheep. Pesticide Science, 55 (1999) 719-725.

(48) Vitayavirasuk, B., Ph.D. Thesis, University of Georgia, Athens, Georgia, 1990.

(49) Karrman, A., van Bavel, B., Jarnberg, U., Hardell, L., Lindstrom, G., Perfluorinated chemicals in relation to other persistent organic pollutants in human blood. Chemosphere, 64 (2006) 1582-1591.

(50) Ahrens, L., Siebert, U., Ebinghaus, R., Temporal trends of polyfluoroalkyl compounds in harbor seals (Phoca vitulina) from the German Bight, 1999-2008. Chemosphere, 76 (2009) 151-158.

(51)   Ahrens, L., Felizeter, S., Ebinghaus, R., Spatial distribution of polyfluoroalkyl compounds in seawater of the German Bight. Chemosphere, 76 (2009) 179-184.

(52)   Schultz, M.M., Barofsky, D.F., Field, J.A., Quantitative determination of fluorinated alkyl substances by large-volume-injection liquid chromatography tandem mass spectrometry - characterization of municipal wastewaters. Environmental Science & Technology, 40 (2006) 289-295.

(53)   Haug, L.S., Thomsen, C., Bechert, G., Time trends and the influence of age and gender on serum concentrations of perfluorinated compounds in archived human samples. Environmental Science & Technology, 43 (2009) 2131-2136.

(54)   Andersen, M.E., Butenhoff, J.L., Chang, S.C., Farrar, D.G., Kennedy, G.L., Lau, C., Olsen, G.W., Seed, J., Wallacekj, K.B., Perfluoroalkyl acids and related chemistries - toxicokinetics and modes of action. Toxicological Sciences, 102 (2008) 3-14.

(55)   Tan, Y.M., Clewell, H.J., Andersen, M.E., Time dependencies in perfluorooctylacids disposition in rat and monkeys: A kinetic analysis. Toxicology Letters, 177 (2008) 38-47.

(56)   Olsen, G.W., Burris, J.M., Ehresman, D.J., Froehlich, J.W., Seacat, A.M., Butenhoff, J.L., Zobel, L.R., Half-life of serum elimination of perfluorooctanesulfonate, perfluorohexanesulfonate, and perfluorooctanoate in retired fluorochemical production workers. Environmental Health Perspectives,

115 (2007) 1298-1305.

(57)   Kestner, T., Fluorochemical isomer distribution by 19F-NMR spectroscopy. Available in the U.S. EPA accession record AR-226-0564. (1997).

Chapter 7

Conclusions and Future Directions

This thesis provides novel information regarding the isomer-specific and enantiomer-specific fate of POPs in the environment. The data and conclusions presented in this thesis are necessary for the continued refinement of our knowledge of POP environmental fate and for the use of enantiomer and isomer signatures for future source apportioning and exposure assessments.

Several main conclusions were presented in the individual chapters of this thesis. In Chapter 2, a novel AA-APPI method was developed, and provided proof of principle of the use of AA-APPI for small molecule analysis. The use of AA-APPI, with 1,4-dibromobutane in toluene as a bromide source, offered increased sensitivity and lower limits of detection than conventional atmospheric pressure photoionization. Minimal matrix effects were found with AA-APPI in sediment extracts spiked post-extraction with HBCD, the model POP compound used in this study, with less than a 6% enhancement in the ion signal. Enantiomer fractions of HBCD were racemic in spiked sediment extracts. This contrasted the more commonly used technique of electrospray ionization, for which matrix effects produced ion signal modification, creating non-racemic measurement artifacts. This study demonstrated that AA-APPI offers a simple means of further extending the range of compounds ionizable by AA-APPI while maintaining minimal matrix effects.

Non-racemic EFs of PCBs 174, 176, and 183 were found in sediments from a sub-tropical estuary heavily contaminated with Aroclor 1268, likely the result of microbial dechlorination. Examination of EFs of possible parent-

daughter congener pairs elucidated possible microbial dechlorination pathways occurring in sediment. Although EFs in grass shrimp mirrored those of sediment, fish species had EFs that differed significantly from sediment or grass shrimp. Similarly, bottlenose dolphins contained non-racemic quantities of PCBs 91, 136, 174, 176, and 183. Non-racemic EFs in these biota were likely a result of both uptake of non-racemic proportions of PCBs from the diet and enantioselective biotransformation.

Blood plasma EFs of chiral chlordanes and atropisomeric PCBs in glaucous gulls from Svalbard, in the Norwegian Arctic, were similar in magnitude and direction to EFs previously reported in glaucous gulls from other Arctic food webs. This suggested overall similarities in the biochemical processes influencing the EFs of bioaccumulated organochlorine contaminants within the food webs at those two locations. EFs in the yolk of eggs collected concurrently from within the same nesting colonies on Svalbard varied with location, laying date, and OC concentrations, and may be influenced by changes in the local feeding ecology between colonies. There were no differences for any analyte between EFs in female gulls compared to those found in egg yolk, indicating that processes involved in the maternal transfer of chlordanes and PCBs to eggs do not modulate the stereochemical ratio between enantiomers. The use of eggs as a valuable and non-invasive means of OC biomonitoring may also extend to enantiomer compositions in glaucous gulls, and perhaps also in other seabird species from Arctic regions.

West Greenland sledge dogs, fed OC-polluted minke whale blubber diets for nearly two years biotransformed α-HCH, oxychlordane, heptachlor epoxide, and PCBs 91, 149, and 183 enantioselectively. Enantiomer distributions varied by tissue for some compounds, including highly enriched distributions of α-HCH in brain tissues and non-racemic distributions in toxicologically sensitive tissues such as thyroid and adrenal gland. Diet influenced differences in enantiomer distributions were also found between exposed and control cohort dogs. Distributions of OC enantiomer were similar between wild polar bears and sledge dogs; however, comparisons of enantiomer-specific biomagnification factors and relative rates of enantiomer-selective biotransformation revealed differences in biotransformation capacity between species. The use of enantiomer-specific biomagnification factors and relative biotransformation rate constants provide more detailed information for making cross-species comparisons of enantiomer distributions in biota.

Finally, male Sprague-Dawley rats eliminated perfluorooctane sulfonamide (PFOSA), a known PFOS precursors, isomer-specifically. Among the two most prominent branched PFOSA isomers, elimination half-lives were relatively rapid compared to linear PFOSA. Consequently, all tissues, blood, and feces were depleted in branched PFOSA isomers. The isomer-specific formation of PFOS was also observed. In comparison to electrochemically fluorinated PFOS, a significant enrichment of 5*m*-PFOS, coupled with a relative depletion of the alpha branched PFOS isomer (1*m*-PFOS), provide the first *in vivo* evidence

that exposure to PFOS precursor compounds alters the observed isomer pattern of PFOS in biota.

Despite the fact that all of the POPs discussed in this thesis are banned or had their use restricted in some capacity does not diminish the need for continued study of legacy POPs. Their continued presence in old reservoirs, for instance PCBs in transformers that are still in use or which have not yet been destroyed, will lead to the continued emission of POPs to the environment, and thus, the continued exposure to POPs by humans and wildlife. Further work should be done on this front to accurately determine the quantity of POPs which may still be released to the environment and develop removal and destructions programs for old stocks.

In regards to the environmental chemistry of POP enantiomers and isomers, more work must be done in the area of enantiomer-specific toxicity. As discussed, the enantiomer distributions of compounds must be known to provide the most accurate risk assessments possible. As a corollary to this, however, is the need for accurate knowledge of enantiomer-specific toxicities. For instance, a specific example as highlighted in this thesis is the need to understand enantiomer-specific protein binding and toxicities of OH-PCBs, which are potent ligands for transthyretin, and may disrupt normal functioning of thyroid hormone transport. The need for accurate knowledge of enantiomer-specific toxicity extends to newer chiral POPs, such as HBCD, as well.

The understanding of basic environmental fate processes affecting

enantiomer and isomer patterns in biotic and abiotic environments warrants more study as well. This knowledge would be beneficial for two fields of study. First, the for accurate assessment of risk, as discussed above. Secondly, is for the use of isomer and enantiomer patterns for source and exposure assessments. In respect to POP enantiomers, it is abundantly clear that biological processes affect enantiomer distributions. However, many of the mechanisms of enantiomer enrichment and confounding factors affecting our interpretation of enantiomer distributions, particularly in biota, remain unclear. A number of these factors have been pointed out throughout this thesis, such as the need for further understanding of dietary influences on enantiomer distributions, and the need to understand the mechanisms of enantiomer-specific biotransformation, in particular, the enzyme/proteins systems involved in enantiomer enrichment. The work presented in Chapters 3 through 5 of this thesis can be further expanded to calculate enantiomer-specific biotransformation rates (as opposed to relative biotransformation rate constants), which will allow for more accurate comparisons among species.

The study of the isomer-specific fate of PFOS and its precursors is still in its infancy. One of the most pressing issues is the uncertainty regarding the differential environmental fate of isomers. Chapter 6 of this thesis, and the studies cited therein, have definitively shown that biological processes can alter the isomer distribution of PFOS. However, isomers have different physical and chemical properties, which may lead to differences in environmental partitioning

coefficients or transformation rates. Further characterization of perfluorochemical isomer patters in all environmental matrices is warranted, as are laboratory based studies into specific environmental fate processes (e.g., microbial degradation).

Finally, scientists must be diligent in continuing to identify new and potential POPs, both *a priori* and those which have already been released into the environment. Despite the knowledge gained in the study of legacy POPs, we humans continue to create, use, and release potentially harmful chemicals into the environment. As such, there will continue to be a need to identify, measure, and study potentially persistent organic pollutants in the environment.

Appendices

Appendix 1: Sample information and enantiomer fractions for sediment and biota from Turtle/Brunswick River estuary

Table A-1-1: Estuary sediment sample information

Sample Name	Sample Type	Location	Depth (cm)	Sum [PCB] (ng/g wet wt.)
311A0-2	Sediment	311A CORE-NORTH MARSH	0-4	0.5
311A10-14	Sediment	311A CORE-NORTH MARSH	10-20	2.25
311A4-6	Sediment	311A CORE-NORTH MARSH	4-6	0.00
311A6-8	Sediment	311A CORE-NORTH MARSH	6-8	0.00
LCP NSM 0-5CM #2	Sediment	NEAR SOUTH MARSH	0-5	0.00
LCP NSM 10-20CM #2	Sediment	NEAR SOUTH MARSH	10-20	0.00
LCP NSM 5-10CM #2	Sediment	NEAR SOUTH MARSH	5-10	0.00
LCP0-2	Sediment	NEAR SOUTH MARSH	0-4	242.00
LCP2-4	Sediment	NEAR SOUTH MARSH	0-4	315.00
LCP4-6	Sediment	NEAR SOUTH MARSH	4-6	688.00
LCP4-6	Sediment	NEAR SOUTH MARSH	4-6	688.00
LCP8-10	Sediment	NEAR SOUTH MARSH	8-10	1150.00
LCPCS 1	Sediment	NEAR SOUTH MARSH	0	0.00
NSM0-5	Sediment	NEAR SOUTH MARSH	0-5	1177.78
NSM10-20	Sediment	NEAR SOUTH MARSH	10-20	165.50
NSM18-22	Sediment	NEAR SOUTH MARSH	10-20	0.00
NSM5-10	Sediment	NEAR SOUTH MARSH	5-10	8000.00
NSM8-10	Sediment	NEAR SOUTH MARSH	8-10	1163.66

Table A-1-2: *Enantiomer fractions in sediment samples*

	Enantiomer Fractions (EFs)				
Sample Name	PCB 91 (CDX)[1]	PCB 91 (CSB)[1]	95 (CDX)[1]	PCB 95 (CSB)[1]	PCB 132 (BGB)[1]
311A0-2	0.480	0.494	NR	0.489	ND
311A10-14	0.486	ND	NR	0.493	0.496
311A4-6	ND	ND	NR	ND	ND
311A6-8	0.438	ND	NR	0.504	ND
LCP NSM 0-5CM #2	ND	ND	ND	ND	ND
LCP NSM 10-20CM #2	ND	ND	ND	ND	ND
LCP NSM 5-10CM #2	ND	ND	ND	ND	ND
LCP0-2	0.410	ND	NR	0.479	ND
LCP2-4	ND	ND	NR	ND	ND
LCP4-6	ND	ND	NR	ND	ND
LCP4-6	0.474	ND	NR	ND	ND
LCP8-10	ND!	ND	NR	ND	ND
LCPCS 1	0.304	ND	NR	0.505	0.496
NSM0-5	ND	ND	NR	ND	ND
NSM10-20	0.485	ND	NR	ND	ND
NSM18-22	~~0.402~~	~~0.134~~	NR	0.406	ND
NSM5-10	ND	ND	NR	ND	NR
NSM8-10	0.221	ND	NR	0.517	NR

[1]Abbreviation in parentheses indicates column used. CDX=Chirasil-Dex; CSB=Cyclosil-B; BGB=BGB-172

264

Enantiomer Fractions (EFs)

Sample Name	PCB 136 (CDX)[1]	PCB 136 (CSB)[1]	PCB 149 (CDX)[1]	PCB 149 (CSB)[1]	PCB 174 (CDX)[1]
311A0-2	0.547	0.557	0.467	0.489	0.858
311A10-14	0.568	ND	0.410	0.489	0.814
311A4-6	0.782	ND	0.498	ND	0.770
311A6-8	0.703	0.681	0.496	0.538	0.853
LCP NSM 0-5CM #2	ND	ND	ND	ND	ND
LCP NSM 10-20CM #2	ND	ND	ND	ND	ND
LCP NSM 5-10CM #2	ND	ND	ND	0.504	ND
LCP0-2	0.789	0.789	0.492	0.505	0.768
LCP2-4	0.789	0.784	0.486	0.499	0.783
LCP4-6	0.799	ND	0.503	0.516	0.764
LCP4-6	0.549	ND	0.477	0.493	0.878
LCP8-10	ND	ND	0.497	0.537	0.813
LCPCS 1	0.565	0.654	0.512	0.547	0.684
NSM0-5	ND	ND	0.460	ND	0.872
NSM10-20	0.838	0.840	0.400	0.415	0.930
NSM18-22	0.942	0.960	0.780	0.821	0.625
NSM5-10	0.867	0.827	0.514	0.542	0.861
NSM8-10	0.852	0.858	0.432	0.460	0.801

[1]Abbreviation in parentheses indicates column used. CDX=Chirasil-Dex; CSB=Cyclosil-B; BGB=BGB-172

Enantiomer Fractions (EFs)

Sample Name	PCB 176 (CDX)[1]	PCB 176 (CSB)[1]	PCB 183 (BGB)[1]
311A0-2	ND	ND	0.651
311A10-14	ND	ND	0.630
311A4-6	ND	ND	0.644
311A6-8	ND	ND	0.648
LCP NSM 0-5CM #2	ND	ND	ND
LCP NSM 10-20CM #2	ND	ND	ND
LCP NSM 5-10CM #2	ND	ND	ND
LCP0-2	0.649	0.655	0.696
LCP2-4	0.658	0.633	0.695
LCP4-6	0.593	ND	ND
LCP4-6	NR	0.667	0.696
LCP8-10	NR	ND	0.703
LCPCS 1	0.611	ND	0.591
NSM0-5	NR	ND	ND
NSM10-20	0.713	0.707	0.480
NSM18-22	0.635	0.627	NR
NSM5-10	ND	ND!	0.470
NSM8-10	0.671	0.647	NR

[1]Abbreviation in parentheses indicates column used. CDX=Chirasil-Dex; CSB=Cyclosil-B; BGB=BGB-172

266

Table A-1-3: Sample information for biota samples

Sample Name	Species	Location	Collection Date	# in composite
PCBC1"F"	Silver perch	PURVIS CREEK	25-Sep-07	20
PCBC2"F"	Silver perch	PURVIS CREEK	25-Sep-07	4
PCBC2"S"	Silver perch	PURVIS CREEK	27-Mar-07	10
PCBC3"F"	Silver perch	PURVIS CREEK	25-Sep-07	11
PCBC3"S"	Silver perch	PURVIS CREEK	27-Mar-07	9
PCBL1"S"	Silver perch	PURVIS CREEK	27-Mar-07	9
PCCN1"F"	Spotted Seatrout	PURVIS CREEK	9-Dec-07	2
PCLX1"F"	Spot	PURVIS CREEK	25-Sep-07	8
PCLX1"S"	Spot	PURVIS CREEK	27-Mar-07	13
PCMC1"F"	Striped mullet	PURVIS CREEK	25-Sep-07	3
PCMC1"S"	Striped mullet	PURVIS CREEK	27-Mar-07	20
PPUGIO	GRASS SHRIMP	PURVIS CREEK	28-Feb-00	0
GS-CC	GRASS SHRIMP	CAUSEWAY CREEK	na	0
GSD-DP	GRASS SHRIMP	DIP POND	na	0
CZM141G	GRASS SHRIMP	PC x CC	na	0
CZM141L	SEATROUT	PC x CC	na	0
CZM141M	GRASS SHRIMP	PC x CC	na	0
CZM43F1	OYSTER COMP	PC x CC	na	0
GSPCC1	GRASS SHRIMP	PURVIS CREEK	na	0
GSPCC2	GRASS SHRIMP	PURVIS CREEK	na	0
FUND-DP	MUMMICHOG (FUNDULUS)	DIP POND	na	0
MOD-DP	RIBBED MUSSEL	DIP POND	na	0
LIP-DP	SNAIL	DIP POND	na	0
SMPWH2	STRIPED MULLET (WHOLE)	PURVIS CREEK	na	0
STIMU1	STRIPED MULLET (WHOLE)	PURVIS CREEK	na	0
12140401	DOLPHIN	Estuary	15-Dec-08	1
12140402	DOLPHIN	Estuary	15-Dec-08	1
12150401	DOLPHIN	Estuary	16-Dec-08	1
12160401	DOLPHIN	Estuary	17-Dec-08	1
12160402	DOLPHIN	Estuary	17-Dec-08	1
12160403	DOLPHIN	Estuary	17-Dec-08	1
12170401	DOLPHIN	Estuary	18-Dec-08	1

267

Table A-1-4: Enantiomer fractions in biota samples

Sample Name	Sum [PCB] (ng/g lipid wt.)	PCB 91 (CDX)[1]	PCB 91 (CSB)[1]
PCBC1"F"	32100	ND	ND
PCBC2"F"	30400	ND	ND
PCBC2"S"	46500	ND	ND
PCBC3"F"	35300	ND	ND
PCBC3"S"	60400	ND	0.559
PCBL1"S"	60400	ND	ND
PCCN1"F"	8210	ND	ND
PCLX1"F"	156000	ND	ND
PCLX1"S"	30400	ND	ND
PCMC1"F"	149000	ND	ND
PCMC1"S"	101000	ND	ND
PPUGIO	138578	ND	ND
GS-CC	4495	ND	ND
GSD-DP	4433	ND	ND
CZM141G	0	NR	ND
CZM141L	2904	ND	ND
CZM141M	0	NR	ND
CZM43F1	83	ND	ND
GSPCC1	566	ND	ND
GSPCC2	405	ND	ND
FUND-DP	62827	ND	ND
MOD-DP	6446	ND	ND
LIP-DP	1990	ND	ND
SMPWH2	0	ND	ND
STIMU1	0	ND	ND
12140401	47700	ND	0.339
12140402	69900	0.312	0.316
12150401	124000	0.121	0.122
12160401	119000	0.196	0.210
12160402	61700	0.310	0.313
12160403	35000	ND	0.462
12170401	84200	0.156	0.161

[1]Abbreviation in parentheses indicates column used. CDX=Chirasil-Dex; CSB=Cyclosil-B; BGB=BGB-1

Enantiomer Fractions (EFs)

Sample Name	95 (CDX)[1]	PCB 95 (CSB)[1]	PCB 132 (BGB)[1]
PCBC1"F"	0.473	0.441	ND
PCBC2"F"	0.395	0.419	ND
PCBC2"S"	0.412	0.413	ND
PCBC3"F"	0.448	0.432	ND
PCBC3"S"	0.444	0.442	ND
PCBL1"S"	0.481	0.442	ND
PCCN1"F"	0.467	0.443	ND
PCLX1"F"	0.379	0.423	ND
PCLX1"S"	0.434	0.420	ND
PCMC1"F"	0.475	0.473	ND
PCMC1"S"	0.478	0.498	ND
PPUGIO	NR	ND	ND
GS-CC	NR	ND	ND
GSD-DP	NR	ND	ND
CZM141G	NR	ND	ND
CZM141L	NR	ND	ND
CZM141M	NR	ND	ND
CZM43F1	NR	ND	ND
GSPCC1	NR	ND	ND
GSPCC2	NR	ND	ND
FUND-DP	NR	ND	ND
MOD-DP	NR	ND	ND
LIP-DP	NR	ND	NR
SMPWH2	NR	ND	ND
STIMU1	NR	ND	NR
12140401	0.419	0.416	NR
12140402	0.486	0.491	NR
12150401	0.527	0.522	NR
12160401	0.499	0.495	NR
12160402	0.489	0.488	NR
12160403	0.490	0.506	NR
12170401	0.525	0.516	NR

[1]Abbreviation in parentheses indicates column used. CDX=Chirasil-Dex; CSB=Cyclosil-B; BGB=BGB-172

Enantiomer Fractions (EFs)

Sample Name	PCB 136 (CDX)[1]	PCB 136 (CSB)[1]	PCB 149 (CDX)[1]	PCB 149 (CSB)[1]
PCBC1"F"	0.729	ND	0.466	0.498
PCBC2"F"	0.740	ND	0.513	0.500
PCBC2"S"	0.743	ND	0.485	0.486
PCBC3"F"	0.768	ND	0.491	0.502
PCBC3"S"	0.780	ND	0.497	0.492
PCBL1"S"	0.702	ND	0.477	0.489
PCCN1"F"	ND	ND	0.576	0.562
PCLX1"F"	0.722	ND	0.599	0.596
PCLX1"S"	0.752	ND	0.514	0.506
PCMC1"F"	0.805	ND	0.355	0.349
PCMC1"S"	0.800	ND	0.323	0.327
PPUGIO	0.816	ND	0.533	ND
GS-CC	ND	ND	ND	ND
GSD-DP	ND	ND	ND	ND
CZM141G	NR	ND	NR	ND
CZM141L	ND	ND	ND	ND
CZM141M	NR	ND	NR	ND
CZM43F1	0.777	ND	0.520	ND
GSPCC1	ND	ND	ND	ND
GSPCC2	ND	ND	0.516	ND
FUND-DP	0.910	ND	0.629	0.680
MOD-DP	ND	ND	ND	ND
LIP-DP	ND	ND	ND	ND
SMPWH2	ND	ND	0.507	ND
STIMU1	ND	ND	ND	ND
12140401	ND	0.571	0.579	0.565
12140402	0.652	0.652	0.533	0.538
12150401	0.539	0.546	0.445	0.448
12160401	0.585	0.592	0.448	0.453
12160402	0.655	0.653	0.537	0.542
12160403	ND	ND	ND	0.494
12170401	0.591	0.585	0.487	0.493

[1]Abbreviation in parentheses indicates column used. CDX=Chirasil-Dex; CSB=Cyclosil-B; BGB=BGB-172

Enantiomer Fractions (EFs)

Sample Name	PCB 174 (CDX)[1]	PCB 176 (CDX)[1]	PCB 176 (CSB)[1]	PCB 183 (BGB)[1]
PCBC1"F"	ND	ND	ND	0.794
PCBC2"F"	ND	ND	ND	0.790
PCBC2"S"	ND	ND	ND	0.810
PCBC3"F"	ND	ND	ND	0.798
PCBC3"S"	ND	ND	ND	0.813
PCBL1"S"	ND	ND	ND	0.798
PCCN1"F"	ND	ND	ND	0.802
PCLX1"F"	ND	ND	ND	0.794
PCLX1"S"	ND	ND	0.669	ND
PCMC1"F"	ND	ND	0.745	0.792
PCMC1"S"	ND	ND	ND	0.798
PPUGIO	ND	ND	ND	0.631
GS-CC	ND	NR	ND	ND
GSD-DP	0.819	NR	ND	ND
CZM141G	NR	NR	ND	ND
CZM141L	ND	ND	ND	ND
CZM141M	NR	NR	ND	ND
CZM43F1	ND	ND	ND	ND
GSPCC1	0.816	ND	ND	0.623
GSPCC2	0.795	ND	ND	0.586
FUND-DP	0.917	0.759	0.764	ND
MOD-DP	ND	NR	ND	ND
LIP-DP	0.861	NR	ND	ND
SMPWH2	ND	ND	ND	NR
STIMU1	0.808	NR	0.659	0.740
12140401	0.704	ND	0.707	0.634
12140402	0.698	0.704	0.632	0.705
12150401	0.700	0.617	0.665	0.628
12160401	0.754	0.659	0.696	0.710
12160402	0.702	0.697	ND	0.715
12160403	ND	ND	ND	0.733
12170401	0.705	0.671	0.652	0.707

[1]Abbreviation in parentheses indicates column used. CDX=Chirasil-Dex; CSB=Cyclosil-B; BGB=BGB-172

271

Appendix 2: Enantiomer fractions in glaucous gull egg yolks and plasma

Table A-2-5: Glaucous gull egg sample information

	Lab code	Collection date	Egg yolk lipid %
GG50	50	5/30	32.2
GG51	51	6/2	31.1
GG52	52	5/30	33.8
GG53	53	5/30	33.9
GG54	54	6/2	30.7
GG55	55	5/31	32.2
GG56	56	6/4	30.5
GG57	57	6/5	30.1
GG58	58	6/1	30.6
GG59	59	6/5	31.3
GG60	60	6/5	28.4
GG61	61	6/2	30.4
GG62	62	6/1	31.7
GG63	63	6/5	33.9
GG64	64	6/1	30.6
GG65	65	6/5	27.2
GG66	66	6/4	34.0
GG67	67	6/1	30.3
GG68	68	6/5	29.4
GG69	69	5/30	30.1
GG70	70	6/1	30.9
GG71	71	6/1	29.7
GG72	72	6/5	28.4
GG73	73	5/30	31.2
GG74	74	6/2	30.7
GG75	75	5/30	30.9
GG76	76	5/31	31.4
GG77	77	6/6	31.5
GG78	78	6/5	28.2
GG79	79	6/2	32.2
GG80	80	6/1	28.3

Table A-2-6: *Enantiomer fractions in glaucous gull egg yolks*

	PCB 95 CDX	PCB 95 CYCB	PCB 91 CDX	PCB 91 CYCB
GG50	ND	ND	ND	ND
GG51	0.417	0.411	ND	ND
GG52	0.601	0.606	ND	ND
GG53	ND	ND	ND	ND
GG54	ND	ND	ND	ND
GG55	0.537	0.605	ND	ND
GG56	ND	ND	ND	ND
GG57	ND	ND	ND	ND
GG58	ND	ND	ND	ND
GG59	ND	ND	ND	ND
GG60	ND	ND	ND	ND
GG61	ND	ND	ND	ND
GG62	ND	ND	ND	ND
GG63	ND	ND	ND	ND
GG64	ND	ND	ND	ND
GG65	ND	ND	ND	ND
GG66	0.533	0.559	ND	ND
GG67	0.658	ND	ND	ND
GG68	ND	ND	ND	ND
GG69	ND	ND	ND	ND
GG70	0.576	0.607	ND	ND
GG71	ND	ND	ND	ND
GG72	ND	ND	ND	ND
GG73	ND	ND	ND	ND
GG74	ND	ND	ND	ND
GG75	ND	ND	ND	ND
GG76	ND	ND	ND	ND
GG77	ND	ND	ND	ND
GG78	0.694	0.600	ND	ND
GG79	ND	ND	ND	ND
GG80	ND	ND	ND	ND

	PCB 84	136 CDX	PCB 136 CYCB	PCB 149 CDX
GG50	ND	ND	ND	0.211
GG51	ND	ND	ND	0.263
GG52	ND	ND	ND	0.241
GG53	ND	ND	ND	0.288
GG54	ND	ND	ND	0.247
GG55	ND	ND	ND	0.300
GG56	ND	ND	ND	0.197
GG57	ND	ND	ND	0.320
GG58	ND	ND	ND	0.142
GG59	ND	ND	ND	0.178
GG60	ND	ND	ND	0.330
GG61	ND	ND	ND	0.284
GG62	ND	ND	ND	0.293
GG63	ND	ND	ND	0.221
GG64	ND	ND	ND	0.188
GG65	ND	ND	ND	0.251
GG66	ND	ND	ND	0.180
GG67	ND	ND	ND	0.197
GG68	ND	ND	ND	0.177
GG69	ND	ND	ND	0.158
GG70	ND	ND	ND	0.223
GG71	ND	ND	ND	0.180
GG72	ND	ND	ND	0.243
GG73	ND	ND	ND	0.167
GG74	ND	ND	ND	0.195
GG75	ND	ND	ND	0.298
GG76	ND	ND	ND	0.190
GG77	ND	ND	ND	0.228
GG78	ND	ND	ND	0.164
GG79	ND	ND	ND	0.185
GG80	ND	ND	ND	0.260

	PCB 149 CYCB	PCB 174 CDX	PCB 174 CYCB	PCB 176 CDX	PCB 183
GG50	0.216	ND	ND	ND	0.481
GG51	0.217	ND	ND	ND	0.429
GG52	0.182	ND	ND	ND	0.436
GG53	0.243	ND	ND	ND	0.449
GG54	0.196	ND	ND	ND	0.417
GG55	0.263	ND	ND	ND	0.455
GG56	0.165	ND	ND	ND	0.379
GG57	0.295	ND	ND	ND	0.393
GG58	0.080	ND	ND	ND	0.496
GG59	0.172	ND	ND	ND	0.338
GG60	ND	ND	ND	ND	ND
GG61	0.272	ND	ND	ND	0.475
GG62	0.251	ND	ND	ND	0.481
GG63	0.160	ND	ND	ND	0.461
GG64	0.143	ND	ND	ND	0.548
GG65	ND	ND	ND	ND	0.298
GG66	0.153	ND	ND	ND	0.474
GG67	0.207	ND	ND	ND	0.512
GG68	0.135	ND	ND	ND	0.440
GG69	0.132	ND	ND	ND	0.484
GG70	0.217	ND	ND	ND	0.572
GG71	ND	ND	ND	ND	0.454
GG72	0.234	ND	ND	ND	0.477
GG73	ND	ND	ND	ND	0.469
GG74	0.157	ND	ND	ND	0.458
GG75	ND	ND	ND	ND	0.471
GG76	0.171	ND	ND	ND	0.443
GG77	0.151	ND	ND	ND	0.365
GG78	0.173	0.699	ND	ND	0.456
GG79	0.110	ND	ND	ND	0.437
GG80	0.222	ND	ND	ND	0.473

Table A-2-7: *Enantiomer fractions in glaucous gull plasma*

Sample	Lab code	Capture date	Sex	plasma lipid %	95 EF	PCB 91
P1	1	7/6	F	0.950	NR	NR
P2	2	6/6	F	0.790	NR	NR
P3	3	13/6	F	0.819	NR	NR
P4	4	11/6	M	0.772	nd	nd
P5	5	12/6	M	0.654	nd	nd
P6	6	6/6	F	0.768	NR	NR
P7	7	15/6	M	1.001	NR	NR
P8	8	21/6	F	0.689	NR	NR
P9	9	23/6	F	0.864	NR	NR
P10	10	1/6	F	1.130	NR	NR
P11	11	6/6	M	0.576	NR	NR
P12	12	11/6	F	0.552	NR	NR
P13	13	4/6	M	0.807	NR	NR
P14	14	7/6	F	0.403	NR	NR
P15	15	30/5	M	0.930	NR	NR
P16	16	7/6	M	0.441	NR	NR
P17	17	8/6	F	0.808	nd	nd
P18	18	8/6	M	0.714	nd	nd
P19	19	11/6	F	0.861	NR	NR
P20	20	15/6	F	0.912	nd	nd
P21	21	30/5	M	0.803	NR	NR
P22	22	5/6	F	0.858	NR	NR
P23	23	5/6	M	0.689	NR	NR
P24	24	1/6	M	0.913	nd	nd
P25	25	5/6	F	0.401	NR	NR
P26	26	30/5	F	0.628	NR	NR
P27	27	5/6	F	0.639	NR	NR
P28	28	2/6	F	0.652	NR	NR
P29	29	15/6	M	0.543	NR	NR
P30	30	30/5	M	1.001	nd	nd
P31	31	15/6	F	0.791	NR	NR
P32	32	3/6	F	1.046	NR	NR
P33	33	2/6	M	0.828	nd	nd
P34	34	5/6	F	1.014	NR	NR
P35	35	7/6	F	1.048	NR	NR
P36	36	15/6	F	1.264	NR	NR
P37	37	2/6	F	1.016	NR	NR
P38	38	3/6	F	1.052	nd	nd
P39	39	1/6	F	1.059	NR	NR
P40	40	3/6	M	0.921	NR	NR
P41	41	23/6	F	0.610	NR	NR
P42	42	4/6	F	0.778	NR	NR
P43	43	8/6	F	1.043	nd	nd
P44	44	12/6	F	0.612	NR	NR
P45	45	3/6	M	0.683	nd	nd
P46	46	4/6	M	0.766	nd	nd
P47	47	1/6	M	0.690	nd	nd
P48	48	12/6	M	0.998	nd	nd
P49	49	31/5	F	1.098	NR	NR

Sample	PCB 84	PCB 136	PCB 149	PCB 176	PCB 174	PCB 183	α−HCH
P1	NR	NR	NR	NR	NR	nd	nd
P2	NR	NR	NR	NR	NR	nd	nd
P3	NR	NR	NR	NR	NR	nd	nd
P4	nd	nd	nd	nd	nd	nd	nd
P5	nd	nd	nd	nd	nd	0.47	nd
P6	NR	NR	NR	NR	NR	0.46	nd
P7	NR	NR	NR	NR	NR	nd	nd
P8	NR	NR	NR	NR	NR	nd	nd
P9	NR	NR	NR	NR	NR	nd	nd
P10	NR	NR	NR	NR	NR	nd	nd
P11	NR	NR	NR	NR	NR	0.55	nd
P12	NR	NR	NR	NR	NR	nd	nd
P13	NR	NR	NR	NR	NR	nd	nd
P14	NR	NR	NR	NR	NR	nd	nd
P15	NR	NR	NR	NR	NR	nd	nd
P16	NR	NR	NR	NR	NR	nd	nd
P17	nd	nd	nd	nd	nd	nd	nd
P18	nd	nd	nd	nd	nd	0.38	nd
P19	NR	NR	NR	NR	NR	NS	nd
P20	nd	nd	nd	nd	nd	0.41	nd
P21	NR	NR	NR	NR	NR	nd	nd
P22	NR	NR	NR	NR	NR	nd	nd
P23	NR	NR	NR	NR	NR	nd	nd
P24	nd	nd	nd	nd	nd	nd	nd
P25	NR	NR	NR	NR	NR	NS	nd
P26	NR	NR	NR	NR	NR	0.38	nd
P27	NR	NR	NR	NR	NR	NS	nd
P28	NR	NR	NR	NR	NR	nd	nd
P29	NR	NR	NR	NR	NR	nd	nd
P30	nd	nd	nd	nd	nd	NS	nd
P31	NR	NR	NR	NR	NR	nd	nd
P32	NR	NR	NR	NR	NR	NS	nd
P33	nd	nd	nd	nd	nd	NS	nd
P34	NR	NR	NR	NR	NR	NS	nd
P35	NR	NR	NR	NR	NR	0.41	nd
P36	NR	NR	NR	NR	NR	nd	nd
P37	NR	NR	NR	NR	NR	nd	nd
P38	nd	nd	nd	nd	nd	0.43	nd
P39	NR	NR	NR	NR	NR	0.51	nd
P40	NR	NR	NR	NR	NR	0.36	nd
P41	NR	NR	NR	NR	NR	nd	nd
P42	NR	NR	NR	NR	NR	0.44	nd
P43	nd	nd	nd	nd	nd	NS	nd
P44	NR	NR	NR	NR	NR	nd	nd
P45	nd	nd	nd	nd	nd	nd	nd
P46	nd	nd	nd	nd	nd	0.43	nd
P47	nd	nd	nd	nd	nd	nd	nd
P48	nd	nd	nd	nd	nd	0.41	nd

277

Sample	HEPX	Oxychlordane	*trans*-Chlordane	*cis*-Chlordane
P1	nq	0.623	nd	nd
P2	nd	nd	nd	nd
P3	nq	int	nd	nd
P4	0.613	0.527	nd	nd
P5	0.765	0.599	nd	nd
P6	nd	int	0.521	nd
P7	nq	0.646	nd	nd
P8	nq	0.568	nd	nd
P9	nd	0.649	nd	nd
P10	nq	nq	nd	nd
P11	nq	0.645	nd	nd
P12	nd	int	0.570	nd
P13	nq	0.631	nd	nd
P14	0.733	0.594	nd	nd
P15	nd	int	nd	nd
P16	nq	int	nd	nd
P17	nq	int	nd	nd
P18	nd	it	nd	nd
P19	0.732	0.588	nd	nd
P20	nd	0.611	nd	nd
P21	0.704	0.649	nd	nd
P22	nd	nq	nd	nd
P23	nq	0.621	nd	nd
P24	0.702	int	0.630	nd
P25	nq	0.728	nd	nd
P26	0.610	0.684	0.525	0.282
P27	nq	0.613	nd	nd
P28	0.659	0.583	nd	nd
P29	0.698	0.662	nd	nd
P30	0.704	0.619	nd	0.309
P31	nd	0.661	nd	nd
P32	0.690	0.621	nd	nd
P33	nd	0.697	nd	nd
P34	0.647	0.673	0.468	0.448
P35	0.706	0.582	nd	nd
P36	nq	0.595	??	??
P37	0.673	int	nd	nd
P38	nd	nd	nd	nd
P39	0.659	0.649	nd	nd
P40	0.720	0.614	0.483	0.225
P41	nd	int	nd	nd
P42	nq	0.676	nd	nd
P43	nd	nd	nd	nd
P44	0.686	0.562	0.542	nd
P45	0.657	0.622	nd	nd
P46	0.650	int	nd	nd
P47	0.722	0.611	nd	nd
P48	int	int	nd	nd
P49	int	0.761	0.449	0.320

Appendix 3: Enantiomer fractions in sledge dog tissues

Table A-3-8: Sledge Dog sample information

Sample	Age (days)	Sex	Age Class	Group
Pelle 223	358	Male	Adult	Control
Pist 221	358	Female	Adult	Control
Pondus 226	358	Male	Adult	Control
Putte 224	358	Male	Adult	Control
Trisse 321	359	Female	Adult	Control
Maja 72	381	Female	Adult	Control
Frida 82	404	unknown	Adult	Control
Lulu 62	500	Female	Adult	Control
Cmila 54	556	Female	Adult	Control
Selma52	556	Female	Adult	Control
Smit 42	635	Female	Adult	Control
Turbo 32	636	Female	Adult	Control
Ping 22	666	Female	Adult	Control
Freda	unknown	unknown	Adult	Control
Mie 725	18	Female	Pup	Control
Mille 722	18	Male	Pup	Control
Minna 723	18	Female	Pup	Control
Molly 724	18	Female	Pup	Control
Moses 726	18	Male	Pup	Control
Trille 325	24	Male	Pup	Control
Tue 324	24	Male	Pup	Control
Tufi 322	24	Female	Pup	Control
Tune 323	24	Male	Pup	Control
Solo 421	79	Female	Pup	Control
Pine 215	342	Female	Adult	Exposed
Prima214	342	Male	Adult	Exposed
Prosit 216	342	Male	Adult	Exposed
Mums 71	381	Female	Adult	Exposed
Fitzen 81	404	Female	Adult	Exposed
Laura 61	500	Female	Adult	Exposed
Chiva 53	556	Female	Adult	Exposed
Senvid 51	556	Female	Adult	Exposed
Smule 41	635	Female	Adult	Exposed
Tufse 31	636	Female	Adult	Exposed
Pong21	666	Female	Adult	Exposed
Mojo	10	Male	Pup	Exposed
Mollo 712	10	Male	Pup	Exposed
Mule 713	10	Male	Pup	Exposed
Miau 721	18	Female	Pup	Exposed
srm 1				
srm 2				

Table A-3-9: *Enantiomer fractions in sledge dog adipose tissue*

Enantiomer Fractions (EF)

Sample	a-HCH (bdex)	a-HCH (BGB)	Oxy	HEPX
Pelle 223	0.692	nd	0.801	nd
Pist 221	0.924	nd	0.815	nd
Pondus 226	0.633	0.598	0.787	nd
Putte 224	nd	0.806	0.796	nd
Trisse 321	0.640	nd	0.801	nd
Maja 72	0.491	0.491	0.687	0.762
Frida 82	0.882	nd	0.793	nd
Lulu 62	0.722	nd	0.730	nd
Cmila 54	0.850	nd	0.764	nd
Selma52	NR	0.846	0.768	0.760
Smit 42	0.821	0.491	0.816	nd
Turbo 32	nd	nd	0.816	nd
Ping 22	0.797	nd	0.802	nd
Freda	0.251	0.367	0.720	0.647
Mie 725	nd	nd	0.709	NR
Mille 722	nd	0.590	0.709	0.792
Minna 723	nd	nd	0.000	0.888
Molly 724	0.452	nd	0.000	1.000
Moses 726	nd	nd	0.706	NR
Trille 325	nd	nd	0.798	NR
Tue 324	nd	nd	0.820	NR
Tufi 322	0.512	nd	NR	NR
Tune 323	0.480	nd	0.000	1.000
Solo 421	0.580	nd	0.802	NR
Pine 215	0.460	0.498	0.635	0.762
Prima214	0.498	0.499	0.626	0.750
Prosit 216	0.485	0.485	0.624	0.765
Mums 71	0.500	0.507	0.651	0.745
Fitzen 81	0.571	0.562	0.693	0.775
Laura 61	0.630	0.631	0.693	0.817
Chiva 53	0.758	0.801	0.733	0.794
Senvid 51	0.452	nd	0.706	NR
Smule 41	0.666	nd	0.746	0.794
Tufse 31	nd	0.700	0.757	0.775
Pong21	0.572	0.647	0.684	0.785
Mojo	0.482	0.484	0.643	0.732
Mollo 712	0.481	0.491	0.650	0.650
Mule 713	0.492	0.915	0.674	0.750
Miau 721	0.563	0.831	0.691	0.737
srm 1	0.586	NR	NR	NR
srm 2	0.589	NR	NR	NR

Enantiomer Fractions (EF)

Sample	TC	CC	PCB 91	PCB 95	PCB 84
Pelle 223	nd	nd	nd	nd	nd
Pist 221	nd	nd	nd	nd	nd
Pondus 226	nd	nd	nd	nd	nd
Putte 224	nd	nd	nd	nd	nd
Trisse 321	nd	nd	nd	nd	nd
Maja 72	nd	0.131	0.321	nd	nd
Frida 82	nd	nd	nd	nd	nd
Lulu 62	nd	nd	nd	nd	nd
Cmila 54	nd	nd	nd	nd	nd
Selma52	nd	nd	nd	nd	nd
Smit 42	nd	nd	nd	nd	nd
Turbo 32	nd	nd	nd	nd	nd
Ping 22	nd	nd	nd	nd	nd
Freda	0.505	nd	nd	nd	nd
Mie 725	nd	nd	nd	nd	nd
Mille 722	nd	nd	nd	nd	nd
Minna 723	nd	nd	nd	nd	nd
Molly 724	0.493	nd	nd	nd	nd
Moses 726	nd	nd	nd	nd	nd
Trille 325	nd	nd	nd	nd	nd
Tue 324	nd	nd	nd	nd	nd
Tufi 322	0.486	nd	nd	nd	nd
Tune 323	0.502	0.366	nd	nd	nd
Solo 421	nd	nd	nd	nd	nd
Pine 215	nd	0.121	0.302	nd	nd
Prima214	nd	nd	0.287	nd	nd
Prosit 216	nd	0.052	0.278	0.361	nd
Mums 71	nd	0.114	0.297	nd	nd
Fitzen 81	0.559	0.158	0.269	nd	nd
Laura 61	nd	0.139	0.314	nd	nd
Chiva 53	nd	0.203	0.341	nd	nd
Senvid 51	nd	nd	nd	nd	nd
Smule 41	nd	nd	nd	nd	nd
Tufse 31	nd	nd	0.294	nd	nd
Pong21	0.573	0.151	0.318	nd	nd
Mojo	0.519	0.209	nd	nd	nd
Mollo 712	nd	nd	nd	nd	nd
Mule 713	nd	nd	nd	nd	nd
Miau 721	0.514	0.235	nd	nd	nd
srm 1	0.856	0.180	0.421	0.485	nd
srm 2	0.854	0.180	0.423	0.491	nd

Enantiomer Fractions (EF)

Sample	PCB 132	PCB 135	PCB 149	PCB 176	PCB 174
Pelle 223	nd	nd	nd	nd	nd
Pist 221	nd	nd	nd	nd	nd
Pondus 226	nd	nd	nd	nd	nd
Putte 224	nd	nd	nd	nd	nd
Trisse 321	nd	nd	nd	nd	nd
Maja 72	0.625	nd	0.315	nd	0.540
Frida 82	nd	nd	nd	nd	nd
Lulu 62	nd	nd	nd	nd	nd
Cmila 54	nd	nd	nd	nd	nd
Selma52	nd	nd	nd	nd	nd
Smit 42	nd	nd	nd	nd	nd
Turbo 32	nd	nd	nd	nd	nd
Ping 22	nd	nd	nd	nd	nd
Freda	nd	nd	nd	nd	nd
Mie 725	nd	nd	nd	nd	nd
Mille 722	nd	nd	nd	nd	nd
Minna 723	nd	nd	nd	nd	nd
Molly 724	nd	nd	nd	nd	nd
Moses 726	nd	nd	nd	nd	nd
Trille 325	nd	nd	nd	nd	nd
Tue 324	nd	nd	nd	nd	nd
Tufi 322	nd	nd	nd	nd	nd
Tune 323	nd	nd	nd	nd	nd
Solo 421	nd	nd	nd	nd	nd
Pine 215	nd	nd	0.145	nd	nd
Prima214	0.591	nd	0.269	nd	0.538
Prosit 216	nd	nd	0.264	nd	0.521
Mums 71	nd	nd	0.233	nd	nd
Fitzen 81	nd	nd	0.171	nd	nd
Laura 61	nd	nd	0.317	nd	nd
Chiva 53	nd	nd	0.268	nd	0.518
Senvid 51	nd	nd	nd	nd	nd
Smule 41	nd	nd	0.319	nd	nd
Tufse 31	nd	nd	0.287	nd	nd
Pong21	nd	nd	0.312	nd	nd
Mojo	nd	nd	0.239	nd	nd
Mollo 712	nd	nd	nd	nd	nd
Mule 713	nd	nd	nd	nd	nd
Miau 721	nd	nd	0.321	nd	nd
srm 1	0.515	0.365	0.463	0.535	0.563
srm 2	0.510	0.378	0.465	0.527	0.557

EF

Sample	PCB 183
Pelle 223	nd
Pist 221	nd
Pondus 226	nd
Putte 224	nd
Trisse 321	nd
Maja 72	0.072
Frida 82	nd
Lulu 62	nd
Cmila 54	nd
Selma52	nd
Smit 42	nd
Turbo 32	nd
Ping 22	nd
Freda	E2 only
Mie 725	nd
Mille 722	nd
Minna 723	nd
Molly 724	nd
Moses 726	nd
Trille 325	nd
Tue 324	nd
Tufi 322	nd
Tune 323	nd
Solo 421	nd
Pine 215	0.112
Prima214	0.216
Prosit 216	0.183
Mums 71	0.142
Fitzen 81	interference
Laura 61	interference
Chiva 53	interference
Senvid 51	E2 only
Smule 41	interference
Tufse 31	E2 only
Pong21	0.043
Mojo	0.082
Mollo 712	0.075
Mule 713	0.092
Miau 721	interference
srm 1	0.486
srm 2	0.480

Table A-3-10: *Enantiomer fractions in sledge dog adrenal tissue*

	Enantiomer Fractions (EF)		
	HCH	TC	CC
Smit42	nd	nd	nd
Pondus226	nd	0.529	nd
Turbo32	nd	0.505	nd
Putte224	nd	nd	nd
Maja72	nd	0.516	nd
Cmilla54	nd	0.537	nd
Trisse321	nd	nd	nd
Trisse322	nd	nd	nd
Lulu62	nd	0.531	nd
Pelle223	nd	0.505	nd
Ping22	nd	0.490	0.485
Ping23	nd	nd	nd
Frida82	nd	nd	nd
Pist221	nd	nd	nd
Selma52	nd	nd	nd
Tufse31	nd	nd	nd
Snehvid-51	0.473	nd	nd
Laura61	0.608	0.518	nd
Pine215	0.431	0.510	0.259
Fitzen81	nd	nd	nd
Prosit216	0.481	0.514	0.360
Chiva53	nd	nd	nd
Mums71	nd	nd	nd
Prima214	nd	nd	nd
Smule41	nd	nd	nd
Smule42	nd	nd	nd

Table A-3-11: *Enantiomer fractions in sledge dog liver tissue*

Liver ID	Dog Name	a-HCH	Oxy	HEPX	TC	CC
22	Ping22	nd	0.841	nd	0.496	0.512
52	Selma52	0.524	0.818	nd	0.501	0.487
54	Cmilla54	nd	0.842	nd	0.504	0.509
62	Lulu62	nd	0.830	nd	0.500	0.491
71	Mums71	nd	0.773	0.685	0.501	0.408
82	Frida82	0.505	0.824	nd	0.501	0.490
221	Pist221	nd	0.840	nd	0.505	0.499
223	Pelle223		0.847	nd		
224	Putte224	nd	0.872	nd	0.506	0.499
226	Pondus226	nd	0.814	nd	0.511	0.471
223-D1-C	Pelle223	nd	0.819	nd	0.506	0.502
223_d2	Pelle223		0.842	nd		
32	Turbo32	0.470	0.817	nd	nd	nd
42	Smit42	nd	0.860	nd	0.504	0.479
321	Trisse321	0.494	0.656	nd	0.502	0.492
31	Tufse31	0.754	0.837	0.751	0.556	0.443
41	Smule41	nd	0.848	0.774	0.501	0.450
51	Snehvid-51	0.535	0.794	0.736	0.511	0.412
61	Laura61	0.653	0.814	0.814	0.508	0.475
72	Maja72	nd	0.813	nd	0.507	0.531
214	Prima214	0.505	0.719	0.715	0.493	0.439
215	Pine215	0.474	0.735	0.717	0.502	0.496
53	Chiva53	0.757	0.803	0.799	0.514	0.469
81	Fitzen81	0.570	0.758	nd	0.500	0.488
216	Prosit216	0.532	0.690	0.681	0.497	0.422
81-DUP1	Fitzen81	0.619		0.738	0.492	0.433
81-DUP2	Fitzen81	0.611	0.797	=	0.507	0.499
SRM1		nd	0.606		nd	nd
SRM2		0.586	0.628	0.503	0.794	0.191

Table A-3-12: *Enantiomer fractions in sledge dog thyroid tissue*

ID	Dog Name	a-HCH	Oxy	HEPX	TC	CC
22	Ping22	nd	nd	nd	nd	0.498
32	Turbo32	nd	nd	nd	nd	nd
42	Smit42	nd	nd	nd	nd	0.533
52	Selma52	nd	0.800	nd	nd	0.487
54	Cmilla54	nd	nd	nd	0.417	0.497
62	Lulu62	nd	nd	nd	0.463	0.480
72	Maja72	nd	0.684	nd	nd	0.499
82	Frida82	nd	nd	nd	nd	nd
221	Pist221	nd	nd	nd	nd	nd
223	Pelle223	nd	nd	nd	nd	0.537
224	Putte224	nd	nd	nd	nd	0.532
226	Pondus226	nd	nd	nd	nd	0.500
321	Trisse321	nd	nd	nd	0.395	0.498
54_dup	Cmilla54	nd	0.770	nd	nd	0.559
72_b	Maja72	nd	nd	nd	nd	nd
maja_72_days	Maja72	nd	nd	nd	nd	nd
31	Tufse31	nd	nd	nd	nd	nd
41	Smule41	nd	nd	nd	nd	nd
51	Snehvid-51	nd	0.690	nd	nd	0.545
53	Chiva53	nd	nd	nd	nd	nd
61	Laura61	nd	0.692	nd	nd	0.491
71	Mums71	nd	nd	nd	nd	0.512
81	Fitzen81	nd	nd	nd	nd	nd
214	Prima214	nd	0.629	0.724	0.718	0.544
215	Pine215	nd	0.643	0.722	0.590	0.514
216	Prosit216	0.656	0.621	0.687	1.000	0.511
41_dup	Smule41	nd	0.740	0.775	nd	0.496
53_dup	Chiva53	nd	nd	nd	nd	nd
61_dup	Laura61	nd	0.721	nd	nd	0.507
tu_31 days	Tufse31	0.738	0.752	0.753	nd	nd
srm 1		0.587	0.606	0.634	0.819	0.830
srm 2		0.591	0.623	0.670	0.814	0.808

Table A-3-13: *Sample information and enantiomer*
fractions in sledge dog brain tissue

Dog Name	ID	Age	Group
Pist221	DB02	Adult	Control
Pondus226	DB03	Adult	Control
Trisse321	DB05	Adult	Control
Smit42	DB06	Adult	Control
Maja72	DB07	Adult	Control
Selma52	DB09	Adult	Control
Pelle223	DB11	Adult	Control
Lulu62	DB15	Adult	Control
Putte224	DB16	Adult	Control
Frida82	DB19	Adult	Control
Ping22	DB20	Adult	Control
Cmilla54	DB21	Adult	Control
Tufse31	DB01	Adult	Exposed
Smule41	DB04	Adult	Exposed
Chiva53	DB08	Adult	Exposed
Prosit216	DB10	Adult	Exposed
Fitzen81	DB13	Adult	Exposed
Prima214	DB18	Adult	Exposed
Laura61	DB23	Adult	Exposed
Laura61	DB24	Adult	Exposed
Snehvid-51	DB25	Adult	Exposed
Snehvid-51	DB26	Adult	Exposed
BL1	DB12		
na	DB14		
na	DB17		
BL2	DB22		

Dog Name	a-HCH	Oxy	HEPX	TC	CC
Pist221	nd	nd	nd	nd	nd
Pondus226	nd	0.860	nd	nd	nd
Trisse321	nd	nd	nd	nd	nd
Smit42	nd	nd	nd	nd	nd
Maja72	nd	0.811	nd	nd	nd
Selma52	nd	nd	nd	nd	nd
Pelle223	nd	nd	nd	nd	nd
Lulu62	nd	nd	nd	nd	nd
Putte224	nd	nd	nd	nd	nd
Frida82	1.000	0.888	nd	0.530	nd
Ping22	nd	0.884	nd	nd	nd
Cmilla54	nd	nd	nd	nd	nd
Tufse31	0.988	0.778	0.806	int	nd
Smule41	0.984	0.754	0.812	0.501	nd
Chiva53	nd	0.784	nd	nd	nd
Prosit216	nd	nd	nd	nd	nd
Fitzen81	nd	0.759	nd	nd	nd
Prima214	0.965	0.642	0.764	0.501	nd
Laura61	nd	0.771	nd	nd	nd
Laura61	0.990	0.736	nd	nd	nd
Snehvid-51	nd	0.710	nd	nd	nd
Snehvid-51	0.973	0.709	nd	nd	nd

Table A-3-14: Enantiomer fractions in exposed sledge dog diet (minke whale blubber)

Sample	BGB	Bdex	BGB		Bdex	
	HCH	HCH	Oxy	HEPX	TC	CC
SD Diet F123 1	0.653	0.664	0.563	interference	nd	0.095
SD Diet F123 2	0.674	nd	0.557	0.187	nd	0.082
SD Diet F123 3	nd	nd	nd	nd	0.498	0.168
SD Diet F123 4	nd	nd	nd	nd	nd	0.092
SD Diet F123 5	nd	nd	nd	nd	nd	nd
SD Diet F123 6	nd	nd	nd	nd	nd	0.087
SD Diet Neutrals 1	nd	nd	nd	nd	nd	nd
SD Diet Neutrals 2	nd	nd	nd	nd	nd	nd
SD Diet Neutrals 3	nd	nd	nd	nd	nd	nd
SD Diet Neutrals 4	0.654	0.656	0.603	0.122	nd	nd
SD Diet Neutrals 5	0.690	0.650	nd	nd	nd	nd
SD Diet Neutrals 6	0.656	0.659	0.553	0.114	nd	nd
SD Diet Neutrals 7	nd	nd	nd	nd	nd	nd
SD Diet Neutrals 8	0.531	nd	0.548	nd	nd	nd

Sample	Chiralsil-dex							
	91	95	84	132	135	149	176
SD Diet F123 1	0.389	0.389	nd	0.460	0.382	0.473	0.505
SD Diet F123 2	0.393	0.329	nd	0.471	0.378	0.470	0.522
SD Diet F123 3	0.424	0.490	nd	0.533	0.379	0.468	0.527
SD Diet F123 4	nd	nd	nd	nd	nd	nd	nd
SD Diet F123 5	nd	nd	nd	nd	nd	nd	nd
SD Diet F123 6	nd	nd	nd	nd	nd	nd	nd
SD Diet Neutrals 1	nd	nd	nd	nd	nd	nd	nd
SD Diet Neutrals 2	nd	nd	nd	nd	nd	nd	nd
SD Diet Neutrals 3	nd	nd	nd	nd	nd	nd	nd
SD Diet Neutrals 4	0.332	nd	nd	0.474	0.337	0.474	0.499
SD Diet Neutrals 5	nd	nd	nd	0.473	0.257	0.474	nd
SD Diet Neutrals 6	0.406	0.530	nd	0.472	0.333	0.475	0.495
SD Diet Neutrals 7	nd	nd	nd	nd	nd	nd	nd
SD Diet Neutrals 8	0.452	nd	nd	0.525	0.304	0.467	nd

290

Sample	CDX 174	BGB 183
SD Diet F123 1	0.493	0.477
SD Diet F123 2	0.493	0.480
SD Diet F123 3	0.576	0.513
SD Diet F123 4	nd	nd
SD Diet F123 5	nd	nd
SD Diet F123 6	nd	nd
SD Diet Neutrals 1	nd	nd
SD Diet Neutrals 2	nd	nd
SD Diet Neutrals 3	nd	nd
SD Diet Neutrals 4	0.488	0.490
SD Diet Neutrals 5	0.483	0.497
SD Diet Neutrals 6	0.493	0.485
SD Diet Neutrals 7	nd	nd
SD Diet Neutrals 8	0.583	0.512

Appendix 4: Sample information and data from Chapter 6-Isomer-Specific

Biotransformation of Perfluorooctane Sulfonamide in Sprague-Dawley Rats
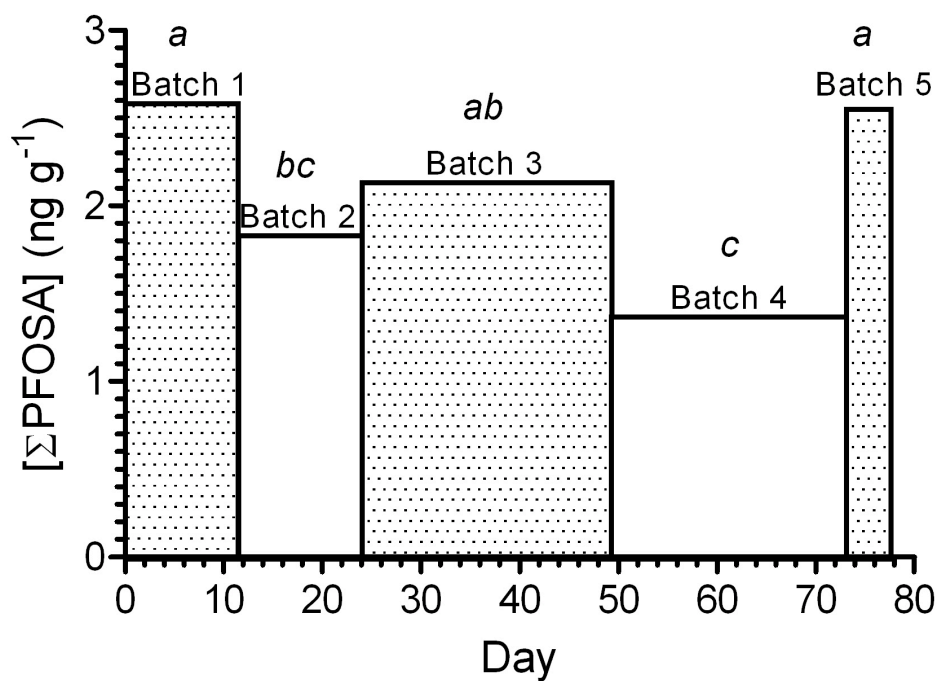
Figure A-4-1: *Concentration of total PFOSA in spiked rat chow as a function of time over the course of the uptake phase. Data expressed as mean ± 1 standard error for n=3. Batches with differing letters above them indicates statistically significant differences (p<0.05).*
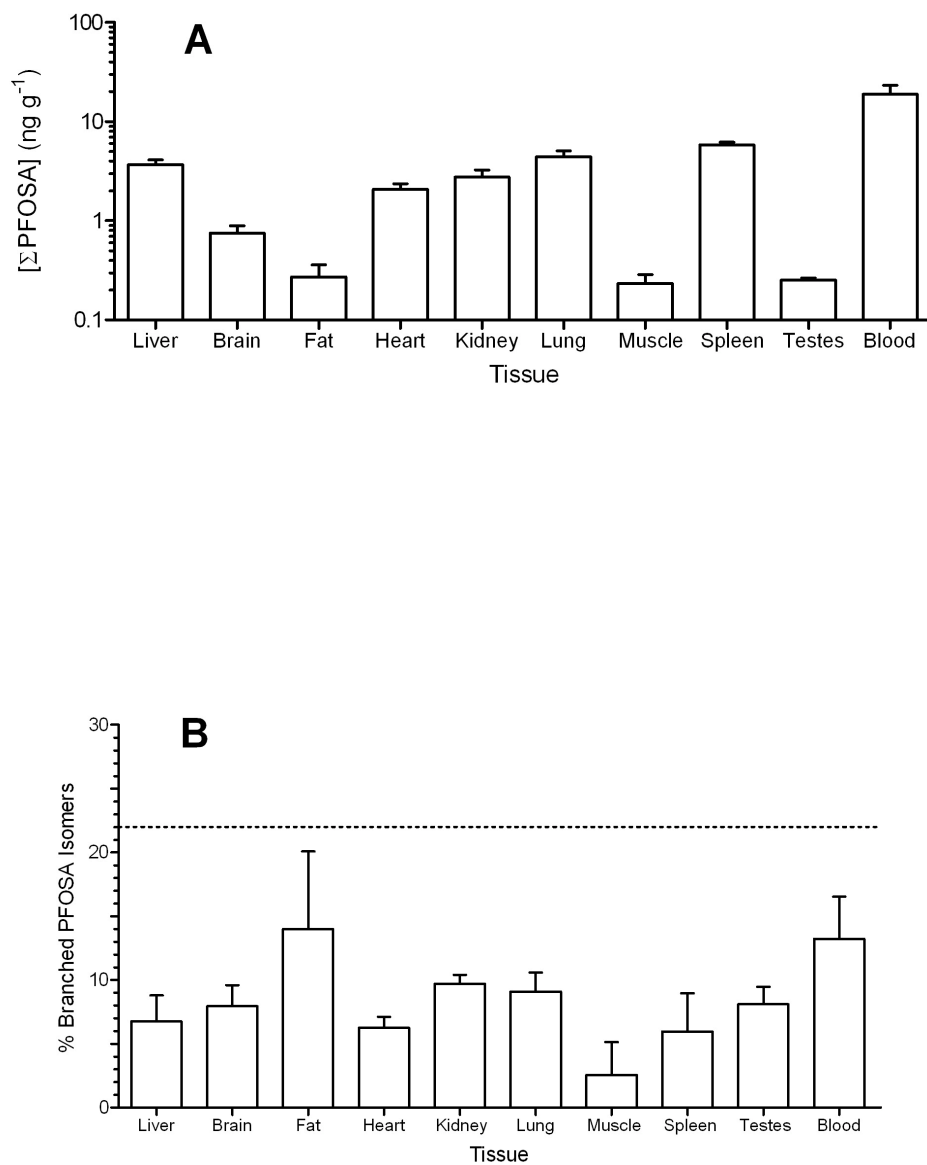
Figure A-4-2: *Concentration of total PFOSA (A) and the percentage of total branched isomers of PFOSA (B) in tissues of rats after 77 days of exposure to electrochemically fluorinated PFOSA via their diet. Data in both plots expressed as mean ± 1 standard error for n=3. Dashed line in (B) represents the mean percentage of branched PFOSA isomers in the food.*
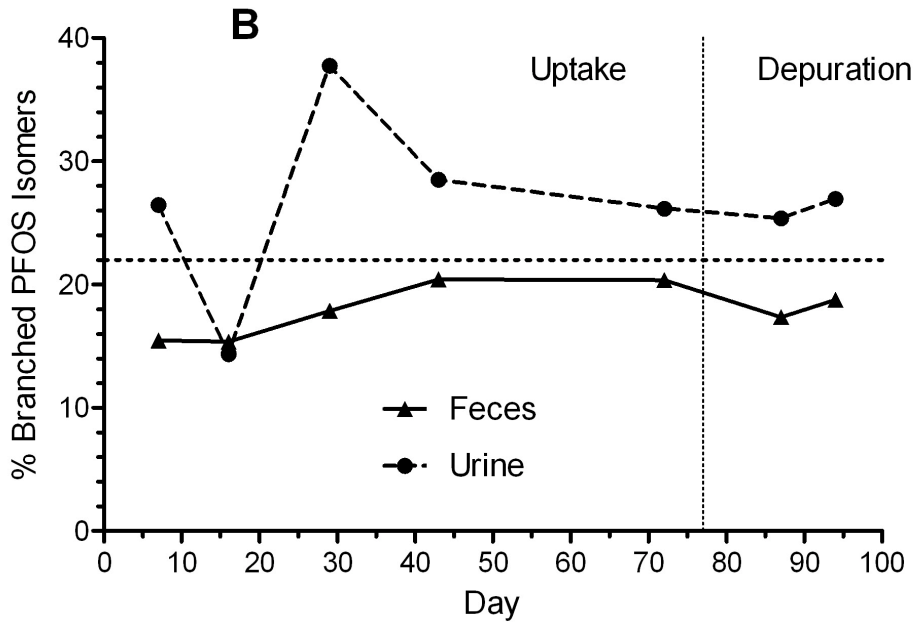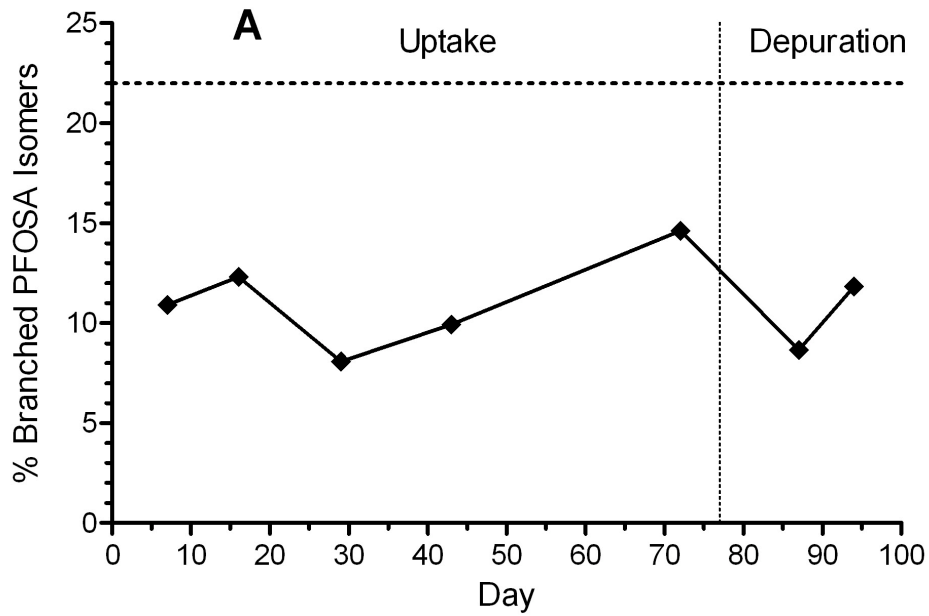
Figure A-4-3: *Percentage of total branched isomers of PFOSA in the feces (A) or percentage of total branched isomers of PFOS in the urine and feces (B) during uptake (days 0 to 77) and depuration (days 78 to 104) phases. Each point represents the mean for n=2. Vertical dashed line delineates the end of the uptake phase. Horizontal dashed line represents the mean percentage of branched PFOSA isomers in the food.*
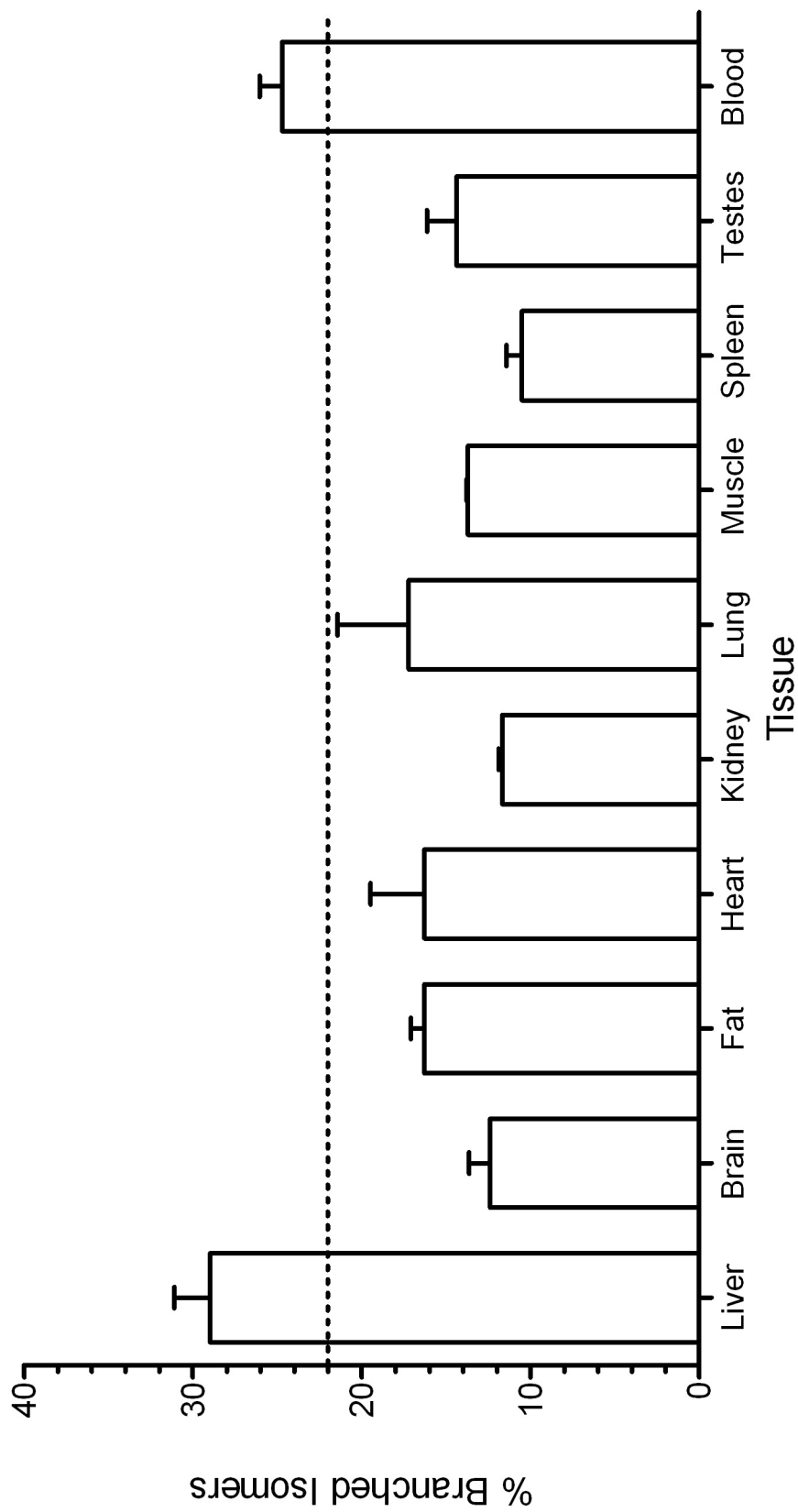
Figure A-4-4: *Percentage of total branched isomers of PFOS in tissues following 77 days of exposure to electrochemically fluorinated PFOSA. Data expressed as mean ± 1 standard error for n=3.*

295

Table A-4-15: Masses of individual rats

Rat ID	6/16/2009	06/23/09	06/25/09	06/30/09	07/08/09	07/14/09	07/21/09	07/28/09	08/05/09
1	0.62	0.62	0.64	0.68	0.70	0.70	0.72	0.76	0.74
2	0.58	0.58	0.60	0.60	0.62	0.62	0.64	0.68	0.68
3	0.60	0.60	0.60	0.58	0.66	0.66	0.68	0.68	0.70
4	0.60	0.60	0.62	0.62	0.62	0.64	0.64	0.66	0.68
5	0.60	0.62	0.60	0.64	0.66	0.66	0.68	0.68	0.68
6	0.50	0.54	0.54	0.54	0.56	0.58	0.58	0.60	0.60
7	0.50	0.56	0.58	0.58	0.58	0.60	0.62	0.60	0.62
8	0.54	0.56	0.56	0.58	0.58	0.60	0.62	0.62	0.64
9	0.64	0.62	0.64	0.68	0.70	0.72	0.74	0.76	0.76
40	0.56	0.54	0.56	0.58	0.60	0.60	0.60	0.62	0.64
50	0.68	0.68	0.64	0.70	0.72	0.74	0.76	0.78	0.80
60	0.62	0.64	0.62	0.64	0.68	0.66	0.68	0.70	0.60

Rat ID	08/18/09	09/01/09	09/15/09	09/29/09	09/30/09	10/01/09	10/06/09	10/13/09	10/26/09
1	0.78	0.78	0.80	0.82	0.82	0.84	0.84	0.84	
2	0.68	0.70	0.74	0.74					
3	0.72	0.72	0.76	0.76					
4	0.70	0.72	0.76	0.80	0.78	0.76	0.80	0.78	0.80
5	0.70	0.72	0.74	0.76					
6	0.62	0.64	0.64	0.64	0.64	0.62	0.64	NA	0.68
7	0.64	0.66	0.66	0.66	0.68	0.66	0.68	0.70	0.70
8	0.66	0.66	0.68	0.70					
9	0.82	0.84	0.86	0.90	0.90	0.88	0.90	0.92	0.94
40	0.68	0.70	0.72	0.74					
50	0.82	0.84	0.88	0.90	0.88	0.90	0.90	0.90	0.94
60	0.76	0.76	0.60	0.78	0.78	0.78	0.78	0.80	0.80

Table A-4- 16: Concentrations and percentage of branched PFOSA isomers in control and spiked rat chow

n-fosa 78

Concentrations
Based on mFOSA

Control		Spike						
6/15/2009	9/21/2009	6/15/2009	6/29/2009	7/14/2009	7/25/2009	8/7/2009	9/2/2009	9/25/2009
0.02	0.00	0.01	0.03	1.9	1.6	1.8	1.2	2.1
0.01	0.02	0.07	0.01	2.1	1.0	1.8	1.1	2.0
0.02	0.02	0.01	0.02	2.0	1.6	1.5	1.0	1.9

total br fosa

Based on mFOSA

Control		Spike						
6/15/2009	9/21/2009	6/15/2009	6/29/2009	7/14/2009	7/25/2009	8/7/2009	9/2/2009	9/25/2009
nd	nd	nd	nd	0.56	0.50	0.45	0.32	0.58
nd	nd	nd	nd	0.66	0.29	0.49	0.32	0.59
nd	nd	nd	nd	0.57	0.47	0.36	0.26	0.51

Total FOSA

Based on mFOSA

Control		Spike						
6/15/2009	9/21/2009	6/15/2009	6/29/2009	7/14/2009	7/25/2009	8/7/2009	9/2/2009	9/25/2009
nd	nd	nd	nd	2.5	2.1	2.2	1.5	2.7
nd	nd	nd	nd	2.7	1.3	2.3	1.4	2.6
nd	nd	nd	nd	2.5	2.1	1.9	1.2	2.4

%Branched

Based on mFOSA

Control		Spike						
6/15/2009	9/21/2009	6/15/2009	6/29/2009	7/14/2009	7/25/2009	8/7/2009	9/2/2009	9/25/2009
nd	nd	nd	nd	0.22	0.24	0.20	0.22	0.22
nd	nd	nd	nd	0.24	0.22	0.22	0.23	0.23
nd	nd	nd	nd	0.23	0.22	0.19	0.21	0.21

297

Table A-4-17: Concentration and branched isomer percentage of PFOS isomers in spiked and control food

Sample	Mass	Concentration (ng/g)							[PFOS]
		1m	3m	4m	5m	totalDM	iso	n-pfos	
C. Food 9/21	1	ND	0.013	0.015	0.049	ND	0.089	1.6	1.7
C.Food 6/15	1.04	ND	ND	ND	ND	ND	ND	0.22	0.2
Food Na2SO4	1.61	ND	ND	ND	ND	ND	ND	ND	0.0
S. Food 9/25	1.02	ND	0.000	0.001	ND	ND	ND	0.72	0.7
S. Food 6/15	1.04	ND	0.005	0.005	0.013	ND	0.032	1.0	1.0
S. Food 6/29	1.02	ND	0.040	0.035	0.120	ND	0.214	2.7	3.1
S. Food 7/14	1.03	ND	0.009	0.006	0.005	ND	0.028	0.82	0.9
S. Food 8/7	1.04	ND	ND	ND	ND	ND	ND	0.38	0.4
S. Food 9/2	1.01	ND	0.036	0.043	0.089	ND	ND	2.9	3.1
Avg Spike	1.03	na	0.018	0.018	0.057	=	0.091	1.4	1.5
SD Spike	0.011	na	0.018	0.019	0.057	=	0.106	1.1	1.2
RSD Spike	1.10	na	102.49	107.64	99.72	=	116.45	77.2	80

Sample	Mass	Isomer Profiles (Mass isomer/mass total)							%Branched
		1m	3m	4m	5m	totalDM	iso	n-pfos	
C. Food 9/21	1	na	0.008	0.009	0.028	na	0.051	0.90	0.10
C.Food 6/15	1.04	na	na	na	na	na	na	1.0	0.00
Food Na2SO4	0	na	na	na	na	na	na	na	na
S. Food 9/25	1.02	na	0.001	0.001	na	na	na	1.0	0.00
S. Food 6/15	1.04	na	0.005	0.005	0.012	na	0.031	0.95	0.05
S. Food 6/29	1.02	na	0.013	0.011	0.038	na	0.068	0.87	0.13
S. Food 7/14	1.03	na	0.010	0.007	0.006	na	0.032	0.94	0.06
S. Food 8/7	1.04	na	na	na	na	na	na	1.0	0.00
S. Food 9/2	1.01	na	0.012	0.014	0.029	na	na	0.95	0.05
Avg Spike	1.03	na	na	na	na	na	na	0.95	0.05
SD Spike	0.011	na	na	na	na	na	na	0.05	0.05
RSD Spike	1.10	na	na	na	na	na	na	5.01	97

Table A-4-18: *Concentrations and percentage of branched PFOS isomers in tissues*

Liver

	Day	1m	3m	4m	5m	TotalDM	isoPFOS 499/80	nPFOS 499/80	isoPFOS 499/99	nPFOS 499/99	Total PFOS	%Branched
2	99	0.35	0.70	0.82	0.95	ND	3.65	101	2.57	98	107	6.04
3	99	0.17	0.34	0.47	0.55	0.04	4.51	107	4.78	108	113	5.40
4	126	0.30	0.50	0.65	0.93	ND	5.28	147	4.62	148	155	4.96
5	99	0.85	42.5	42.9	55.8	10.8	155	936	159	884	1244	24.8
6	126	1.10	82.5	62.4	50.5	9.5	198	1053	218	995	1457	27.8
7	126	1.25	70.3	68.0	84.6	14.0	213	1281	238	1243	1733	26.1
8	99	1.86	99.7	84.3	89.5	20.4	253	1238	283	1183	1786	30.7
9	126	0.61	32.7	29.6	33.2	6.2	90.8	637	97.3	597	830	23.3
40	99	1.40	73.5	68.4	84.4	25.1	218	1026	238	1026	1497	31.4
50	126	0.81	67.1	62.0	62.7	15.7	176	835	184	800	1219	31.5
60	126	0.74	25.4	27.2	42.3	6.9	114	598	126	600	814	26.6

Brain

	Day	1m	3m	4m	5m	TotalDM	isoPFOS 499/80	nPFOS 499/80	isoPFOS 499/99	nPFOS 499/99	Total PFOS	%Branched
2	99	ND	ND	ND	ND	ND	0.26	3.22	ND	2.38	3.47	7.4
3	99	ND	0.12	ND	0.42	ND	0.62	8.21	0.74	8.63	9.37	12.4
4	126	ND	0.14	0.11	0.46	ND	0.62	8.03	0.78	8.55	9.35	14.2
5	99	0.04	0.06	0.06	0.26	ND	0.61	9.24	0.43	9.14	10.3	10.0
6	126	ND	0.14	0.08	0.47	ND	0.74	10.3	0.54	11.0	11.8	12.2
7	126	ND	0.03	0.07	0.19	ND	0.36	5.08	0.29	4.92	5.73	11.4
8	99	0.13	0.21	0.07	0.73	0.03	1.03	12.6	0.84	13.0	14.6	14.2
9	126	ND	0.10	ND	0.33	ND	0.45	5.28	0.37	5.37	6.28	15.9
40	99	ND	0.13	0.05	0.43	0.02	0.56	7.93	0.62	7.78	9.12	13.0
50	126	ND	ND	ND	ND	ND	0.50	7.56	0.17	6.29	8.06	6.19
60	126	ND	0.16	0.09	0.55	ND	0.85	11.6	0.88	11.3	13.2	12.4

Rat	Day	1m	3m	4m	5m	TotalDM	isoPFOS 499/80	nPFOS 499/80	isoPFOS 499/99	nPFOS 499/99	Total PFOS	%Branched
2	99	ND	0.048	ND	0.17	ND	0.23	2.89	0.24	2.99	3.34	13.4
3	99	ND	0.028	ND	0.10	ND	0.11	1.43	0.12	1.59	1.66	14.0
4	126	0.030	0.054	0.052	0.18	0.00	0.18	3.62	0.24	3.67	4.12	12.3
5	99	0.041	0.053	0.061	0.27	ND	0.63	5.76	0.58	5.97	6.82	15.5
6	126	0.031	0.049	0.058	0.36	0.01	0.89	10.5	0.91	10.6	11.9	11.7
7	126	0.032	0.059	0.063	0.39	ND	0.79	8.08	0.72	8.30	9.41	14.1
8	99	0.062	0.230	0.091	0.77	0.02	1.12	12.5	1.16	13.2	14.8	15.5
9	126	0.030	0.053	0.050	0.23	0.01	0.63	6.46	0.64	6.63	7.46	13.4
40	99	ND	0.282	0.079	0.91	ND	1.30	11.8	1.09	12.8	14.3	17.9
50	126	0.028	0.043	0.060	0.34	0.01	0.69	7.44	0.52	7.75	8.62	13.7
60	126	0.028	0.050	ND	0.27	0.01	0.62	5.54	0.51	5.88	6.51	15.0

Heart

Rat	Day	1m	3m	4m	5m	TotalDM	isoPFOS 499/80	nPFOS 499/80	isoPFOS 499/99	nPFOS 499/99	Total PFOS	%Branched
2	99	0.046	0.084	0.061	0.287	ND	0.384	3.24	0.28	3.41	4.10	21.0
3	99											
4	126	ND	0.095	0.163	0.577	0.0357	1.21	12.0	1.21	11.8	14.1	14.8
5	99	ND	0.094	ND	0.323	ND	0.451	7.82	0.720	7.47	8.69	10.0
6	126	ND	0.213	0.392	2.88	ND	4.99	48.4	5.37	50.0	56.8	14.9
7	126	0.097	0.145	0.206	1.42	ND	2.82	26.1	2.56	26.3	30.8	15.2
8	99	0.143	0.487	0.267	1.61	ND	2.71	22.5	2.69	24.4	27.7	18.8
9	126	ND	0.065	ND	0.213	ND	0.710	7.61	0.66	9.03	8.60	11.5
40	99	ND	0.304	ND	1.04	0.0239	1.29	10.6	0.96	11.6	13.2	20.1
50	126	ND	0.389	0.197	1.33	ND	1.82	17.4	1.58	17.1	21.1	17.7
60	126	0.103	0.572	0.189	1.96	0.0860	3.19	29.2	2.47	29.1	35.3	17.3

Kidney

Rat	Day	1m	3m	4m	5m	TotalDM	isoPFOS 499/80	nPFOS 499/80	isoPFOS 499/99	nPFOS 499/99	Total PFOS	%Branched
2	99	ND	0.0478	0.0649	0.5994	0.01	1.16	20.6	1.25	19.9	22.4	8.4
3	99	ND	ND	ND	0.0141	0.00	0.195	7.89	ND	7.63	8.10	2.6
4	126	ND	0.0020	ND	0.0022	ND	0.372	9.92	0.43	9.97	10.3	3.7
5	99	ND	0.1336	0.130	1.62	0.04	2.94	36.8	2.91	36.7	41.7	11.7
6	126	0.0871	0.654	1.30	4.88	0.17	12.7	104	10.4	99.7	124	15.9
7	126	0.0796	0.564	0.262	1.92	ND	3.30	58.0	3.34	58.6	64.2	9.5
8	99	0.1259	0.281	0.428	3.34	0.10	6.61	85.0	5.74	81.3	95.9	11.4
9	126	ND	0.247	0.382	2.02	0.06	3.89	54.0	3.42	51.9	60.6	10.9
40	99	0.0486	0.120	0.207	2.13	0.06	3.69	45.8	3.67	44.1	52.1	12.0
50	126	0.0487	0.230	0.417	2.56	0.08	5.48	61.2	5.14	60.7	70.0	12.6
60	126	ND	0.0837	0.149	1.66	0.02	3.05	36.8	2.64	36.4	41.8	11.9

Lung

Rat	Day	1m	3m	4m	5m	TotalDM	isoPFOS 499/80	nPFOS 499/80	isoPFOS 499/99	nPFOS 499/99	Total PFOS	%Branched
2	99	0.053	0.043	0.056	0.126	ND	0.390	6.19	0.36	6.18	6.86	9.7
3	99	0.062	0.087	0.100	0.298	ND	0.549	4.17	0.45	4.28	5.27	20.8
4	126	ND	ND	ND	ND	ND	ND	12.1	ND	ND	12.1	0.0
5	99	0.077	0.15	0.20	1.37	0.05	2.50	13.2	2.02	13.6	17.5	24.8
6	126											
7	126	0.34	0.52	0.93	5.69	0.19	11.25	89.4	10.2	92.4	108	17.5
8	99	0.29	0.81	0.70	4.51	1.30	10.68	92.2	8.50	90.9	110	16.6
9	126	0.10	0.47	0.37	1.93	0.08	6.36	49.6	4.30	50.9	58.9	15.8
40	99	ND	ND	ND	2.59	ND	6.91	82.9	4.76	73.6	92.4	10.3
50	126	ND	0.14	ND	0.41	ND	0.80	6.85	0.75	6.79	8.19	16.4
60	126	0.16	0.42	0.41	2.90	0.11	6.89	40.2	5.11	41.4	51.1	21.3

Muscle

Rat	Day	1m	3m	4m	5m	TotalDM	isoPFOS 499/80	nPFOS 499/80	isoPFOS 499/99	nPFOS 499/99	Total PFOS	%Branched
2	99	ND	ND	ND	ND	ND	0.14	1.41	ND	1.37	1.55	9.22
3	99	ND	0.06	ND	0.10	ND	0.31	3.13	0.33	2.88	3.59	13.0
4	126	ND	0.04	ND	0.16	ND	0.26	3.75	ND	3.06	4.21	10.9
5	99	ND	0.07	ND	0.21	ND	0.61	5.60	0.49	5.83	6.49	13.7
6	126	ND	0.06	0.08	0.37	0.02	0.78	7.43	0.65	8.00	8.74	14.9
7	126	0.03	0.09	0.10	0.34	ND	0.72	7.85	0.72	7.51	9.14	14.0
8	99	ND	0.08	0.09	0.36	0.02	0.76	8.15	0.69	8.19	9.46	13.9
9	126	ND	0.04	ND	0.23	ND	0.61	5.36	0.52	5.01	6.25	14.2
40	99	ND	0.05	0.06	0.24	ND	0.40	4.83	0.28	4.91	5.59	13.6
50	126	ND	0.18	0.20	0.63	0.04	1.07	9.77	0.97	8.60	11.88	17.7
60	126	ND	0.02	0.01	0.15	ND	0.27	2.26	0.27	2.48	2.72	16.8

Spleen

Rat	Day	1m	3m	4m	5m	TotalDM	isoPFOS 499/80	nPFOS 499/80	isoPFOS 499/99	nPFOS 499/99	Total PFOS	%Branched
2	99	0.12	0.13	ND	0.51	ND	1.29	15.3	1.42	15.0	17.4	11.8
3	99	ND	ND	ND	ND	ND	1.22	11.5	ND	10.2	12.7	9.60
4	126	ND	0.23	ND	0.78	ND	0.96	7.45	0.61	7.67	9.41	20.9
5	99	ND	0.09	ND	0.70	ND	1.38	16.8	1.67	20.3	18.9	11.4
6	126	ND	0.11	0.19	0.98	ND	2.70	32.4	2.13	31.9	36.4	10.9
7	126	0.13	1.03	0.42	3.40	ND	6.14	42.1	5.39	43.0	53.2	20.9
8	99											
9	126	ND	0.22	0.14	0.74	ND	0.66	9.11	0.84	9.46	10.9	16.2
40	99	ND	0.30	ND	1.04	0.01	1.74	19.1	1.56	19.5	22.2	13.9
50	126	ND	ND	ND	ND	ND	1.34	21.4	0.48	19.6	22.7	5.90
60	126	ND	0.09	0.11	0.80	ND	1.78	20.4	1.72	20.7	23.1	12.0

Testes

	Day	1m	3m	4m	5m	TotalDM	isoPFOS 499/80	nPFOS 499/80	isoPFOS 499/99	nPFOS 499/99	Total PFOS	%Branched
2	99	ND	ND	ND	ND	ND	ND	1.07	ND	0.38	1.07	0.0
3	99	ND	ND	ND	ND	ND	1.79	37.1	0.59	25.3	38.9	4.61
4	126	ND	ND	ND	ND	0.00	0.14	2.86	ND	2.63	3.00	4.59
5	99	ND	0.07	0.00	0.71	ND	1.19	11.58	1.10	12.0	13.5	14.5
6	126	ND	ND	ND	ND	ND	1.95	24.3	ND	24.8	26.2	7.44
7	126	ND	0.07	ND	0.99	ND	2.14	30.8	2.28	30.7	34.0	9.43
8	99	0.00	0.05	ND	0.70	ND	1.56	18.2	0.79	17.4	20.6	11.3
9	126	ND	ND	ND	0.31	ND	1.02	11.8	ND	13.0	13.2	10.1
40	99	ND	0.05	0.04	0.92	ND	1.50	12.0	1.29	11.6	14.5	17.4
50	126	ND	ND	ND	0.55	ND	1.31	14.2	0.93	13.2	16.1	11.6
60	126	ND	ND	ND	ND	ND	1.56	14.0	0.73	14.6	15.6	10.0

303

Table A-4-19: *Concentrations and percentage of branched PFOSA isomers in rat tissues*

Concentration (ng/g)
Liver

Sample	Day	Σbranched PFOSA	n-FOSA	Total FOSA	%Branched
2	99	ND	ND	0.00	N/A
3	99	ND	ND	0.00	N/A
5	99	0.11	2.75	2.85	3.70
8	99	0.38	3.92	4.30	8.85
40	99	0.14	3.79	3.92	3.53
4	126	ND	ND	0.00	N/A
6	126	ND	0.22	0.22	N/A
7	126	ND	0.30	0.30	N/A
9	126	ND	0.06	0.06	N/A
50	126	ND	0.08	0.08	N/A
60	126	0.00	0.17	0.17	2.76

Brain

Sample	Day	Σbranched PFOSA	n-FOSA	Total FOSA	%Branched
2	99	ND	ND	0.00	N/A
3	99	ND	ND	0.00	N/A
5	99	0.02	0.49	0.52	4.25
8	99	0.06	0.96	1.01	5.68
40	99	0.07	0.66	0.72	9.08
4	126	ND	ND	0.00	N/A
6	126	ND	ND	0.00	N/A
7	126	ND	0.05	0.05	N/A
9	126	ND	0.02	0.02	N/A
50	126	ND	0.02	0.02	N/A
60	126	ND	0.04	0.04	N/A

Fat

Sample	Day	Σbranched PFOSA	n-FOSA	Total FOSA	%Branched
2	99	ND	ND	0.00	N/A
3	99	ND	ND	0.00	N/A
5	99	0.03	0.40	0.44	7.96
8	99	0.06	0.17	0.23	25.7
40	99	0.01	0.15	0.15	4.82
4	126	ND	0.02	0.02	N/A
6	126	ND	0.15	0.15	N/A
7	126	ND	0.04	0.04	N/A
9	126	ND	0.02	0.02	N/A
50	126	ND	0.01	0.01	N/A
60	126	ND	0.02	0.02	N/A

Heart

Sample	Day	Σbranched PFOSA	n-FOSA	Total FOSA	%Branched
2	99	ND	ND	0.00	N/A
3	99				
4	126	ND	0.05	0.05	N/A
5	99	0.09	1.75	1.84	5.13
6	126	ND	0.13	0.13	N/A
7	126	ND	0.15	0.15	N/A
8	99	0.16	2.51	2.67	5.95
9	126	ND	0.06	0.06	N/A
40	99	0.06	1.67	1.73	3.52
50	126	ND	0.07	0.07	N/A
60	126	ND	0.08	0.08	N/A

Kidney

Sample	Day	Σbranched PFOSA	n-FOSA	Total FOSA	%Branched
2	99	ND	0.02	0.02	N/A
3	99	ND	ND	0.00	N/A
4	126	ND	0.03	0.03	N/A
5	99	0.13	1.88	2.01	6.67
6	126	ND	0.14	0.14	N/A
7	126	ND	0.12	0.12	N/A
8	99	0.33	3.37	3.69	8.85
9	126	ND	ND	0.00	N/A
40	99	0.20	2.35	2.56	8.00
50	126	ND	0.05	0.05	N/A
60	126	0.00	0.09	0.09	2.92

Lung

Sample	Day	Σbranched PFOSA	n-FOSA	Total FOSA	%Branched
2	99	ND	0.02	0.02	N/A
3	99	ND	0.02	0.02	N/A
4	126	ND	ND	0.00	N/A
5	99	0.25	3.95	4.20	6.05
6	126				
7	126	ND	0.22	0.22	N/A
8	99	0.33	5.34	5.67	5.88
9	126	0.00	0.08	0.08	5.67
40	99	0.34	3.07	3.42	10.0
50	126	0.00	0.13	0.14	2.60
60	126	ND	0.21	0.21	N/A

Muscle

Sample	Day	Σbranched PFOSA	n-FOSA	Total FOSA	%Branched
2	99	ND	ND	0.00	N/A
3	99	ND	ND	0.00	N/A
4	126	ND	0.05	0.05	N/A
5	99	ND	0.34	0.34	N/A
6	126	ND	0.03	0.03	N/A
7	126	ND	ND	0.00	N/A
8	99	0.01	0.16	0.17	6.07
9	126	ND	0.01	0.01	N/A
40	99	ND	0.19	0.19	N/A
50	126	ND	ND	0.00	N/A
60	126	ND	0.01	0.01	N/A

Spleen

Sample	Day	Σbranched PFOSA	n-FOSA	Total FOSA	%Branched
2	99	ND	0.12	0.12	N/A
3	99	ND	ND	0.00	N/A
4	126	ND	0.03	0.03	N/A
5	99	0.47	5.72	6.19	7.56
6	126	ND	ND	0.00	N/A
7	126	0.01	0.23	0.23	2.57
8	99				
9	126	ND	ND	0.00	N/A
40	99	0.36	5.03	5.39	6.77
50	126	0.00	0.12	0.13	3.57
60	126				

Testes

Sample	Day	Σbranched PFOSA	n-FOSA	Total FOSA	%Branched
2	99	ND	ND	0.00	N/A
3	99	ND	ND	0.00	N/A
4	126	ND	ND	0.00	N/A
5	99	0.11	2.75	2.85	3.70
6	126	ND	0.22	0.22	N/A
7	126	ND	0.30	0.30	N/A
8	99	0.38	3.92	4.30	8.85
9	126	ND	0.06	0.06	N/A
40	99	0.14	3.79	3.92	3.53
50	126	ND	0.08	0.08	N/A

Table A-4-20: Concentrations of PFOSA in rat whole blood

n-PFOSA

Day						Rat						
	1	2	3	4	5	6	7	8	9	40	50	60
0	0.91	0.11	0.38	NA	2.21	NA	0.16	0.04	0.14	NA	NA	0.17
14	NA	NA	0.03	0.13	12.8	27.4	38.0	13.0	12.2	15.2	31.2	18.4
22	0.06	0.03	0.04	NA	5.0	23.9	39.6	6.4	12.4	10.1	30.6	15.5
35	0.47	0.09	NA	NA	NA	6.1	14.8	25.3	53.7	20.9	40.5	92.7
49	0.04	0.16	0.33	0.10	26.5	17.4	40.0	20.7	23.4	31.6	28.1	NA
63	0.00	0.11	0.15	0.06	12.4	14.6	21.2	18.2	8.62	20.6	19.0	6.76
77	0.09	NA	1.32	3.79	12.1	7.33	30.0	22.0	3.46	12.5	16.1	NA
78	0.00	NA	NA	0.00	NA	5.68	29.1	NA	3.71	NA	28.1	8.81
79	0.19	NA	NA	0.06	NA	1.72	36.9	NA	221	NA	10.5	5.31
84	0.20	NA	NA	2.11	NA	14.4	17.8	NA	8.56	NA	7.23	3.92
91	0.23	NA	NA	0.07	NA	6.8	6.18	NA	1.39	NA	3.64	1.85
98	0.36	NA	NA	2.59	NA	2.51	3.57	NA	1.35	NA	1.23	NA
104	NA	NA	NA	0.06	NA	0.95	0.79	NA	0.68	NA	0.43	0.43

Total branched PFOSA

Day						Rat						
	1	2	3	4	5	6	7	8	9	40	50	60
0	0.02	0.00	0.00	NA	0.08	NA	0.00	0.00	0.00	NA	NA	0.01
14	NA	NA	0.00	0.00	2.99	4.00	9.68	3.36	6.35	3.12	6.79	6.86
22	0.00	0.00	0.00	NA	0.83	8.79	8.24	0.24	2.69	1.99	15.4	2.76
35	0.00	0.01	NA	NA	NA	1.35	3.52	6.14	15.6	5.24	12.7	20.7
49	0.00	0.02	0.09	0.00	1.43	3.54	14.3	3.49	3.11	3.42	1.91	NA
63	0.01	0.04	0.00	0.00	1.97	2.06	3.57	3.43	0.26	3.06	7.67	0.36
77	0.00	NA	0.19	0.00	12.0	0.23	9.91	4.25	0.52	2.50	3.69	NA
78	0.00	NA	NA	0.00	NA	0.88	5.73	NA	0.63	NA	10.3	2.53
79	0.06	NA	NA	0.00	NA	0.17	4.78	NA	34.0	NA	4.36	0.61
84	0.05	NA	NA	0.97	NA	1.40	1.79	NA	0.28	NA	1.72	0.15
91	0.06	NA	NA	0.00	NA	0.10	0.51	NA	0.05	NA	0.54	0.05
98	0.06	NA	NA	0.42	NA	0.02	0.20	NA	0.34	NA	0.15	NA

Total PFOSA

Day					Rat							
	1	2	3	4	5	6	7	8	9	40	50	60
0	0.92	0.11	0.38	NA	2.29	31.4	0.16	0.04	0.14			0.18
14	NA	NA	0.03	0.13	15.8	32.7	47.7	16.4	18.6	18.3	38.0	25.3
22	0.06	0.03	0.04	NA	5.78	7.43	47.8	6.61	15.1	12.1	46.0	18.2
35	0.47	0.10	NA	NA		21.0	18.3	31.4	69.3	26.1	53.2	113.4
49	0.04	0.18	0.42	0.10	27.9	16.6	54.4	24.2	26.5	35.1	30.0	
63	0.01	0.15	0.15	0.06	14.3	7.55	24.7	21.6	8.89	23.66	26.66	7.12
77	0.09	NA	1.51	3.79	24.1	6.56	39.9	26.3	3.99	15.0	19.8	
78	0.00	NA	NA	0.00	NA	1.88	34.9	NA	4.34	NA	38.4	11.3
79	0.25	NA	NA	0.06	NA	15.8	41.7	NA		NA	14.8	5.92
84	0.25	NA	NA	3.08	NA	6.89	19.6	NA	8.84	NA	8.95	4.07
91	0.30	NA	NA	0.07	NA	2.52	6.69	NA	1.44	NA	4.18	1.91
98	0.42	NA	NA	3.01	NA	0.98	3.77	NA	1.69	NA	1.38	NA
104	NA	NA	NA	0.07	NA		0.81	NA	0.75	NA	0.47	0.49

%branched

Day					Rat							
	1	2	3	4	5	6	7	8	9	40	50	60
0	1.66	0.00	0.00	NA	3.46	NA	0.00	3.10	0.00	NA	NA	5.86
14	NA	NA	0.00	0.77	18.9	12.8	20.3	20.5	34.2	17.1	17.9	27.1
22	0.00	11.5	8.04	NA	14.4	26.9	17.2	3.66	17.9	16.5	33.5	15.2
35	0.00	10.4	NA	NA	NA	18.2	19.2	19.5	22.6	20.1	23.8	18.2
49	3.62	11.3	21.4	0.00	5.11	16.9	26.4	14.4	11.7	9.75	6.37	NA
63	100.00	27.7	0.00	0.00	13.7	12.4	14.4	15.8	2.98	12.9	28.8	5.02
77	0.00	NA	12.6	0.00	50.0	2.99	24.8	16.2	13.1	16.7	18.7	NA
78	NA	NA	NA	NA	NA	13.4	16.4	NA	14.5	NA	26.9	22.3
79	22.70	NA	NA	0.00	NA	8.86	11.5	NA	13.4	NA	29.4	10.3
84	19.99	NA	NA	31.5	NA	8.88	9.12	NA	3.18	NA	19.2	3.72
91	21.57	NA	NA	0.00	NA	1.51	7.57	NA	3.21	NA	12.8	2.85
98	14.86	NA	NA	13.9	NA	0.78	5.19	NA	20.0	NA	11.1	NA
104	NA	NA	NA	15.3	NA	3.47	3.02	NA	8.64	NA	7.90	12.3

Table A-4-21: Control and growth corrected concentrations of PFOS isomers in rat whole blood

1m

						Rat						
Day	1	2	3	4	5	6	7	8	9	40	50	60
0	0.032	<control	0.299	<control	0.055	<control	<control	<control	<control	<control	<control	<control
14	<control	0.003	NA	<control	0.031	0.068	0.104	0.041	0.018	0.018	0.042	0.028
22	0.058	<control	<control	0.011	0.025	0.124	0.004	0.122	0.055	0.039	0.089	0.088
35	<control	<control	<control	0.043	0.017	0.157	0.089	0.123	0.036	-0.015	0.051	0.063
49	<control	0.060	<control	<control	0.009	0.110	0.051	0.162	0.045	0.044	0.155	0.024
63	NA	<control	<control	0.015	0.039	0.206	0.089	0.190	0.028	0.070	0.110	0.031
77	0.161	<control	<control	0.036	0.050	-0.071	0.121	0.242	0.069	0.057	0.355	0.189
78	0.000	NA	NA	NA	NA	0.209	0.103	NA	0.044	NA	0.117	0.116
79	0.061	NA	NA	0.000	NA	0.263	0.146	NA	0.053	NA	0.107	0.204
84	<control	NA	NA	0.000	NA	0.128	0.109	NA	-0.021	NA	0.069	0.422
91	0.162	NA	NA	0.000	NA	0.072	0.031	NA	0.041	NA	0.133	0.050
98	0.174	NA	NA	0.000	NA	0.228	0.230	NA	0.063	NA	0.196	0.196
104	NA	NA	NA	0.000	NA	0.217	0.195	NA	0.069	NA	0.105	0.182

3m

						Rat						
Day	1	2	3	4	5	6	7	8	9	40	50	60
0	<control	<control	0.350	<control	<control	<control	<control	<control	<control	<control	<control	<control
14	0.005	0.000	NA	0.000	0.058	0.178	0.156	0.064	0.039	0.045	0.048	0.045
22	0.023	<control	<control	0.008	0.051	0.260	0.039	0.159	0.048	0.047	0.067	0.085
35	0.015	<control	0.003	0.007	0.061	0.415	0.068	0.170	0.079	0.043	0.062	0.057
49	<control	<control	0.005	<control	0.041	0.329	0.092	0.222	0.096	0.123	0.160	0.058
63	NA	<control	0.018	0.001	0.106	0.310	0.156	0.237	0.056	0.146	0.253	0.064
77	0.148	<control	<control	0.012	0.110	-0.012	0.231	0.259	0.222	0.090	0.591	0.312
78	0.000	NA	NA	NA	NA	0.645	0.252	NA	0.176	NA	0.363	0.192
79	0.083	NA	NA	0.000	NA	0.588	0.260	NA	0.174	NA	0.323	0.433
84	0.031	NA	NA	0.000	NA	0.406	0.238	NA	0.121	NA	0.297	0.240
91	0.133	NA	NA	0.000	NA	0.398	0.194	NA	0.239	NA	0.286	0.156
98	0.021	NA	NA	0.000	NA	0.368	0.342	NA	0.100	NA	0.255	0.098
104	NA	NA	NA	0.000	NA	0.58	0.28	NA	0.13	NA	0.17	0.22

4m

Rat

Day	1	2	3	4	5	6	7	8	9	40	50	60
0	<control	<control	<control	<control	<control	<control	<control	<control	<control	<control	<control	<control
14	0.007	<control	NA	0.001	0.072	0.207	0.217	0.084	0.081	0.054	0.104	0.082
22	0.031	<control	<control	0.005	0.061	0.326	0.126	0.202	0.111	0.056	0.131	0.149
35	<control	<control	0.007	0.008	0.100	0.587	0.205	0.224	0.165	0.055	0.151	0.112
49	<control	0.023	<control	<control	0.080	0.500	0.188	0.321	0.215	0.167	0.298	0.123
63	NA	<control	0.032	<control	0.141	<control	0.297	0.369	0.183	0.181	0.437	0.130
77	0.162	<control	<control	0.016	0.154	0.670	0.384	0.327	0.381	0.128	0.916	0.504
78	0.000	NA	NA	NA	NA	1.085	0.463	NA	-0.070	NA	0.617	0.365
79	0.092	NA	NA	0.000	NA	0.968	0.488	NA	0.327	NA	0.587	0.475
84	0.009	NA	NA	0.000	NA	0.673	0.387	NA	0.281	NA	0.421	0.535
91	0.203	NA	NA	0.000	NA	0.699	0.314	NA	0.400	NA	0.495	0.317
98	0.079	NA	NA	0.000	NA	0.654	0.422	NA	0.177	NA	0.010	0.241
104	NA	NA	NA	0.000	NA	0.797	0.351	NA	0.275	NA	0.277	0.341

5m

Rat

Day	1	2	3	4	5	6	7	8	9	40	50	60
0	<control	<control	0.785	<control	<control	<control	<control	<control	<control	<control	<control	<control
14	0.031	<control	NA	<control	0.509	1.41	1.13	0.671	0.676	0.551	1.01	0.920
22	0.116	<control	<control	0.023	0.587	2.14	1.15	1.40	0.977	0.688	1.45	1.45
35	<control	<control	0.039	0.017	1.03	4.09	1.98	1.98	1.52	0.663	1.80	1.51
49	<control	<control	<control	<control	0.951	3.74	1.69	2.43	2.12	1.85	2.61	1.66
63	NA	<control	0.102	<control	1.44	5.50	2.66	3.49	2.02	1.92	3.72	2.01
77	0.388	<control	<control	0.048	1.69	5.02	3.18	3.22	3.11	1.73	4.75	4.70
78	0.000	NA	NA	NA	NA	6.72	3.97	NA	2.65	NA	4.62	4.00
79	0.263	NA	NA	0.000	NA	5.88	3.71	NA	2.95	NA	4.27	2.99
84	0.075	NA	NA	0.000	NA	4.66	3.23	NA	2.61	NA	3.44	3.89
91	0.510	NA	NA	0.000	NA	4.42	2.80	NA	2.73	NA	3.21	3.15
98	0.290	NA	NA	0.000	NA	4.41	3.70	NA	2.04	NA	3.18	2.80
104	NA	NA	NA	0.000	NA	4.62	2.42	NA	1.99	NA	2.03	3.66

iso

Rat

Day	1	2	3	4	5	6	7	8	9	40	50	60
0	<control	<control	1.627	<control	<control	<control	control	control	control	control	control	control
14	0.011	<control	NA	0.018	0.532	1.42	1.62	0.774	0.810	0.560	1.050	0.827
22	0.293	<control	<control	0.077	0.596	2.40	1.20	1.60	1.07	0.736	1.44	1.52
35	0.013	<control	0.100	0.035	0.999	4.15	2.49	2.29	1.74	0.860	2.13	1.43
49	<control	0.105	0.011	<control	0.899	4.20	1.91	2.78	2.36	2.06	2.73	1.75
63	NA	<control	0.307	<control	1.595	5.54	3.24	4.10	2.21	2.04	4.66	2.09
77	0.743	<control	<control	0.132	1.942	5.69	4.09	3.80	3.92	1.86	7.12	6.30
78	0.000	NA	NA	NA	NA	7.99	4.27	NA	3.31	NA	5.70	5.30
79	0.628	NA	NA	0.000	NA	7.37	4.33	NA	3.53	NA	5.53	4.39
84	0.189	NA	NA	0.000	NA	5.85	3.65	NA	3.29	NA	4.44	4.82
91	1.267	NA	NA	0.000	NA	5.63	3.44	NA	3.89	NA	4.18	3.71
98	0.592	NA	NA	0.000	NA	5.50	4.58	NA	2.39	NA	4.38	3.57
104	NA	NA	NA	0.000	NA	6.18	3.25	NA	2.86	NA	2.74	4.35

totalDM

Rat

Day	1	2	3	4	5	6	7	8	9	40	50	60
0	<control	<control	<control	<control	<control	<control	<control	<control	<control	<control	<control	<control
14	0.011	0.000	NA	0.000	0.089	0.301	0.004	0.145	0.146	0.112	0.226	0.244
22	0.039	0.000	0.000	0.000	0.119	0.334	0.136	0.245	0.175	0.132	0.269	0.229
35	<control	<control	0.078	<control	0.114	0.553	0.159	0.266	0.214	0.101	0.250	0.202
49	<control	0.024	<control	0.031	0.099	0.511	0.204	0.376	0.317	0.281	0.374	0.232
63	NA	<control	0.000	0.000	0.254	0.446	0.278	0.425	0.323	0.319	0.617	0.282
77	0.144	0.000	NA	NA	0.280	0.000	0.433	0.416	0.467	0.237	0.854	0.741
78	0.000	NA	NA	0.000	NA	0.818	0.489	NA	0.435	NA	0.747	0.695
79	0.099	NA	NA	0.000	NA	0.785	0.580	NA	0.502	NA	0.626	0.425
84	0.005	NA	NA	0.000	NA	0.573	0.299	NA	0.344	NA	0.486	0.592
91	0.142	NA	NA	0.000	NA	0.529	0.258	NA	0.445	NA	0.531	0.427
98	0.019	NA	NA	0.000	NA	0.543	0.417	NA	0.301	NA	0.485	0.395
104	NA	NA	NA	0.000	NA	0.508	0.179	NA	0.283	NA	0.300	0.460

n-pfos

Rat

Day	1	2	3	4	5	6	7	8	9	40	50	60
0	<control	<control	<control	<control	<control	<control	<control	<control	<control	<control	<control	<control
14	0.432	<control	NA	0.18	3.26	7.37	13.65	6.06	5.52	3.39	5.48	3.64
22	5.33	<control	<control	0.92	4.79	13.8	9.90	12.4	6.8	7.38	9.53	8.74
35	0.981	<control	<control	2.32	6.02	22.1	16.5	16.3	12.3	8.90	11.95	7.88
49	<control	1.62	<control	<control	7.81	22.5	16.2	18.1	13.2	12.0	16.8	8.38
63	NA	<control	2.71	<control	8.79	31.1	18.9	22.8	11.4	12.3	25.2	7.67
77	7.757	<control	<control	1.85	9.01	42.2	30.4	21.6	22.1	10.8	55.8	32.8
78	0.000	NA	NA	NA	NA	49.2	30.7	NA	20.6	NA	35.7	27.4
79	8.556	NA	NA	0.000	NA	47.1	29.6	NA	21.3	NA	38.1	30.6
84	2.791	NA	NA	0.000	NA	35.0	29.5	NA	19.4	NA	32.3	26.6
91	9.756	NA	NA	0.000	NA	32.3	24.5	NA	19.5	NA	27.8	17.2
98	5.535	NA	NA	0.000	NA	30.6	27.2	NA	13.7	NA	24.3	16.5
104	NA	NA	NA	0.000	NA	39.1	24.7	NA	16.9	NA	20.0	21.8

total PFOS

Rat

Day	1	2	3	4	5	6	7	8	9	40	50	60
0	<control	<control	<control	<control	<control	<control	<control	<control	<control	<control	<control	<control
14	0.475	<control	NA	0.192	4.46	10.7	16.9	7.69	7.15	4.62	7.73	5.55
22	5.85	<control	<control	1.04	6.11	19.1	12.4	15.9	9.10	8.95	12.7	12.0
35	0.972	<control	<control	2.43	8.23	31.5	21.3	21.0	15.9	10.5	16.1	11.1
49	<control	1.88	<control	<control	9.79	31.3	20.2	24.0	18.0	16.3	22.8	12.0
63	NA	<control	3.18	-0.40	12.1	42.6	25.3	31.2	15.9	16.7	34.4	12.0
77	9.36	<control	<control	2.10	13.0	53.5	38.4	29.5	29.8	14.7	69.5	44.8
78	0.00	NA	NA	NA	NA	65.9	39.8	NA	26.7	NA	47.1	37.4
79	9.68	NA	NA	0.00	NA	62.2	38.5	NA	28.4	NA	48.9	39.1
84	3.09	NA	NA	0.00	NA	46.7	37.1	NA	25.6	NA	40.9	36.5
91	12.0	NA	NA	0.00	NA	43.5	31.3	NA	26.8	NA	36.2	24.6
98	6.69	NA	NA	0.00	NA	41.8	36.4	NA	18.5	NA	32.3	23.4
104	NA	NA	NA	0.00	NA	51.5	31.2	NA	22.2	NA	25.4	30.5

%Branched

					Rat							
Day	1	2	3	4	5	6	7	8	9	40	50	60
0	17.4	16.4	15.2	13.8	35.5	16.3	13.8	15.9	14.9	16.5	15.4	15.2
14	9.04	7.64	NA	7.64	26.9	30.8	19.1	21.2	22.7	26.6	29.1	34.3
22	8.91	8.95	15.7	11.9	21.6	27.5	20.3	22.0	24.9	17.5	25.0	27.4
35	-0.9	36.3	-8.38	4.6	26.8	29.9	22.7	22.8	22.3	15.3	26.0	28.7
49	13.6	13.9	10.7	14.4	20.2	28.3	19.5	24.6	26.8	26.1	26.1	30.1
63	NA	15.7	14.9	9.42	27.5	27.0	25.4	26.9	28.3	26.2	26.7	36.0
77	17.1	9.89	13.2	11.6	30.5	21.1	20.8	26.6	25.9	26.3	19.8	26.8
78	NA	NA	NA	NA	NA	25.3	22.8	NA	22.9	NA	24.2	26.7
79	11.6	NA	NA	NA	NA	24.2	23.2	NA	24.8	NA	22.1	21.7
84	9.82	NA	NA	NA	NA	25.1	20.5	NA	24.5	NA	21.2	27.2
91	18.9	NA	NA	NA	NA	29.5	21.7	NA	27.2	NA	23.0	30.1
98	17.3	NA	NA	NA	NA	26.7	25.4	NA	25.9	NA	24.8	29.5
104	NA	NA	NA	NA	NA	24.0	20.8	NA	24.0	NA	21.0	28.7

313